A Systematic Experimental and Computational Approach to Investigating Phosphotyrosine Signaling Networks

A systematic experimental and computational approach to investigating phosphotyrosine signaling networks

A dissertation presented

By

Grigoriy Koytiger

To

The Department of Chemistry and Chemical Biology

in partial fulfillment of the requirements

for the degree of

Doctor of Philosophy

In the subject of

Chemistry

Harvard University

Cambridge, Massachusetts

April 2013

Thesis Advisor: Prof. Peter Sorger Grigoriy Koytiger

A systematic experimental and computational approach to investigating phosphotyrosine signaling networks

Abstract

Mutation and over-expression of Receptor Tyrosine Kinases (RTKs) or the proteins they regulate serve as oncogenic drivers in diverse cancers. RTKs catalyze the transfer of phosphate from ATP to the hydroxyl group on tyrosine. The proximal stretch of amino acids including this post translational modification is then able to be recognized by SH2 and PTB domains. Chapter 1 details our work to better understand RTK signaling and its link to oncogenesis using protein microarrays to systematically and quantitatively measure interactions between virtually every SH2 or PTB domain encoded in the human genome and all known sites of tyrosine phosphorylation on 40 out of the 53 Receptor Tyrosine Kinases.

Chapter 2 expands upon this work to study the next layer of binding among SH2 and PTB domain-containing adaptor proteins themselves. We found that adaptor proteins, like RTKs, have many high affinity bindings sites for other adaptor proteins. In addition, proteins driving oncogenesis, including both receptors and adaptor proteins, tend to be highly interconnected via a network of SH2 and PTB domain-mediated interactions. Our results suggest that network topological properties such as connectivity can be used to prioritize new drug targets in these well-studied signaling networks.

Despite the extensive work presented here on experimentally determining interactions, we nevertheless are unable to keep up with the discovery of new sites of tyrosine phosphorylation by high throughput mass spectrometry as well as their mutation in cancer

discovered by next generation tumor sequencing approaches. Chapter 3 introduces work in progress to build a unified predictive model of SH2 domain interactions via integration of diverse data sets of binding as well as crystal structures of domain-peptide interactions. This model will enable researchers discovering new phosphorylation events or mutations to be able to predict potential interaction partners and thereby elucidate novel functional mechanisms.

Table of Contents

Abstract

1. Overview of Phosphotyrosine Signaling

1.1. Signal Initiation

1.2. SH2 Domains

1.2.1. Structure

1.2.2. Function

1.3. PTB Domains

1.3.1. Structure

1.3.2. Function

1.4. Pathways

1.4.1. PI3K/AKT Pathway

1.4.2. Ras/MAPK Pathway

1.4.3. PLC-γ/ PKC

1.4.4. STAT

1.5. Challenges to the Pathway View of Signaling

1.6. Phosphotyrosine Signaling in Disease

1.7. Qualitative Methods to Study SH2/PTB Domain Interactions

1.8. Quantitative Protein Domain Microarrays

1.8.1. Previous Publications

1.8.2. Experimental Procedures

1.8.2.1. Peptide Synthesis and Purification

1.8.2.2. Production and Purification of Domains

1.8.2.3. Printing and Processing of Arrays

1.8.2.4. Data Analysis Pipeline

1.9. Prediction of SH2 Domain Interactions

1.9.1. Position Specific Scoring Matrix Based Methods

1.9.2. Neural Network Based Methods

2. A Systems Biology Approach to Uncover the RTK Interactome

2.1. Introduction

2.2. Data Collection

2.3. Oncogenic RTKs are highly connected Results

2.4. Materials and methods

2.4.1. Determining Interaction Affinity

2.4.2. Determining Oncogene Status

2.4.3. Statistical Tests for Enrichment of Binding

2.4.4. Peptides Derived from RTKs

3. Systematic Investigation of Adaptor-Adaptor Interactions

3.1. Introduction

3.2. Oncogenic Adaptors are highly connected

3.3. Materials and methods

3.3.1. Determining Oncogene Status

3.3.2. RTK and Adaptors Expression in Tumor Samples

3.3.3. Adaptor Phosphopeptides

4. Modeling of SH2 Domain Interactions

4.1. Introduction

4.2. Model Inputs

4.3. Model Fitting

4.4. Assessing Model Performance

4.5. Applying the model to study cancer

5. Conclusions and Future Direction

5.1. From Molecular Machines to Pleomorphic Ensembles

5.2. From Data Explosion to Data Saturation

5.3. From Narrative Knowledge to Database Knowledge

6. Appendix

6.1. SH2 and PTB Domains Used in These Studies

6.2. Sub micromolar interactions identified in these studies

Acknowledgements

It is difficult to overstate the enormous contributions of other people to the work presented here. It truly would not have been possible for me to achieve even a small fraction without the wonderful support of my lab mates, collaborators and friends.

First, I would like to thank my advisors Profs. Gavin MacBeath and Peter Sorger. Gavin believed in my ability to excel in his lab despite my background being in organic chemistry. He has provided an extraordinary help in guiding my research and refining the writing describing it. He has pushed me to think larger and motivated me to pursue projects that pushed the limits of what I thought possible for me to do. It has truly been a marvelous experience to work in his lab. Peter graciously took in the members of the MacBeath lab and managed to seamlessly integrate us. I have never felt out of place and anything less than a full team member. My success would be difficult without Peter's incisive insight and extensive knowledge of seemingly all topics of cell biology.

The members of the MacBeath and Sorger labs have been some of the most intelligent and hardworking people that I have had the pleasure to know. They create a stimulating, exciting and collaborative environment, which is a joy to work in. I would like to especially thank three members of the lab for their extensive contributions to my progress: Dr. Alexis Kaushanksy, Dr. Taran Gujral and Dr. Marina Chan. When entering the MacBeath lab, I knew next to nothing about executing molecular biology research. Alexis taught me everything from the basic protocols, to how to print SH2 domain arrays and how to think about the data that I generate. I will never forget her patience with me and her ability to dedicate her own time to assisting me. Through her actions Alexis taught me not only how to be a great scientist, but also how to be a great mentor. Drs. Taran Gujral and Marina Chan have been wonderful colleagues with whom I

have had many illuminating scientific discussions. Their dedication, intelligence and genuine good nature are an inspiration to me. I will miss the time we spend theorizing, chatting and laughing.

I would also like to thank Dr. Mohammed AlQuarashi. I wish all collaborations are as fruitful, stress free and enlightening. The modeling work described in this thesis would simply be impossible without Mohammed. His intelligence, computational savvy and curiosity amaze me. Often a quick chat with Mohammed about our project morphs into an illuminating multi hour discussion spanning science, philosophy and politics.

I wish all the people that have helped me along the way to my doctorate the best of luck in their future endeavors. I hope to one day return the favor for what you all have given me.

Part One: Overview of Phosphotyrosine Signaling

1.1 Signal Initiation

Phosphotyrosine (pTyr) signaling networks evolved in Metazoans to process extracellular cues and elicit cellular responses such as differentiation, proliferation or migration. Phosphotyrosine signaling emerges from the dynamic interplay of 4 domain types, the Tyrosine Kinase (TK) domain, the Src Homology 2 (SH2) domains, the Phosphotyrosine Binding (PTB) domain and the Tyrosine Phosphatase domain (Lemmon and Schlessinger 2010).

Canonical phosphotyrosine signaling is initiated when a ligand binds to the extracellular domain of its cognate Receptor Tyrosine Kinase (RTK), inducing the receptor's transition from a catalytically inactive to active form. However, there are notable differences among the receptors in the organization of their inactive and active forms as well as the mechanism of the transition between the two. The current view is that the majority of receptors exist as monomers in their inactive form and ligand binding induces dimerization and activation. However, there are exceptions to this rule. Insulin and IGF1R receptors exist as preformed dimers and ligand binding induces a conformational change that induces activation. EGFR can also exist in inactive oligomers of unknown size. Moreover, Eph receptors require the formation of larger oligomers at sites of cell-cell contact to be fully activated .

Ligand-induced dimerization primarily exists on a mechanistic continuum from purely ligand mediated to receptor mediated, defined by the composition of the dimerization interface. In a purely ligand-mediated mode, a bivalent ligand is able to simultaneously interact with two receptors leading to receptor crosslinking with no receptor-receptor contacts made extracellularly. An exemplar of this mode is NTRK1, whose ligand, NGF is shown in a crystal structure to make up the entire dimer interface (Wehrman et al. 2007). At the opposite

mechanistic end is EGFR, whose ligand EGF binds to only one receptor molecule, inducing a conformational change extracellularly. This exposes a dimerization arm, which is then able to interact with another molecule of EGFR (Burgess et al. 2003). Another distinct class of mechanism is exemplified by RET, where the ligand GDNF binds the coreceptor GFRα and the complex subsequently induces receptor dimerization (Schlee, Carmillo, and Whitty 2006).

Dimerization relieves cis-autoinhibitory contacts with the kinase domain by trans-phosphorylation. These autoinhibitory contacts are typically with the activation loop (Nolen, Taylor, and Ghosh 2004), but can also be to the juxtamembrane region (Till et al. 2002) or with the C-terminus (Niu, Peters, and Kontos 2002). The kinase domain then becomes fully active and catalyzes the auto-phosphorylation of intracellular tyrosine residues (Lemmon and Schlessinger 2010). These phosphotyrosine residues can then be recognized selectively by the approximately 120 SH2 and 44 PTB domains. Upon recruitment, many adaptor proteins bearing SH2 and PTB domains themselves become phosphorylated on tyrosine residues by active receptor or cytosolic tyrosine kinases. This second set of phosphorylation events leads to the recruitment of additional SH2 and PTB domain-containing proteins. SH2 and PTB domains also undergo rapid binding and unbinding.

Signal termination can occur when tyrosine phosphatase domains hydrolyze the phosphate. However, this system is highly dynamic with rapid turnover of the phosphate. Phosphotyrosines have half-lives of a few seconds, and thus turn over hundreds of times during the course of early signaling events. Once a receptor's kinase domain is inhibited by a drug, it rapidly loses its phosphorylation with half-lives on the order of 15 seconds. This signal ablation propogates to downstream components with SHC also becoming rapidly dephosphorylated

(Kleiman et al. 2011). Rapid dynamics allows SH2 and PTB domain binding to be effectively non-competitive, allowing for a given site to interact with many adaptors. It also allows adaptors to rapidly interact with many neighboring RTKs.

1.2. SH2 Domains

1.2.1 Structure

SH2 domains correspond to a conserved stretch of approximately 100 residues with a characteristic fold composed of two α–helices that flank an anti-parallel β sheet comprising three to four β strands. The phosphotyrosine residue binds the more conserved N-terminal region of the protein containing an arginine. In a couple of SH2 domains such as those found on the proteins Tyk2 and Rin2, however the arginine is mutated leading to an apparent loss of phosphotyrosine binding capacity (B. A. Liu et al. 2006). The domain also binds residues primarily C-terminal to the phosphotyrosine in the more variable C-terminus. Variation in those contact residues allows for sequence selectivity to be achieved between ligand and domain (Figure 1.1). A unique class of SH2-like domains is the CBL tyrosine kinase-binding (TKB) domain. While sharing little sequence similarity with SH2 domains, the TKB domain possesses a highly similar fold and shares the canonical arginine residue that is required for phosphotyrosine recognition.

Figure 1.1: Complex of SH2 domain with peptide. X-ray crystal structure of the SH2 domain of LCK is shown in complex with the phosphopeptide EPQyEEIPIYL (PDB ID 1LCJ). The peptide takes on an extended conformation within the SH2 domain binding groove.

Residues outside the canonical binding pocket can also facilitate target recognition. For example, a crystal structure of the complex between FGFR1 and PLC-γ showed a secondary binding site on the SH2 domain for the kinase domain, which further strengthened the interaction. However, most of the binding energy still came from the canonical binding mode (Bae et al. 2009). This coupled with the success of peptide-based methods of identifying new interactions as well as capturing known interactions, argues for the continued use of peptides in research.

SH2 domain–peptide interactions are typically of moderate affinity from 0.1 μM to 5 μM. A recent study shows, however, that SH2 domains are not optimized for maximum affinity. "Superbinder" SH2 domains can be generated through a triple point mutation resulting in a domain with identical ligand selectivity but capable of sub-nanomolar affinity. These superbinder domains effectively blocked signaling when expressed in cells, showing that the moderate affinity is critical for proper function of the network (Kaneko et al. 2012). Reduced affinity can minimize cross target binding as well as increase the dynamics of the network by speeding up dissociation.

1.2.2 Function

SH2 domain-containing proteins carry out at least three distinctive functions within cells: scaffold, enzymes and transcription factors.

The enzymatic class of proteins shares a common property in that their substrates are membrane localized. SH2 domain binding to membrane bound targets brings the catalytic domains in close proximity to their substrates and thereby facilitates catalytic activity. For instance, the vast majority of cytosolic tyrosine kinases (CTKs), such as Src and Abl1, also contain SH2 domains. SH2 domain binding relieves auto inhibitory interactions and liberates the tyrosine kinase domain to phosphorylate additional substrates. This typically proceeds in a processive fashion, generating additional sites of tyrosine phosphorylation on a target, which can be further recognized by the SH2 domain. CTKs are also capable of phosphorylating tyrosine residues on RTKs, expanding the repertoire of interactions possible on the receptor. Another class of enzymatic proteins, such as PLC-γ and PI3K, act upon phosphoinositides, a type of membrane lipid. These proteins typically also possess a PH domain, capable of recognizing

these phospholipds, which stabilizes membrane association and increases the lifetime of these membrane scaffolds. SH2 domains are also present on proteins such as RASA1 containing G-protein activating domains (GAPs) or the VAV family of guanine exchange factors (GEFs).

Most enzymatic proteins are involved in relaying and amplifying signals downstream of RTKs, causing additional rounds of activation. A notable exception is CBL. CBL contains ubiquitin ligase activity allowing for it to poly-ubiquinate receptors interacting with the SH2 domain. This leads to receptor internalization and subsequent degradation. This is a form of negative feedback loop, which serves to attenuate signals downstream of RTKs. Also, tyrosine phosphatases such as PTPN11 and PTPN6 become active by engagement of their SH2 domains. They catalyze the hydrolysis of phosphotyrosine, which for the most part leads to a decrease in signaling.

However, even these negative regulatory units can often have contradictory signal amplification properties. CBL-promoted internalization of catalytically active receptors allows them to reach additional intracellular substrates. PTPN11 can dephosphorylate negative regulatory sites on proteins such as SRC, which can lead to signal amplification. In fact, PTPN11 misregulation can lead to amplified ERK signaling and can drive oncogenesis.

Scaffold proteins contain additional protein interaction domains such as PTB or SH3 domains. An example is Grb2, which contains one SH2 domain and two SH3 domains. The N-terminal SH3 domain interacts with a proline-rich region in SOS, which activates Ras, initiating the MAPK cascade. The C-terminal SH3 domain is simultaneously capable of binding a proline rich region of Gab1. Grb2 interaction with an RTK also brings this protein in close proximity.

Gab1 is subsequently able to become tyrosine phosphorylated itself, which presents sites of recruitment for PI3K (Salcini et al. 1994).

1.3 PTB Domains

1.3.1 Structure

In contrast to SH2 domains, PTB domains constitute a smaller but more diverse class of phosphotyrosine recognition modules. They can be broadly divided into three families, the phosphotyrosine-dependent Shc-like and IRS-like class and the phosphorylation-independent Dab-like class. They share little sequence homology among themselves and are characterized instead by a distinct PH-like fold.

PTB domains recognize peptides in quite a distinct manner from SH2 domains. In contrast to the extended conformation, peptides take on a β-turn conformation in the PTB binding pocket (DiNitto and Lambright 2006). Sequence selectivity is achieved by the peptide N-terminal residues forming an anti-parallel β-strand with the domain. The canonical motif of PTB domains is NPXpY, although peptides matching that motif are recognized differently by the domains (Smith et al. 2006).

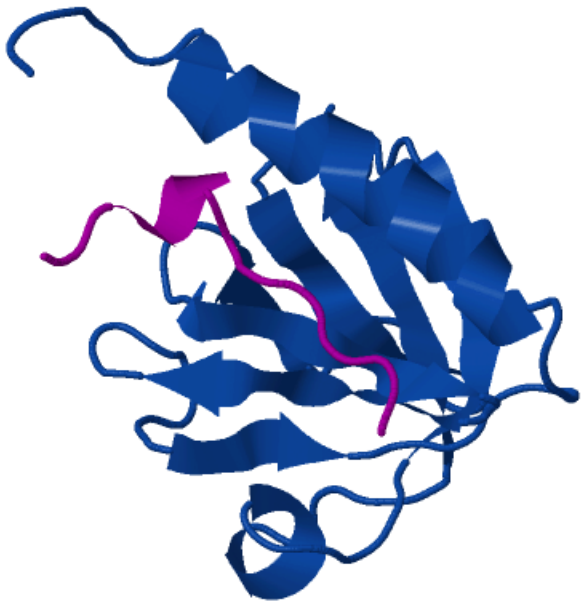

Figure 1.2: Prototypical PDB-peptide complex. IRS1-PTB Domain interacts with a IL-4 receptor derived phosphopeptide (PDB: 1IRS). The peptide (pink) takes on a β-turn L-shaped conformation within the binding pocket. The interaction is phosphotyrosine-dependent.

Most PTB domains fall within the phosphotyrosine-independent Dab class. In fact, some of these domains dissociate from their ligand upon phosphorylation. For instance, the Numb PTB domain binds to the sequence NVYYY in E-cadherin, but phosphorylation by Src abrogates binding (Wang et al. 2009).

1.3.2 Function

PTB domain-containing proteins are typically involved in phosphotyrosine signaling as scaffolds. Shc recognizes phosphopeptides primarily through its PTB domain primarily, and only secondarily its SH2 domain. Upon binding receptor through its PTB domain, Shc becomes tyrosine phosphorylated on Tyr427 of SHC1 (or Tyr317 in the p52 SHC1 isoform). This provides a binding site for Grb2 and thereby induces activation of the RAS/MAPK kinase cascade (Salcini et al. 1994). Similarly, FRS2α and FRS2β mediate many of the signals downstream of the FGFR family and NTRK family of receptors (Lemmon and Schlessinger 2010).

Dok (downstream of tyrosine kinase) family of proteins play many diverse roles, typically as negative regulators of many signaling pathways such as in adaptive and innate immunity (Mashima et al. 2013). Tensin family members can serve as tumor suppressors through their constitutive interaction with the DLC (deleted in liver cancer) genes. These examples, while not exhaustive, are illustrative of the many diverse roles played by PTB domain-containing proteins both in normal and disease physiology.

1.4 Pathways

Molecular pathways prototypically have a "bow-tie" structure, where many extracellular cues bind distinct receptors. Activated receptors are capable of binding a myriad of adaptors which then relay signals to very few conserved processes that integrate the diverse signals. They subsequently activate a wide set of effectors to elicit distinct phenotypic responses. There are four canonical RTK pathways –PI3K/AKT/mTOR, RAS/MAPK, PLC-γ/ PKC, and STAT – that are activated by a wide array of the receptors (Lemmon and Schlessinger 2010).

1.4.1 PI3K/AKT/mTOR

RTK activation can lead to the recruitment of PI3K either directly through phosphorylation sites on the receptor or indirectly through adaptor intermediates such as IRS1 or Gab1. PI3K is composed of two subunits, the p85 regulatory subunit containing two SH2 domains and the p110 catalytic subunit containing a lipid kinase. Engagement of the SH2 domains on p85 relieves autoinhibitory contacts as well as localizes the protein complex to the membrane. This activates the p110 subunit and brings it in close proximity to its primary substrate phosphoinositide (4,5) phosphate (PIP2). The enzyme catalyzes phosphotransfer from ATP to the 3' hydroxyl on PIP2, generating the critical secondary messenger PIP3.

PIP3 is capable of being recognized by the PH domains of 3'-phoshoinositde-dependent kinase (PDK1) and protein kinase B (Akt), leading to their translocation to the membrane. This brings the two enzymes into close proximity, leading to the phosphorylation of Akt by PDK1 and its subsequent activation. Akt is at the center of the "bow-tie" network, and is able to modulate cellular phenotype such as modulating protein synthesis via the mTOR complex, inhibiting apoptosis by phosphorylation of BAD and inducing cell-cycle entry by phosphorylation of GSK-3.

There are multiple mechanisms for signal attenuation of this pathway. For instance, inositol phosphatases such as PTEN and SHIP catalyze the dephosphorylation of PIP3. PP2A and PHLPP directly dephosphorylate Akt, inactivating the kinase. Akt also engages in negative feedback loops primarily at the transcriptional level. It inhibits FOXO-mediated RTK transcription as well as IRS1 transcription through mTORC1. For this reason, therapeutic

treatment with inhibitors targeting this pathway has the unintended effect of upregulating kinase signaling (Chandarlapaty et al. 2011).

1.4.2 RAS/MAPK

Activation of the MAPK pathway requires the membrane localization of the guanine nucleotide exchange factor son of sevenless (SOS). SOS is constitutively associated with Grb2 through an interaction mediated by the Grb2 SH3 domain and a proline rich region on SOS. This complex can be directly recruited to the membrane by direct binding of the Grb2 SH2 domain to an activated RTK. Conversely, the complex can be recruited indirectly through Shc, which becomes tyrosine phosphorylated upon recruitment to the membrane, which creates a binding site for Grb2 (Salcini et al. 1994).

Membrane localized SOS promotes the nucleotide exchange of GDP for GTP on the prenylated RAS family of proteins: KRAS, NRAS and HRAS. GTP bound RAS activates RAF, which phosphorylates and activates the MAPK kinases, MEK1 and MEK2. MEK can then subsequently activate the ERK family of kinases, whose downstream targets include the transcription factors CREB and c-Jun (Downward 2003).

1.4.3 PLC-γ/PKC

PLC-γ contains two SH2 domains, which act normally to suppress catalytic function (Carpenter and Ji 1999). Like many enzymatic SH2 domain-containing proteins, engagement of the SH2 domains by activated receptors liberates the auto-inhibitory conformation and promotes enzymatic activity. For instance, binding of the N-terminal SH2 domain of PLC-γ to PDGFR

leads to the phosphorylation of Tyr771, Tyr783 and Tyr1254 and the activation of the enzyme (Kim et al. 1991).

PLC-γ catalyzes the hydrolysis of PIP2, generating two secondary messengers diacylglycerol (DAG) and inositoyl 1,4,5-triphosphate (IP_3). IP3 binding to its endoplasmic reticulum (ER)-localized receptor, IP3R, leads to the release of calcium ions from the ER. This leads to the activation of calmodulin and related kinases. DAG and calcium also combine to activate protein kinase C (PKC), which is a central hub of this pathway and mediates many of the physiological responses downstream of PLC-γ (Choi, Ryu, and Suh 2007).

1.4.4 STAT

The signal transducer and activator of transcription (STAT) family of proteins is among the simplest of the pathways activated downstream of RTKs. This class of SH2 domain-containing proteins is unique in also functioning as transcription factors. They are therefore able to directly couple receptor activation to changes in gene expression.

Inactive STATs exist as monomers in the cytosol. Binding by the SH2 domain and subsequent tyrosine phosphorylation allows the STAT proteins to dimerize by reciprocal binding of the pTyr by the SH2 domain. Active dimers are then able to translocate to the nucleus and initiate the transcription of numerous genes (Harrison 2012).

1.5 Challenges to the Pathway View of Signaling

The term pathway implies linearity and modularity in the interacting components described above. Indeed, this was the consensus view of these networks for a long time with the

MAPK signaling pathway being the prototypical example (Lemmon and Schlessinger 2010). However, as more data have been collected, this conception has proved increasingly inadequate.

RTKs share a similar set of interactors and activate many of the same response pathways. They do not, however, necessarily elicit the same phenotypes. For example, both EGFR and NTRK1 induce MAPK signaling in PC12 cells, but EGFR triggers proliferation whereas NTRK1 promotes differentiation (Marshall 1995). Both of these phenotypes are dependent on ERK activity. However, even the act of overexpressing EGFR in those cells can shift the response from proliferation to differentiation. This is thought to be due to the differential recruitment of negative and positive feedback mechanisms within the MAPK pathway (Santos, Verveer, and Bastiaens 2007). This phenomenon is also observed clinically, where only a subset of RTKs have been shown to drive cancer despite sharing many downstream pathways (Santarius et al. 2010). Current qualitative representations of signaling networks as linear cascades are inadequate to explain the diverse phenotypes that arise downstream of different RTKs (Lemmon and Schlessinger 2010).

Increasing understanding of pathway crosstalk has also undermined the concept of pathway modularity. In a purely modular network, the activity of one pathway does not affect the activity of another. However, this is clearly not the case. For instance, PLC-γ catalyzes the hydrolysis of PIP2 whereas PI3K catalyzes its phosphorylation. Whichever is recruited first to the activated receptor will rapidly deplete the substrate for the second (Mayer, Blinov, and Loew 2009). This is also seen in the clinic where single drug targeting of the MAPK or PI3K pathways leads to the undesired effect of up regulating the other pathway (Khalili et al. 2012; Won et al. 2012).

1.6 Phosphotyrosine Signaling in Disease

Aberrant signal processing by RTK signaling networks has been causally linked to cancer development, maintenance, and progression in many human tissues. Well-studied examples include overexpression of ERBB2 in breast cancer (Perren 1991), KIT in testicular germ cell tumors (McIntyre et al. 2005), and MET in gastric cancer (Comoglio, Giordano, and Trusolino 2008). Constitutive activating mutations of RTKs, such as those observed in the RET kinase (Mulligan et al. 1993; Hofstra et al. 1994) in multiple endocrine neoplasia type 2 or KIT in gastrointestinal stromal tumors (Hirota et al. 1998) are also capable of driving oncogenesis.

Underscoring the critical role played by RTKs in cancer is the considerable effort underway to develop drugs targeting them. There are two classes of drugs in development, antibody therapeutics target the extracellular portions of receptors and small molecule tyrosine kinase domain inhibitors that bind in the ATP recognition region of the RTKs and interfere with its ability to catalyze phosphorylation. Tyrosine kinase inhibitors typically have the drawback of being cross-reactive with other targets leading to potential side effects. Antibodies on the other hand typically have insufficient efficacy as monotherapies (Lemmon and Schlessinger 2010). Both drug classes almost invariably lead to drug resistance caused by tumor mutations that abrogate the tumor's dependence on the targeted RTK or the affinity of the inhibitor to its target (Engelman and Settleman 2008).

Table 1.1: Phosphotyrosine signaling components are targeted by clinical drugs. Both antibody and small molecule inhibitors of kinases are clinically used to treat cancer. Despite considerable effort, SH2 and phosphatases have so far not been effectively drugged (Lemmon and Schlessinger 2010).

Small Molecule	Mab	Target	Disease	Year of approval
Imatinib (Gleevec)		PDGFR, KIT, Abl, Arg	CML, GIST	2001
Gefitinib (Iressa)		EGFR	Esophageal cancer, Glioma	2003
Erlotinib (Tarceva)		EGFR	Esophageal cancer, Glioma	2004
Sorafenib (Nexavar)		Raf, VEGFR, PDGFR, Flt3, KIT	Renal cell carcinoma	2005
Sunitinib (Sutent)		KIT, VEGFR, PDGFR, Flt3	Renal cell carcinoma, GIST, Endocrine pancreatic cancer	2006
Desatinib (Sprycel)		Abl, Arg, KIT, PDGFR, Src	Gleevec-resistant CML	2007
Nilotinib (Tasigna)		Abl, Arg, KIT, PDGFR	Gleevec-resistant CML	2007
Lapatinib (Tykerb)		EGFR, ErbB2	Mammary carcinoma	2007
	Trastuzumab (Herceptin)	ErbB2	Mammary carcinoma	1998
	Cetuximab (Erbitux)	EGFR	Colorectal cancer, Head and neck cancer	2004
	Bevacizumab (Avastin)	VEGF	Lung cancer, Colorectal cancer	2004
	Panitumumab (Vectibix)	EGFR	Colorectal cancer	2006

Similarly to RTKs, mutation or overexpression of SH2 domain-containing cytosolic proteins such as ABL kinase (Druker et al. 2001) or the PI3K p85 regulatory subunit (Cheung et al. 2011) can also drive cancer, in these cases by inducing constitutive enzymatic activity that is decoupled from upstream signaling events. Drugs targeting the catalytic activity of Abl are already in clinical use (Goldman and Melo 2003) and inhibitors of PI3K are in development (Howes et al. 2007).

Phosphotyrosine signaling abnormalities have also been shown to promote diseases outside of cancer. The virally transcribed protein $p28^{sis}$ activates PDGFR in an autocrine loop leading to pro-survival signaling. The avian erythroblastosis virus encodes a truncated form of EGFR that becomes constitutively active. Bacterial proteins are also capable of becoming tyrosine phosphorylated and interacting with SH2 and PTB domain-containing proteins to rewire signaling for their advantage (Boettcher et al. 2010; Mehlitz et al. 2010).

1.7 Qualitative Methods to Study SH2/PTB Domain Interactions

Systematic methods that have been used to study the binding properties of these phosphotyrosine interacting domains can be broadly divided into two classes – display and array. Display methods can use phosphopeptide libraries attached to beads, phage or as nucleotide-peptide hybrids. Binders are then isolated and typically the interacting peptides are identified in bulk, giving a frequency distribution of the presence of each amino acid at the individual positions of the peptide (Zhou et al. 1993). The positive features of these methods are their capacity to encode large libraries and thereby probe a wide range of interactions. The drawback is that most of the sequences assayed are not physiological and thus their interactions shed little

light on cellular function. Moreover, the assay is competitive so high affinity non-physiological sequences sequester the protein away from more physiologically relevant but weaker binding peptides.

Peptide array methods typically involve direct synthesis on a membrane using the SPOTS method (Rodriguez et al. 2004; B. A. Liu et al. 2010). These membranes can then be directly probed with labeled domain and detected or the peptides can be cleaved off the membrane and arrayed in higher density on another surface (Miller et al. 2008). This method has the advantage of being able to assay the domains against the same set of peptides, facilitating systematic comparison in the recognition properties of these domains. Also, because these peptides are spatially isolated, identifying which peptide interacts with a given domain is operationally simpler than in the display methods. The addressable sequence space is lower for this assay; however, recent advances in generating high density peptide arrays should minimize this gap (Breitling et al. 2009).

The drawback to all these methods is that they are non-quantitative. Their signal is usually directly proportional to the amount of a given peptide. If one sequence is synthesized with a higher yield on a membrane, it will yield a higher signal than a peptide of equal affinity but lower synthetic yield. The relationship between spot intensity and affinity is a complicated one and can invert when probing at different concentrations. This makes comparisons across peptides and domains difficult (Gordus and MacBeath 2006; Jones et al. 2005).

1.8 Quantitative Protein Domain Microarrays

To overcome many of these challenges, the MacBeath lab has developed quantitative protein domain microarrays. In this approach, 134 purified recombinant SH2 and PTB domains were printed as microarrays in individual wells of 96-well microtiter plates. The arrays were then probed with fluorescently labeled phosphopeptides derived from known sites of tyrosine phosphorylation on human proteins. By probing the array with eight different concentrations of each peptide, full saturation binding curves were obtained, providing an estimate of the equilibrium dissociation constant for each biochemical interaction. One advantage of this method is that its quantitative nature allows facile comparison of interaction strength across domains and peptides. Nitrocellulose membranes used in peptide arrays have also notably higher background fluorescence than the glass surfaces used for domain arrays. On-membrane synthesis also does not allow for peptide purification. This can result in signal that can potentially be a result of binding to mis-synthesized peptides.

Previous work focused on nine RTKs: FGFR1, IGF1R, MET, NTRK2, PDGFRβ and the four ErbB receptors (Jones et al. 2005; Kaushansky et al. 2008). We have further validated many of the measured interactions in a cellular context by testing novel binding partners and by comparison with known interactions (Jung et al. 2011; Mehlitz et al. 2010; Boettcher et al. 2010). This work forms the foundation for the majority of the experimental work detailed in this thesis, which describes utilizing this approach to systematically quantify, on a nearly proteome-wide level, interactions between SH2 or PTB domains and known sites of tyrosine phosphorylation on both human RTKs and the adaptor proteins themselves. This represents an order of magnitude more interactions than have been tested in any previous publication.

1.9 Prediction of SH2 Domain Interactions

Previous systematic research on the binding specificity of SH2/PTB domains has been performed using phosphorylated peptide libraries. Early studies of this type uncovered consensus binding motifs of many SH2 domains (Huang et al. 2008; Rodriguez et al. 2004; Zhou et al. 1993). It was hoped that these motifs contained within them sufficient information to predict all known interaction sites of that domain. It is now apparent, however, that these motifs are simplified views of *in vivo* selectivity and that specificity is also defined by "anti-motifs" representing excluded contacts for SH2 domains (B. A. Liu et al. 2010), SH3 domains (Gorelik, Stanger, and Davidson 2011), and probably other modular interaction domains as well. This lack of positional independence makes it very difficult to predict accurately whether an SH2 or PTB domain will bind to a particular sequence in vivo.

Despite the challenges of prediction, the explosion of high throughput mass spectrometric studies has led to the discovery of many sites of tyrosine phosphorylation whose functional importance is unknown (Guo et al. 2008; Rikova et al. 2007). Moreover, genome-wide tumor sequencing efforts are identifying mutations near tyrosine phosphorylation sites that can perturb binding. Biochemical studies continue to lag behind in their ability to characterize and ascribe functional roles to these data. Development of an accurate predictive model can provide biological hypotheses that can be rapidly tested by researchers. Work towards development of such a model and its application to study disease will also be discussed in this thesis.

Part 2: A Systems Biology Approach to Uncover the RTK Interactome

2.1 Introduction

Recently, Barabási and colleagues advanced a mathematical argument that network driver nodes, the nodes that control information flow in a network, should not be highly interconnected (Y.-Y. Liu, Slotine, and Barabási 2011). If this notion is extended to cancer, in which signaling networks are substantially altered or rewired, we would expect that proteins driving oncogenesis would not be highly interconnected. We sought to determine experimentally if there is indeed a link between network connectivity and the propensity of a protein to drive cancer. In making this determination, we cannot rely solely on literature-derived interaction networks (Jonsson and Bates 2006; Wachi, Yoneda, and Wu 2005) as they are confounded by study bias (Hakes, Robertson, and Oliver 2005; Hakes et al. 2008). Specifically, oncogenic proteins are more intensively studied than non-oncogenic proteins, potentially resulting in a bias in terms of number of binding partners. As a means to collect systematic pTyr-mediated interaction data, *in vivo* methods like the yeast two-hybrid system are not suitable as they do not allow for control over post-translational modification events (Phizicky et al. 2003). Systematic co-immunoprecipitation coupled with mass spectrometry is also problematic, as many interactions mediated by tyrosine phosphorylation are transient, with half lives on the order of seconds, and any particular cell type expresses only a subset of the proteome (Mayer, Blinov, and Loew 2009).

To circumvent these limitations, we used protein domain microarrays to systematically probe and quantify every possible interaction between human SH2 or PTB domains and sites of tyrosine of RTKs. Overall, we found we find a very high degree of connectivity that challenges conventional, linear views of receptor-adapter interaction. Moreover, RTKs and adaptor proteins that have been shown to play a causal role in cancer tend to mediate more interactions than those

that do not. This suggests that these connectivity profiles may provide insight into how networks are rewired and may help prioritize new targets for anti-cancer drug discovery.

RESULTS AND DISCUSSION

2.2 Data collection

We started by compiling a list of known sites of tyrosine phosphorylation on human RTKs and on all SH2 and PTB domain-containing proteins listed in the PhosphoSitePlus database (Hornbeck et al. 2011). We restricted our studies to experimentally verified sites of tyrosine phosphorylation as nonphysiologically relevant sites, when artificially phosphorylated, may also bind SH2/PTB domains (Kaushansky, Gordus, Chang, et al. 2008) and thereby confound any systems level conclusions drawn from the resulting data. We focused on 40 of the 53 Uniprot-annotated RTKs that had more than three phosphorylation sites to include only those receptors whose biology is sufficiently understood to enable systematic comparison. This resulted in a total of 729 unique phosphopeptides that we successfully synthesized, fluorescently labeled, and purified using high performance liquid chromatography. We then used each of the peptides to probe microarrays comprising virtually every human SH2 and PTB domain. The arrays were probed at eight concentrations of each peptide, ranging from 10 nM to 5 μM (see, for example, Fig. 2.1A). By repeating this process for each phosphopeptide we were able to generate a quantitative interaction map for the receptor (Fig. 2.1B). This process was repeated for all of the remaining RTKs to generate, for the first time, a global, systematic, and unbiased view of RTK recruitment (Fig. 2.1C). Only interactions with $K_D < 1$ μM are included in these diagrams. SH2 domain-mediated interactions of lower affinity have been shown to be physiologically relevant intramolecularly, but it is generally accepted that most *bona fide* intermolecular

interactions exhibit dissociation constants below 1 µM (Ladbury et al. 1995; Piccione et al. 1993; Bibbins, Boeuf, and Varmus 1993). The complete list of sub-micromolar interactions is provided in Table 2 of the Appendix.

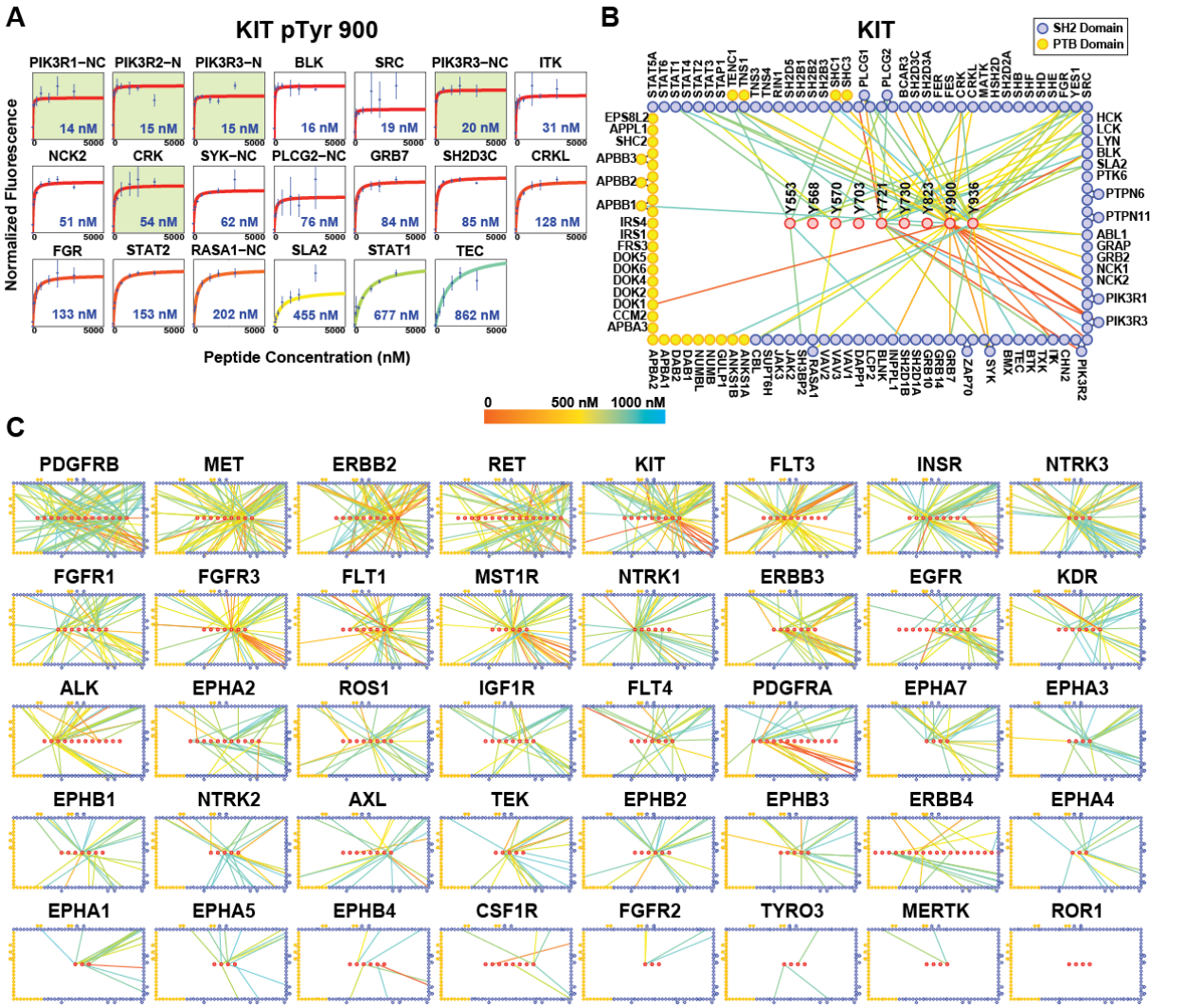

Figure 2.1: Determining binding affinity for SH2/PTB domains to phosphopeptides. (**A**) Example titration of 5 (6)-TAMRA-labeled phosphopeptide corresponding to the sequence encompassing KIT-pTyr900. Titrations highlighted in green correspond to previously-identified binding partners (Lennartsson et al. 2003). Curves are colored according to affinity (see legend) (**B**) Total connectivity for phosphorylation sites of the oncogenic RTK, KIT. Red circles corresponding to phosphorylation sites, blue circles to SH2 domains, and yellow circles to PTB domains. Lines are colored according to affinity. (**C**) Visualization of the binding profile of the 40 RTKs analyzed in the study. RTKs are sorted in descending order by the total number of links with affinities lower than 1 µM.

As with any assay, one invariably encounters false positives and false negatives. With protein domain microarrays, the most frequent source of false positives is nonspecific binding between peptide and domain, whereas false negatives likely arise from low surface activity of the domains, presumably because some domains denature on the slide surface or are preferentially immobilized in a way that blocks access to the binding site. To estimate the stochastic false positive rate, we conservatively assumed that domains having the lowest frequency of binding were actually inactive in our assay and exhibited no true-positive interactions (any interactions identified for these domains are by definition false positives). We observed that domains in the bottom 20% of the binding frequency spectrum accounted for 20 interactions out of the 37,490 titrations performed on the domains, corresponding to a stochastic false positive rate of 5.33×10^{-4}. If we extend this rate to all the titrations performed (195,546), we estimate that 104 of the 2,808 interactions we identified are liable to be stochastic false positives (false discovery rate of 3.72%). As there is no reason to believe that false positive errors are observed preferentially with phosphopeptides derived from cancer-causing proteins, the primary conclusions of this study are not affected.

Another potential limitation of our approach is that the current list of physiological sites of tyrosine phosphorylation in PhosphoSitePlus may be incomplete. This would be particularly problematic if non-oncogenic RTKs were less well annotated than oncogenic ones. To investigate this possibility, we used phosphotyrosine-directed mass spectrometry (Kaushansky, Gordus, Budnik, et al. 2008, 4) to study six non-oncogenic members of the Ephrin class of RTKs – EphA2, EphA3, EphA4, EphB2, EphB3 and EphB4. We overexpressed each receptor in HEK293T cells, a procedure that induced receptor auto-activation and phosphorylation in all six cases. Receptors were then immunoprecipitated using an anti-pTyr antibody and subjected to

targeted and untargeted μLC-MS/MS. Using this approach, we were able to identify 32 out of the 38 known sites of intracellular tyrosine phosphorylation (84% sensitivity). Remarkably, we did not identify any sites of tyrosine phosphorylation beyond those already reported in the PhosphoSitePlus database. This suggests that the many high throughput, pTyr-directed mass spectrometric studies that have been used to populate PhosphoSitePlus are not biased against non-oncogenic receptors and that the existing list of tyrosine phosphorylation events, at least on RTKs, is nearly complete.

2.3 Oncogenic RTKs are highly connected

By examining the connectivity profile of the 40 RTKs at various affinity thresholds (Fig. 2.2 A), we sought to identify whether a link exists between connectivity and oncogenicity. We determined whether or not an RTK is an oncogene based on its inclusion in the Sanger Institute's Cancer Gene Census (Santarius et al. 2010) (http://www.sanger.ac.uk/genetics/CGP/Census/), which seeks to determine a strict causal (and not merely correlative) relationship between cancer development and mutation and/or overexpression of a given gene. Based on these assignments, we found that oncogenic RTKs have a significantly higher median connectivity in our interaction dataset than non-oncogenic RTKs. At an affinity threshold of 1 μM, for example, the median number of binding partners is 21 for non-oncogenic RTKs and 56 for oncogenic receptors, corresponding to a ~2.5-fold difference in the number of interactions (Mann-Whitney U-test $p=2.77x10^{-5}$). Non-oncogenic RTKs also have a median of six phosphorylation sites, whereas oncogenic RTKs have nine phosphorylation sites (Mann-Whitney U-test p=0.007), corresponding to a 50% increase. This indicates that the primary reason for the increased connectivity of oncogenic RTKs is the presence of more promiscuous pTyr docking sites and

only secondarily an increase in the number of docking sites (Figure 2.2A). For instance, the non-oncogenic receptor CSF1R, although it has twice as many phosphorylation sites as NTRK3 (8 vs. 4), has far fewer high-affinity (K_D<1 μM) binding partners (6 vs. 58) (Figure 2.2 B). In addition, the RTK with the greatest number of phosphorylation sites in our study is the non-oncogenic ERBB4 with 16. ERBB4 has only 18 binding partners, however, which places it in the bottom 25% of the RTKs we studied.

Many interactions annotated here may be of too low affinity to bind at appreciable levels to a receptor that is present at low surface density or at a low level of activation. When a cell becomes malignant, however, gene amplification or overexpression may make phosphorylated receptors (or adaptors) sufficiently abundant that low affinity interactions are enabled and downstream signaling activated. This notion is supported by the observation, in PC12 cells, that EGFR mediates proliferation when present at normal levels but differentiation when overexpressed (Marshall 1995). These phenomena cannot be captured in qualitative diagrams of signaling and highlight the need to think of these interactions as being contextually conditional and existing on a quantitative spectrum without a single fixed threshold.

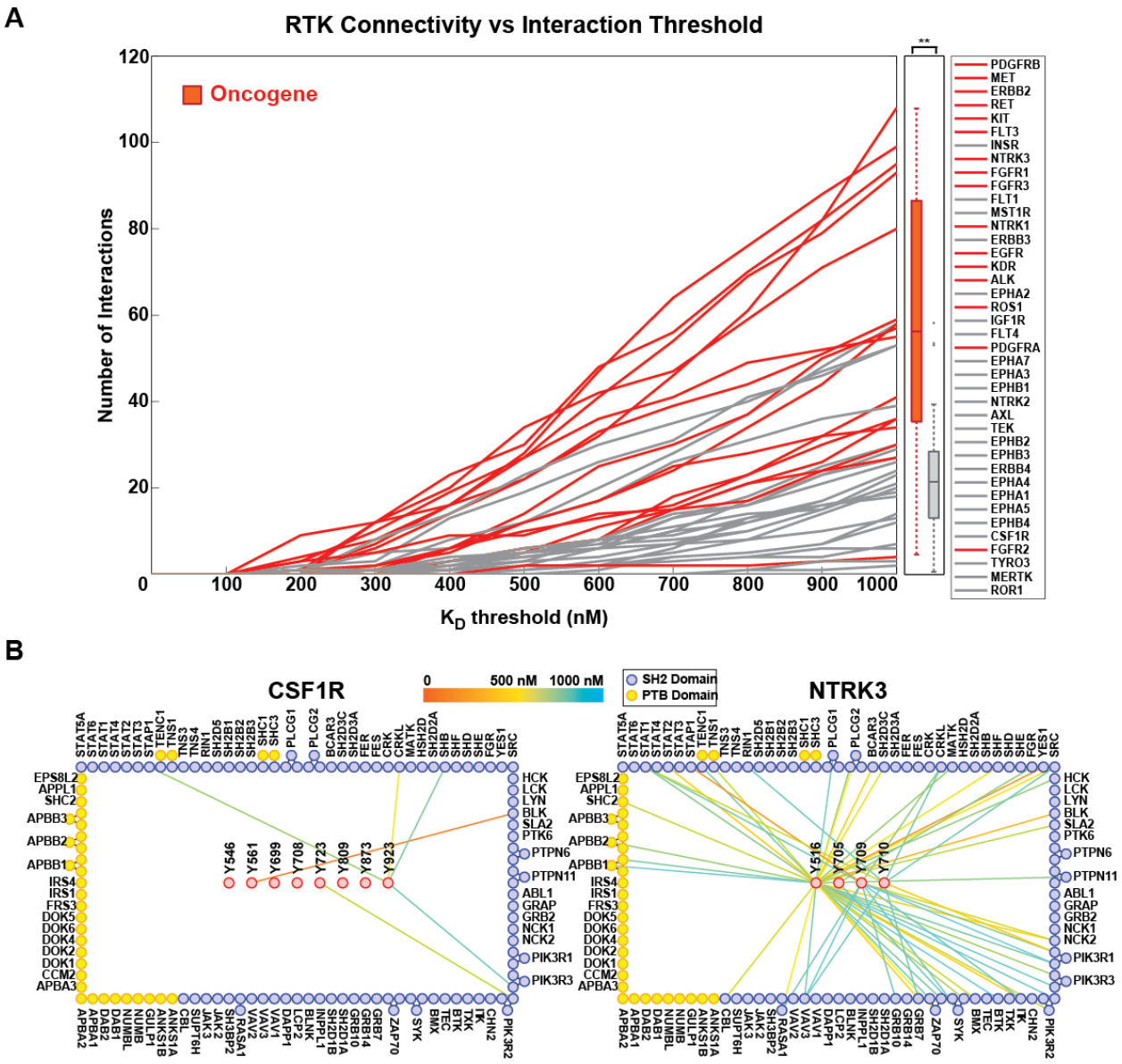

Figure 2.2: Oncogenic RTKs are enriched for binding partners. (**A**) Cumulative density distribution of RTK interactions at different affinity thresholds. Oncogenic RTKs in red have significantly more binding partners than non-oncogenic RTKs in grey; median of 56 vs. 21 interactions with affinity less than 1 μM (Mann-Whitney U-Test $p=2.8x10^{-5}$). (**B**) Example of connectivity between sites of tyrosine phosphorylation on the non-oncogenic RTK CSF1R and SH2/PTB domains.

2.4 Materials and methods

A detailed protocol for preparing protein domain microarrays has been described previously (Kaushansky et al. 2010).

2.4.1 Determining interaction affinity

Following peptide binding, arrays were scanned at multiple PMT voltages on a Tecan LS400 microarray scanner on both Cy5 and Cy3 channels. Spots with saturated pixels were eliminated. The remaining spots were fit to a line that allows for the conversion of all the Cy3 values measured at different PMT voltages to the same scale. The fold-over-background value of a titration was determined by taking the trimmed mean of the Cy3 values for each domain-peptide titration divided by the Cy3 values of the Thioredoxin control spots. The mean Cy3 value of the Thioredoxin control spots was then subtracted from the Cy3 value of the domain spot and the spots were normalized by the Cy5 value.

Each domain was printed in quadruplicate in each well and the arrays were probed using eight different concentrations of each peptide, ranging from 5 μM down to 10 nM. These 32 data points were then fit to the following equation using MATLAB®'s robust fit function with bisquare weights:

$$F_{obs} = F_{max}[\text{Peptide}] / (K_D + [\text{Peptide}]) \quad \text{Eq. 1}$$

where F_{obs} is the mean fluorescence of replicate spots, F_{max} is the fluorescence at saturation, [Peptide] is the total concentration of phosphopeptide, and K_D is the equilibrium dissociation constant. Robust fitting procedures are more resistant to the presence of outlier data resulting from missed spots, fluorescent debris or other aberrations (Huber 2003). Only titrations with

fold-over-background values in the top 10% of the data and R^2 values over 0.9 were kept. Replicate affinities were then averaged in log space. The MATLAB® code used to perform the analysis is supplied in supplementary information.

2.4.2 Determining oncogene status

Oncogene status for RTKs was determined using the Sanger Institute Cancer Gene Census (Futreal et al. 2004; Santarius et al. 2010). The Sanger list contains only those genes for which a strong causal link to cancer has been established.

2.4.3 Statistical tests for enrichment of binding

To test against the null hypothesis that the distribution of connectivity is equivalent for both Oncogene and non-Oncogene classes, we performed the non-parametric Mann-Whitney U test in MATLAB® R2011a (The MathWorks, Inc., Natick, MA). Only those interactions with dissociation constants below 1 μM were considered.

2.4.4 Peptides derived from RTKs

Table 2.1 RTK Phosphopeptides

Gene	pTyr	Peptide Sequence	Uniprot
ALK	Y1078	MQMELQSPEyKLSKLRT	Q9UM73
ALK	Y1092	LRTSTIMTDyNPNYCFA	Q9UM73
ALK	Y1096	TIMTDYNPNyCFAGKTS	Q9UM73
ALK	Y1131	LGHGAFGEVyEGQVSGM	Q9UM73
ALK	Y1278	GDFGMARDIyRASYYRK	Q9UM73
ALK	Y1282	MARDIYRASyYRKGGCA	Q9UM73
ALK	Y1283	ARDIYRASYyRKGGCAM	Q9UM73
ALK	Y1359	PPKNCPGPVyRIMTQCW	Q9UM73
ALK	Y1507	KPTSLWNPTyGSWFTEK	Q9UM73
ALK	Y1584	RHFPCGNVNyGYQQQGL	Q9UM73

Table 2.1 RTK Phosphopeptides (Continued)

ALK	Y1586	FPCGNVNYGyQQQGLPL	Q9UM73
ALK	Y1604	AATAPGAGHyEDTILKS	Q9UM73
AXL	Y481	VHRRKKETRyGEVFEPT	P30530
AXL	Y698	ADFGLSKKIyNGDYYRQ	P30530
AXL	Y702	LSKKIYNGDyYRQGRIA	P30530
AXL	Y703	SKKIYNGDYyRQGRIAK	P30530
AXL	Y726	AIESLADRVyTSKSDVW	P30530
AXL	Y759	QPADCLDGLyALMSRCW	P30530
AXL	Y821	PAQEPDEILyVNMDEGG	P30530
AXL	Y866	AAEVHPAGRyVLCPSTT	P30530
CSF1R	Y546	LYKYKQKPKyQVRWKII	P07333
CSF1R	Y561	IIESYEGNSyTFIDPTQ	P07333
CSF1R	Y699	GQDPEGGVDyKNIHLEK	P07333
CSF1R	Y708	YKNIHLEKKyVRRDSGF	P07333
CSF1R	Y723	GFSSQGVDTyVEMRPVS	P07333
CSF1R	Y809	ARDIMNDSNyIVKGNAR	P07333
CSF1R	Y873	KFYKLVKDGyQMAQPAF	P07333
CSF1R	Y923	AQEDRRERDyTNLPSSS	P07333
EGFR	Y727	LGSGAFGTVyKGLWIPE	P00533
EGFR	Y869	KLLGAEEKEyHAEGGKV	P00533
EGFR	Y944	QPPICTIDVyMIMVKCW	P00533
EGFR	Y978	SKMARDPQRyLVIQGDE	P00533
EGFR	Y998	LPSPTDSNFyRALMDEE	P00533
EGFR	Y1016	MDDVVDADEyLIPQQGF	P00533
EGFR	Y1069	IKEDSFLQRySSDPTGA	P00533
EGFR	Y1092	DDTFLPVPEyINQSVPK	P00533
EGFR	Y1125	NPAPSRDPHyQDPHSTA	P00533
EGFR	Y1138	HSTAVGNPEyLNTVQPT	P00533
EGFR	Y1172	HQISLDNPDyQQDFFPK	P00533
EGFR	Y1197	KGSTAENAEyLRVAPQS	P00533
EPHA1	Y599	REDKLWLKPyVDLQAYE	P21709
EPHA1	Y605	LKPYVDLQAyEDPAQGA	P21709
EPHA1	Y781	RLLDDFDGTyETQGGKI	P21709
EPHA2	Y575	RARQSPEDVyFSKSEQL	P29317
EPHA2	Y588	SEQLKPLKTyVDPHTYE	P29317
EPHA2	Y594	LKTYVDPHTyEDPNQAV	P29317
EPHA2	Y628	IGAGEFGEVyKGMLKTS	P29317

Table 2.1 RTK Phosphopeptides (Continued)

EPHA2	Y694	YKPMMIITEyMENGALD	P29317
EPHA2	Y735	GMKYLANMNyVHRDLAA	P29317
EPHA2	Y772	VLEDDPEATyTTSGGKI	P29317
EPHA2	Y791	RWTAPEAISyRKFTSAS	P29317
EPHA2	Y921	WLESIKMQQyTEHFMAA	P29317
EPHA2	Y930	YTEHFMAAGyTAIEKVV	P29317
EPHA2	Y960	LPGHQKRIAySLLGLKD	P29317
EPHA3	Y596	HLKLPGLRTyVDPHTYE	P29320
EPHA3	Y602	LRTYVDPHTyEDPTQAV	P29320
EPHA3	Y779	VLEDDPEAAyTTRGGKI	P29320
EPHA3	Y937	CKEIFTGVEySSCDTIA	P29320
EPHA4	Y596	KHLNQGVRTyVDPFTYE	P54764
EPHA4	Y602	VRTYVDPFTyEDPNQAV	P54764
EPHA4	Y779	VLEDDPEAAyTTRGGKI	P54764
EPHA5	Y650	HIKLPGVRTyIDPHTYE	P54756
EPHA5	Y656	VRTYIDPHTyEDPNQAV	P54756
EPHA5	Y833	VLEDDPEAAyTTRGGKI	P54756
EPHA5	Y967	EHSPLGSGAyRSVGEWL	P54756
EPHA7	Y597	ADQEGDEELyFHFKFPG	Q15375
EPHA7	Y608	HFKFPGTKTyIDPETYE	Q15375
EPHA7	Y614	TKTYIDPETyEDPNRAV	Q15375
EPHA7	Y791	VIEDDPEAVyTTTGGKI	Q15375
EPHB1	Y575	KRAYSKEAVySDKLQHY	P54762
EPHB1	Y582	AVYSDKLQHySTGRGSP	P54762
EPHB1	Y594	GRGSPGMKIyIDPFTYE	P54762
EPHB1	Y600	MKIYIDPFTyEDPNEAV	P54762
EPHB1	Y634	IGAGEFGEVyKGRLKLP	P54762
EPHB1	Y778	LQDDTSDPTyTSSLGGK	P54762
EPHB1	Y928	WLSAIKMVQyRDSFLTA	P54762
EPHB2	Y577	RGFERADSEyTDKLQHY	P29323
EPHB2	Y584	SEYTDKLQHyTSGHMTP	P29323
EPHB2	Y596	GHMTPGMKIyIDPFTYE	P29323
EPHB2	Y602	MKIYIDPFTyEDPNEAV	P29323
EPHB2	Y780	LEDDTSDPTyTSALGGK	P29323
EPHB2	Y912	PLLDRTIPDyTSFNTVD	P29323
EPHB3	Y600	SEYTEKLQQyIAPGMKV	P54753
EPHB3	Y608	QYIAPGMKVyIDPFTYE	P54753

Table 2.1 RTK Phosphopeptides (Continued)

EPHB3	Y614	MKVYIDPFTyEDPNEAV	P54753
EPHB3	Y754	GMKYLSEMNyVHRDLAA	P54753
EPHB3	Y924	PLLDRTVPDyTTFTTVG	P54753
EPHB4	Y574	KQSNGREAEySDKHGQY	P54760
EPHB4	Y581	AEYSDKHGQyLIGHGTK	P54760
EPHB4	Y596	TKVYIDPFTyEDPNEAV	P54760
EPHB4	Y614	EFAKEIDVSyVKIEEVI	P54760
EPHB4	Y774	LEENSSDPTyTSSLGGK	P54760
EPHB4	Y906	PLLDQRQPHySAFGSVG	P54760
ERBB2	Y735	LGSGAFGTVyKGIWIPD	P04626
ERBB2	Y877	RLLDIDETEyHADGGKV	P04626
ERBB2	Y1005	PASPLDSTFyRSLLEDD	P04626
ERBB2	Y1023	MGDLVDAEEyLVPQQGF	P04626
ERBB2	Y1112	THDPSPLQRySEDPTVP	P04626
ERBB2	Y1127	VPLPSETDGyVAPLTCS	P04626
ERBB2	Y1139	PLTCSPQPEyVNQPDVR	P04626
ERBB2	Y1196	FGGAVENPEyLTPQGGA	P04626
ERBB2	Y1221	AFSPAFDNLyYWDQDPP	P04626
ERBB2	Y1222	FSPAFDNLYyWDQDPPE	P04626
ERBB3	Y1054	QSLLSPSSGyMPMNQGN	P21860
ERBB3	Y1197	TEEEDEDEEyEYMNRRR	P21860
ERBB3	Y1199	EEDEDEEYEyMNRRRRH	P21860
ERBB3	Y1262	GTTPDEDYEyMNRQRDG	P21860
ERBB3	Y1276	RDGGGPGGDyAAMGACP	P21860
ERBB3	Y1289	GACPASEQGyEEMRAFQ	P21860
ERBB3	Y1328	TDSAFDNPDyWHSRLFP	P21860
ERBB4	Y875	RLLEGDEKEyNADGGKM	Q15303
ERBB4	Y1035	QAFNIPPPIyTSRARID	Q15303
ERBB4	Y1056	EIGHSPPPAyTPMSGNQ	Q15303
ERBB4	Y1066	TPMSGNQFVyRDGGFAA	Q15303
ERBB4	Y1081	AAEQGVSVPyRAPTSTI	Q15303
ERBB4	Y1128	VQEDSSTQRySADPTVF	Q15303
ERBB4	Y1150	PRGELDEEGyMTPMRDK	Q15303
ERBB4	Y1162	PMRDKPKQEyLNPVEEN	Q15303
ERBB4	Y1188	DLQALDNPEyHNASNGP	Q15303
ERBB4	Y1202	NGPPKAEDEyVNEPLYL	Q15303
ERBB4	Y1208	EDEYVNEPLyLNTFANT	Q15303

Table 2.1 RTK Phosphopeptides (Continued)

ERBB4	Y1221	FANTLGKAEyLKNNILS	Q15303
ERBB4	Y1242	AKKAFDNPDyWNHSLPP	Q15303
ERBB4	Y1258	PRSTLQHPDyLQEYSTK	Q15303
ERBB4	Y1262	LQHPDYLQEySTKYFYK	Q15303
ERBB4	Y1266	DYLQEYSTKyFYKQNGR	Q15303
ERBB4	Y1268	LQEYSTKYFyKQNGRIR	Q15303
ERBB4	Y1284	RPIVAENPEyLSEFSLK	Q15303
ERBB4	Y1301	PGTVLPPPPyRHRNTVV	Q15303
FGFR1	Y463	TPMLAGVSEyELPEDPR	P11362
FGFR1	Y585	QARRPPGLEyCYNPSHN	P11362
FGFR1	Y605	RRPPGLEYCyNPSHNPE	P11362
FGFR1	Y653	LARDIHHIDyYKKTTNG	P11362
FGFR1	Y653	SSKDLVSCAyQVARGME	P11362
FGFR1	Y654	ARDIHHIDYyKKTTNGR	P11362
FGFR1	Y730	KPSNCTNELyMMMRDCW	P11362
FGFR1	Y766	IVALTSNQEyLDLSMPL	P11362
FGFR2	Y466	TPMLAGVSEyELPEDPK	P21802
FGFR2	Y586	RARRPPGMEySYDINRV	P21802
FGFR2	Y588	RRPPGMEYSyDINRVPE	P21802
FGFR3	Y577	RARRPPGLDySFDTCKP	P22607
FGFR3	Y599	TFKDLVSCAyQVARGME	P22607
FGFR3	Y647	LARDVHNLDyYKKTTNG	P22607
FGFR3	Y648	ARDVHNLDYyKKTTNGR	P22607
FGFR3	Y724	KPANCTHDLyMIMRECW	P22607
FGFR3	Y760	VLTVTSTDEyLDLSAPF	P22607
FGFR3	Y770	LDLSAPFEQySPGGQDT	P22607
FLT1	Y794	RSSSEIKTDyLSIIMDP	P17948
FLT1	Y1048	CDFGLARDIyKNPDYVR	P17948
FLT1	Y1053	ARDIYKNPDyVRKGDTR	P17948
FLT1	Y1169	ANVQQDGKDyIPINAIL	P17948
FLT1	Y1213	NSGSSDDVRyVNAFKFM	P17948
FLT1	Y1242	PNATSMFDDyQGDSSTL	P17948
FLT1	Y1327	IACCSPPPDyNSVVLYS	P17948
FLT1	Y1333	PPDYNSVVLySTPPI--	P17948
FLT3	Y572	CHKYKKQFRyESQLQMV	P36888
FLT3	Y589	LDLSAPFEQySPGGQDT	P36888
FLT3	Y591	QVTGSSDNEyFYVDFRE	P36888

Table 2.1 RTK Phosphopeptides (Continued)

FLT3	Y597	EYFYVDFREyEYDLKWE	P36888
FLT3	Y599	FYVDFREYEyDLKWEFP	P36888
FLT3	Y726	IFKEHNFSFyPTFQSHP	P36888
FLT3	Y768	SFHSEDEIEyENQKRLE	P36888
FLT3	Y842	ARDIMSDSNyVVRGNAR	P36888
FLT3	Y955	QLADAEEAMyQNVDGRV	P36888
FLT3	Y969	GRVSECPHTyQNRRPFS	P36888
FLT4	Y830	PAHADIKTGyLSIIMDP	P35916
FLT4	Y833	EVPLEEQCEyLSYDASQ	P35916
FLT4	Y853	LEEQCEYLSyDASQWEF	P35916
FLT4	Y1063	CDFGLARDIyKDPDYVR	P35916
FLT4	Y1068	ARDIYKDPDyVRKGSAR	P35916
FLT4	Y1333	RGARGGQVFyNSEYGEL	P35916
FLT4	Y1337	GGQVFYNSEyGELSEPS	P35916
IGF1R	Y973	NSRLGNGVLyASVNPEY	P08069
IGF1R	Y980	VLYASVNPEyFSAADVY	P08069
IGF1R	Y1161	GDFGMTRDIyETDYYRK	P08069
IGF1R	Y1165	MTRDIYETDyYRKGGKG	P08069
IGF1R	Y1166	TRDIYETDYyRKGGKGL	P08069
IGF1R	Y1280	EPGFREVSFyYSEENKL	P08069
IGF1R	Y1281	PGFREVSFYySEENKLP	P08069
IGF1R	Y1346	RASFDERQPyAHMNGGR	P08069
INSR	Y992	QPDGPLGPLyASSNPEY	P06213
INSR	Y999	PLYASSNPEyLSASDVF	P06213
INSR	Y1011	ASDVFPCSVyVPDEWEV	P06213
INSR	Y1149	AAEIADGMAyLNAKKFV	P06213
INSR	Y1185	GDFGMTRDIyETDYYRK	P06213
INSR	Y1189	MTRDIYETDyYRKGGKG	P06213
INSR	Y1190	TRDIYETDYyRKGGKGL	P06213
INSR	Y1355	GSSLGFKRSyEEHIPYT	P06213
INSR	Y1361	KRSYEEHIPyTHMNGGK	P06213
KDR	Y801	ANGGELKTGyLSIVMDP	P35968
KDR	Y951	GARFRQGKDyVGAIPVD	P35968
KDR	Y996	EEEEAPEDLyKDFLTLE	P35968
KDR	Y1054	CDFGLARDIyKDPDYVR	P35968
KDR	Y1059	ARDIYKDPDyVRKGDAR	P35968
KDR	Y1175	ANAQQDGKDyIVLPISE	P35968

Table 2.1 RTK Phosphopeptides (Continued)

KDR	Y1214	EEVCDPKFHyDNTAGIS	P35968
KIT	Y553	TYKYLQKPMyEVQWKVV	P10721
KIT	Y568	VVEEINGNNyVYIDPTQ	P10721
KIT	Y570	EEINGNNYVyIDPTQLP	P10721
KIT	Y703	QEDHAEAALyKNLLHSK	P10721
KIT	Y721	SSCSDSTNEyMDMKPGV	P10721
KIT	Y730	YMDMKPGVSyVVPTKAD	P10721
KIT	Y823	ARDIKNDSNyVVKGNAR	P10721
KIT	Y900	SPEHAPAEMyDIMKTCW	P10721
KIT	Y936	QISESTNHIySNLANCS	P10721
MERTK	Y749	ADFGLSKKIySGDYYRQ	Q12866
MERTK	Y753	LSKKIYSGDyYRQGRIA	Q12866
MERTK	Y754	SKKIYSGDYyRQGRIAK	Q12866
MERTK	Y929	HDSKPHEGRyILNGGSE	Q12866
MET	Y1003	EMVSNESVDyRATFPED	P08581
MET	Y1093	IGRGHFGCVyHGTLLDN	P08581
MET	Y1230	ADFGLARDMyDKEYYSV	P08581
MET	Y1234	LARDMYDKEyYSVHNKT	P08581
MET	Y1235	ARDMYDKEYySVHNKTG	P08581
MET	Y1313	QPEYCPDPLyEVMLKCW	P08581
MET	Y1349	IFSTFIGEHyVHVNATY	P08581
MET	Y1356	EHYVHVNATyVNVKCVA	P08581
MET	Y1365	YVNVKCVAPyPSLLSSE	P08581
MST1R	Y1017	LPILYSGSDyRSGLALP	Q04912
MST1R	Y1238	LARDILDREyYSVQQHR	Q04912
MST1R	Y1239	ARDILDREYySVQQHRH	Q04912
MST1R	Y1317	QPEYCPDSLyQVMQQCW	Q04912
MST1R	Y1353	IVSALLGDHyVQLPATY	Q04912
MST1R	Y1360	DHYVQLPATyMNLGPST	Q04912
NTRK1	Y496	QGHIIENPQyFSDACVH	P04629
NTRK1	Y676	GDFGMSRDIySTDYYRV	P04629
NTRK1	Y680	MSRDIYSTDyYRVGGRT	P04629
NTRK1	Y681	SRDIYSTDYyRVGGRTM	P04629
NTRK1	Y757	RPRACPPEVyAIMRGCW	P04629
NTRK1	Y791	QALAQAPPVyLDVLG--	P04629
NTRK2	Y516	KIPVIENPQyFGITNSQ	Q16620
NTRK2	Y702	GDFGMSRDVySTDYYRV	Q16620

Table 2.1 RTK Phosphopeptides (Continued)

NTRK2	Y706	MSRDVYSTDyYRVGGHT	Q16620
NTRK2	Y707	SRDVYSTDYyRVGGHTM	Q16620
NTRK2	Y817	QNLAKASPVyLDILG--	Q16620
NTRK3	Y516	RIPVIENPQyFRQGHNC	Q16288
NTRK3	Y705	GDFGMSRDVySTDYYRV	Q16288
NTRK3	Y709	MSRDVYSTDyYRVGGHT	Q16288
NTRK3	Y710	SRDVYSTDYyRVGGHTM	Q16288
PDGFRA	Y572	ESISPDGHEyIYVDPMQ	P16234
PDGFRA	Y574	ISPDGHEYIyVDPMQLP	P16234
PDGFRA	Y613	FGKVVEGTAyGLSRSQP	P16234
PDGFRA	Y731	ILSFENNGDyMDMKQAD	P16234
PDGFRA	Y742	DMKQADTTQyVPMLERK	P16234
PDGFRA	Y754	MLERKEVSKySDIQRSL	P16234
PDGFRA	Y768	RSLYDRPASyKKKSMLD	P16234
PDGFRA	Y849	ARDIMHDSNyVSKGSTF	P16234
PDGFRA	Y944	SEPEKRPSFyHLSEIVE	P16234
PDGFRA	Y958	IVENLLPGQyKKSYEKI	P16234
PDGFRA	Y962	LLPGQYKKSyEKIHLDF	P16234
PDGFRA	Y988	RMRVDSDNAyIGVTYKN	P16234
PDGFRA	Y1018	EQRLSADSGyIIPLPDI	P16234
PDGFRB	Y562	IMLWQKKPRyEIRWKVI	P09619
PDGFRB	Y579	ESVSSDGHEyIYVDPMQ	P09619
PDGFRB	Y581	VSSDGHEYIyVDPMQLP	P09619
PDGFRB	Y740	SLTGESDGGyMDMSKDE	P09619
PDGFRB	Y751	DMSKDESVDyVPMLDMK	P09619
PDGFRB	Y763	MLDMKGDVKyADIESSN	P09619
PDGFRB	Y771	KYADIESSNyMAPYDNY	P09619
PDGFRB	Y775	IESSNYMAPyDNYVPSA	P09619
PDGFRB	Y778	SNYMAPYDNyVPSAPER	P09619
PDGFRB	Y857	ARDIMRDSNyISKGSTF	P09619
PDGFRB	Y934	QPAHASDEIyEIMQKCW	P09619
PDGFRB	Y970	LLGEGYKKKyQQVDEEF	P09619
PDGFRB	Y1009	SPLDTSSVLyTAVQPNE	P09619
PDGFRB	Y1021	VQPNEGDNDyIIPLPDP	P09619
RET	Y687	RPAQAFPVSySSSGARR	P07949
RET	Y752	AFHLKGRAGyTTVAVKM	P07949
RET	Y791	VNHPHVIKLyGACSQDG	P07949

Table 2.1 RTK Phosphopeptides (Continued)

RET	Y806	DGPLLLIVEyAKYGSLR	P07949
RET	Y826	RESRKVGPGyLGSGGSR	P07949
RET	Y864	AWQISQGMQyLAEMKLV	P07949
RET	Y900	SDFGLSRDVyEEDSYVK	P07949
RET	Y905	SRDVYEEDSyVKRSQGR	P07949
RET	Y928	AIESLFDHIyTTQSDVW	P07949
RET	Y952	EIVTLGGNPyPGIPPER	P07949
RET	Y981	RPDNCSEEMyRLMLQCW	P07949
RET	Y1015	EKMMVKRRDyLDLAAST	P07949
RET	Y1029	ASTPSDSLIyDDGLSEE	P07949
RET	Y1062	PSTWIENKLyGMSDPNW	P07949
RET	Y1090	DGTNTGFPRyPNDSVYA	P07949
RET	Y1096	FPRYPNDSVyANWMLSP	P07949
ROR1	Y786	PVSNLSNPRyPNYMFPS	Q01973
ROR1	Y789	NLSNPRYPNyMFPSQGI	Q01973
ROR1	Y828	INGYPIPPGyAAFPAAH	Q01973
ROR1	Y836	GYAAFPAAHyQPTGPPR	Q01973
ROS1	Y1923	AGVGLANACyAIHTLPT	P08922
ROS1	Y2110	GDFGLARDIyKNDYYRK	P08922
ROS1	Y2114	LARDIYKNDyYRKRGEG	P08922
ROS1	Y2115	ARDIYKNDYyRKRGEGL	P08922
ROS1	Y2274	ETKNREGLNyMVLATEC	P08922
ROS1	Y2323	DFCQEKQVAyCPSGKPE	P08922
ROS1	Y2334	PSGKPEGLNyACLTHSG	P08922
ROS1	Y2342	NYACLTHSGyGDGSD--	P08922
TEK	Y992	FGLSRGQEVyVKKTMGR	Q02763
TEK	Y1048	YCGMTCAELyEKLPQGY	Q02763
TEK	Y1102	NRMLEERKTyVNTTLYE	Q02763
TEK	Y1108	RKTYVNTTLyEKFTYAG	Q02763
TEK	Y1113	NTTLYEKFTyAGIDCSA	Q02763
TYRO3	Y681	ADFGLSRKIySGDYYRQ	Q06418
TYRO3	Y685	LSRKIYSGDyYRQGCAS	Q06418
TYRO3	Y686	SRKIYSGDYyRQGCASK	Q06418
TYRO3	Y828	LELPGRDQPySGAGDGS	Q06418

Part 3: Systematic Investigation of Adaptor-Adaptor Interactions

3.1 Introduction

Focusing only on the initial recruitment of adaptors to RTKs provides an incomplete view of the full complexity of early RTK signaling. Adaptors can themselves become tyrosine phosphorylated and interact with each other, forming multi-protein complexes at the receptor. By systematically probing our SH2/PTB domain microarrays with phosphopeptides derived from 334 known pTyr sites on adaptor proteins, we identified a dense network of interactions among the adaptor proteins themselves (Fig. 3.1A and Table 6.2 in the appendix). For example, the well-studied tyrosine kinase ABL1, which is responsible for driving the development of chronic myeloid leukemia when fused with the protein BCR, is currently annotated to mediate 15 interactions through its SH2 domain (Colicelli 2010). In our study, we identified 53 biochemical binding partners (Figure 3.1B), including known interactions with DAB1, ERBB2, PTK2 and SHC1 (Colicelli 2010). Our data may also resolve some outstanding questions in the field. For example, it has previously been reported that the Vav1 SH2 domain binds to a phosphorylation site on BCR/ABL and that this interaction is critical for activation of Rac-1 and BCR/ABL-mediated leukemogenesis. Previous attempts to identify the site of binding by constructing a series of Tyr to Phe mutants, focusing in particular on the Vav1 consensus binding motif, were unsuccessful (Bassermann et al. 2002). Our data reveal an interaction between Vav1 and pTyr917 of BCR/ABL (Uniprot id: A9UF07), which was not included in the earlier mutagenesis experiments.

RTK-mediated activation of the MAPK pathway is well studied (Tidyman and Rauen 2009; McKay and Morrison 2007), but we nevertheless find many new interactions that impinge on this pathway. RTKs vary in their ability to recruit early signaling proteins in this pathway,

such as SHC1, GRB2, and PTPN11. Here, we find that these adaptors have the potential to interact with many other signaling proteins as well, increasing the complexity of MAPK pathway activation (Fig. 3.1 D). This view aligns well with the idea that RTKs function not as discrete molecular machines, as typically depicted, but as pleomorphic ensembles that are highly complex and dynamic with many rapidly interchanging states (Mayer, Blinov, and Loew 2009; Kleiman et al. 2011).

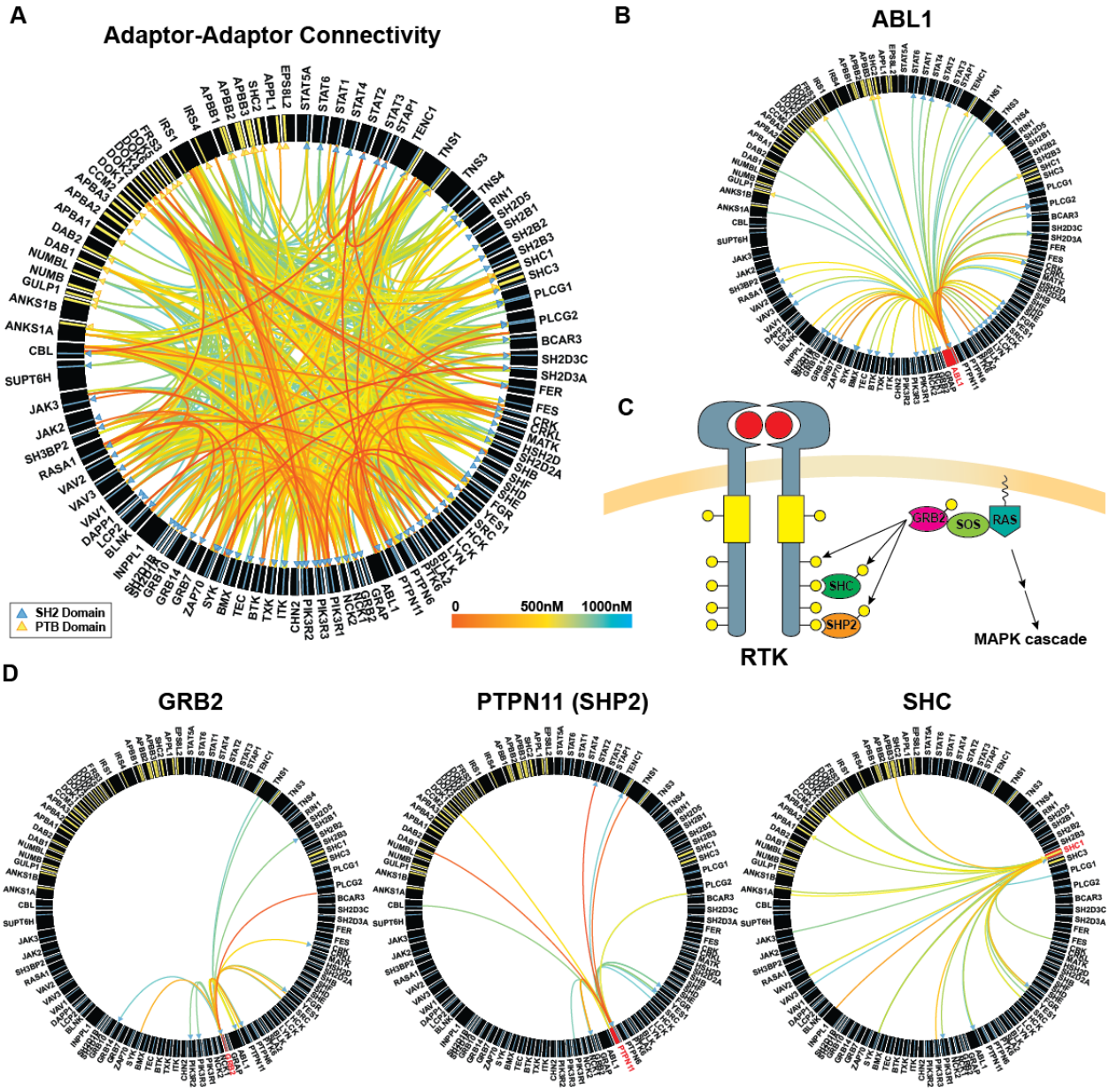

Figure 3.1: Adaptors are densely interconnected. (**A**) Adaptor proteins displayed in a circle with the size of the band corresponding to protein length (Krzywinski et al. 2009). Lines begin at sites of tyrosine phosphorylation and terminate in either a yellow triangle corresponding to a PTB domain or a blue triangle corresponding to an SH2 domain and are color coded according to affinity. (**B**) Visualization of the binding partners of ABL1 SH2 domain (in-links) and phosphorylation sites of ABL1 (out-links). (**C**) RTK activation of the MAPK cascade is a varied process that integrates binding of GRB2 to SHC1 and SHP2 as well as to the RTK. (**D**) The combinatorial complexity of RTK activation of MAPK is liable to be even greater as GRB2, SHC1 and PTPN11 (SHP2) are also capable of binding other adaptors, as can be seen by the diagrams, as well as other RTKs (not visualized).

3.2 Oncogenic adaptors are highly connected

To probe the relationship between connectivity and oncogenicity in the adaptor-adaptor layer of binding, we organized domains by sequence similarity (Fig. 3.2A) (Letunic and Bork 2011). The blue bars indicate how many peptides bind to each domain (in-links) and the green bars show how many binding partners interact with phosphorylation sites on the corresponding protein (out-links). Simple inspection reveals a wide range of binding promiscuity within the SH2 and PTB domain families. For example, proteins in the SRC, HCK, and PI3K N-terminal families of domains have relatively high numbers of binding partners and are frequently annotated as oncogenes. When we sort the domains by the number of in-links and out-links, from least to most connected, it is clear that oncogenic proteins (red) are preferentially enriched among proteins with high in-connectivity (median 20 vs. 8 in-links, Mann-Whitney U test $p= 3.4x10^{-3}$), high out-connectivity (median 9 vs. 1 out-links, Mann-Whitney U test $p=1.0x10^{-4}$), or both (Fig. 4B). Because the adaptors are likely to amplify signals downstream of RTKs, especially those without intrinsic catalytic activity themselves, we used an expanded definition of oncogene that incorporates additional cancer gene lists as well as the Sanger list (see Methods).

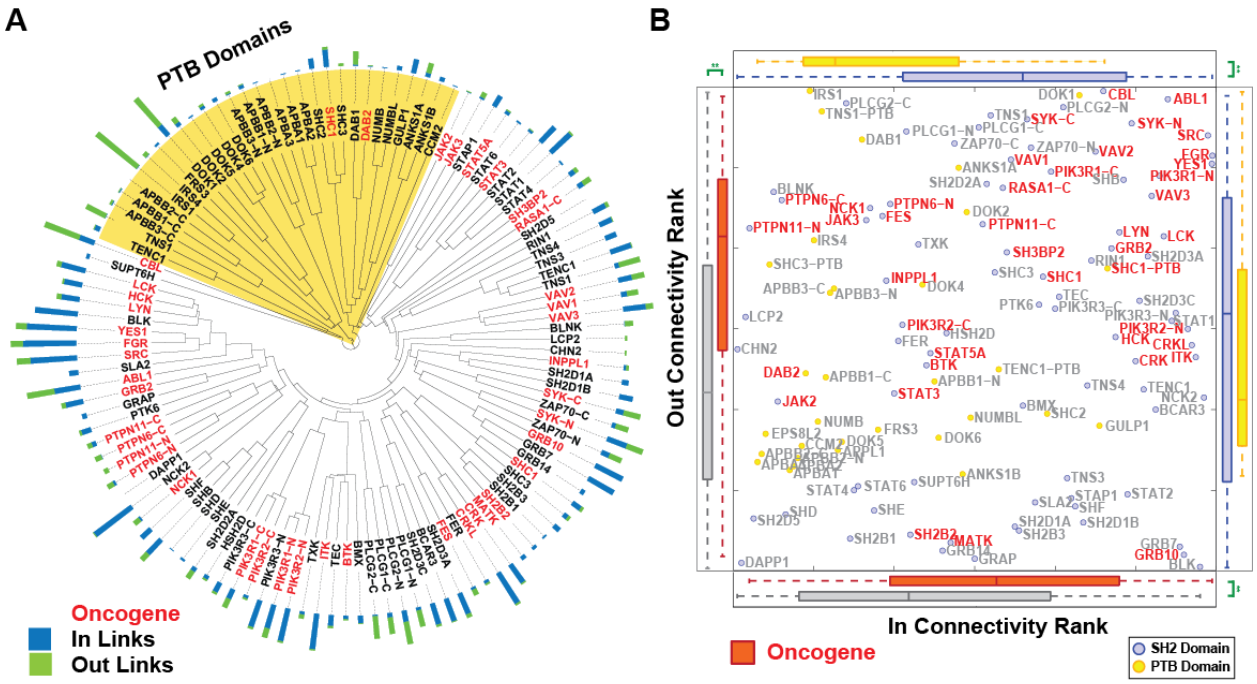

Figure 3.2: Oncogenic adaptors are more highly promiscuous. (**A**) Phylogeny of adaptors shows that genetically related domains share similar binding profiles. For example the SRC class (SRC, YES1, FGR) of tyrosine kinases all show a large number of in-links. This can be due to sequence determinants of selectivity as well as the bias in the phosphoproteome to sequences that interact with the domain family. (**B**) Adaptors sorted according to the number of peptides with which they interact (in-links; the X axis) and the number of adaptors that interact with them (out-links; Y axis). Oncogenic adaptors have both higher median in-links (20 vs. 8, Mann-Whitney U test $p= 3.4x10^{-3}$) and out-links (9 vs. 1, Mann-Whitney U test $p=1.0x10^{-4}$) than non-oncogenic adaptors. SH2 domains bind a higher median number of peptides (15.5 vs. 2, Mann-Whitney U test $p=1.7x10^{-6}$) but share a similar number of out-links (Mann-Whitney U Test $p>0.01$).

The quantitative interaction data generated in this study should prove generally useful in the fields of network modeling (Chen et al. 2009) and interaction prediction (Miller et al. 2008). With the caveat that our data necessarily include false positives and false negatives, we also hope that the novel interactions identified in these studies will aid efforts to uncover signaling pathways downstream of RTKs.

Our work shows that the genes whose mutation or overexpression drives cancer tend to be highly connected hubs. Moreover, the most highly connected proteins in our networks are the primary targets of anti-cancer drugs (e.g., erlotonib for EGFR (Raymond, Faivre, and Armand 2000), lapatanib for ERBB2 (Burris et al. 2005), vandetanib for RET (Degrauwe et al. 2012), sunitinib for KIT (Demetri et al. 14), and imatanib for ABL1 (Druker et al. 2001)). Analogously, viral proteins preferentially target hub proteins during infection (Calderwood et al. 2007; Shapira et al. 2009). This combined evidence suggests that disease states arise preferentially from the perturbation of network hubs and drugs should target these same hub proteins.

In conclusion, we have generated a systematic map covering a substantial fraction of the potential interactions between SH2 or PTB domains and sites of tyrosine phosphorylation on RTKs and adaptor proteins. These interactions are very poorly represented in existing unbiased human interactomes (Rual et al. 2005; Venkatesan et al. 2009) despite extensive evidence that they play essential roles in signal transduction. We observe a high degree of connectivity among RTKs and adaptor proteins, and among adaptor proteins themselves. This is in contrast to the usual depiction of receptor-proximal signaling as a series of linear pathways connecting sites of tyrosine phosphorylation on RTKs to a few adaptor proteins and then to a few core signaling molecules such as ERK and AKT. Of course, the actual complexity of the resulting network in

any particular cell type depends not only on the affinities of the interactions, as determined here, but also on the relative abundance of RTKs and SH2/PTB-containing proteins. mRNA sequencing data of 1430 diverse tumor types collected by the TCGA consortium shows that they express a median of 78% of the phosphotyrosine signaling proteins analyzed in this study. In fact, over half of these proteins are expressed ubiquitously (in >95% of the tumor samples; Figure 3.3). Thus, it is highly likely that receptor and adaptor proteins combine to form a highly interconnected mesh with the potential to perform complex signal processing functions.

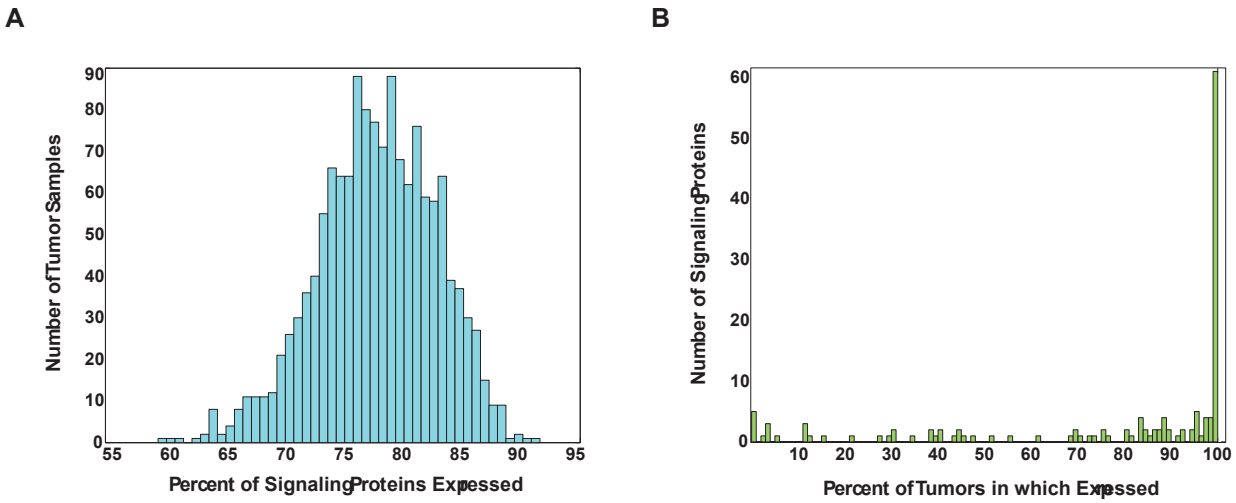

Figure 3.3 Tumors Widely Express RTKs and adaptors. (A) Tumor expression data of 1437 tumors from breast cancer, colon and rectal adenocarcinoma, and clear cell kidney cancer collected by The Cancer Genome Atlas Network was analyzed for RTK and adaptor protein expression. Tumors express a median of 78% of the phosphotyrosine signaling proteins. (B) Expression of signaling proteins varies widely with 52% of phosphotyrosine signaling proteins are expressed nearly ubiquitously (>95%) of tumors and other proteins having more restricted expression.

3.3 Materials and methods

The protocols for this chapter are identical to those of Part 2, except where described below.

3.3.1 Determining onocogene status

Since many SH2/PTB domain-containing proteins have no catalytic activity of their own, they serve principally to amplify and propagate signals from upstream proteins, a less stringent criterion for oncogene assignment was used. For this reason, adaptors were assigned as having a role in cancer by their presence in a union of the Sanger list and other cancer gene lists (Huret et al. 2000; Sjöblom et al. 2006; Akagi et al. 2004) compiled by the Bushman lab (http://microb230.med.upenn.edu/links/genelist).

3.3.2 RTK and adaptor expression in tumor samples

cBio Cancer Genomics Data Server Matlab Toolbox v1.04 was used to retrieve mRNA sequencing data corresponding to 1437 tumors from breast cancer, colon and rectal adenocarcinoma (T. C. G. A. Network 2012) and clear cell kidney cancer collected by The Cancer Genome Atlas Network. We used a 1 read per kilobase of exon model per million mapped reads (RPKM) threshold to separate genes that are expressed. This threshold has been shown to correspond to 1 transcript per C2C12 cell (Mortazavi et al. 2008) and optimizes overlap with mass spectrometry results in HeLa cells (Nagaraj et al. 2011). We consider this to be an upper bound estimate to the total number of potential interaction partners.

3.3.3 Adaptor Phosphopeptides

Table 3.1 Adaptor Phosphopeptides

Gene	Uniprot	pTyr	Peptide Sequence
ABL1	P00519	Y89	NDPNLFVALyDFVASGD
ABL1	P00519	Y134	NGQGWVPSNyITPVNSL
ABL1	P00519	Y191	ISLRYEGRVyHYRINTA
ABL1	P00519	Y204	INTASDGKLyVSSESRF
ABL1	P00519	Y234	ADGLITTLHyPAPKRNK
ABL1	P00519	Y245	APKRNKPTVyGVSPNYD
ABL1	P00519	Y251	PTVYGVSPNyDKWEMER
ABL1	P00519	Y272	MKHKLGGGQyGEVYEGV
ABL1	P00519	Y276	LGGGQYGEVyEGVWKKY
ABL1	P00519	Y283	EVYEGVWKKySLTVAVK
ABL1	P00519	Y412	LSRLMTGDTyTAHAGAK
ABL1	P00519	Y488	RPEGCPEKVyELMRACW
ABL2	P42684	Y161	NGQGWVPSNyITPVNSL
ABL2	P42684	Y231	INTTADGKVyVTAESRF
ABL2	P42684	Y261	ADGLVTTLHyPAPKCNK
ABL2	P42684	Y272	APKCNKPTVyGVSPIHD
ABL2	P42684	Y303	LGGGQYGEVyVGVWKKY
ABL2	P42684	Y515	QPEGCPPKVyELMRACW
ABL2	P42684	Y568	AASSSSVVPyLPRLPIL
ABL2	P42684	Y683	EMENQPHKKyELTGNFS
ABL2	P42684	Y718	EANLVPPKCyGGSFAQR
ANKS1A	Q92625	Y454	AAREEDEHPyELLLTAE
ANKS1A	Q92625	Y833	IIASLADRPyEEPPQKP
APBB1	O00213	Y547	ELVQKFQVYyLGNVPVA
APBB3	O95704	Y291	DAVSQAAQKyEALYMGT
BCAR3	O75815	Y42	PLAEHRPDAyQDVSIHG
BCAR3	O75815	Y117	PHLLDPTVEyVKFSKER
BCAR3	O75815	Y266	VPLRCLEEHyGTSPGQA
BCAR3	O75815	Y429	SAWLNSEANyCELNPAF
BLNK	Q8WV28	Y72	QWSDDFDSDyENPDEHS
BLNK	Q8WV28	Y84	PDEHSDSEMyVMPAEEN
BLNK	Q8WV28	Y96	PAEENADDSyEPPPVEQ
BLNK	Q8WV28	Y178	KGLLEDEADyVVPVEDN
BLNK	Q8WV28	Y189	VPVEDNDENyIHPTESS

Table 3.1 Adaptor Phosphopeptides (Continued)

BMX	P51813	Y40	FVLTKTNLSyYEYDKMK
BMX	P51813	Y216	PSSSTSLAQyDSNSKKI
BMX	P51813	Y224	QYDSNSKKIyGSQPNFN
BMX	P51813	Y566	MTRYVLDDQyVSSVGTK
BTK	Q06187	Y223	SELKKVVALyDYMPMNA
BTK	Q06187	Y225	LKKVVALYDyMPMNAND
BTK	Q06187	Y361	FSTIPELINyHQHNSAG
BTK	Q06187	Y375	SAGLISRLKyPVSQQNK
BTK	Q06187	Y511	CKDVCEAMEyLESKQFL
BTK	Q06187	Y551	LSRYVLDDEyTSSVGSK
CBL	P22681	Y337	LIDGFREGFyLFPDGRN
CBL	P22681	Y368	DHIKVTQEQyELYCEMG
CBL	P22681	Y371	KVTQEQYELyCEMGSTF
CBL	P22681	Y455	GAEGAPSPNyDDDDDER
CBL	P22681	Y552	PPPPPPDRPySVGAESR
CBL	P22681	Y674	KPSSSANAIySLAARPL
CBL	P22681	Y700	QCEGEEDTEyMTPSSRP
CBL	P22681	Y731	CDQQIDSCTyEAMYNIQ
CBL	P22681	Y774	EESENEDDGyDVPKPPV
CBLB	Q13191	Y363	KVTQEQYELyCEMGSTF
CBLB	Q13191	Y709	DPVEEDDDEyKIPSSHP
CBLB	Q13191	Y889	VKTNRTSQDyDQLPSCS
CBLC	Q9ULV8	Y144	LHALFPGGKyCGHMYQL
CHN2	P52757	Y21	SSVSSDAEEyQPPIWKS
CHN2	P52757	Y153	ISKMTTNPIyEHIGYAT
CHN2	P52757	Y158	TNPIYEHIGyATLLREK
CHN2	P52757	Y1087	PLLSSQRRSyAFETQAN
CRK	P46108	Y108	ALLEFYKIHyLDTTTLI
CRK	P46108	Y136	VILRQEEAEyVRALFDF
CRK	P46108	Y190	MIPVPYVEKyRPASASV
CRK	P46108	Y221	PLGGPEPGPyAQPSVNT
CRK	P46108	Y251	VIQKRVPNAyDKTALAL
CRKL	P46109	Y127	LPTAEDNLEyVRTLYDF
CRKL	P46109	Y132	DNLEYVRTLyDFPGNDA
CRKL	P46109	Y198	KHGNRNSNSyGIPEPAH
CRKL	P46109	Y207	YGIPEPAHAyAQPQTTT
CRKL	P46109	Y251	AIQKRVPCAyDKTALAL

Table 3.1 Adaptor Phosphopeptides (Continued)

CSK	P41240	Y184	GTVAAQDEFyRSGWALN
CSK	P41240	Y263	VIVEEKGGLyIVTEYMA
CTNNB1	P35222	Y30	AVSHWQQQSyLDSGIHS
CTNNB1	P35222	Y64	EDVDTSQVLyEWEQGFS
CTNNB1	P35222	Y86	EQVADIDGQyAMTRAQR
CTNNB1	P35222	Y142	KHAVVNLINyQDDAELA
CTNNB1	P35222	Y331	QALVNIMRTyTYEKLLW
CTNNB1	P35222	Y333	LVNIMRTYTyEKLLWTT
CTNNB1	P35222	Y489	MAQNAVRLHyGLPVVVK
CTNNB1	P35222	Y654	HSRNEGVATyAAAVLFR
CTNNB1	P35222	Y670	RMSEDKPQDyKKRLSVE
CTNNB1	P35222	Y716	LGYRQDDPSyRSFHSGG
DAB1	O75553	Y198	LEEDVEDPVyQYIVFEA
DAB1	O75553	Y220	RDPETEENIyQVPTSQK
DAB1	O75553	Y232	PTSQKKEGVyDVPKSQP
DAB2	P98082	Y170	DLKDLFQVIyNVKKKEE
DAB2	P98082	Y342	NGPLNGDVDyFGQQFDQ
DOK1	Q99704	Y146	ALEMLENSLySPTWEGS
DOK1	Q99704	Y203	ILEPLLSWPyTLLRRYG
DOK1	Q99704	Y296	ELLDSPPALyAEPLDSL
DOK1	Q99704	Y315	APCPSQDSLySDPLDST
DOK1	Q99704	Y337	EGVQRKKPLyWDLYEHA
DOK1	Q99704	Y341	RKKPLYWDLyEHAQQQL
DOK1	Q99704	Y362	LTDPKEDPIyDEPEGLA
DOK1	Q99704	Y377	LAPVPPQGLyDLPREPK
DOK1	Q99704	Y398	CQARVKEEGyELPYNPA
DOK1	Q99704	Y402	VKEEGYELPyNPATDDY
DOK1	Q99704	Y409	LPYNPATDDyAVPPPRS
DOK1	Q99704	Y449	GIKSHNSALySQVQKSG
DOK2	O60496	Y139	RPCMEENELySSAVTVG
DOK2	O60496	Y271	ASLPRPDSPySRPHDSL
DOK2	O60496	Y299	PRPRGQEGEyAVPFDAV
DOK2	O60496	Y345	TLPPRPDHIyDEPEGVA
DOK3	Q7L591	Y208	LVPMEENSIySSWQEVG
DOK3	Q7L591	Y381	EPNDLASGLyASVCKRA
DOK3	Q7L591	Y432	SRSPTTSPIyHNGQDLS
DOK3	Q7L591	Y453	ANDSTLEAQyRRLLELD

Table 3.1 Adaptor Phosphopeptides (Continued)

DOK4	Q8TEW6	Y165	KLQITHENIyLWDIHNP
DOK4	Q8TEW6	Y255	RLLNKGTEHySYPCTPT
FER	P16591	Y229	KALKGIFDEySQITSLV
FER	P16591	Y402	GKEPPPVVNyEEDARSV
FER	P16591	Y615	LQEAKILKQyDHPNIVK
FER	P16591	Y714	MSRQEDGGVySSSGLKQ
FES	P07332	Y156	RDSAQAKRKyQEASKDK
FES	P07332	Y261	AARIQPEAEyQGFLRQY
FES	P07332	Y614	LQEARILKQySHPNIVR
FES	P07332	Y713	MSREEADGVyAASGGLR
FES	P07332	Y811	GQRPSFSTIyQELQSIR
FGR	P09769	Y28	AGLEGDFRSyGAADHYG
FGR	P09769	Y34	FRSYGAADHyGPDPTKA
FGR	P09769	Y180	RESETTKGAySLSIRDW
FGR	P09769	Y208	KIRKLDMGGyYITTRVQ
FGR	P09769	Y209	IRKLDMGGYyITTRVQF
FGR	P09769	Y412	LARLIKDDEyNPCQGSK
FGR	P09769	Y523	DYFTSAEPQyQPGDQT-
FRS2	Q8WU20	Y196	LVAEEQVHTyVNTTGVQ
FRS2	Q8WU20	Y306	DAPSVNKLVyENINGLS
FRS2	Q8WU20	Y349	AQRRTALLNyENLPSLP
FRS2	Q8WU20	Y392	HNNLDPMHNyVNTENVT
FRS2	Q8WU20	Y436	PSLEHRQLNyIQVDLEG
FYN	P06241	Y28	DGSLNQSSGyRYGTDPT
FYN	P06241	Y185	RESETTKGAySLSIRDW
FYN	P06241	Y213	KIRKLDNGGyYITTRAQ
FYN	P06241	Y214	IRKLDNGGYyITTRAQF
FYN	P06241	Y420	LARLIEDNEyTARQGAK
FYN	P06241	Y440	KWTAPEAALyGRFTIKS
FYN	P06241	Y531	DYFTATEPQyQPGENL-
GAB1	Q13480	Y242	NGFFQQQMIyDSPPSRA
GAB1	Q13480	Y259	PSASVDSSLyNLPRSYS
GAB1	Q13480	Y285	SSTEADGELyVFNTPSG
GAB1	Q13480	Y307	TQMRHVSISyDIPPTPG
GAB1	Q13480	Y317	DIPPTPGNTyQIPRTFP
GAB1	Q13480	Y373	RTASDTDSSyCIPTAGM
GAB1	Q13480	Y406	RKDASSQDCyDIPRAFP

Table 3.1 Adaptor Phosphopeptides (Continued)

GAB1	Q13480	Y447	VSSEELDENyVPMNPNS
GAB1	Q13480	Y472	FTEPIQEANyVPMTPGT
GAB2	Q9UQC2	Y643	SVTSDEKVDyVQVDKEK
GRAP2	O75791	Y45	KAELGSQEGyVPKNFID
GRB10	Q13322	Y67	DMNASLESLySACSMQS
GRB10	Q13322	Y404	RLLKYGMLLyQNYRIPQ
GRB2	P62993	Y209	GQTGMFPRNyVTPVNRN
GRB7	Q14451	Y107	ASRPHVVKVySEDGACR
HCK	P08631	Y127	RSLATRKEGyIPSNYVA
HCK	P08631	Y209	IRTLDNGGFyISPRSTF
HCK	P08631	Y411	LARVIEDNEyTAREGAK
HCK	P08631	Y515	YIQSVLDDFyTATESQY
HCK	P08631	Y522	DFYTATESQyQQQP---
HSH2D	Q96JZ2	Y265	GDPTSGDRGyTDPCVAT
INPPL1	O15357	Y671	RYERGSRDTyAWHKQKP
INPPL1	O15357	Y886	ERLGTRERLyEWISIDK
INPPL1	O15357	Y986	PKNSFNNPAyYVLEGVP
INPPL1	O15357	Y987	KNSFNNPAYyVLEGVPH
INPPL1	O15357	Y1135	MAKTLSEVDyAPAGPAR
INPPL1	O15357	Y1162	QPPRGLPSDyGRPLSFP
IRS1	P35568	Y46	EAGGPARLEyYENEKKW
IRS1	P35568	Y465	ARGEEELSNyICMGGKG
IRS1	P35568	Y612	SSTLHTDDGyMPMSPGV
IRS1	P35568	Y632	PSGRKGSGDyMPMSPKS
IRS1	P35568	Y662	HPQRVDPNGyMMMSPSG
IRS1	P35568	Y732	GKLLPCTGDyMNMSPVG
IRS1	P35568	Y896	PPEPKSPGEyVNIEFGS
IRS1	P35568	Y941	REEETGTEEyMKMDLGP
IRS1	P35568	Y989	RAVPSSRGDyMTMQMSC
IRS1	P35568	Y1179	AGGLENGLNyIDLDLVK
IRS1	P35568	Y1229	RRSSEDLSAyASISFQK
IRS2	Q9Y4H2	Y628	SSPKVAYHPyPEDYGDI
IRS2	Q9Y4H2	Y632	VAYHPYPEDyGDIEIGS
IRS2	Q9Y4H2	Y653	SSNLGADDGyMPMTPGA
IRS2	Q9Y4H2	Y675	GSGSCRSDDyMPMSPAS
IRS2	Q9Y4H2	Y823	YTCGGDSDQyVLMSSPV
IRS4	O14654	Y717	ATPLVSSSDyMPMAPQN

Table 3.1 Adaptor Phosphopeptides (Continued)

IRS4	O14654	Y743	RSPFEDSRGyMMMFPRV
IRS4	O14654	Y921	QREADSSSDyVNMDFTK
IRS4	O14654	Y1038	MALADSAIRyDAETGRI
ITK	Q08881	Y180	PEETVVIALyDYQTNDP
ITK	Q08881	Y512	MTRFVLDDQyTSSTGTK
JAK2	O60674	Y119	HNVLYRIRFyFPRWYCS
JAK2	O60674	Y221	KCIRAKIQDyHILTRKR
JAK2	O60674	Y570	KGVRREVGDyGQLHETE
JAK2	O60674	Y790	ANLINNCMDyEPDFRPS
JAK2	O60674	Y813	DLNSLFTPDyELLTEND
JAK2	O60674	Y931	RRNLKLIMEyLPYGSLR
JAK2	O60674	Y956	RIDHIKLLQyTSQICKG
JAK2	O60674	Y966	TSQICKGMEyLGTKRYI
JAK2	O60674	Y1007	TKVLPQDKEyYKVKEPG
JAK2	O60674	Y1008	KVLPQDKEYyKVKEPGE
JAK3	P52333	Y785	DLNSLISSDyELLSDPT
JAK3	P52333	Y904	RQSLRLVMEyLPSGCLR
JAK3	P52333	Y939	SSQICKGMEyLGSRRCV
JAK3	P52333	Y980	AKLLPLDKDyYVVREPG
JAK3	P52333	Y981	KLLPLDKDYyVVREPGQ
LCK	P06239	Y192	IRNLDNGGFyISPRITF
LCK	P06239	Y394	LARLIEDNEyTAREGAK
LCK	P06239	Y505	DFFTATEGQyQPQP---
LCP2	Q13094	Y113	GWSSFEEDDyESPNDDQ
LCP2	Q13094	Y128	DQDGEDDGDyESPNEEE
LCP2	Q13094	Y145	EAPVEDDADyEPPPSND
LCP2	Q13094	Y173	KPFPNSNSMyIDRPPSG
LYN	P07948	Y32	PVRNTERTIyVRDPTSN
LYN	P07948	Y117	KKEGFIPSNyVAKLNTL
LYN	P07948	Y193	KIRSLDNGGyYISPRIT
LYN	P07948	Y194	IRSLDNGGYyISPRITF
LYN	P07948	Y265	GQFGEVWMGyYNNSTKV
LYN	P07948	Y306	LQHDKLVRLyAVVTREE
LYN	P07948	Y316	AVVTREEPIyIITEYMA
LYN	P07948	Y397	LARVIEDNEyTAREGAK
LYN	P07948	Y460	DVMTALSQGyRMPRVEN
LYN	P07948	Y473	RVENCPDELyDIMKMCW

Table 3.1 Adaptor Phosphopeptides (Continued)

LYN	P07948	Y501	YLQSVLDDFyTATEGQY
LYN	P07948	Y508	DFYTATEGQyQQQP---
MAPRE1	Q15691	Y124	FDANYDGKDyDPVAARQ
NCK1	P16333	Y105	SFVDPGERLyDLNMPAY
NCK1	P16333	Y112	RLYDLNMPAyVKFNYMA
NCK1	P16333	Y268	LEPSPPQCDyIRPSLTG
NCK2	O43639	Y50	VRNAANRTGyVPSNYVE
NCK2	O43639	Y99	SPTPSTDAEyPANGSGA
NCK2	O43639	Y110	ANGSGADRIyDLNIPAF
PIK3C2B	O00750	Y228	QGRLLGSVDyDGINDAI
PIK3C2B	O00750	Y685	YGFAEPYNLySSLKELV
PIK3C2B	O00750	Y1056	KGIVPRDCSyFNSNAVP
PIK3C2G	O75747	Y419	IRKYDFHLKyLLKTQEN
PIK3C2G	O75747	Y1437	SVPLDKEKWyPLGNSII
PIK3CA	P42336	Y508	SVSREAGFSySHAGLSN
PIK3CB	P42338	Y246	KEDEVSPYDyVLQVSGR
PIK3CB	P42338	Y425	STKTINPSKyQTIRKAG
PIK3CB	P42338	Y772	NPCVILSELyVEKCKYM
PIK3CB	P42338	Y962	RERVPFILTyDFIHVIQ
PIK3CD	O00329	Y440	QLKTGERCLyMWPSVPD
PIK3CD	O00329	Y484	LPEVAPHPVyYPALEKI
PIK3CD	O00329	Y485	PEVAPHPVYyPALEKIL
PIK3CD	O00329	Y524	LERRGSGELyEHEKDLV
PIK3CD	O00329	Y936	RERVPFILTyDFVHVIQ
PIK3R1	P27986	Y368	DASTKMHGDyTLTLRKG
PIK3R1	P27986	Y452	EAVGKKLHEyNTQFQEK
PIK3R1	P27986	Y463	TQFQEKSREyDRLYEEY
PIK3R1	P27986	Y467	EKSREYDRLyEEYTRTS
PIK3R1	P27986	Y470	REYDRLYEEyTRTSQEI
PIK3R1	P27986	Y528	KEIQRIMHNyDKLKSRI
PIK3R1	P27986	Y556	EDLKKQAAEyREIDKRM
PIK3R1	P27986	Y580	IQLRKTRDQyLMWLTQK
PIK3R1	P27986	Y607	LGNENTEDQySLVEDDE
PIK3R1	P27986	Y699	YGFAEPYNLySSLKELV
PIK3R2	O00459	Y365	DASSKIQGEyTLTLRKG
PIK3R2	O00459	Y464	DKSREYDQLyEEYTRTS
PIK3R2	O00459	Y467	REYDQLYEEyTRTSQEL

Table 3.1 Adaptor Phosphopeptides (Continued)

PIK3R2	O00459	Y605	GIKNETEDQyALMEDED
PIK3R3	Q92569	Y195	SQYQEKSKEyDRLYEEY
PIK3R3	Q92569	Y199	EKSKEYDRLyEEYTRTS
PIK3R3	Q92569	Y202	KEYDRLYEEyTRTSQEI
PIK3R3	Q92569	Y341	IKNEDADENyFINEEDE
PLCG1	P19174	Y472	HKKLAEGSAyEEVPTSM
PLCG1	P19174	Y481	YEEVPTSMMySENDISN
PLCG1	P19174	Y771	EKIGTAEPDyGALYEGR
PLCG1	P19174	Y775	TAEPDYGALyEGRNPGF
PLCG1	P19174	Y783	LYEGRNPGFyVEANPMP
PLCG1	P19174	Y977	EKIGTERACyRDMSSFP
PLCG1	P19174	Y1253	AREGSFESRyQQPFEDF
PLCG2	P16885	Y733	SLYRKMRLRyPVTPELL
PLCG2	P16885	Y743	PVTPELLERyNMERDIN
PLCG2	P16885	Y753	NMERDINSLyDVSRMYV
PLCG2	P16885	Y759	NSLYDVSRMyVDPSEIN
PLCG2	P16885	Y780	QRTVKALYDyKAKRSDE
PLCG2	P16885	Y1197	PVLESEEELySSCRQLR
PLCG2	P16885	Y1217	EELNNQLFLyDTHQNLR
PLCG2	P16885	Y1245	SVNENQLQLyQEKCNKR
PTK2	Q05397	Y5	-----MAAAyLDPNLNH
PTK2	Q05397	Y148	EDKPTLNFFyQQVKSDY
PTK2	Q05397	Y155	FFYQQVKSDyMLEIADQ
PTK2	Q05397	Y397	AVSVSETDDyAEIIDEE
PTK2	Q05397	Y407	AEIIDEEDTyTMPSTRD
PTK2	Q05397	Y441	QFGDVHQGIyMSPENPA
PTK2	Q05397	Y570	KLGDFGLSRyMEDSTYY
PTK2	Q05397	Y576	LSRYMEDSTyYKASKGK
PTK2	Q05397	Y577	SRYMEDSTYyKASKGKL
PTK2	Q05397	Y720	APPKPSRPGyPSPRSSE
PTK2	Q05397	Y861	QGPIGNQHIyQPVGKPD
PTK2	Q05397	Y925	NLDRSNDKVyENVTGLV
PTK2	Q05397	Y1007	INKMKLAQQyVMTSLQQ
PTK2B	Q14289	Y402	ESCSIESDIyAEIPDET
PTK2B	Q14289	Y579	LSRYIEDEDyYKASVTR
PTK2B	Q14289	Y580	SRYIEDEDYyKASVTRL
PTK2B	Q14289	Y683	ELVCSLSDVyQMEKDIA

Table 3.1 Adaptor Phosphopeptides (Continued)

PTK2B	Q14289	Y699	AMEQERNARyRTPKILE
PTK2B	Q14289	Y722	PPPKPSRPKyRPPPQTN
PTK2B	Q14289	Y756	SPTLTSPMEyPSPVNSL
PTK2B	Q14289	Y819	KQQKQMVEDyQWLRQEE
PTK2B	Q14289	Y834	EEKSLDPMVyMNDKSPL
PTK2B	Q14289	Y849	PLTPEKEVGyLEFTGPP
PTK2B	Q14289	Y881	NLDRTDDLVyLNVMELV
PTK2B	Q14289	Y906	ELCQLPPEGyVVVVKNV
PTK6	Q13882	Y114	RVSEKPSADyVLSVRDT
PTK6	Q13882	Y342	LARLIKEDVyLSHDHNI
PTK6	Q13882	Y351	YLSHDHNIPyKWTAPEA
PTK6	Q13882	Y447	RERLSSFTSyENPT---
PTPN11	Q06124	Y62	HIKIQNTGDyYDLYGGE
PTPN11	Q06124	Y63	IKIQNTGDYyDLYGGEK
PTPN11	Q06124	Y279	RQENKNKNRyKNILPFD
PTPN11	Q06124	Y304	GDPNEPVSDyINANIIM
PTPN11	Q06124	Y546	QKSKRKGHEyTNIKYSL
PTPN11	Q06124	Y584	EMREDSARVyENVGLMQ
PTPN6	P29350	Y301	RDSNIPGSDyINANYIK
PTPN6	P29350	Y374	TREVGMQRAyGPYSVTN
PTPN6	P29350	Y377	VGMQRAYGPySVTNCGE
PTPN6	P29350	Y390	NCGEHDTTEyKLRTLQV
PTPN6	P29350	Y536	QSQKGQESEyGNITYPP
PTPN6	P29350	Y541	QESEYGNITyPPAMKNA
PTPN6	P29350	Y564	TSSKHKEDVyENLHTKN
RASA1	P20936	Y239	FRIIAMCGDyYIGGRRF
RASA1	P20936	Y460	NDTVDGKEIyNTIRRKT
RASA1	P20936	Y615	LPVKHFTNPyCNIYLNS
RIN1	Q13671	Y36	REKPAQDPLyDVPNASG
RIN1	Q13671	Y632	CFQHLLRVAyQDPSSGC
SH2B1	Q9NRF2	Y55	RLYLASHPQyAGPGAEA
SH2B3	Q9UQQ2	Y273	TRLEMPDNLyTFVLKVK
SH2D2A	Q9NP31	Y39	TRRSCQNLGyTAASPQA
SH2D2A	Q9NP31	Y216	SKSQDPNPQySPIIKQG
SH2D2A	Q9NP31	Y260	AKPQLPPEVyTIPVPRH
SH2D2A	Q9NP31	Y280	PRPKPSNPIyNEPDEPI
SH2D2A	Q9NP31	Y290	NEPDEPIAFyAMGRGSP

Table 3.1 Adaptor Phosphopeptides (Continued)

SH2D2A	Q9NP31	Y305	SPGEAPSNIyVEVEDEG
SH2D3A	Q9BRG2	Y16	GEDLAGQPWyHGLLSRQ
SH2D3A	Q9BRG2	Y95	PSIPALVHSyMTGRRPL
SH2D3A	Q9BRG2	Y231	PDASERPPTyCELVPRV
SH2D3C	Q8N5H7	Y183	AGEPEAGSDyVKFSKEK
SH2D3C	Q8N5H7	Y495	SYSDPDSGHyCQLQPPV
SH3BP2	P78314	Y174	SPYPTDNEDyEHDDEDD
SH3BP2	P78314	Y183	YEHDDEDDSyLEPDSPE
SH3BP2	P78314	Y448	TGGDDSDEDyEKVPLPN
SHB	Q15464	Y96	QKERDFEDPyNGPGSSL
SHB	Q15464	Y114	KLRAMCRLDyCGGSGEP
SHB	Q15464	Y246	KDKVTIADDySDPFDAK
SHB	Q15464	Y268	KAGKGESAGyMEPYEAQ
SHB	Q15464	Y272	GESAGYMEPyEAQRIMT
SHB	Q15464	Y297	RSQHKGIQLyDTPYEPE
SHB	Q15464	Y301	KGIQLYDTPyEPEGQSV
SHB	Q15464	Y336	QDDDRPADEyDQPWEWN
SHC1	P29353	Y349	EEEEPPDHQyYNDFPGK
SHC1	P29353	Y350	EEEPPDHQYyNDFPGKE
SHC1	P29353	Y427	GRELFDDPSyVNVQNLD
SHC3	Q92529	Y341	EEGDGSDHPyYNSIPSK
SHC3	Q92529	Y342	EGDGSDHPYyNSIPSKM
SHC3	Q92529	Y379	AQFAGKEQTyYQGRHLG
SHC3	Q92529	Y380	QFAGKEQTYyQGRHLGD
SHC3	Q92529	Y406	PLRQGSSDIySTPEGKL
SHC3	Q92529	Y424	DASSKIQGEyTLTLRKG
SOS1	Q07889	Y1065	LQQEPRKISySRIPESE
SRC	P12931	Y187	RESETTKGAyCLSVSDF
SRC	P12931	Y216	IRKLDSGGFyITSRTQF
SRC	P12931	Y338	YAVVSEEPIyIVTEYMS
SRC	P12931	Y419	LARLIEDNEyTARQGAK
SRC	P12931	Y438	KWTAPEAALyGRFTIKS
SRC	P12931	Y521	EYLQAFLEDyFTSTEPQ
SRC	P12931	Y530	DYFTSTEPQyQPGENL-
STAT1	P42224	Y203	QEQLLLKKMyLMLDNKR
STAT1	P42224	Y701	ELDGPKGTGyIKTELIS
STAT2	P52630	Y631	KVLIYSVQPyTKEVLQS

Table 3.1 Adaptor Phosphopeptides (Continued)

STAT2	P52630	Y690	KVNLQERRKyLKHRLIV
STAT3	P40763	Y539	EKLLGPGVNySGCQITW
STAT3	P40763	Y686	IPKEEAFGKyCRPESQE
STAT3	P40763	Y705	EADPGSAAPyLKTKFIC
STAT4	Q14765	Y355	LLIKLPELNyQVKVKAS
STAT4	Q14765	Y693	RPTERGDKGyVPSVFIP
STAT5A	P42229	Y90	FLLKIKLGHyATQLQKT
STAT5A	P42229	Y694	PVLAKAVDGyVKPQIKQ
STAT5B	P51692	Y90	FLLKIKLGHyATQLQNT
STAT5B	P51692	Y665	LADRLGDLNyLIYVFPD
STAT5B	P51692	Y679	FPDRPKDEVySKYYTPV
STAT5B	P51692	Y699	SATAKAVDGyVKPQIKQ
STAT5B	P51692	Y725	ADAGGGSATyMDQAPSP
STAT5B	P51692	Y740	SPAVCPQAHyNMYPQNP
STAT5B	P51692	Y743	VCPQAHYNMyPQNPDSV
STAT6	P42226	Y641	EQMGKDGRGyVPATIKM
SYK	P43405	Y74	TIERELNGTyAIAGGRT
SYK	P43405	Y203	IRARDNNGSyALCLLHE
SYK	P43405	Y244	DTLWQLVEHySYKADGL
SYK	P43405	Y296	GGIISRIKSySFPKPGH
SYK	P43405	Y323	QESTVSFNPyEPELAPW
SYK	P43405	Y348	EALPMDTEVyESPYADP
SYK	P43405	Y352	MDTEVYESPyADPEEIR
SYK	P43405	Y525	SKALRADENyYKAQTHG
SYK	P43405	Y526	KALRADENYyKAQTHGK
SYK	P43405	Y568	GVLMWEAFSyGQKPYRG
TEC	P42680	Y206	DLRLERGQEyLILEKND
TEC	P42680	Y228	ARDKYGNEGyIPSNYVT
TEC	P42680	Y519	MARYVLDDQyTSSSGAK
TENC1	Q63HR2	Y483	TRGPLDGSPyAQVQRPP
TNS1	Q9HBL0	Y168	QPSQRRYVHyFSGLLSG
TNS1	Q9HBL0	Y327	ENGPSVSVDyNTSDPLI
TNS1	Q9HBL0	Y339	SDPLIRWDSyDNFSGHR
TNS1	Q9HBL0	Y366	TQGPLDGSLyAKVKKKD
TNS1	Q9HBL0	Y609	WPQPVTTSHyAHDPSGM
TNS1	Q9HBL0	Y766	HPLTQSRSGyIPSGHSL
TNS1	Q9HBL0	Y796	VPPGRSYSPyDYQPCLA

Table 3.1 Adaptor Phosphopeptides (Continued)

TNS1	Q9HBL0	Y903	RRRAASDGQyENQSPEA
TNS1	Q9HBL0	Y1144	SPLPTVGSSySSPDYSL
TNS1	Q9HBL0	Y1149	VGSSYSSPDySLQHFSS
TNS1	Q9HBL0	Y1254	SLCRHPAGVyQVSGLHN
TNS1	Q9HBL0	Y1323	SPCLDRHVAyGGYSTPE
TNS1	Q9HBL0	Y1326	LDRHVAYGGySTPEDRR
TNS1	Q9HBL0	Y1345	LSRQSSASGyQAPSTPS
TNS1	Q9HBL0	Y1404	GDRAGSLPNyATINGKV
TNS1	Q9HBL0	Y1440	SHTLPDFSKySMPDNSP
TNS4	Q8IZW8	Y150	EESEALDIKyIEVTSAR
TNS4	Q8IZW8	Y284	SASPVSDVSyMFGSSQS
TXK	P42681	Y91	EEKIQVKALyDFLPREP
TXK	P42681	Y420	MTRYVLDDEyVSSFGAK
VAV1	P15498	Y142	EESVGDEDIySGLSDQI
VAV1	P15498	Y160	DTVEEDEDLyDCVENEE
VAV1	P15498	Y174	NEEAEGDEIyEDLMRSE
VAV1	P15498	Y280	IKYKERFLVyGRYCSQV
VAV1	P15498	Y791	KYFGTAKARyDFCARDR
VAV1	P15498	Y826	QQGWWRGEIyGRVGWFP
VAV2	P52735	Y142	ETTENDDDVyRSLEELA
VAV2	P52735	Y159	DEHDLGEDIyDCVPCED
VAV2	P52735	Y172	PCEDGGDDIyEDIIKVE
VAV3	Q9UKW4	Y173	YGEDEGGEVyEDLMKAE
YES1	P07947	Y32	EPVSTSVSHyGAEPTTV
YES1	P07947	Y194	RESETTKGAySLSIRDW
YES1	P07947	Y222	KIRKLDNGGyYITTRAQ
YES1	P07947	Y223	IRKLDNGGYyITTRAQF
YES1	P07947	Y426	LARLIEDNEyTARQGAK
YES1	P07947	Y446	KWTAPEAALyGRFTIKS
YES1	P07947	Y537	DYFTATEPQyQPGENL-
ZAP70	P43403	Y46	RQCLRSLGGyVLSLVHD
ZAP70	P43403	Y69	PIERQLNGTyAIAGGKA
ZAP70	P43403	Y126	CLRDAMVRDyVRQTWKL
ZAP70	P43403	Y164	TTAHERMPWyHSSLTRE
ZAP70	P43403	Y178	TREEAERKLySGAQTDG
ZAP70	P43403	Y248	LKLKADGLIyCLKEACP
ZAP70	P43403	Y292	RIDTLNSDGyTPEPARI

Table 3.1 Adaptor Phosphopeptides (Continued)

ZAP70	P43403	Y315	RPMPMDTSVyESPYSDP
ZAP70	P43403	Y319	MDTSVYESPySDPEELK
ZAP70	P43403	Y474	RNVLLVNRHyAKISDFG
ZAP70	P43403	Y492	SKALGADDSyYTARSAG
ZAP70	P43403	Y493	KALGADDSYyTARSAGK

Part 4: Modeling SH2 Domain Interactions

4.1 Introduction

High throughput approaches have led to an explosion of data on SH2 domain-mediated interactions. Despite this, there are two critical issues that limit their utility to biologists: completeness and accuracy. The continued discovery of new phosphorylation sites as well as mutations affecting these sites will ensure that an experimental dataset will be incomplete as soon as it is collected. Moreover, as is the limitation with all experimental approaches, the dataset will invariably contain false positive and false negatives. Further complicating the issue is that there is no confidence score associated with most interactions, meaning that large-scale datasets are potentially erroneous in unknown ways.

One can try to come to grips with these problems in an *ad hoc* manner. For example, if a researcher discovers a new phosphorylation site and is curious as to what it might interact with, they can find the closest peptide by sequence. However, two sequences might be very similar in regions that are irrelevant for SH2 domain recognition. To overcome this challenge the researcher will apply prior knowledge from crystal structures as to which residues make contact with the domain and are therefore likely to be of importance. To deal with the question of accuracy, one can also evaluate how similar a given interaction is to other related peptide-domain pairs in the dataset. If it is more similar to the binders, then it is more likely to be a true positive interaction. The utility of *ad hoc* mental models for the task of identifying new interactions is nevertheless limited and this has spurred the creation of computational predictive models (Table 4.1).

Table 4.1: Summary of predictive SH2 domain models. There are five models that have previously been developed to analyze SH2 domains. PSSM models have been the most popular in part because they are directly measured from experiment. All models use almost exclusively one data type to build the predictor.

Method Name	Model Type	Training Data	Reference
Scansite	PSSM	Peptide Library	(Obenauer, Cantley, and Yaffe 2003)
SMALI	PSSM	OPAL	(Huang et al. 2008)
DomPep	PSSM	OPAL	(Li et al. 2011)
NetPhorest	NN	Peptide Array	(Miller et al. 2008)
Wunderlich	AA-Potential	Domain Array	(Wunderlich and Mirny 2009)

The most common strategy, employed by the Scansite, SMALI and DomPep methods is to generate a position specific scoring matrix (PSSM). For the Scansite method, the underlying data are derived from a degenerate peptide library that is incubated with a target domain. The binding peptides are then isolated and sequenced by Edman degradation. In the oriented peptide library (OPAL) approach used by SMALI, a single residue is fixed at a given position. The peptides are synthesized on a membrane using the SPOTs method (Frank 2002) and incubated with a domain. Differences in spot intensity for the various mutants are used to infer peptide selectivity at a given position. Because of experimental uncertainty in the derived PSSMs, the same group that developed SMALI also derived an approach, termed DomPep, that would average similar PSSMs from sequence-related domains and find improvements in performance (Li et al. 2011).

NetPhorest incorporates the PSSMs of SMALI and Scansite but also trains neural network (nn)-based models on peptide array data that were collected by the Cesarini lab (Miller et al. 2008). Where the neural networks outperformed the PSSMs, they were used instead. This

method is an ensemble of optimal domain-specific models. The limitation of domain-specific models is that they do not allow for evidential support from closely related domains such as for example Crk and CrkL, which share many of the same binding partners.

The Wunderlich model (Wunderlich and Mirny 2009) provides the principle foundation for the model that we will adopt in our approach. The model starts with the intuitive premise that the energy of binding of a given peptide and domain pair is the summation of the energies of all the amino acid – amino acid (AA-AA) contacts between the two. By incorporating structural information from SH2 domain-peptide complexes, Wunderlich and Mirny derived a contact map and fit an energy potential that maximally segregated the previously determined (Jones et al. 2005) binding and non-binding complexes. The principle limitation of this approach is that it fits a single energy potential, thereby assuming that every contact has an identical energy profile. This was primarily driven by the limitation of using a small training dataset (190 positive interactions), which does not have enough information to constrain a more complex model and would therefore result in overfitting.

The success of a computational modeling endeavor is dependent on many things including the choice of a suitable modeling approach, accuracy and diversity of the underlying training data, and the inclusion of prior knowledge. Despite their success, we postulated that previous efforts can be improved in all these criteria. As a modeling approach, PSSMs are not very suitable for SH2 domains because they assume that all positions contribute equally to binding. This is in contradiction with knowledge about SH2 domain biology. All methods previous have also used almost exclusively a single data source for their training information. This allows for easy standardization and comparison of data points but incurs the risk of modeling assay bias and not underlying biology. Only Wunderlich and Mirny, have utilized any

of the additional knowledge such as structure and amino acid composition of the SH2 domains to improve their performance.

RESULTS AND DISUCSSION

4.2 Model Inputs

To expand beyond the previous modeling approaches, we made several improvements. We expanded the training data to include data derived from multiple publications (Table 4.2) spanning distinct assay types, including domain array (Koytiger et al. 2013), peptide array (Miller et al. 2008; B. A. Liu et al. 2012) and solution phase fluorescence polarization (Hause et al. 2012). We also sought to further expand the data types to use additional peptide array data (Huang et al. 2008) as well as low throughput experimental data annotated by Phospho.ELM (Dinkel et al. 2011) and PhosphositePlus (Hornbeck et al. 2011).

Table 4.2: Input binding data for model training. We collated all available systematic data collection efforts on SH2 domain binding for model training across multiple assay types.

Data Type	Peptide #	Domain #	Binding #	Reference
Domain Array	724	88	2114	Koytiger et al. 2013
Peptide Array	981	69	8114	Miller et al. 2008b
Peptide Array	191	40	730	B. A. Liu et al. 2012
FP	72	74	213	Hause et al. 2012

The expansion of training data allows us to also use an improved modeling approach with minimal built in assumptions. However, there are two key assumptions in our model. The first is that the probability that a peptide-domain pair will be experimentally identified as being a “true

binder" is related to the energy of binding, which is the linear summation of the energy of the individual domain-peptide contacts (Figure 4.1).

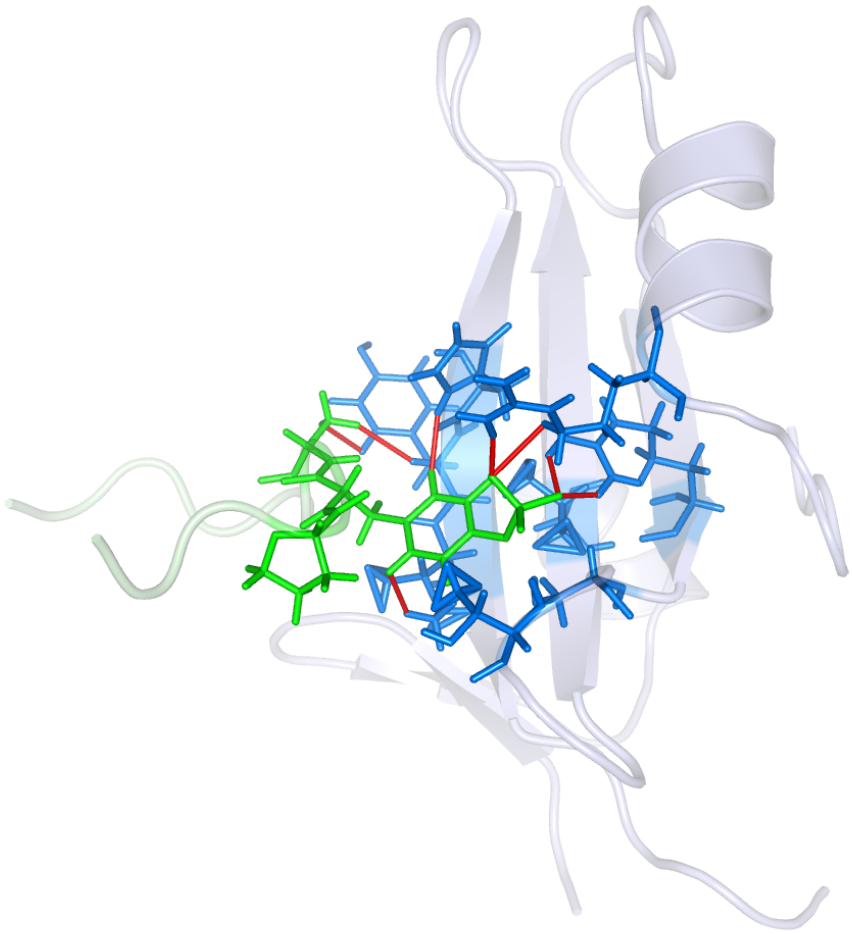

Figure 4.1: Schematic representation of the structure model. Amino acids on the SH2 domain (blue) make contact (red lines) with the amino acids on the peptide (green). These interactions can be either repulsive or attractive and when summed correspond to the overall energy of the interaction between a peptide and a domain

We used 25 structures of SH2 domains in complex with peptide ligands, downloaded from the PDB (Sussman et al. 1998) (Table 4.3). To allow for mapping of domains onto the

structures, all domains and structures were aligned to the 106 amino acid Hidden Markov Model (HMM) profile of the SH2 domain from the SCOP database (Andreeva et al. 2007). The advantages of using a previously verified alignment over an in-house-generated multiple sequence alignment are that SCOP uses structural information to guide the alignment and that the entirety of SH2 domain sequence knowledge is used for the alignment instead of just the domains under study here. The SCOP HMM also generates a high quality, largely gap free alignment of the domains in a manner that is wholly transparent and reproducible by other researchers. We also standardized all peptides to 15-mer length, with the 8^{th} position being the phosphotyrosine.

We also made the approximation that the contact map among different domain-peptide pairs is the same. This is justified by analysis of the entirety of the solved structures of SH2 – phosphopeptide complexes showing minimal variation in the contact distances (Figure 4.2). When determining the contact distance we use the distance between the two closest atoms between each residue pair.

Table 4.3: SH2 Domain structures used in model construction. Each structure was retrieved from the PDB, aligned to the SCOP SH2 domain HMM and used to compute the average contact map with the peptide ligand.

PDB ID	SH2 Domain
1AOT	FYN
1YVL	STAT1
2HDX	SH2B1
3MAZ	STAP1
1MW4	GRB7
1JU5	CRK
1D4W	SH2D1A
1TCE	SHC1
2PLD	PLCG1
2LCT	VAV1
1A81	SYK-N
2ETZ	ITK
1CSY	SYK-C
3PFV	CBLB
1LCJ	LCK
1I3Z	SH2D1B
1QG1	GRB2
2IUH	PIK3R1-N
1SPS	SRC
1R1Q	GRAP2
2CIA	NCK2
1PIC	PIK3R1-C
2CI9	NCK1
2HMH	SOCS3
2VIF	SOCS6

A

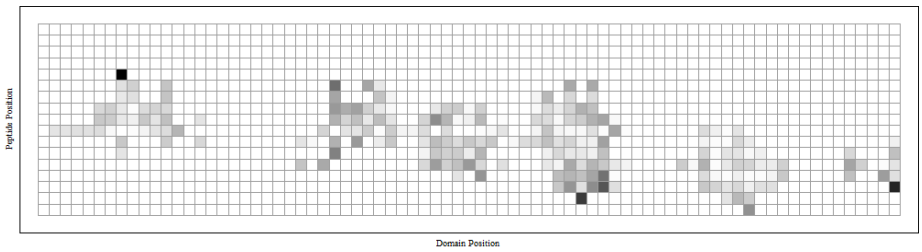

B

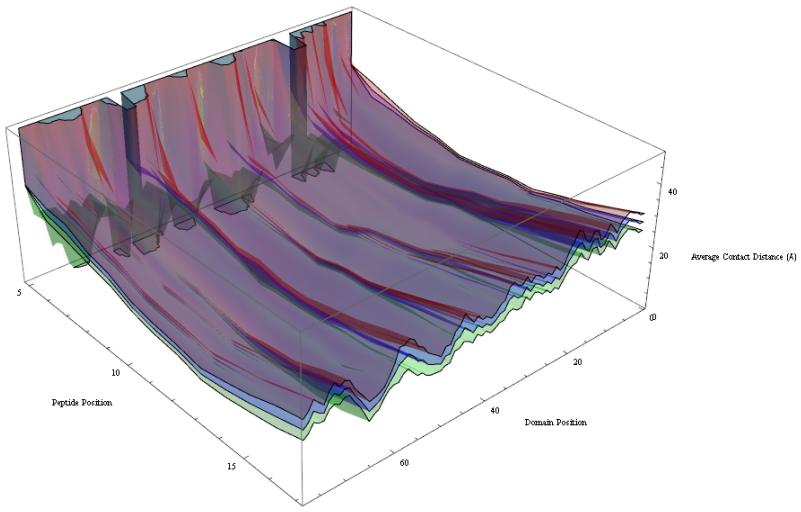

Figure 4.2 SH2-peptide complexes are structurally similar. **(A)** Average contact map of all structures of SH2 domain- peptide complexes. The x-axis corresponds to positions on the SH2 domain aligned to the SCOP HMM and the y-axis to positions on the peptide. The darker the boxes indicate closer distances between the positions structurally. **(B)** Distribution of contact distances of all the structures. The blue sheet represents the average distance, the green sheet the minimal distance and the red the maximum. Areas where distance is 0 indicate regions of no data.

4.3 Model Fitting

The amino acid sequence of the peptide and SH2 domain are represented as a series of 21 × 21 matrices (20 amino acid types plus a gap value). There is a single positive entry in this matrix corresponding to each pair. Since there are 106 positions in the domain HMM and 15 in

the peptide, this makes for 106×15 or 1590 pairwise interaction pairs. These inputs are then concatenated and reshaped into an input vector of length 701,190 (106×15×21×21).

Since the number of input features is much larger than the training data, there is a great chance of model overfitting. This risk is mitigated in two ways: removing all features past a certain cutoff distance and using an L1 penalty for model complexity. L1 penalty's effect is to shrink the coefficients of most parameters to 0, thus giving a sparse solution (Hastie, Tibshirani, and Friedman 2009). It requires as its input, a parameter lambda which dictates how aggressively this shrinkage will occur. This is intuitively useful, since we know in biology that recognition occurs by direct contact with a subset of positions. Since we do not know *a priori* what is the optimal cutoff distance and lambda parameter, we use a cross validation approach to empirically determine their values (Figure 4.3). We perform 6-fold cross-validation, training the model on 5/6ths of the dataset and assessing its performance on the remaining 1/6th. How we evaluated the performance of the model will be discussed later.

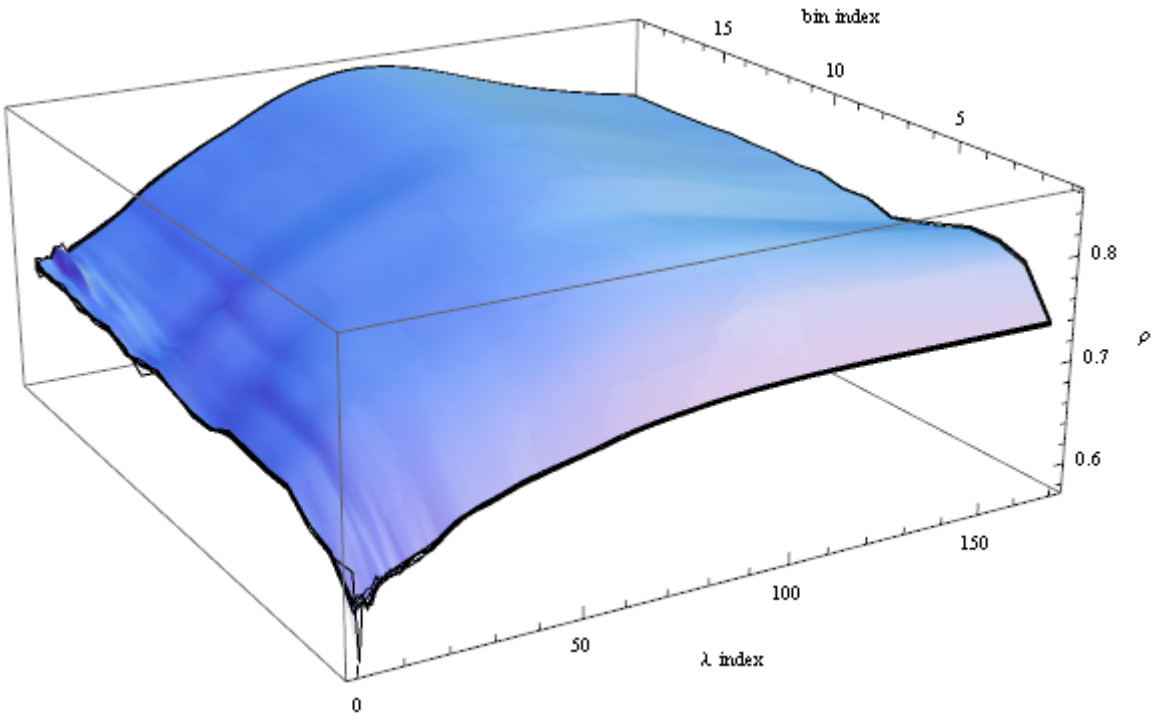

Figure 4.3: Landscape of model performance. Shows the cross validation performance results (ROC AUC) (z-axis) as the lambda paramater (x-axis) and the cutoff distance (y-axis) are altered.

Because the actual modeling work was performed by my collaborator, Dr. Mohammed AlQuarashi, I will not discuss this work in great detail in this thesis. However, by framing the model as described above, we were able to derive a sparse, stable solution to the energetic contribution of each position. We found that a 15 angstrom cutoff distance optimized cross validation performance while balancing computational complexity of the model. The output of the model is a probability which can be directly interpretted as the probability in the training data that a certain interaction will be declared as occuring (Figure 4.4).

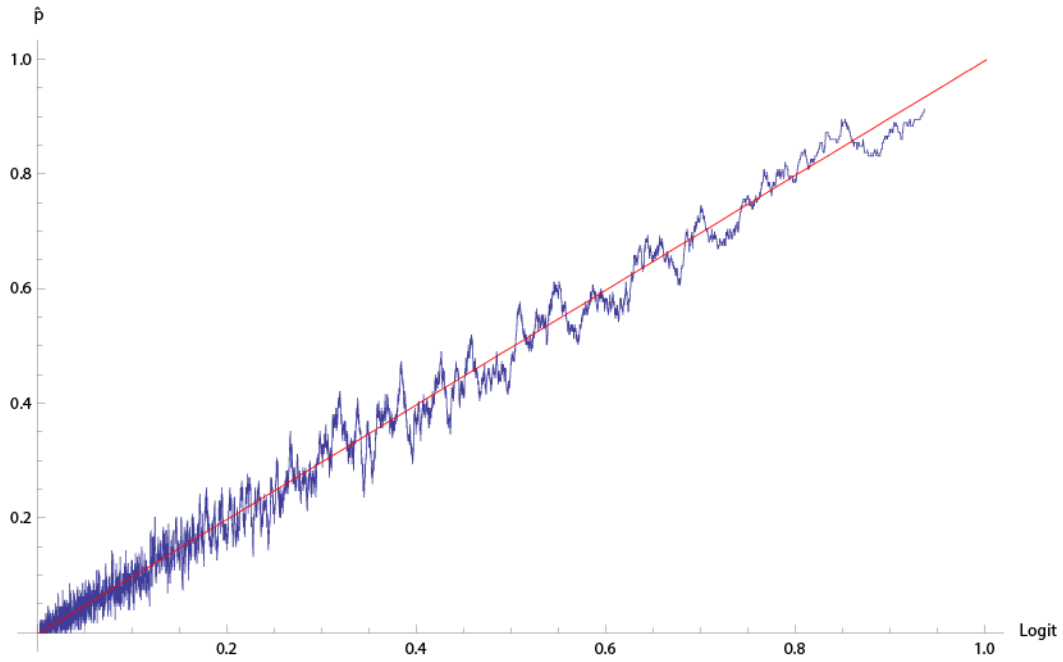

Figure 4.4: Model probabilities are equivalent to experimental probabilities. Bins of data are taken along different model output probabilities (x-axis) and determined what fraction binds (y-axis). The red line shows a perfect correspondence. This shows that the model output is directly interpretable

The energetic terms fit by the model also largely behave as we would expect them to from biological intuition. Oppositely charged amino acids tend to favor binding and also distant contacts tend to have weaker energetic contributions to binding as compared to closer contacts (Figure 4.5). These intuitions were not included in the formulation of the model *a priori* and indicate that part of the performance of the model is likely due to its capturing information about the underlying structural biology.

A.

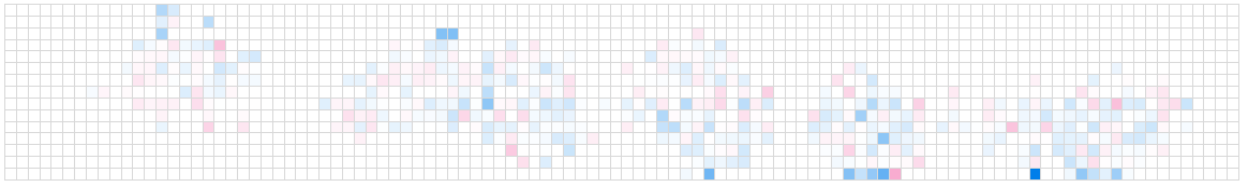

B.

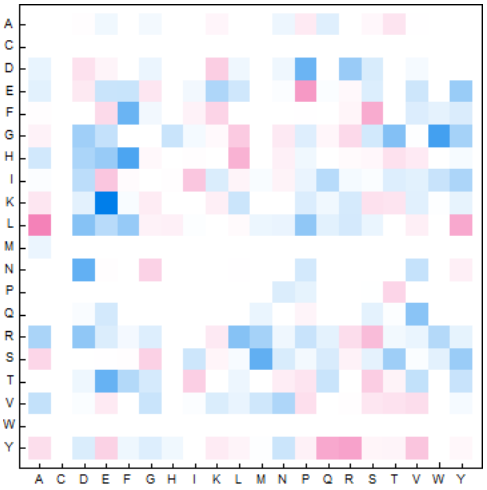

C.

Figure 4.5: Energy matrices fit by the model (A) Peptide positions are in the y-axis and domain positions are in the x-axis. Every square at the intersection contains a predicted 21 x 2`1 energy matrix (all amino acids plus gap value). The color indicates the sum of the terms in the matrix with blue indicating attraction and red indicating repulsion. **(B)** Average interaction matrix from all position pairs. Note the general recapitulation of known attraction between oppositely charged amino acids (K-E, D-R, etc.) **(C)** Potentials as they change by distance. Note the higher level of activity in more proximal pairs. Recapitulates known behavior of interactions to get weaker as they get further apart

3.4 Assessing Model Performance

To assess the performance of the model and to facilitate its comparison to other modeling efforts, we use the area under the curve (AUC) of the receiver operating characteristic (ROC) (Mason and Graham 2002). Since our input data are largely negative (92%), we cannot use simple accuracy measures as a model would get 92% accuracy simply by assigning every prediction as non-binding. ROC curves are generated by plotting the true positive rate (TPR) or sensitivity of the model on the y-axis and the false positive rate (FPR) or the 1-specificity of the model on the x-axis. The equations for the two are:

$$TPR = \frac{TP}{TP + FN} \qquad FPR = \frac{FP}{FP + TN}$$

where TP is the number of true positives (predicted binding events that are experimentally confirmed), FN is the number of false negatives (predicted non-binding events that are experimentally determined to be binding), FP is the number of false positives (predicted binding events that are experimentally shown to be negative), and TN is the number of true negatives (correctly predicted non-binding events). The ROC curve is generated by relaxing the threshold by which the model calls a positive interaction, gradually bringing in lower confidence predictions and calculating the TPR and FPR at each threshold. Because this analysis can be confounded by experimental error in the training data, we chose to use the solution phase fluorescence polarization dataset (Hause et al. 2012), which is liable to be the highest quality. The fluorescence polarization data constitute 72 phospho-peptides derived from all tyrosine sites on the ERBB family of receptors.

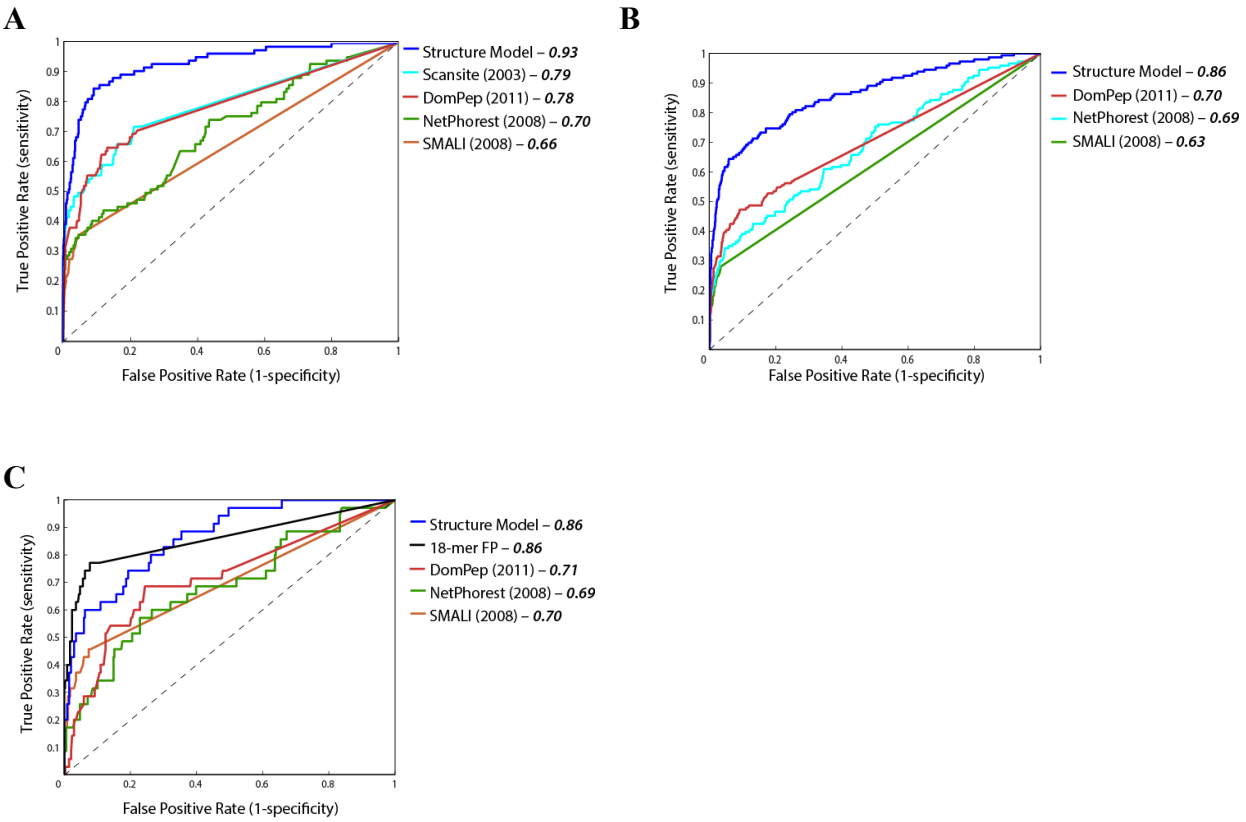

Figure 4.6: Reciever operating characteristic (ROC) curves of predictive models (A) Assesses the performance of 5 available predictors across the 72 peptides analyzed by fluorescence polarization of 15 domains common to all the predictors. This corresponds to 146 positive and 2842 negative interactions. Numbers in bold show the area under the curve (AUC), for reference, a perfect predictor would have an AUC of 1 and a random predictor 0.5. **(B)** Similar to (A) but eliminates the Scansite predictor, which allows comparison of a larger subset of domains, 58 in total. All predictors here perform worse indicating these domains are harder to predict. **(C)** Restricts the analysis to the 6 peptides which have FP experimental replicates using larger peptides. The "scores" from the FP assay are their association constants. Note performance of replicate experiments is similar to structure model

To compare the predictors in a fair way, we constructed ROC curves only on domains modeled by all of them. By taking the area under the curve (AUC) of the ROC curve, we get an unbiased metric of the performance of the predictors. For reference, a random predictor will have an AUC of 0.5, corresponding to an equivalent false and true positive rate, whereas a perfect

predictor will have and AUC of 1.0, corresponding to predicting all true positives and no false positives at all thresholds. When comparing all predictors, we see that the model described here substantially outperforms every other published method, with an AUC of 0.93 compared to the next nearest predictor of 0.79 (Figure 4.6A). Another way to assess model performance is to compare only on high confidence region of predictions, for example, only those that correspond to a false positive rate of 5%. At such a FPR, our model has a true positive rate (TPR) of 75%, whereas the next most accurate model, Scansite, has a 50% TPR. Since Scansite only offers predictions for a small subset of all human SH2 domains, we can also look more broadly by eliminating it from the analysis (Figure 4.6B). In this larger and more diverse subset of domains, our model still outperforms all other predictors with an AUC of 0.86 compared to 0.70 for the nearest predictor, DomPep. Similarly at 5% FPR, Dompep has 40% TPR while our model has a 60% TPR. In both tests, our model is able to predict 50% more accurately than previously developed methods.

The ultimate test, however, is if the model can perform as well as high quality experimental data. To assess this, we again used the data of Hause et al.. In this case, we relied on experiments in which they re-probed 6 peptides using a slightly longer version of the peptide (18 vs 13-mers). As the additional length is far away from the SH2 domain binding site, this change should have no effect on the assay results. The peptides were probed on average three times and the average K_D was calculated. This should result in a very high quality dataset, better than most high throughput experimental data that were used to train our model. We assigned the score for the "predictions" of the 18-mers as being the association constant, because we reasoned that the stronger the binding, the more likely the interaction is to be real and rediscovered. As can be seen in Figure 4.6C, the AUC of both the structure model and the solution phase assay is

0.86. At 5% FPR, the 18-mer FP "predictions" have a TPR of 68%, whereas our model's performance over this same subset is 51%, indicating the experiment is still better at high confidence threshold. However, as the two experiments are of the same type, they probably share similar systematic errors, including similar domains and peptide artifacts. The experiment was also not performed blind, thus replication of non-agreeing data points is likely. In the future, we will use for our "gold standard" data points which come at the intersection of these different assays. That is, we will count high confidence binding and non-binding events, those that have support from at least two distinct assays.

3.5 Applying the model to study cancer

A functioning, high quality model allows us to derive an unbiased protein-protein interaction network mediated by phosphotyrosine. To do this, we extracted all known phosphorylation sites from PhosphositePlus (Hornbeck et al. 2011) and remove all sites that only have one reference to minimize spurious phosphorylation events. We then predicted, using our model, the SH2 domain binding profile of each site and integrated the probabilities to achieve an overall probability that the SH2 domain-containing and phosphotyrosine-containing proteins will interact. The resulting graph is shown in Figure 4.6 and represents a cutoff of 50% confidence in an interaction. This cutoff was chosen to ease visualization as the network increases rapidly in size as the threshold is lowered. As anticipated, the predicted network captures many known interactions (e.g. PI3K family with ERRB3, CRK family with BCAR1/p130Cas among others) and predicts many interactions that have not previously been described. We are currently

investigating the biological relevance of some of these predicted interactions.

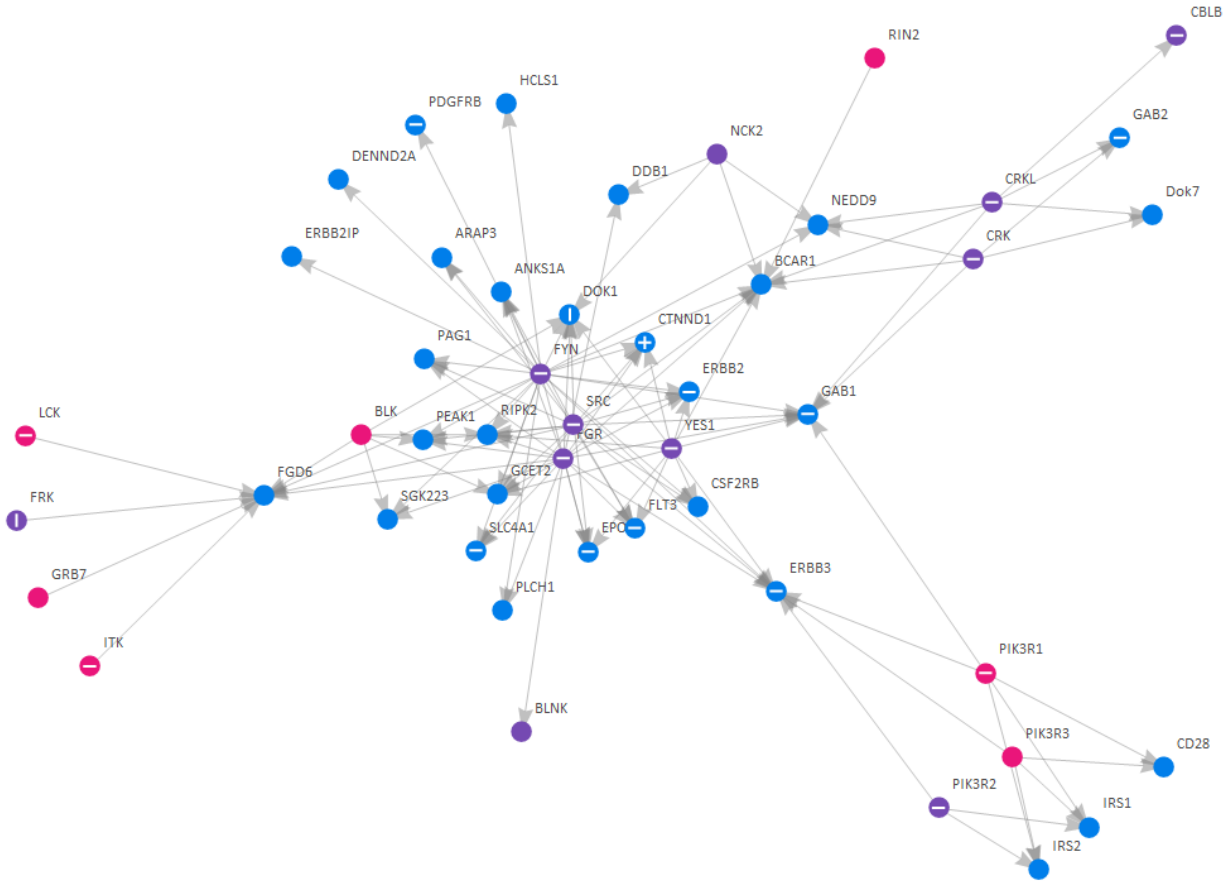

Figure 4.7: Proteome wide wild type signaling network. Purple and pink circles indicate SH2 domain containing proteins. Blue and pink circles indicate phosphotyrosine containing proteins. Arrows start from the SH2 protein and end at the phosphotyrosine protein. Horizontal white lines indicate oncogenes and vertical white lines indicate tumor suppressors.

Phosphotyrosine signaling plays a well-documented role in cancer. It is not surprising, therefore, that many of the somatic mutations being discovered by high throughput sequencing methods modify regions of sequence surrounding sites of tyrosine phosphorylation as well as regions of the SH2 domain. Our model potentially provides insight into how such mutations could rewire phosphotyrosine signaling networks. To investigate this application, we extracted all the data available from version 62 of the Catalog of Somatic Mutations in Cancer (COSMIC)

(Bamford et al. 2004) and mapped them onto sites of tyrosine phosphorylation using a custom built MATLAB pipeline. This yielded in excess of 58,000 cancer mutations that affect sites of tyrosine phosphorylation (although significantly fewer if one only considers high confidence sites of tyrosine phosphorylation). Many of the SNPs are identical in sequence but come from multiple samples or affect the same phosphorylation site; this gives us an additional genomic prior when interpreting the data. We can compute the probability that, given a random mutation that affects the sequence surrounding a site of tyrosine phosphorylation, it will affect a protein-protein interaction, either by forming a new interaction or removing an existing interaction. We perform this analysis on individual cancer types in the data and map the interactions that are highly likely to get rewired (Figure 4.7). We are seeking to experimentally validate the predicted effect of these mutations on a subset of the interactions.

A **Squamos Cell Carcinoma**

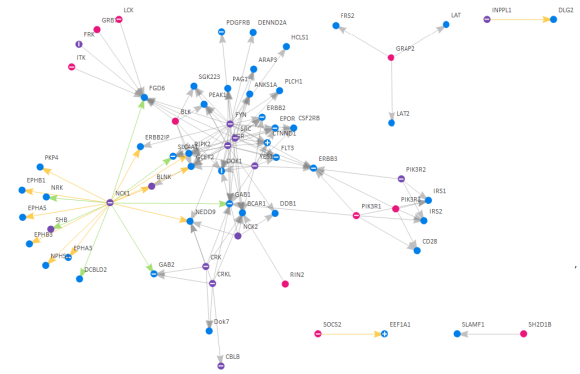

B **Serous Carcinoma**

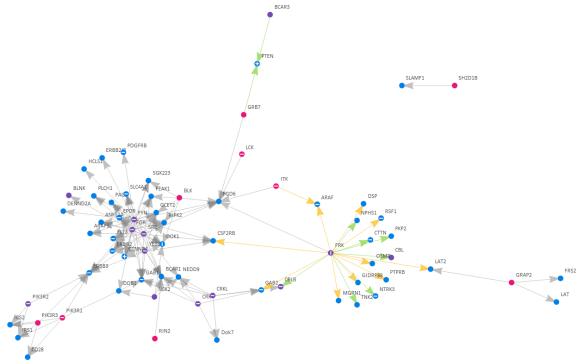

C **Endometroid Carcinoma**

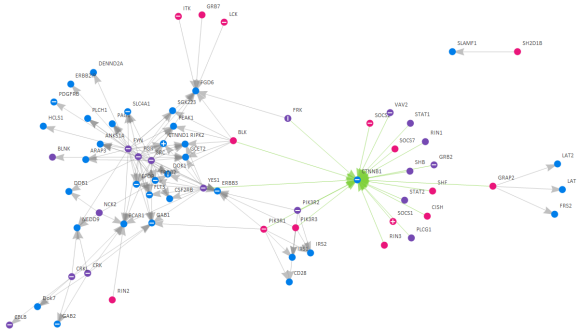

D **Adenocarcinoma**

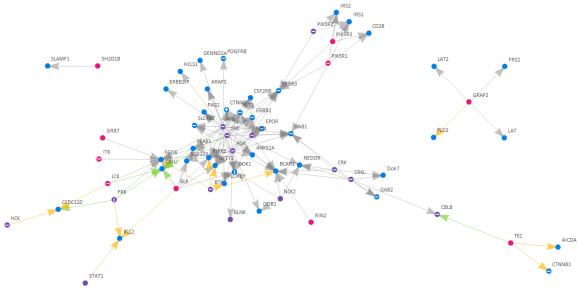

Figure 4.8: Integrated probabilities of network rewiring. Likely new edges are colored green, likely destroyed edges are colored in orange. For additional information on interpreting the graph, see the caption for Figure 4.6.

We are also seeking to expand the analysis further to understand network rewiring from short deletions, truncations, insertions and rearrangements. Another avenue of analysis is to incorporate protein expression levels from mRNAseq data to understand how fluctuations in protein concentration in cancer affect the underlying signaling network. The primary source of

the information will come from the TCGA project's efforts in characterizing tumor samples (T. C. G. A. R. Network 2011) from a wide variety of cancer types. The model provides the organizing framework to facilitate our understanding of how networks function under changing contexts and how they are rewired to promote oncogenesis. This process is performed in a completely unbiased manner, which has the potential to shed light on interesting new biology and hopefully ultimately inform patient treatment.

Another avenue of research enabled by the model is a result of its capacity to take as its input an arbitrary SH2 domain. Researchers studying model organism systems such as mice can generate similar interaction graphs as those highlighted here for mouse SH2 domains. Knowing where the networks are similar to humans and where they diverge can facilitate cross-species comparative network biology. This can also be useful when studying drug action and efficacy in other organisms, to understand where an animal is an appropriate model system. Relevant pre-clinical results are more likely from networks that are predicted to be highly conserved cross-species.

In conclusion, the modeling work presented here enables multiple areas of further research. To facilitate this, we plan to develop an accessible web-based tool that will allow the scientific community to use this model freely.

Part 5: Conclusions and Future Directions

In this chapter, I will speculate as to the implications of the research presented above and the overall future direction of the field. Largely this chapter will discuss how this and related work is supplementing our current understanding of molecular biology, which is based on mental models and taxonomy. What is emerging is a more holistic and systematic understanding enabled by large-scale data and computation, where the criterion of understanding is prediction.

5. 1 From Molecular Machines to Pleomorphic Ensembles

Much of our current understanding of biology comes from pioneering discovery studies that would identify a new gene and attempt to characterize its particular function. However, it is now understood that genes do not convey function in isolation. Conversely, most traits are complex; there is no single "obesity gene" for instance. The study of protein interactions has also started with with publication of a new protein-protein interaction followed by some basic characterization as to "what it does." This too is reductionist as proteins interactions are embedded in a dense network, in which function changes with context and fluctuation in concentration. The explosion of characterized biochemical interactions resulting from high throughput and predictive approaches has provided a challenge in understanding what they all do.

The common framework for understanding such interactions is to imagine protein complexes as molecular machines that carry out some discrete function. An example of this would be the complexes nucleated by an RTK and GRB2, namely GRB2-SOS1 and GRB2-GAB1. The RTK-GRB2-SOS1 machine recruits and activates the components of the MAPK pathway (as described in the introduction) and RTK-GRB2-GAB1 has a similar function for the PI3K pathway (Lemmon and Schlessinger 2010). This pathway is so illustrated in textbooks and

is one of the foundational pieces of "what we really know" about RTK signaling. The diagrams and the mental models implicitly assume that identity of the RTK is irrelevant and the concentrations of the components of this machine are irrelevant except in the trivial case where the components are non-expressed. These mental models simply cannot integrate a piece of information such as a recent study showing that in signaling downstream of the RTK RON (MST1R), which is very closely related to MET, GRB2 plays an antagonistic role in activation of the MAPK and PI3K pathways. In fact, siRNA-mediated knockdown of GRB2 led to a nearly three-fold increase in phospho-AKT and a twofold increase in phospho-MAPK downstream of RON activation (Chaudhuri et al. 2011). Mutation of the RON phosphotyrosine site responsible for GRB2 recruitment to the sequence found in MET did not change this antagonistic role of GRB2, ruling out an affinity argument. This example highlights the challenges in linking even well studied molecular complexes to phenotypes and function and the ability of the same core components to carry out different function in even subtly different contexts.

Examples such as these as well as the rich binding data collected in the research detailed in this thesis highlight the need to rethink how signaling complexes behave *in vivo*. Activated receptors nucleate a wide variety of complexes that interact with each other in many unexpected and subtle ways to generate a phenotypic outcome. This allows these networks to have distinct input-output relationships depending on context. Understanding this complex, dynamic process will remain a daunting challenge, requiring the extensive use of computational modeling.

5.2 From Data Explosion to Data Saturation

The sequencing of the human genome greatly enabled the study of molecular biology systematically. In our instance, the annotation of all SH2 domain-containing proteins in the

human proteome has enabled us to study them as a family instead of single proteins. The concomitant development of new technologies in miniaturization (e.g. microarrays) has allowed these studies to proceed in a cost-economical and scalable way. Numerous studies such as ours were enabled and this led to a massive increase in the data generated in the field.

Development of the computational model presented in this work shows us the utility and limitation of the large quantity of data generated since then. We have built a model that performs as well as biochemical methods in identifying interactions. This allows us to make the next leap of several orders of magnitude over experimental data. Future researchers will no longer need to perform unbiased high throughput SH2 domain research such as the type that I have described in Part 1 and 2. We seem to have the data necessary to train computational models and thereby infer the remainder of the interactome. There might be a need for targeted approaches that seek to probe domains or peptides that are currently poorly predicted by our model or which behave poorly in current experimental set ups. However, even new methodologies that identify SH2 domain binding partners, when used in the same unbiased way that currently serves to train our model, would suffer from the rule of diminishing returns.

A similar development is going on in the complementary field of phosphotyrosine site identification. In our study, we performed mass spectrometry on six receptors in 2008 and found many sites of tyrosine phosphorylation, the vast majority of them being novel. However, in the process of collecting and analyzing our data other labs performing high throughput mass spectrometry discovered all of the novel sites that we identified. This rapid transition highlights that much of the effort needed to identify new sites is redundant data and that truly new sites of tyrosine phosphorylation that have not been discovered are probably limited in number.

Moreover, whereas previous studies requiring a comprehensive list of phosphorylation sites would merge multiple different databases, in this study we actually pruned data out of one database to choose only the high confidence data. This again due to the transition that has rapidly occurred from being data quality not quantity limited.

These arguments are of course not to say that we have saturated all the potential data types. For instance, we do not know what cell types these predicted interactions would be active in, the interplay of these interacting proteins and the dynamic properties of these systems in the cell. Development of new experimental methods will allow the collection of new complementary data types to those that are currently available and will greatly assist in this endeavor. Thus merging distinct data types into a coherent framework will be the way forward to understanding the cell and not merely the scaling up of existing data collection endeavors. Genomics has provided us the nodes of the protein interaction network, proteomics the edges, but the challenging part of interpreting these data systematically is still largely in its infancy.

5.3 From Narrative Knowledge to Database Knowledge

The explosion of journals and articles focused on the life sciences coupled with the massive increase in data generation has rendered the individual researcher unable to acquire and evaluate any significant portion of the current scientific output. Coupled with the fact that results of scientific inquiry are often ambiguous and filled with false positives and false negatives, it will increasingly be realized that without computation our ability to process scientific information is woefully inadequate.

This problem is especially manifest in "omics" data. In a prototypical high-throughput study, the generated large-scale dataset is used to cherry pick a couple of data points for follow up research and "assay validation." To perhaps the majority of the readership of the final paper, the high throughput data become irrelevant and only the narrative constructed around the small-scale study is understood and remembered. Our ability to generate genuinely useful and predictive models out of the high throughput data is currently limited.

Low throughput experiments suffer a related problem. While in isolation they often convey an understandable narrative and couch results in familiar cause-effect structure, that coherency is lost when the information is aggregated. This is a product of several related factors: literature text mining is in its infancy, extracting data computationally from free flowing text very difficult (and time consuming, even for knowledgeable researchers), experimental results are by their nature ambiguous and often incommensurate with each other. For instance, in the determination of a protein-protein interaction, it is often not known whether the interaction is indirect or direct, what its affinity is, and what post translational modifications are required, making comparison of different assay results challenging. In our experience in generating the model in Section 3, we found that database aggregation of previously published, low throughput experiments was on the whole of worse quality than high throughput data (data not shown), similar to the experience of others (Cusick et al. 2009).

Despite the caveats of computation, data that are not computationally interpretable will become progressively marginalized as we try to understand the totality of molecular biology. Integrating publications mentally is already highly difficult if not impossible. Our work on the structure-based model shows one way forward in understanding large interlinked datasets. By

combining what is known about SH2 domain sequence, its structure and the plethora of computationally interpretable binding data in an intuitive framework, we have generated a program that understands SH2 domain binding in a way that a human brain simply cannot. Computation will not replace but instead augment researchers in their investigations into biological systems.

Our model is a dynamic program that sits at the intersection of five different databases: Uniprot, PhosphositePlus (Hornbeck et al. 2011), the PDB, COSMIC (Bamford et al. 2004) and the informal database merging all known SH2 domain-mediated interactions. This allows our model to dynamically process and keep up to date with all these data sources in a way that static papers do not. Moreover, our assumptions and analyses are codified such that anyone who finds methodological improvements can immediately make changes. This is in contrast to much of the experimental literature that is often ambiguous, making it extremely difficult to disprove or improve upon.

In conclusion, biology is truly complex. If we hope to understand it in totality, we must organize experimental data in machine readable databases and develop computational algorithms that link these databases with each other. This will allow for the systematic synthesis of all the information and the generation of predictive models across multiple scales, from the biochemical (e.g. SH2 domain-peptide interactions) to molecular biology (e.g. cell signaling models) with the ultimate goal being patient level models that predict disease and aid in optimizing therapy.

BIBLIOGRAPHY

Akagi, Keiko, Takeshi Suzuki, Robert M Stephens, Nancy A Jenkins, and Neal G Copeland. 2004. "RTCGD: Retroviral Tagged Cancer Gene Database." *Nucleic Acids Research* 32 (Database issue) (January 1): D523–527. doi:10.1093/nar/gkh013.

Andreeva, Antonina, Dave Howorth, John-Marc Chandonia, Steven E. Brenner, Tim J. P. Hubbard, Cyrus Chothia, and Alexey G. Murzin. 2007. "Data Growth and Its Impact on the SCOP Database: New Developments." *Nucleic Acids Research* (November 13). doi:10.1093/nar/gkm993. http://nar.oxfordjournals.org/content/early/2007/11/13/nar.gkm993.

Bae, Jae Hyun, Erin Denise Lew, Satoru Yuzawa, Francisco Tomé, Irit Lax, and Joseph Schlessinger. 2009. "The Selectivity of Receptor Tyrosine Kinase Signaling Is Controlled by a Secondary SH2 Domain Binding Site." *Cell* 138 (3) (August 7): 514–524. doi:10.1016/j.cell.2009.05.028.

Bamford, S, E Dawson, S Forbes, J Clements, R Pettett, A Dogan, A Flanagan, et al. 2004. "The COSMIC (Catalogue of Somatic Mutations in Cancer) Database and Website." *British Journal of Cancer* 91 (2) (July 19): 355–358. doi:10.1038/sj.bjc.6601894.

Bassermann, Florian, Thomas Jahn, Cornelius Miething, Petra Seipel, Ren-Yuan Bai, Sunita Coutinho, Victor L. Tybulewicz, Christian Peschel, and Justus Duyster. 2002. "Association of Bcr-Abl with the Proto-oncogene Vav Is Implicated in Activation of the Rac-1 Pathway." *Journal of Biological Chemistry* 277 (14) (April 5): 12437–12445. doi:10.1074/jbc.M112397200.

Bibbins, K. B., H. Boeuf, and H. E. Varmus. 1993. "Binding of the Src SH2 Domain to Phosphopeptides Is Determined by Residues in Both the SH2 Domain and the Phosphopeptides." *Molecular and Cellular Biology* 13 (12) (December 1): 7278–7287. doi:10.1128/MCB.13.12.7278.

Boettcher, Jan Peter, Marieluise Kirchner, Yuri Churin, Alexis Kaushansky, Malvika Pompaiah, Hans Thorn, Volker Brinkmann, Gavin Macbeath, and Thomas F Meyer. 2010. "Tyrosine-phosphorylated Caveolin-1 Blocks Bacterial Uptake by Inducing Vav2-RhoA-mediated Cytoskeletal Rearrangements." *PLoS Biology* 8 (8). doi:10.1371/journal.pbio.1000457.

Breitling, Frank, Alexander Nesterov, Volker Stadler, Thomas Felgenhauer, and F Ralf Bischoff. 2009. "High-density Peptide Arrays." *Molecular bioSystems* 5 (3) (March): 224–234. doi:10.1039/b819850k.

Burgess, Antony W, Hyun-Soo Cho, Charles Eigenbrot, Kathryn M Ferguson, Thomas P.J Garrett, Daniel J Leahy, Mark A Lemmon, Mark X Sliwkowski, Colin W Ward, and Shigeyuki Yokoyama. 2003. "An Open-and-Shut Case? Recent Insights into the Activation of EGF/ErbB Receptors." *Molecular Cell* 12 (3) (September): 541–552. doi:10.1016/S1097-2765(03)00350-2.

Burris, Howard A, 3rd, Herbert I Hurwitz, E Claire Dees, Afshin Dowlati, Kimberly L Blackwell, Bert O'Neil, Paul K Marcom, et al. 2005. "Phase I Safety, Pharmacokinetics, and Clinical Activity Study of Lapatinib (GW572016), a Reversible Dual Inhibitor of Epidermal Growth Factor Receptor Tyrosine Kinases, in Heavily Pretreated Patients with Metastatic Carcinomas." *Journal of Clinical Oncology: Official Journal of the American Society of Clinical Oncology* 23 (23) (August 10): 5305–5313. doi:10.1200/JCO.2005.16.584.

Calderwood, Michael A., Kavitha Venkatesan, Li Xing, Michael R. Chase, Alexei Vazquez, Amy M. Holthaus, Alexandra E. Ewence, et al. 2007. "Epstein–Barr Virus and Virus Human Protein Interaction Maps." *Proceedings of the National Academy of Sciences* 104 (18) (May 1): 7606–7611. doi:10.1073/pnas.0702332104.

Carpenter, Graham, and Qun-sheng Ji. 1999. "Phospholipase C-γ as a Signal-Transducing Element." *Experimental Cell Research* 253 (1) (November 25): 15–24. doi:10.1006/excr.1999.4671.

Chandarlapaty, Sarat, Ayana Sawai, Maurizio Scaltriti, Vanessa Rodrik-Outmezguine, Olivera Grbovic-Huezo, Violeta Serra, Pradip K. Majumder, Jose Baselga, and Neal Rosen. 2011. "AKT Inhibition Relieves Feedback Suppression of Receptor Tyrosine Kinase Expression and Activity." *Cancer Cell* 19 (1) (January 18): 58–71. doi:10.1016/j.ccr.2010.10.031.

Chaudhuri, Amitabha, Ming-Hong Xie, Becky Yang, Kaushiki Mahapatra, Jinfeng Liu, Scot Marsters, Sweta Bodepudi, and Avi Ashkenazi. 2011. "Distinct Involvement of the Gab1 and Grb2 Adaptor Proteins in Signal Transduction by the Related Receptor Tyrosine Kinases RON and MET." *The Journal of Biological Chemistry* 286 (37) (September 16): 32762–32774. doi:10.1074/jbc.M111.239384.

Chen, William W, Birgit Schoeberl, Paul J Jasper, Mario Niepel, Ulrik B Nielsen, Douglas A Lauffenburger, and Peter K Sorger. 2009. "Input-output Behavior of ErbB Signaling Pathways as Revealed by a Mass Action Model Trained Against Dynamic Data." *Molecular Systems Biology* 5: 239. doi:10.1038/msb.2008.74.

Cheung, Lydia W.T., Bryan T. Hennessy, Jie Li, Shuangxing Yu, Andrea P. Myers, Bojana Djordjevic, Yiling Lu, et al. 2011. "High Frequency of PIK3R1 and PIK3R2 Mutations in Endometrial Cancer Elucidates a Novel Mechanism for Regulation of PTEN Protein Stability." *Cancer Discovery* 1 (2) (July 1): 170–185. doi:10.1158/2159-8290.CD-11-0039.

Choi, Jang Hyun, Sung Ho Ryu, and Pann-Ghill Suh. 2007. "On/Off-regulation of Phospholipase C-γ1-mediated Signal Transduction." *Advances in Enzyme Regulation* 47 (1): 104–116. doi:10.1016/j.advenzreg.2006.12.010.

Colicelli, John. 2010. "ABL Tyrosine Kinases: Evolution of Function, Regulation, and Specificity." *Science Signaling* 3 (139): re6. doi:10.1126/scisignal.3139re6.

Comoglio, Paolo M., Silvia Giordano, and Livio Trusolino. 2008. “Drug Development of MET Inhibitors: Targeting Oncogene Addiction and Expedience.” *Nature Reviews Drug Discovery* 7 (6) (June 1): 504–516. doi:10.1038/nrd2530.

Cusick, Michael E, Haiyuan Yu, Alex Smolyar, Kavitha Venkatesan, Anne-Ruxandra Carvunis, Nicolas Simonis, Jean-François Rual, et al. 2009. “Literature-curated Protein Interaction Datasets.” *Nature Methods* 6 (1) (January): 39–46. doi:10.1038/nmeth.1284.

Degrauwe, Nils, Julie Ann Sosa, Sanziana Roman, and Hari A Deshpande. 2012. “Vandetanib for the Treatment of Metastatic Medullary Thyroid Cancer.” *Clinical Medicine Insights. Oncology* 6: 243–252. doi:10.4137/CMO.S7999.

Demetri, George D, Allan T van Oosterom, Christopher R Garrett, Martin E Blackstein, Manisha H Shah, Jaap Verweij, Grant McArthur, et al. 14. “Efficacy and Safety of Sunitinib in Patients with Advanced Gastrointestinal Stromal Tumour after Failure of Imatinib: a Randomised Controlled Trial.” *The Lancet* 368 (9544): 1329–1338. doi:10.1016/S0140-6736(06)69446-4.

DiNitto, Jonathan P, and David G Lambright. 2006. “Membrane and Juxtamembrane Targeting by PH and PTB Domains.” *Biochimica et Biophysica Acta* 1761 (8) (August): 850–867. doi:10.1016/j.bbalip.2006.04.008.

Dinkel, Holger, Claudia Chica, Allegra Via, Cathryn M Gould, Lars J Jensen, Toby J Gibson, and Francesca Diella. 2011. “Phospho.ELM: a Database of Phosphorylation Sites--update 2011.” *Nucleic Acids Research* 39 (Database issue) (January): D261–267. doi:10.1093/nar/gkq1104.

Downward, Julian. 2003. “Targeting RAS Signalling Pathways in Cancer Therapy.” *Nature Reviews Cancer* 3 (1) (January 1): 11–22. doi:10.1038/nrc969.

Druker, B J, C L Sawyers, H Kantarjian, D J Resta, S F Reese, J M Ford, R Capdeville, and M Talpaz. 2001. “Activity of a Specific Inhibitor of the BCR-ABL Tyrosine Kinase in the Blast Crisis of Chronic Myeloid Leukemia and Acute Lymphoblastic Leukemia with the Philadelphia Chromosome.” *The New England Journal of Medicine* 344 (14) (April 5): 1038–1042. doi:10.1056/NEJM200104053441402.

Engelman, Jeffrey A, and Jeffrey Settleman. 2008. “Acquired Resistance to Tyrosine Kinase Inhibitors During Cancer Therapy.” *Current Opinion in Genetics & Development* 18 (1) (February): 73–79. doi:10.1016/j.gde.2008.01.004.

Frank, Ronald. 2002. “The SPOT-synthesis Technique. Synthetic Peptide Arrays on Membrane Supports--principles and Applications.” *Journal of Immunological Methods* 267 (1) (September 1): 13–26.

Futreal, P. Andrew, Lachlan Coin, Mhairi Marshall, Thomas Down, Timothy Hubbard, Richard Wooster, Nazneen Rahman, and Michael R. Stratton. 2004. “A Census of Human Cancer Genes.” *Nature Reviews Cancer* 4 (3) (March 1): 177–183. doi:10.1038/nrc1299.

Goldman, John M., and Junia V. Melo. 2003. “Chronic Myeloid Leukemia — Advances in Biology and New Approaches to Treatment.” *New England Journal of Medicine* 349 (15): 1451–1464. doi:10.1056/NEJMra020777.

Gordus, Andrew, and Gavin MacBeath. 2006. “Circumventing the Problems Caused by Protein Diversity in Microarrays: Implications for Protein Interaction Networks.” *Journal of the American Chemical Society* 128 (42) (October 25): 13668–13669. doi:10.1021/ja065381g.

Gorelik, Maryna, Karen Stanger, and Alan R Davidson. 2011. “A Conserved Residue in the Yeast Bem1p SH3 Domain Maintains the High Level of Binding Specificity Required for Function.” *The Journal of Biological Chemistry* 286 (22) (June 3): 19470–19477. doi:10.1074/jbc.M111.229294.

Guo, Ailan, Judit Villén, Jon Kornhauser, Kimberly A Lee, Matthew P Stokes, Klarisa Rikova, Anthony Possemato, et al. 2008. “Signaling Networks Assembled by Oncogenic EGFR and c-Met.” *Proceedings of the National Academy of Sciences of the United States of America* 105 (2) (January 15): 692–697. doi:10.1073/pnas.0707270105.

Hakes, Luke, John W Pinney, David L Robertson, and Simon C Lovell. 2008. “Protein-protein Interaction Networks and Biology--what’s the Connection?” *Nature Biotechnology* 26 (1) (January): 69–72. doi:10.1038/nbt0108-69.

Hakes, Luke, David L Robertson, and Stephen G Oliver. 2005. “Effect of Dataset Selection on the Topological Interpretation of Protein Interaction Networks.” *BMC Genomics* 6 (September 20): 131. doi:10.1186/1471-2164-6-131.

Harrison, Douglas A. 2012. “The JAK/STAT Pathway.” *Cold Spring Harbor Perspectives in Biology* 4 (3) (March 1). doi:10.1101/cshperspect.a011205. http://cshperspectives.cshlp.org/content/4/3/a011205.

Hastie, Trevor, Robert Tibshirani, and Jerome Friedman. 2009. *The Elements of Statistical Learning: Data Mining, Inference, and Prediction, Second Edition*. 0002-2009. Corr. 3rd. Springer.

Hause, Ronald J, Jr, Kin K Leung, John L Barkinge, Mark F Ciaccio, Chih-Pin Chuu, and Richard B Jones. 2012. “Comprehensive Binary Interaction Mapping of SH2 Domains via Fluorescence Polarization Reveals Novel Functional Diversification of ErbB Receptors.” *PloS One* 7 (9): e44471. doi:10.1371/journal.pone.0044471.

Himanen, Juha-Pekka, and Dimitar B Nikolov. 2003. “Eph Signaling: a Structural View.” *Trends in Neurosciences* 26 (1) (January): 46–51. doi:10.1016/S0166-2236(02)00005-X.

Hirota, Seiichi, Koji Isozaki, Yasuhiro Moriyama, Koji Hashimoto, Toshirou Nishida, Shingo Ishiguro, Kiyoshi Kawano, et al. 1998. “Gain-of-Function Mutations of C-kit in Human Gastrointestinal Stromal Tumors.” *Science* 279 (5350) (January 23): 577–580. doi:10.1126/science.279.5350.577.

Hofstra, R M, R M Landsvater, I Ceccherini, R P Stulp, T Stelwagen, Y Luo, B Pasini, J W Höppener, H K van Amstel, and G Romeo. 1994. “A Mutation in the RET Proto-oncogene Associated with Multiple Endocrine Neoplasia Type 2B and Sporadic Medullary Thyroid Carcinoma.” *Nature* 367 (6461) (January 27): 375–376. doi:10.1038/367375a0.

Hornbeck, Peter V., Jon M. Kornhauser, Sasha Tkachev, Bin Zhang, Elżbieta Skrzypek, Beth Murray, Vaughan Latham, and Michael Sullivan. 2011. “PhosphoSitePlus: a Comprehensive Resource for Investigating the Structure and Function of Experimentally Determined Post-translational Modifications in Man and Mouse.” *Nucleic Acids Research* (December 1). doi:10.1093/nar/gkr1122. http://nar.oxfordjournals.org/content/early/2011/11/30/nar.gkr1122.

Howes, Amy L, Gary G Chiang, Elizabeth S Lang, Caroline B Ho, Garth Powis, Kristiina Vuori, and Robert T Abraham. 2007. “The Phosphatidylinositol 3-kinase Inhibitor, PX-866, Is a Potent Inhibitor of Cancer Cell Motility and Growth in Three-dimensional Cultures.” *Molecular Cancer Therapeutics* 6 (9) (September): 2505–2514. doi:10.1158/1535-7163.MCT-06-0698.

Huang, Haiming, Lei Li, Chenggang Wu, David Schibli, Karen Colwill, Sucan Ma, Chengjun Li, et al. 2008. “Defining the Specificity Space of the Human Src Homology 2 Domain.” *Molecular & Cellular Proteomics* 7 (4) (April 1): 768–784. doi:10.1074/mcp.M700312-MCP200.

Huber, Peter J. 2003. *Robust Statistics*. John Wiley & Sons.

Huret, Jean-Loup, Sylvaine Le Minor, Franck Dorkeld, Philippe Dessen, and Alain Bernheim. 2000. “Atlas of Genetics and Cytogenetics in Oncology and Haematology, an Interactive Database.” *Nucleic Acids Research* 28 (1) (January 1): 349–351.

Jones, Richard B., Andrew Gordus, Jordan A. Krall, and Gavin MacBeath. 2005. “A Quantitative Protein Interaction Network for the ErbB Receptors Using Protein Microarrays.” *Nature* 439 (7073) (November 6): 168. doi:10.1038/nature04177.

Jonsson, Pall F., and Paul A. Bates. 2006. “Global Topological Features of Cancer Proteins in the Human Interactome.” *Bioinformatics* 22 (18) (September 15): 2291–2297. doi:10.1093/bioinformatics/btl390.

Jung, Andre Scott, Alexis Kaushansky, Gavin Macbeath, and Kenneth Kaushansky. 2011. “Tensin2 Is a Novel Mediator in Thrombopoietin (TPO)-induced Cellular Proliferation by Promoting Akt Signaling.” *Cell Cycle (Georgetown, Tex.)* 10 (11) (June 1): 1838–1844.

Kaneko, Tomonori, Haiming Huang, Xuan Cao, Xing Li, Chengjun Li, Courtney Voss, Sachdev S. Sidhu, and Shawn S. C. Li. 2012. “Superbinder SH2 Domains Act as Antagonists of

Cell Signaling." *Science Signaling* 5 (243) (September 25): ra68. doi:10.1126/scisignal.2003021.

Kaushansky, Alexis, John E Allen, Andrew Gordus, Michael A Stiffler, Ethan S Karp, Bryan H Chang, and Gavin MacBeath. 2010. "Quantifying Protein-protein Interactions in High Throughput Using Protein Domain Microarrays." *Nature Protocols* 5 (4) (April): 773–790. doi:10.1038/nprot.2010.36.

Kaushansky, Alexis, Andrew Gordus, Bogdan A Budnik, William S Lane, John Rush, and Gavin MacBeath. 2008. "System-wide Investigation of ErbB4 Reveals 19 Sites of Tyr Phosphorylation That Are Unusually Selective in Their Recruitment Properties." *Chemistry & Biology* 15 (8) (August 25): 808–817. doi:10.1016/j.chembiol.2008.07.006.

Kaushansky, Alexis, Andrew Gordus, Bryan Chang, John Rush, and Gavin MacBeath. 2008. "A Quantitative Study of the Recruitment Potential of All Intracellular Tyrosine Residues on EGFR, FGFR1 and IGF1R." *Molecular bioSystems* 4 (6) (June): 643–653. doi:10.1039/b801018h.

Khalili, Jahan S., Xiaoxing Yu, Ji Wang, Brendan C. Hayes, Michael A. Davies, Gregory Lizee, Bita Esmaeli, and Scott E. Woodman. 2012. "Combination Small Molecule MEK and PI3K Inhibition Enhances Uveal Melanoma Cell Death in a Mutant GNAQ- and GNA11-Dependent Manner." *Clinical Cancer Research* 18 (16) (August 15): 4345–4355. doi:10.1158/1078-0432.CCR-11-3227.

Kim, Ha Kun, Jae Won Kim, Asher Zilberstein, Benjamin Margolis, Jin Gwan Kim, Joseph Schlessinger, and Sue Goo Rhee. 1991. "PDGF Stimulation of Inositol Phospholipid Hydrolysis Requires PLC-γ1 Phosphorylation on Tyrosine Residues 783 and 1254." *Cell* 65 (3) (May 3): 435–441. doi:10.1016/0092-8674(91)90461-7.

Kleiman, Laura B, Thomas Maiwald, Holger Conzelmann, Douglas A Lauffenburger, and Peter K Sorger. 2011. "Rapid Phospho-turnover by Receptor Tyrosine Kinases Impacts Downstream Signaling and Drug Binding." *Molecular Cell* 43 (5) (September 2): 723–737. doi:10.1016/j.molcel.2011.07.014.

Koytiger, Grigoriy, Alexis Kaushansky, Andrew Gordus, John Rush, Peter K. Sorger, and Gavin MacBeath. 2013. "Phosphotyrosine Signaling Proteins That Drive Oncogenesis Tend to Be Highly Interconnected." *Molecular & Cellular Proteomics* (January 28). doi:10.1074/mcp.M112.025858. http://www.mcponline.org/content/early/2013/01/28/mcp.M112.025858.

Krzywinski, M., J. Schein, I. Birol, J. Connors, R. Gascoyne, D. Horsman, S. J. Jones, and M. A. Marra. 2009. "Circos: An Information Aesthetic for Comparative Genomics." *Genome Research* 19 (9) (June 18): 1639–1645. doi:10.1101/gr.092759.109.

Ladbury, J E, M A Lemmon, M Zhou, J Green, M C Botfield, and J Schlessinger. 1995. "Measurement of the Binding of Tyrosyl Phosphopeptides to SH2 Domains: a

Reappraisal." *Proceedings of the National Academy of Sciences of the United States of America* 92 (8) (April 11): 3199–3203.

Lemmon, Mark A, and Joseph Schlessinger. 2010. "Cell Signaling by Receptor Tyrosine Kinases." *Cell* 141 (7) (May 25): 1117–1134. doi:10.1016/j.cell.2010.06.011.

Lennartsson, Johan, Christer Wernstedt, Ulla Engström, Ulf Hellman, and Lars Rönnstrand. 2003. "Identification of Tyr900 in the Kinase Domain of c-Kit as a Src-dependent Phosphorylation Site Mediating Interaction with c-Crk." *Experimental Cell Research* 288 (1) (August 1): 110–118. doi:10.1016/S0014-4827(03)00206-4.

Letunic, I., and P. Bork. 2011. "Interactive Tree Of Life V2: Online Annotation and Display of Phylogenetic Trees Made Easy." *Nucleic Acids Research* 39 (Web Server) (April 5): W475–W478. doi:10.1093/nar/gkr201.

Li, Lei, Bing Zhao, Jun Du, Kaizhong Zhang, Charles X. Ling, and Shawn Shun-Cheng Li. 2011. "DomPep—A General Method for Predicting Modular Domain-Mediated Protein-Protein Interactions." *PLoS ONE* 6 (10) (October 7): e25528. doi:10.1371/journal.pone.0025528.

Liu, Bernard A, Karl Jablonowski, Eshana E Shah, Brett W Engelmann, Richard B Jones, and Piers D Nash. 2010. "SH2 Domains Recognize Contextual Peptide Sequence Information to Determine Selectivity." *Molecular & Cellular Proteomics: MCP* 9 (11) (November): 2391–2404. doi:10.1074/mcp.M110.001586.

Liu, Bernard A., Brett W. Engelmann, Karl Jablonowski, Katherine Higginbotham, Andrew S. Stergachis, and Piers D. Nash. 2012. "SRC Homology 2 Domain Binding Sites in Insulin, IGF-1 and FGF Receptor Mediated Signaling Networks Reveal an Extensive Potential Interactome." *Cell Communication and Signaling* 10 (1) (September 14): 27. doi:10.1186/1478-811X-10-27.

Liu, Bernard A., Karl Jablonowski, Monica Raina, Michael Arcé, Tony Pawson, and Piers D. Nash. 2006. "The Human and Mouse Complement of SH2 Domain Proteins—Establishing the Boundaries of Phosphotyrosine Signaling." *Molecular Cell* 22 (6) (June 23): 851–868. doi:10.1016/j.molcel.2006.06.001.

Liu, Yang-Yu, Jean-Jacques Slotine, and Albert-László Barabási. 2011. "Controllability of Complex Networks." *Nature* 473 (7346) (May 12): 167–173. doi:10.1038/nature10011.

Marshall, C.J. 1995. "Specificity of Receptor Tyrosine Kinase Signaling: Transient Versus Sustained Extracellular Signal-regulated Kinase Activation." *Cell* 80 (2) (January 27): 179–185. doi:10.1016/0092-8674(95)90401-8.

Mashima, Ryuichi, Sumimasa Arimura, Shuhei Kajikawa, Hideaki Oda, Susumu Nakae, and Yuji Yamanashi. 2013. "Dok Adaptors Play Anti-inflammatory Roles in Pulmonary Homeostasis." *Genes to Cells* 18 (1): 56–65. doi:10.1111/gtc.12016.

Mason, S. J., and N. E. Graham. 2002. “Areas Beneath the Relative Operating Characteristics (ROC) and Relative Operating Levels (ROL) Curves: Statistical Significance and Interpretation.” *Quarterly Journal of the Royal Meteorological Society* 128 (584): 2145–2166. doi:10.1256/003590002320603584.

Mayer, Bruce J, Michael L Blinov, and Leslie M Loew. 2009. “Molecular Machines or Pleiomorphic Ensembles: Signaling Complexes Revisited.” *Journal of Biology* 8 (9) (October 16): 81. doi:10.1186/jbiol185.

McIntyre, Alan, Brenda Summersgill, Beata Grygalewicz, Ad J.M. Gillis, J. Stoop, Ruud J.H.L.M. van Gurp, Nening Dennis, et al. 2005. “Amplification and Overexpression of the KIT Gene Is Associated with Progression in the Seminoma Subtype of Testicular Germ Cell Tumors of Adolescents and Adults.” *Cancer Research* 65 (18) (September 15): 8085–8089. doi:10.1158/0008-5472.CAN-05-0471.

McKay, M M, and D K Morrison. 2007. “Integrating Signals from RTKs to ERK/MAPK.” *Oncogene* 26 (22) (May 14): 3113–3121. doi:10.1038/sj.onc.1210394.

Mehlitz, Adrian, Sebastian Banhart, André P Mäurer, Alexis Kaushansky, Andrew G Gordus, Julia Zielecki, Gavin Macbeath, and Thomas F Meyer. 2010. “Tarp Regulates Early Chlamydia-induced Host Cell Survival through Interactions with the Human Adaptor Protein SHC1.” *The Journal of Cell Biology* 190 (1) (July 12): 143–157. doi:10.1083/jcb.200909095.

Miller, Martin Lee, Lars Juhl Jensen, Francesca Diella, Claus Jørgensen, Michele Tinti, Lei Li, Marilyn Hsiung, et al. 2008. “Linear Motif Atlas for Phosphorylation-dependent Signaling.” *Science Signaling* 1 (35): ra2. doi:10.1126/scisignal.1159433.

Mortazavi, Ali, Brian A. Williams, Kenneth McCue, Lorian Schaeffer, and Barbara Wold. 2008. “Mapping and Quantifying Mammalian Transcriptomes by RNA-Seq.” *Nature Methods* 5 (7) (July 1): 621–628. doi:10.1038/nmeth.1226.

Mulligan, L M, J B Kwok, C S Healey, M J Elsdon, C Eng, E Gardner, D R Love, S E Mole, J K Moore, and L Papi. 1993. “Germ-line Mutations of the RET Proto-oncogene in Multiple Endocrine Neoplasia Type 2A.” *Nature* 363 (6428) (June 3): 458–460. doi:10.1038/363458a0.

Nagaraj, Nagarjuna, Jacek R Wisniewski, Tamar Geiger, Juergen Cox, Martin Kircher, Janet Kelso, Svante Pääbo, and Matthias Mann. 2011. “Deep Proteome and Transcriptome Mapping of a Human Cancer Cell Line.” *Molecular Systems Biology* 7: 548. doi:10.1038/msb.2011.81.

Network, The Cancer Genome Atlas. 2012. “Comprehensive Molecular Characterization of Human Colon and Rectal Cancer.” *Nature* 487 (7407) (July 19): 330–337. doi:10.1038/nature11252.

Network, The Cancer Genome Atlas Research. 2011. “Integrated Genomic Analyses of Ovarian Carcinoma.” *Nature* 474 (7353) (June 30): 609–615. doi:10.1038/nature10166.

Niu, Xi-Lin, Kevin G. Peters, and Christopher D. Kontos. 2002. “Deletion of the Carboxyl Terminus of Tie2 Enhances Kinase Activity, Signaling, and Function EVIDENCE FOR AN AUTOINHIBITORY MECHANISM.” *Journal of Biological Chemistry* 277 (35) (August 30): 31768–31773. doi:10.1074/jbc.M203995200.

Nolen, Brad, Susan Taylor, and Gourisankar Ghosh. 2004. “Regulation of Protein Kinases: Controlling Activity through Activation Segment Conformation.” *Molecular Cell* 15 (5) (September 10): 661–675. doi:10.1016/j.molcel.2004.08.024.

Obenauer, John C, Lewis C Cantley, and Michael B Yaffe. 2003. “Scansite 2.0: Proteome-wide Prediction of Cell Signaling Interactions Using Short Sequence Motifs.” *Nucleic Acids Research* 31 (13) (July 1): 3635–3641.

Perren, T J. 1991. “c-erbB-2 Oncogene as a Prognostic Marker in Breast Cancer.” *British Journal of Cancer* 63 (3) (March): 328–332.

Phizicky, Eric, Philippe I. H. Bastiaens, Heng Zhu, Michael Snyder, and Stanley Fields. 2003. “Protein Analysis on a Proteomic Scale.” *Nature* 422 (6928) (March 13): 208–215. doi:10.1038/nature01512.

Piccione, Elizabeth, Randi D. Case, Susan M. Domchek, Patrick Hu, Manas Chaudhuri, Jonathan M. Backer, Joseph Schlessinger, and Steven E. Shoelson. 1993. “Phosphatidylinositol 3-kinase P85 SH2 Domain Specificity Defined by Direct phosphopeptide/SH2 Domain Binding.” *Biochemistry* 32 (13) (April 1): 3197–3202. doi:10.1021/bi00064a001.

Raymond, E, S Faivre, and J P Armand. 2000. “Epidermal Growth Factor Receptor Tyrosine Kinase as a Target for Anticancer Therapy.” *Drugs* 60 Suppl 1: 15–23; discussion 41–42.

Rikova, Klarisa, Ailan Guo, Qingfu Zeng, Anthony Possemato, Jian Yu, Herbert Haack, Julie Nardone, et al. 2007. “Global Survey of Phosphotyrosine Signaling Identifies Oncogenic Kinases in Lung Cancer.” *Cell* 131 (6) (December 14): 1190–1203. doi:10.1016/j.cell.2007.11.025.

Rodriguez, Maria, Shawn S.-C. Li, J. Wade Harper, and Zhou Songyang. 2004. “An Oriented Peptide Array Library (OPAL) Strategy to Study Protein-Protein Interactions.” *Journal of Biological Chemistry* 279 (10) (March 5): 8802–8807. doi:10.1074/jbc.M311886200.

Rual, Jean-François, Kavitha Venkatesan, Tong Hao, Tomoko Hirozane-Kishikawa, Amélie Dricot, Ning Li, Gabriel F. Berriz, et al. 2005. “Towards a Proteome-scale Map of the Human Protein–protein Interaction Network.” *Nature* 437 (7062) (September 28): 1173–1178. doi:10.1038/nature04209.

Salcini, A E, J McGlade, G Pelicci, I Nicoletti, T Pawson, and P G Pelicci. 1994. “Formation of Shc-Grb2 Complexes Is Necessary to Induce Neoplastic Transformation by Overexpression of Shc Proteins.” *Oncogene* 9 (10) (October): 2827–2836.

Santarius, Thomas, Janet Shipley, Daniel Brewer, Michael R Stratton, and Colin S Cooper. 2010. “A Census of Amplified and Overexpressed Human Cancer Genes.” *Nature Reviews. Cancer* 10 (1) (January): 59–64. doi:10.1038/nrc2771.

Santos, Silvia D. M., Peter J. Verveer, and Philippe I. H. Bastiaens. 2007. “Growth Factor-induced MAPK Network Topology Shapes Erk Response Determining PC-12 Cell Fate.” *Nature Cell Biology* 9 (3) (March): 324–330. doi:10.1038/ncb1543.

Schlee, Sandra, Paul Carmillo, and Adrian Whitty. 2006. “Quantitative Analysis of the Activation Mechanism of the Multicomponent Growth-factor Receptor Ret.” *Nature Chemical Biology* 2 (11): 636–644. doi:10.1038/nchembio823.

Shapira, Sagi D., Irit Gat-Viks, Bennett O.V. Shum, Amelie Dricot, Marciela M. de Grace, Liguo Wu, Piyush B. Gupta, et al. 2009. “A Physical and Regulatory Map of Host-Influenza Interactions Reveals Pathways in H1N1 Infection.” *Cell* 139 (7) (December 24): 1255–1267. doi:10.1016/j.cell.2009.12.018.

Sjöblom, Tobias, Siân Jones, Laura D Wood, D Williams Parsons, Jimmy Lin, Thomas D Barber, Diana Mandelker, et al. 2006. “The Consensus Coding Sequences of Human Breast and Colorectal Cancers.” *Science (New York, N.Y.)* 314 (5797) (October 13): 268–274. doi:10.1126/science.1133427.

Smith, Matthew J, W. Rod Hardy, James M Murphy, Nina Jones, and Tony Pawson. 2006. “Screening for PTB Domain Binding Partners and Ligand Specificity Using Proteome-Derived NPXY Peptide Arrays.” *Molecular and Cellular Biology* 26 (22) (November 15): 8461–8474. doi:10.1128/MCB.01491-06.

Sussman, J L, D Lin, J Jiang, N O Manning, J Prilusky, O Ritter, and E E Abola. 1998. “Protein Data Bank (PDB): Database of Three-dimensional Structural Information of Biological Macromolecules.” *Acta Crystallographica. Section D, Biological Crystallography* 54 (Pt 6 Pt 1) (November 1): 1078–1084.

Tidyman, William E., and Katherine A. Rauen. 2009. “The RASopathies: Developmental Syndromes of Ras/MAPK Pathway Dysregulation.” *Current Opinion in Genetics & Development* 19 (3) (June): 230–236. doi:10.1016/j.gde.2009.04.001.

Till, Jeffrey H., Manuel Becerra, Anke Watty, Yun Lu, Yuliang Ma, Thomas A. Neubert, Steven J. Burden, and Stevan R. Hubbard. 2002. “Crystal Structure of the MuSK Tyrosine Kinase: Insights into Receptor Autoregulation.” *Structure* 10 (9) (September): 1187–1196. doi:10.1016/S0969-2126(02)00814-6.

Venkatesan, Kavitha, Jean-François Rual, Alexei Vazquez, Ulrich Stelzl, Irma Lemmens, Tomoko Hirozane-Kishikawa, Tong Hao, et al. 2009. "An Empirical Framework for Binary Interactome Mapping." *Nature Methods* 6 (1): 83–90. doi:10.1038/nmeth.1280.

Wachi, Shinichiro, Ken Yoneda, and Reen Wu. 2005. "Interactome-transcriptome Analysis Reveals the High Centrality of Genes Differentially Expressed in Lung Cancer Tissues." *Bioinformatics* 21 (23) (December 1): 4205–4208. doi:10.1093/bioinformatics/bti688.

Wang, Zezhou, Shelley Sandiford, Chenggang Wu, and Shawn Shun-Cheng Li. 2009. "Numb Regulates Cell-cell Adhesion and Polarity in Response to Tyrosine Kinase Signalling." *The EMBO Journal* 28 (16) (August 19): 2360–2373. doi:10.1038/emboj.2009.190.

Wehrman, Tom, Xiaolin He, Bill Raab, Abhiram Dukipatti, Helen Blau, and K. Christopher Garcia. 2007. "Structural and Mechanistic Insights into Nerve Growth Factor Interactions with the TrkA and P75 Receptors." *Neuron* 53 (1) (January 4): 25–38. doi:10.1016/j.neuron.2006.09.034.

Won, Jae-Kyung, Hee Won Yang, Sung-Young Shin, Jong Hoon Lee, Won Do Heo, and Kwang-Hyun Cho. 2012. "The Crossregulation Between ERK and PI3K Signaling Pathways Determines the Tumoricidal Efficacy of MEK Inhibitor." *Journal of Molecular Cell Biology* 4 (3) (June 1): 153–163. doi:10.1093/jmcb/mjs021.

Wunderlich, Zeba, and Leonid A. Mirny. 2009. "Using Genome-wide Measurements for Computational Prediction of SH2-peptide Interactions." *Nucleic Acids Research* 37 (14) (August): 4629–4641. doi:10.1093/nar/gkp394.

Zhou, Songyang, Steven E. Shoelson, Manas Chaudhuri, Gerald Gish, Tony Pawson, Wayne G. Haser, Fred King, et al. 1993. "SH2 Domains Recognize Specific Phosphopeptide Sequences." *Cell* 72 (5) (March 12): 767–778. doi:10.1016/0092-8674(93)90404-E.

APPENDIX

Table 6.1: SH2 and PTB Domains Used in These Studies

Domain	Uniprot	Domain	Start	End
ABL1	P00519	SH2	112	232
BCAR3	O75815	SH2	135	260
BLK	P51451	SH2	112	231
BLNK	Q8WV28	SH2	333	456
BMX	P51813	SH2	284	404
BTK	Q06187	SH2	265	396
CBL	P22681	SH2	47	351
CHN2	P52757	SH2	49	161
CRK	P46108	SH2	1	129
CRKL	P46109	SH2	1	114
DAPP1	Q9UN19	SH2	20	144
FER	P16591	SH2	444	557
FES	P07332	SH2	450	553
FGR	P09769	SH2	127	251
GRAP	Q13588	SH2	49	158
GRB10	Q13322	SH2	479	592
GRB14	Q14449	SH2	424	538
GRB2	P62993	SH2	46	158
GRB7	Q14451	SH2	417	532
HCK	P08631	SH2	134	253
HSH2D	Q96JZ2	SH2	14	132
INPPL1	O15357	SH2	8	131
ITK	Q08881	SH2	220	348
JAK2	O60674	SH2	385	505
JAK3	P52333	SH2	358	484
LCK	P06239	SH2	110	234
LCP2	Q13094	SH2	410	533
LYN	P07948	SH2	114	236
MATK	P42679	SH2	108	224
NCK1	P16333	SH2	270	377
NCK2	O43639	SH2	270	378
PIK3R1-N	P27986	SH2	319	432
PIK3R1-C	P27986	SH2	610	722
PIK3R1-NC	P27986	SH2	434	612

Table 6.1: SH2 and PTB Domains Used in These Studies (Continued)

PIK3R2-N	O00459	SH2	318	431
PIK3R2-C	O00459	SH2	608	726
PIK3R2-NC	O00459	SH2	431	610
PIK3R3-N	Q92569	SH2	53	166
PIK3R3-C	Q92569	SH2	345	461
PIK3R3-NC	Q92569	SH2	166	345
PLCG1-N	P19174	SH2	537	660
PLCG1-C	P19174	SH2	652	762
PLCG1-NC	P19174	SH2	539	664
PLCG2	P16885	SH2	518	643
PLCG2-C	P16885	SH2	631	747
PLCG2-NC	P16885	SH2	520	749
PTK6	Q13882	SH2	62	182
PTPN11-N	Q06124	SH2	1	103
PTPN11-C	Q06124	SH2	101	222
PTPN11-NC	Q06124	SH2	1	222
PTPN6	P29350	SH2	97	221
PTPN6-N	P29350	SH2	1	102
PTPN6-NC	P29350	SH2	1	221
RASA1-C	P20936	SH2	335	448
RASA1-NC	P20936	SH2	168	452
RIN1	Q13671	SH2	54	175
SH2B1	Q9NRF2	SH2	510	630
SH2B2	O14492	SH2	404	523
SH2B3	Q9UQQ2	SH2	348	495
SH2D1A	O60880	SH2	1	108
SH2D1B	O14796	SH2	1	110
SH2D2A	Q9NP31	SH2	79	232
SH2D3A	Q9BRG2	SH2	3	120
SH2D3C	Q8N5H7	SH2	207	326
SH2D5	Q6ZV89	SH2	200	312
SH3BP2	P78314	SH2	449	559
SHB	Q15464	SH2	394	507
SHC1	P29353	SH2	474	581
SHC3	Q92529	SH2	484	592
SHD	Q96IW2	SH2	229	340
SHE	Q5VZ18	SH2	381	493

Table 6.1: SH2 and PTB Domains Used in These Studies (Continued)

SHF	Q7M4L6	SH2	311	423
SLA2	Q9H6Q3	SH2	82	201
SRC	P12931	SH2	134	258
STAP1	Q9ULZ2	SH2	167	285
STAT1	P42224	SH2	565	698
STAT2	P52630	SH2	562	684
STAT3	P40763	SH2	567	688
STAT4	Q14765	SH2	557	679
STAT5A	P42229	SH2	577	687
STAT6	P42226	SH2	521	630
SUPT6H	Q7KZ85	SH2	1304	1446
SYK-C	P43405	SH2	147	269
SYK-N	P43405	SH2	1	112
SYK-NC	P43405	SH2	1	273
TEC	P42680	SH2	235	357
TENC1	Q63HR2	SH2	1121	1259
TNS1	Q9HBL0	SH2	1442	1573
TNS3	Q68CZ2	SH2	1161	1286
TNS4	Q8IZW8	SH2	438	564
TXK	P42681	SH2	138	256
VAV1	P15498	SH2	658	769
VAV2	P52735	SH2	659	772
VAV3	Q9UKW4	SH2	656	768
YES1	P07947	SH2	144	266
ZAP70-C	P43403	SH2	142	264
ZAP70-N	P43403	SH2	1	118
ZAP70-NC	P43403	SH2	1	268
ANKS1A	Q92625	PTB	924	1092
ANKS1B	Q7Z6G8	PTB	1023	1225
APBA1	Q02410	PTB	420	671
APBA2	Q99767	PTB	313	581
APBA3	O96018	PTB	179	387
APBB1-N	O00213	PTB	332	522
APBB1-C	O00213	PTB	523	708
APBB1-NC	O00213	PTB	332	710
APBB2-N	Q92870	PTB	417	565
APBB2-C	Q92870	PTB	565	755

Table 6.1: SH2 and PTB Domains Used in These Studies (Continued)

APBB2-NC	Q92870	PTB	419	759
APBB3-N	O95704	PTB	81	266
APBB3-C	O95704	PTB	266	481
APBB3-NC	O95704	PTB	81	505
APPL1	Q9UKG1	PTB	491	632
CCM2	Q9BSQ5	PTB	51	235
DAB1	O75553	PTB	1	227
DAB2	P98082	PTB	1	226
DOK1	Q99704	PTB	121	290
DOK2	O60496	PTB	115	280
DOK4	Q8TEW6	PTB	101	258
DOK5	Q9P104	PTB	101	268
DOK6	Q6PKX4	PTB	105	262
EPS8L2	Q9H6S3	PTB	52	204
FRS3	O43559	PTB	1	140
GULP1	Q9UBP9	PTB	13	165
IRS1	P35568	PTB	114	308
IRS4	O14654	PTB	199	364
NUMB	P49757	PTB	1	220
NUMBL	Q9Y6R0	PTB	51	251
SHC1-PTB	P29353	PTB	121	379
SHC2	P98077	PTB	94	330
SHC3	Q92529	PTB	224	319
TENC1-PTB	Q63HR2	PTB	1260	1405
TNS1-PTB	Q9HBL0	PTB	1574	1725

Table 6.2: Sub micromolar interactions identified in these studies

Adaptor	Uniprot Id	Protein	pY Site	Uniprot Id	Kd (μM)
PIK3R1-N	P27986	EPHA3	Y779	P29320	0.992842
PIK3R1-N	P27986	EPHA4	Y779	P54764	0.992842
PIK3R1-N	P27986	EPHA5	Y833	P54756	0.992842
PIK3R1-N	P27986	EPHA4	Y602	P54764	0.431994
PIK3R1-N	P27986	FGFR1	Y730	P11362	0.426785
PIK3R1-N	P27986	FGFR3	Y724	P22607	0.244469
PIK3R1-N	P27986	FLT1	Y1213	P17948	0.796538
PIK3R1-N	P27986	KDR	Y1059	P35968	0.762434
PIK3R1-N	P27986	KIT	Y900	P10721	0.513097
PIK3R1-N	P27986	MST1R	Y1317	Q04912	0.216106
PIK3R1-N	P27986	NTRK2	Y706	Q16620	0.786309
PIK3R1-N	P27986	NTRK3	Y709	Q16288	0.786309
PIK3R1-N	P27986	NTRK2	Y707	Q16620	0.395866
PIK3R1-N	P27986	NTRK3	Y710	Q16288	0.395866
PIK3R1-N	P27986	PDGFRA	Y742	P16234	0.360627
PIK3R1-N	P27986	PDGFRB	Y740	P09619	0.155778
PIK3R1-N	P27986	ERBB4	Y1056	Q15303	0.710236
PIK3R1-N	P27986	ERBB2	Y1139	P04626	0.753057
PIK3R1-N	P27986	ERBB3	Y1197	P21860	0.147163
PIK3R1-N	P27986	ABL2	Y515	P42684	0.295444
PIK3R1-N	P27986	ZAP70	Y493	P43403	0.629901
PIK3R1-N	P27986	TXK	Y420	P42681	0.393795
PIK3R1-N	P27986	FES	Y811	P07332	0.386173
PIK3R1-N	P27986	PLCG1	Y775	P19174	0.698607
PIK3R1-N	P27986	PLCG2	Y1217	P16885	0.667422
PIK3R1-N	P27986	GRAP2	Y45	O75791	0.526474
PIK3R1-N	P27986	NCK1	Y268	P16333	0.578606
PIK3R1-N	P27986	SHC1	Y427	P29353	0.689798
PIK3R1-N	P27986	JAK3	Y785	P52333	0.180054
PIK3R1-N	P27986	SH2D3A	Y231	Q9BRG2	0.694002
PIK3R1-N	P27986	SH2D2A	Y280	Q9NP31	0.861829
PIK3R1-N	P27986	VAV2	Y172	P52735	0.713453
PIK3R1-N	P27986	PTPN6	Y536	P29350	0.654597
PIK3R1-N	P27986	CBL	Y371	P22681	0.600737
PIK3R1-N	P27986	CBLB	Y363	Q13191	0.600737
PIK3R1-N	P27986	DOK1	Y362	Q99704	0.31038

Table 6.2: Sub micromolar interactions identified in these studies (Continued)

PIK3R1-N	P27986	EPHB4	Y774	P54760	0.145616
PIK3R1-N	P27986	IRS1	Y465	P35568	0.758214
PIK3R1-N	P27986	IRS1	Y612	P35568	0.297814
PIK3R1-N	P27986	IRS1	Y989	P35568	0.617862
PIK3R1-N	P27986	ZAP70	Y319	P43403	0.584842
PIK3R1-N	P27986	BMX	Y216	P51813	0.507805
PIK3R1-N	P27986	PDGFRB	Y934	P09619	0.612879
PIK3R1-N	P27986	ROS1	Y2342	P08922	0.675277
PIK3R1-N	P27986	PIK3CB	Y246	P42338	0.653475
PIK3R1-N	P27986	NCK2	Y50	O43639	0.581543
PIK3R1-N	P27986	SHB	Y272	Q15464	0.603671
PIK3R1-N	P27986	IRS4	Y921	O14654	0.306591
PIK3R1-N	P27986	ANKS1A	Y454	Q92625	0.968243
PIK3R1-C	P27986	EPHA3	Y596	P29320	0.866703
PIK3R1-C	P27986	FGFR1	Y463	P11362	0.357871
PIK3R1-C	P27986	FGFR1	Y730	P11362	0.351668
PIK3R1-C	P27986	FGFR3	Y724	P22607	0.278032
PIK3R1-C	P27986	NTRK1	Y496	P04629	0.875405
PIK3R1-C	P27986	NTRK2	Y706	Q16620	0.992394
PIK3R1-C	P27986	NTRK3	Y709	Q16288	0.992394
PIK3R1-C	P27986	NTRK3	Y516	Q16288	0.867029
PIK3R1-C	P27986	ROS1	Y2334	P08922	0.956608
PIK3R1-C	P27986	RET	Y952	P07949	0.726299
PIK3R1-C	P27986	EPHA2	Y735	P29317	0.867606
PIK3R1-C	P27986	ABL1	Y412	P00519	0.351166
PIK3R1-C	P27986	FGR	Y412	P09769	0.948546
PIK3R1-C	P27986	PLCG1	Y783	P19174	0.830702
PIK3R1-C	P27986	VAV2	Y172	P52735	0.969825
PIK3R1-C	P27986	IRS1	Y662	P35568	0.647556
PIK3R1-C	P27986	IRS1	Y989	P35568	0.933089
PIK3R1-C	P27986	ZAP70	Y69	P43403	0.531278
PIK3R1-C	P27986	SRC	Y521	P12931	0.472004
PIK3R1-C	P27986	BTK	Y225	Q06187	0.220062
PIK3R1-C	P27986	IRS4	Y921	O14654	0.530788
PIK3R1-NC	P27986	EPHA3	Y602	P29320	0.989368
PIK3R1-NC	P27986	FGFR1	Y730	P11362	0.508023
PIK3R1-NC	P27986	FGFR3	Y724	P22607	0.24913
PIK3R1-NC	P27986	FLT1	Y1213	P17948	0.327832
PIK3R1-NC	P27986	IGF1R	Y1346	P08069	0.563199
PIK3R1-NC	P27986	INSR	Y1011	P06213	0.616807

Table 6.2: Sub micromolar interactions identified in these studies (Continued)

PIK3R1-NC	P27986	INSR	Y1361	P06213	0.277565
PIK3R1-NC	P27986	KDR	Y1059	P35968	0.998675
PIK3R1-NC	P27986	KIT	Y900	P10721	0.157236
PIK3R1-NC	P27986	MET	Y1356	P08581	0.408076
PIK3R1-NC	P27986	MST1R	Y1317	Q04912	0.213602
PIK3R1-NC	P27986	NTRK1	Y496	P04629	0.72195
PIK3R1-NC	P27986	PDGFRA	Y574	P16234	0.252781
PIK3R1-NC	P27986	PDGFRB	Y579	P09619	0.995754
PIK3R1-NC	P27986	PDGFRB	Y740	P09619	0.332446
PIK3R1-NC	P27986	PDGFRB	Y763	P09619	0.423616
PIK3R1-NC	P27986	RET	Y981	P07949	0.262998
PIK3R1-NC	P27986	ERBB4	Y1056	Q15303	0.814685
PIK3R1-NC	P27986	EGFR	Y998	P00533	0.330541
PIK3R1-NC	P27986	EGFR	Y1016	P00533	0.216375
PIK3R1-NC	P27986	EGFR	Y1092	P00533	0.433733
PIK3R1-NC	P27986	EGFR	Y1138	P00533	0.807115
PIK3R1-NC	P27986	ERBB2	Y1221	P04626	0.728121
PIK3R1-NC	P27986	ERBB3	Y1054	P21860	0.945453
PIK3R1-NC	P27986	ERBB3	Y1199	P21860	0.727357
PIK3R1-NC	P27986	ERBB3	Y1276	P21860	0.319315
PIK3R1-NC	P27986	RET	Y952	P07949	0.619382
PIK3R1-NC	P27986	EPHA2	Y628	P29317	0.8053
PIK3R1-NC	P27986	EPHA2	Y921	P29317	0.745884
PIK3R1-NC	P27986	ABL2	Y515	P42684	0.137027
PIK3R1-NC	P27986	FYN	Y420	P06241	0.453753
PIK3R1-NC	P27986	SRC	Y419	P12931	0.453753
PIK3R1-NC	P27986	YES1	Y426	P07947	0.453753
PIK3R1-NC	P27986	ZAP70	Y248	P43403	0.720679
PIK3R1-NC	P27986	TXK	Y420	P42681	0.222524
PIK3R1-NC	P27986	HCK	Y209	P08631	0.729415
PIK3R1-NC	P27986	PTK6	Y342	Q13882	0.417406
PIK3R1-NC	P27986	FES	Y811	P07332	0.677834
PIK3R1-NC	P27986	PLCG1	Y783	P19174	0.749776
PIK3R1-NC	P27986	NCK1	Y268	P16333	0.878331
PIK3R1-NC	P27986	SH3BP2	Y183	P78314	0.731312
PIK3R1-NC	P27986	JAK3	Y785	P52333	0.252956
PIK3R1-NC	P27986	BLNK	Y84	Q8WV28	0.166578
PIK3R1-NC	P27986	VAV1	Y160	P15498	0.784962
PIK3R1-NC	P27986	VAV1	Y174	P15498	0.361554
PIK3R1-NC	P27986	PTPN6	Y564	P29350	0.455606

Table 6.2: Sub micromolar interactions identified in these studies (Continued)

PIK3R1-NC	P27986	CBL	Y368	P22681	0.499943
PIK3R1-NC	P27986	CBL	Y371	P22681	0.330579
PIK3R1-NC	P27986	CBLB	Y363	Q13191	0.330579
PIK3R1-NC	P27986	CBL	Y700	P22681	0.813982
PIK3R1-NC	P27986	DOK1	Y146	Q99704	0.718682
PIK3R1-NC	P27986	EPHB3	Y608	P54753	0.57567
PIK3R1-NC	P27986	IRS1	Y941	P35568	0.145369
PIK3R1-NC	P27986	IRS1	Y989	P35568	0.286464
PIK3R1-NC	P27986	IRS2	Y653	Q9Y4H2	0.566533
PIK3R1-NC	P27986	GAB1	Y373	Q13480	0.62363
PIK3R1-NC	P27986	CSK	Y263	P41240	0.674614
PLCG1-N	P19174	KIT	Y721	P10721	0.156814
PLCG1-N	P19174	ROS1	Y2274	P08922	0.321813
PLCG1-N	P19174	FRS2	Y436	Q8WU20	0.751277
PLCG1-N	P19174	ERBB2	Y1127	P04626	0.43883
PLCG1-N	P19174	FGFR2	Y466	P21802	0.447897
PLCG1-N	P19174	IRS4	Y921	O14654	0.846191
PLCG1-C	P19174	AXL	Y866	P30530	0.467486
PLCG1-C	P19174	FGFR1	Y585	P11362	0.950479
PLCG1-C	P19174	NTRK1	Y496	P04629	0.767983
PLCG1-C	P19174	EPHA7	Y608	Q15375	0.829249
PLCG1-C	P19174	PLCG2	Y1245	P16885	0.649951
PLCG1-C	P19174	CBL	Y371	P22681	0.645106
PLCG1-C	P19174	CBLB	Y363	Q13191	0.645106
PLCG1-C	P19174	HSH2D	Y265	Q96JZ2	0.640045
PLCG1-C	P19174	PTK2B	Y849	Q14289	0.869204
PLCG1-NC	P19174	FGFR3	Y724	P22607	0.463045
PLCG1-NC	P19174	FLT1	Y1327	P17948	0.826507
PLCG1-NC	P19174	FLT1	Y1333	P17948	0.508594
PLCG1-NC	P19174	KIT	Y721	P10721	0.341182
PLCG1-NC	P19174	KIT	Y900	P10721	0.782461
PLCG1-NC	P19174	KIT	Y936	P10721	0.895221
PLCG1-NC	P19174	MET	Y1365	P08581	0.991527
PLCG1-NC	P19174	MST1R	Y1317	Q04912	0.969104
PLCG1-NC	P19174	NTRK3	Y516	Q16288	0.920632
PLCG1-NC	P19174	ERBB2	Y1139	P04626	0.711685
PLCG1-NC	P19174	ERBB3	Y1289	P21860	0.604968
PLCG1-NC	P19174	TXK	Y420	P42681	0.772389
PLCG1-NC	P19174	PLCG1	Y472	P19174	0.627038
PLCG1-NC	P19174	PLCG1	Y783	P19174	0.558081

Table 6.2: Sub micromolar interactions identified in these studies (Continued)

PLCG1-NC	P19174	PLCG2	Y1217	P16885	0.617156
PLCG1-NC	P19174	NCK1	Y268	P16333	0.763537
PLCG1-NC	P19174	CBL	Y371	P22681	0.698794
PLCG1-NC	P19174	CBLB	Y363	Q13191	0.698794
PLCG1-NC	P19174	EPHA5	Y656	P54756	0.94524
PLCG1-NC	P19174	ERBB2	Y1127	P04626	0.284964
PLCG1-NC	P19174	IRS1	Y465	P35568	0.499646
PLCG1-NC	P19174	KIT	Y730	P10721	0.792031
PLCG1-NC	P19174	FGFR2	Y466	P21802	0.498434
PLCG1-NC	P19174	ABL1	Y204	P00519	0.931565
PLCG1-NC	P19174	MERTK	Y929	Q12866	0.904937
PLCG1-NC	P19174	PIK3CB	Y246	P42338	0.907801
PLCG1-NC	P19174	PLCG1	Y1253	P19174	0.680696
PLCG1-NC	P19174	PLCG2	Y759	P16885	0.714683
PLCG1-NC	P19174	NCK1	Y112	P16333	0.596646
PLCG1-NC	P19174	BCAR3	Y117	O75815	0.566937
PLCG1-NC	P19174	BCAR3	Y429	O75815	0.912581
PLCG1-NC	P19174	PTPN6	Y541	P29350	0.570099
PLCG1-NC	P19174	CBL	Y731	P22681	0.578916
PLCG1-NC	P19174	CBLB	Y889	Q13191	0.724476
PLCG1-NC	P19174	STAT1	Y203	P42224	0.906056
PLCG1-NC	P19174	APBB1	Y547	O00213	0.787488
PLCG1-NC	P19174	IRS4	Y921	O14654	0.614164
PLCG1-NC	P19174	CSK	Y263	P41240	0.928201
PLCG1-NC	P19174	PTK2	Y5	Q05397	0.3871
PLCG1-NC	P19174	PTK2B	Y849	Q14289	0.48127
PLCG1-NC	P19174	CTNNB1	Y64	P35222	0.569265
PTPN11-C	Q06124	PDGFRB	Y740	P09619	0.223661
PTPN11-C	Q06124	ROS1	Y2274	P08922	0.511486
PTPN11-C	Q06124	EPHA7	Y791	Q15375	0.782353
PTPN11-C	Q06124	FYN	Y420	P06241	0.966945
PTPN11-C	Q06124	SRC	Y419	P12931	0.966945
PTPN11-C	Q06124	YES1	Y426	P07947	0.966945
PTPN11-C	Q06124	GRB2	Y209	P62993	0.927502
PTPN11-C	Q06124	PIK3R1	Y467	P27986	0.896784
PTPN11-C	Q06124	TNS1	Y339	Q9HBL0	0.199096
PTPN11-NC	Q06124	FLT1	Y1327	P17948	0.492911
PTPN11-NC	Q06124	INSR	Y1011	P06213	0.743534
PTPN11-NC	Q06124	FLT4	Y1063	P35916	0.753535
PTPN11-NC	Q06124	KDR	Y1054	P35968	0.753535

Table 6.2: Sub micromolar interactions identified in these studies (Continued)

PTPN11-NC	Q06124	NTRK3	Y516	Q16288	0.790381
PTPN11-NC	Q06124	FRS2	Y436	Q8WU20	0.792149
PTPN11-NC	Q06124	PLCG2	Y1217	P16885	0.487206
PTPN11-NC	Q06124	PLCG2	Y1245	P16885	0.890514
PTPN11-NC	Q06124	CBL	Y371	P22681	0.779886
PTPN11-NC	Q06124	CBLB	Y363	Q13191	0.779886
PTPN11-NC	Q06124	DAB1	Y220	O75553	0.187434
PTPN11-NC	Q06124	DOK1	Y146	Q99704	0.434321
PTPN11-NC	Q06124	IRS2	Y675	Q9Y4H2	0.648714
APBB1-N	O00213	EPHA3	Y596	P29320	0.423237
APBB1-N	O00213	PLCG2	Y1245	P16885	0.963279
APBB1-N	O00213	DOK1	Y315	Q99704	0.754687
APBB1-N	O00213	IRS1	Y465	P35568	0.916948
APBB1-N	O00213	IRS2	Y675	Q9Y4H2	0.866369
APBB1-N	O00213	ABL2	Y683	P42684	0.946056
APBB1-N	O00213	SYK	Y203	P43405	0.892074
APBB1-C	O00213	NTRK3	Y516	Q16288	0.868648
APBB1-C	O00213	IRS1	Y465	P35568	0.973194
APBB2-N	Q92870	VAV2	Y172	P52735	0.864078
APBB3-N	O95704	IRS1	Y989	P35568	0.746694
APBB3-N	O95704	ABL1	Y191	P00519	0.917416
APBB3-C	O95704	IRS2	Y675	Q9Y4H2	0.31856
APBB3-C	O95704	ABL1	Y191	P00519	0.777657
APBA1	Q02410	SHC1	Y350	P29353	0.686694
APBA2	Q99767	DOK1	Y315	Q99704	0.991871
STAT1	P42224	ALK	Y1092	Q9UM73	0.597352
STAT1	P42224	ALK	Y1096	Q9UM73	0.611407
STAT1	P42224	FGFR1	Y730	P11362	0.377798
STAT1	P42224	FGFR3	Y724	P22607	0.881298
STAT1	P42224	FLT1	Y1327	P17948	0.923726
STAT1	P42224	FLT3	Y597	P36888	0.551359
STAT1	P42224	FLT3	Y599	P36888	0.4865
STAT1	P42224	FLT4	Y1337	P35916	0.765492
STAT1	P42224	IGF1R	Y1161	P08069	0.865635
STAT1	P42224	INSR	Y1185	P06213	0.865635
STAT1	P42224	IGF1R	Y1280	P08069	0.675169
STAT1	P42224	INSR	Y1011	P06213	0.768642
STAT1	P42224	KIT	Y570	P10721	0.798863
STAT1	P42224	KIT	Y900	P10721	0.942345
STAT1	P42224	MST1R	Y1317	Q04912	0.741368

Table 6.2: Sub micromolar interactions identified in these studies (Continued)

STAT1	P42224	NTRK1	Y496	P04629	0.647238
STAT1	P42224	NTRK2	Y706	Q16620	0.891127
STAT1	P42224	NTRK3	Y709	Q16288	0.891127
STAT1	P42224	NTRK2	Y707	Q16620	0.607542
STAT1	P42224	NTRK3	Y710	Q16288	0.607542
STAT1	P42224	NTRK3	Y516	Q16288	0.799565
STAT1	P42224	PDGFRB	Y581	P09619	0.625261
STAT1	P42224	PDGFRB	Y751	P09619	0.870689
STAT1	P42224	PDGFRB	Y775	P09619	0.463376
STAT1	P42224	PDGFRB	Y1021	P09619	0.925029
STAT1	P42224	RET	Y791	P07949	0.485331
STAT1	P42224	RET	Y806	P07949	0.642974
STAT1	P42224	RET	Y981	P07949	0.590296
STAT1	P42224	TEK	Y1102	Q02763	0.960307
STAT1	P42224	ERBB2	Y1221	P04626	0.73832
STAT1	P42224	ERBB2	Y1222	P04626	0.36864
STAT1	P42224	FGR	Y412	P09769	0.653203
STAT1	P42224	ZAP70	Y315	P43403	0.934525
STAT1	P42224	ZAP70	Y474	P43403	0.760738
STAT1	P42224	FES	Y811	P07332	0.488148
STAT1	P42224	PLCG2	Y743	P16885	0.463266
STAT1	P42224	GRAP2	Y45	O75791	0.43481
STAT1	P42224	RASA1	Y615	P20936	0.575295
STAT1	P42224	SH2D2A	Y39	Q9NP31	0.70762
STAT1	P42224	SH2D2A	Y290	Q9NP31	0.955433
STAT1	P42224	PTPN6	Y536	P29350	0.754849
STAT1	P42224	DOK1	Y398	Q99704	0.653589
STAT1	P42224	FLT4	Y853	P35916	0.817403
STAT1	P42224	EPHA2	Y694	P29317	0.394144
STAT1	P42224	PDGFRA	Y958	P16234	0.955757
STAT1	P42224	ABL2	Y568	P42684	0.596368
STAT1	P42224	ABL1	Y191	P00519	0.869398
STAT1	P42224	ZAP70	Y69	P43403	0.379163
STAT1	P42224	STAT3	Y686	P40763	0.154844
STAT1	P42224	TNS1	Y339	Q9HBL0	0.590149
STAT1	P42224	TNS1	Y1404	Q9HBL0	0.84694
STAT1	P42224	DOK3	Y432	Q7L591	0.380145
STAT1	P42224	CSK	Y263	P41240	0.586253
STAT1	P42224	PTK2	Y5	Q05397	0.538651
STAT2	P52630	ALK	Y1092	Q9UM73	0.457682

Table 6.2: Sub micromolar interactions identified in these studies (Continued)

STAT2	P52630	AXL	Y866	P30530	0.786808
STAT2	P52630	FGFR1	Y730	P11362	0.971215
STAT2	P52630	FGFR3	Y724	P22607	0.453742
STAT2	P52630	FLT1	Y1333	P17948	0.634384
STAT2	P52630	FLT3	Y591	P36888	0.902217
STAT2	P52630	FLT3	Y597	P36888	0.319258
STAT2	P52630	FLT3	Y599	P36888	0.474452
STAT2	P52630	FLT4	Y1337	P35916	0.764998
STAT2	P52630	IGF1R	Y1280	P08069	0.747779
STAT2	P52630	INSR	Y1011	P06213	0.547969
STAT2	P52630	KDR	Y996	P35968	0.903331
STAT2	P52630	KIT	Y570	P10721	0.551262
STAT2	P52630	KIT	Y900	P10721	0.760358
STAT2	P52630	KIT	Y936	P10721	0.778786
STAT2	P52630	MET	Y1313	P08581	0.393904
STAT2	P52630	MET	Y1356	P08581	0.434497
STAT2	P52630	MST1R	Y1317	Q04912	0.352203
STAT2	P52630	NTRK3	Y516	Q16288	0.396016
STAT2	P52630	PDGFRB	Y1009	P09619	0.835574
STAT2	P52630	RET	Y981	P07949	0.154832
STAT2	P52630	RET	Y1096	P07949	0.966577
STAT2	P52630	ROS1	Y2274	P08922	0.780933
STAT2	P52630	ERBB2	Y1023	P04626	0.70289
STAT2	P52630	ERBB2	Y1221	P04626	0.56298
STAT2	P52630	ERBB2	Y1222	P04626	0.307909
STAT2	P52630	LCK	Y192	P06239	0.718302
STAT2	P52630	PLCG2	Y1245	P16885	0.88968
STAT2	P52630	RASA1	Y615	P20936	0.336722
STAT2	P52630	INSR	Y1149	P06213	0.434825
STAT2	P52630	IRS1	Y732	P35568	0.828657
STAT2	P52630	IRS2	Y628	Q9Y4H2	0.595462
STAT2	P52630	IRS2	Y823	Q9Y4H2	0.96041
STAT2	P52630	MERTK	Y929	Q12866	0.723573
STAT2	P52630	PIK3R3	Y199	Q92569	0.460031
STAT2	P52630	PIK3R3	Y202	Q92569	0.885941
STAT2	P52630	FER	Y615	P16591	0.188177
STAT2	P52630	PTPN11	Y279	Q06124	0.136066
STAT2	P52630	TNS1	Y339	Q9HBL0	0.977454
STAT2	P52630	TNS1	Y609	Q9HBL0	0.161107
STAT2	P52630	TNS1	Y1323	Q9HBL0	0.803293

Table 6.2: Sub micromolar interactions identified in these studies (Continued)

STAT3	P40763	EPHA4	Y596	P54764	0.967603
STAT3	P40763	ABL1	Y412	P00519	0.6392
STAT3	P40763	DOK1	Y315	Q99704	0.634271
STAT3	P40763	IRS1	Y732	P35568	0.96908
STAT3	P40763	IRS2	Y675	Q9Y4H2	0.782215
STAT4	Q14765	ABL1	Y412	P00519	0.768737
STAT4	Q14765	ABL1	Y488	P00519	0.718808
STAT4	Q14765	DOK1	Y315	Q99704	0.96734
STAT5A	P42229	FLT4	Y1068	P35916	0.136262
STAT5A	P42229	INSR	Y1149	P06213	0.542657
STAT5A	P42229	IRS1	Y465	P35568	0.69113
STAT5A	P42229	IRS2	Y823	Q9Y4H2	0.791466
STAT5A	P42229	TNS1	Y366	Q9HBL0	0.741576
STAT5A	P42229	TNS1	Y796	Q9HBL0	0.405017
STAT5A	P42229	CSK	Y263	P41240	0.999448
STAT6	P42226	PLCG2	Y1245	P16885	0.996953
STAT6	P42226	ABL1	Y191	P00519	0.839248
STAT6	P42226	TNS1	Y796	Q9HBL0	0.785009
FGR	P09769	ALK	Y1092	Q9UM73	0.807365
FGR	P09769	EPHA4	Y602	P54764	0.692983
FGR	P09769	EPHB1	Y600	P54762	0.813246
FGR	P09769	EPHB2	Y602	P29323	0.813246
FGR	P09769	FGFR3	Y724	P22607	0.652358
FGR	P09769	FGFR3	Y770	P22607	0.961136
FGR	P09769	FLT3	Y589	P36888	0.961136
FGR	P09769	FLT3	Y597	P36888	0.283126
FGR	P09769	FLT3	Y599	P36888	0.356976
FGR	P09769	FLT4	Y1063	P35916	0.461362
FGR	P09769	KDR	Y1054	P35968	0.461362
FGR	P09769	KIT	Y721	P10721	0.4756
FGR	P09769	KIT	Y900	P10721	0.415806
FGR	P09769	KIT	Y936	P10721	0.650369
FGR	P09769	MET	Y1313	P08581	0.209711
FGR	P09769	MET	Y1356	P08581	0.947853
FGR	P09769	MST1R	Y1317	Q04912	0.495535
FGR	P09769	NTRK1	Y496	P04629	0.845914
FGR	P09769	NTRK2	Y702	Q16620	0.768861
FGR	P09769	NTRK3	Y705	Q16288	0.768861
FGR	P09769	PDGFRB	Y740	P09619	0.705074
FGR	P09769	RET	Y900	P07949	0.741499

Table 6.2: Sub micromolar interactions identified in these studies (Continued)

FGR	P09769	RET	Y1096	P07949	0.755762
FGR	P09769	EGFR	Y1172	P00533	0.681239
FGR	P09769	ERBB2	Y1221	P04626	0.431439
FGR	P09769	ERBB3	Y1197	P21860	0.706646
FGR	P09769	ERBB3	Y1289	P21860	0.358075
FGR	P09769	EPHA2	Y735	P29317	0.969841
FGR	P09769	EPHA7	Y597	Q15375	0.673411
FGR	P09769	EPHA7	Y614	Q15375	0.660769
FGR	P09769	ABL1	Y245	P00519	0.782787
FGR	P09769	ABL1	Y276	P00519	0.369299
FGR	P09769	FYN	Y420	P06241	0.532507
FGR	P09769	SRC	Y419	P12931	0.532507
FGR	P09769	YES1	Y426	P07947	0.532507
FGR	P09769	EPHA1	Y605	P21709	0.69312
FGR	P09769	SYK	Y323	P43405	0.475592
FGR	P09769	HCK	Y209	P08631	0.909464
FGR	P09769	PTK6	Y342	Q13882	0.546378
FGR	P09769	LCK	Y192	P06239	0.930584
FGR	P09769	FES	Y811	P07332	0.769762
FGR	P09769	PLCG1	Y771	P19174	0.917296
FGR	P09769	PTPN11	Y62	Q06124	0.860495
FGR	P09769	SH3BP2	Y174	P78314	0.6036
FGR	P09769	SH3BP2	Y183	P78314	0.659309
FGR	P09769	SHC1	Y349	P29353	0.368218
FGR	P09769	SHC1	Y427	P29353	0.920724
FGR	P09769	JAK3	Y785	P52333	0.889518
FGR	P09769	LCP2	Y128	Q13094	0.587323
FGR	P09769	LCP2	Y145	Q13094	0.846775
FGR	P09769	BLNK	Y72	Q8WV28	0.562045
FGR	P09769	BLNK	Y84	Q8WV28	0.841612
FGR	P09769	BLNK	Y178	Q8WV28	0.717231
FGR	P09769	SH2D2A	Y305	Q9NP31	0.809557
FGR	P09769	SH2D3C	Y495	Q8N5H7	0.852269
FGR	P09769	VAV1	Y142	P15498	0.721767
FGR	P09769	VAV1	Y174	P15498	0.550635
FGR	P09769	VAV2	Y159	P52735	0.576858
FGR	P09769	VAV2	Y172	P52735	0.686303
FGR	P09769	CBL	Y368	P22681	0.620303
FGR	P09769	CBL	Y371	P22681	0.702645
FGR	P09769	CBLB	Y363	Q13191	0.702645

Table 6.2: Sub micromolar interactions identified in these studies (Continued)

FGR	P09769	CBL	Y774	P22681	0.501711
FGR	P09769	DAB1	Y198	O75553	0.389253
FGR	P09769	DOK1	Y146	Q99704	0.752308
FGR	P09769	DOK1	Y296	Q99704	0.732111
FGR	P09769	DOK1	Y315	Q99704	0.771126
FGR	P09769	DOK1	Y362	Q99704	0.708328
FGR	P09769	DOK1	Y377	Q99704	0.849714
FGR	P09769	DOK2	Y345	O60496	0.979642
FGR	P09769	EPHA3	Y937	P29320	0.65836
FGR	P09769	EPHB3	Y608	P54753	0.827312
FGR	P09769	EPHB3	Y754	P54753	0.66284
FGR	P09769	EPHB4	Y596	P54760	0.947729
FGR	P09769	IRS1	Y662	P35568	0.562586
FGR	P09769	IRS1	Y896	P35568	0.953107
FGR	P09769	IRS1	Y989	P35568	0.766203
FGR	P09769	IRS1	Y1179	P35568	0.805941
FGR	P09769	IRS2	Y632	Q9Y4H2	0.76278
FGR	P09769	IRS2	Y653	Q9Y4H2	0.996095
FGR	P09769	IRS2	Y823	Q9Y4H2	0.962522
FGR	P09769	GAB1	Y406	Q13480	0.271278
FGR	P09769	FGFR2	Y466	P21802	0.872532
FGR	P09769	EPHA2	Y930	P29317	0.8007
FGR	P09769	ZAP70	Y319	P43403	0.995828
FGR	P09769	PIK3R1	Y528	P27986	0.876338
FGR	P09769	ZAP70	Y69	P43403	0.772009
FGR	P09769	SYK	Y203	P43405	0.985349
FGR	P09769	PLCG1	Y1253	P19174	0.896801
FGR	P09769	PTPN11	Y584	Q06124	0.83587
FGR	P09769	RIN1	Y632	Q13671	0.707133
FGR	P09769	CHN2	Y21	P52757	0.893389
FGR	P09769	BCAR3	Y429	O75815	0.765136
FGR	P09769	VAV1	Y826	P15498	0.443437
FGR	P09769	VAV3	Y173	Q9UKW4	0.749646
FGR	P09769	SHB	Y297	Q15464	0.765108
FGR	P09769	SHB	Y336	Q15464	0.359336
FGR	P09769	TNS1	Y796	Q9HBL0	0.794286
FGR	P09769	CBL	Y731	P22681	0.430551
FGR	P09769	APBB1	Y547	O00213	0.766893
FGR	P09769	DAB2	Y342	P98082	0.607378
FGR	P09769	DOK3	Y208	Q7L591	0.552494

Table 6.2: Sub micromolar interactions identified in these studies (Continued)

FGR	P09769	DOK4	Y255	Q8TEW6	0.626702
FGR	P09769	IRS4	Y921	O14654	0.611249
FGR	P09769	CSK	Y263	P41240	0.574304
FGR	P09769	PTK2	Y861	Q05397	0.734391
FGR	P09769	PTK2B	Y580	Q14289	0.602848
FGR	P09769	PTK2B	Y834	Q14289	0.821619
GRB2	P62993	FGFR3	Y724	P22607	0.762506
GRB2	P62993	FLT1	Y1213	P17948	0.366702
GRB2	P62993	INSR	Y1011	P06213	0.807897
GRB2	P62993	KIT	Y936	P10721	0.406433
GRB2	P62993	MET	Y1313	P08581	0.90774
GRB2	P62993	MET	Y1356	P08581	0.262136
GRB2	P62993	MST1R	Y1317	Q04912	0.970287
GRB2	P62993	RET	Y1096	P07949	0.158621
GRB2	P62993	TEK	Y1113	Q02763	0.954263
GRB2	P62993	FRS2	Y196	Q8WU20	0.761346
GRB2	P62993	EGFR	Y1092	P00533	0.312085
GRB2	P62993	EGFR	Y1138	P00533	0.38272
GRB2	P62993	ERBB2	Y1139	P04626	0.529508
GRB2	P62993	EPHA7	Y614	Q15375	0.67471
GRB2	P62993	ABL1	Y276	P00519	0.47088
GRB2	P62993	FYN	Y420	P06241	0.363214
GRB2	P62993	SRC	Y419	P12931	0.363214
GRB2	P62993	YES1	Y426	P07947	0.363214
GRB2	P62993	PLCG2	Y1217	P16885	0.169385
GRB2	P62993	EPHB1	Y575	P54762	0.689033
GRB2	P62993	ERBB2	Y735	P04626	0.701509
GRB2	P62993	ERBB2	Y1005	P04626	0.903653
GRB2	P62993	ABL2	Y272	P42684	0.582755
GRB2	P62993	ABL2	Y683	P42684	0.977271
GRB2	P62993	ABL1	Y191	P00519	0.820656
GRB2	P62993	ABL1	Y234	P00519	0.849815
GRB2	P62993	SRC	Y521	P12931	0.804124
GRB2	P62993	SYK	Y203	P43405	0.342176
GRB2	P62993	FYN	Y531	P06241	0.63852
GRB2	P62993	YES1	Y537	P07947	0.63852
GRB2	P62993	PTPN11	Y279	Q06124	0.306572
GRB2	P62993	PTPN11	Y304	Q06124	0.628023
GRB2	P62993	PTPN11	Y584	Q06124	0.43784
GRB2	P62993	TNS1	Y366	Q9HBL0	0.91334

Table 6.2: Sub micromolar interactions identified in these studies (Continued)

GRB2	P62993	TNS1	Y903	Q9HBL0	0.828437
GRB2	P62993	CSK	Y263	P41240	0.65581
GRAP	Q13588	INSR	Y1011	P06213	0.473537
GRAP	Q13588	MET	Y1356	P08581	0.971152
GRAP	Q13588	NTRK1	Y496	P04629	0.654807
GRAP	Q13588	PDGFRB	Y581	P09619	0.454764
GRAP	Q13588	RET	Y1096	P07949	0.834892
GRAP	Q13588	ABL2	Y515	P42684	0.788826
GRAP	Q13588	ABL1	Y276	P00519	0.535505
GRAP	Q13588	PLCG1	Y775	P19174	0.953276
GRAP	Q13588	ANKS1A	Y833	Q92625	0.416368
CRK	P46108	ALK	Y1092	Q9UM73	0.960923
CRK	P46108	FGFR1	Y653	P11362	0.782345
CRK	P46108	FGFR1	Y654	P11362	0.867506
CRK	P46108	FGFR3	Y648	P22607	0.470982
CRK	P46108	FGFR3	Y724	P22607	0.544314
CRK	P46108	FLT1	Y1327	P17948	0.537132
CRK	P46108	KIT	Y900	P10721	0.334269
CRK	P46108	KIT	Y936	P10721	0.855645
CRK	P46108	PDGFRB	Y581	P09619	0.809281
CRK	P46108	PDGFRB	Y775	P09619	0.348979
CRK	P46108	RET	Y981	P07949	0.242159
CRK	P46108	RET	Y1062	P07949	0.890518
CRK	P46108	ZAP70	Y248	P43403	0.865993
CRK	P46108	AXL	Y759	P30530	0.420886
CRK	P46108	TXK	Y91	P42681	0.84179
CRK	P46108	HCK	Y209	P08631	0.17982
CRK	P46108	LCK	Y192	P06239	0.355726
CRK	P46108	RASA1	Y460	P20936	0.93526
CRK	P46108	VAV2	Y172	P52735	0.844312
CRK	P46108	CBL	Y337	P22681	0.916979
CRK	P46108	CBL	Y700	P22681	0.250844
CRK	P46108	CBL	Y774	P22681	0.96678
CRK	P46108	DAB1	Y220	O75553	0.827471
CRK	P46108	ERBB2	Y1127	P04626	0.913481
CRK	P46108	FLT1	Y1048	P17948	0.530287
CRK	P46108	KIT	Y730	P10721	0.807238
CRK	P46108	SYK	Y352	P43405	0.14203
CRK	P46108	TYRO3	Y686	Q06418	0.780138
CRK	P46108	PIK3R1	Y528	P27986	0.409337

Table 6.2: Sub micromolar interactions identified in these studies (Continued)

CRK	P46108	PIK3CD	Y440	O00329	0.87878
CRK	P46108	SRC	Y187	P12931	0.951278
CRK	P46108	LYN	Y194	P07948	0.366867
CRK	P46108	LYN	Y265	P07948	0.329713
CRK	P46108	LYN	Y460	P07948	0.472918
CRK	P46108	SHC3	Y342	Q92529	0.439218
CRK	P46108	RIN1	Y632	Q13671	0.532582
CRK	P46108	SHB	Y297	Q15464	0.7483
CRK	P46108	TNS1	Y339	Q9HBL0	0.857306
CRK	P46108	TNS1	Y1345	Q9HBL0	0.580296
CRK	P46108	CBLB	Y709	Q13191	0.410687
CRK	P46108	CBLB	Y889	Q13191	0.212974
CRK	P46108	STAT1	Y203	P42224	0.367567
CRK	P46108	DOK4	Y255	Q8TEW6	0.173799
CRK	P46108	PTK2B	Y834	Q14289	0.296704
NCK1	P16333	RIN1	Y36	Q13671	0.773345
NCK1	P16333	CBL	Y368	P22681	0.61497
NCK1	P16333	IRS2	Y675	Q9Y4H2	0.969245
NCK1	P16333	SHB	Y297	Q15464	0.712148
SRC	P12931	ALK	Y1092	Q9UM73	0.60043
SRC	P12931	ALK	Y1096	Q9UM73	0.832896
SRC	P12931	AXL	Y866	P30530	0.920576
SRC	P12931	FGFR1	Y653	P11362	0.910884
SRC	P12931	FGFR3	Y724	P22607	0.600336
SRC	P12931	FLT1	Y1327	P17948	0.728706
SRC	P12931	FLT1	Y1333	P17948	0.714631
SRC	P12931	FLT3	Y591	P36888	0.946893
SRC	P12931	FLT3	Y597	P36888	0.304586
SRC	P12931	FLT4	Y1337	P35916	0.83551
SRC	P12931	IGF1R	Y1161	P08069	0.893775
SRC	P12931	INSR	Y1185	P06213	0.893775
SRC	P12931	IGF1R	Y1165	P08069	0.84471
SRC	P12931	INSR	Y1189	P06213	0.84471
SRC	P12931	IGF1R	Y1281	P08069	0.929541
SRC	P12931	INSR	Y1011	P06213	0.656615
SRC	P12931	INSR	Y1355	P06213	0.902995
SRC	P12931	FLT4	Y1063	P35916	0.530055
SRC	P12931	KDR	Y1054	P35968	0.530055
SRC	P12931	KIT	Y721	P10721	0.865338
SRC	P12931	KIT	Y900	P10721	0.419736

Table 6.2: Sub micromolar interactions identified in these studies (Continued)

SRC	P12931	MET	Y1313	P08581	0.620978
SRC	P12931	MET	Y1349	P08581	0.579156
SRC	P12931	MET	Y1356	P08581	0.48307
SRC	P12931	MET	Y1365	P08581	0.82532
SRC	P12931	MST1R	Y1317	Q04912	0.850414
SRC	P12931	NTRK2	Y707	Q16620	0.893073
SRC	P12931	NTRK3	Y710	Q16288	0.893073
SRC	P12931	NTRK2	Y817	Q16620	0.329342
SRC	P12931	NTRK3	Y516	Q16288	0.442639
SRC	P12931	PDGFRA	Y574	P16234	0.581626
SRC	P12931	PDGFRB	Y581	P09619	0.954544
SRC	P12931	PDGFRB	Y778	P09619	0.975133
SRC	P12931	RET	Y981	P07949	0.342694
SRC	P12931	RET	Y1096	P07949	0.752956
SRC	P12931	TEK	Y1048	Q02763	0.357874
SRC	P12931	ERBB2	Y1139	P04626	0.991981
SRC	P12931	ERBB2	Y1222	P04626	0.283326
SRC	P12931	ERBB3	Y1197	P21860	0.697298
SRC	P12931	ERBB3	Y1276	P21860	0.755275
SRC	P12931	RET	Y952	P07949	0.484765
SRC	P12931	EPHA2	Y575	P29317	0.840205
SRC	P12931	EPHA2	Y735	P29317	0.958006
SRC	P12931	EPHA2	Y772	P29317	0.752683
SRC	P12931	EPHA7	Y597	Q15375	0.908591
SRC	P12931	ABL2	Y515	P42684	0.993295
SRC	P12931	ABL1	Y276	P00519	0.507701
SRC	P12931	EPHA1	Y605	P21709	0.963384
SRC	P12931	TXK	Y91	P42681	0.617408
SRC	P12931	PTK6	Y447	Q13882	0.951337
SRC	P12931	PLCG1	Y472	P19174	0.763502
SRC	P12931	PLCG2	Y743	P16885	0.995082
SRC	P12931	GRAP2	Y45	O75791	0.745513
SRC	P12931	SH3BP2	Y183	P78314	0.853914
SRC	P12931	BLNK	Y72	Q8WV28	0.83476
SRC	P12931	SH2D2A	Y305	Q9NP31	0.765588
SRC	P12931	VAV1	Y160	P15498	0.557238
SRC	P12931	VAV2	Y172	P52735	0.94891
SRC	P12931	CBL	Y337	P22681	0.977717
SRC	P12931	CBL	Y368	P22681	0.748399
SRC	P12931	DAB1	Y198	O75553	0.592214

Table 6.2: Sub micromolar interactions identified in these studies (Continued)

SRC	P12931	DOK1	Y146	Q99704	0.810844
SRC	P12931	DOK1	Y203	Q99704	0.79574
SRC	P12931	DOK1	Y315	Q99704	0.935102
SRC	P12931	DOK1	Y409	Q99704	0.619481
SRC	P12931	EPHB3	Y754	P54753	0.924912
SRC	P12931	ERBB2	Y1127	P04626	0.706778
SRC	P12931	IRS1	Y732	P35568	0.864099
SRC	P12931	IRS1	Y989	P35568	0.836248
SRC	P12931	IRS2	Y632	Q9Y4H2	0.786089
SRC	P12931	GAB1	Y373	Q13480	0.762992
SRC	P12931	GAB1	Y406	Q13480	0.917565
SRC	P12931	KIT	Y553	P10721	0.902571
SRC	P12931	PDGFRB	Y934	P09619	0.689683
SRC	P12931	ROS1	Y2115	P08922	0.911802
SRC	P12931	TENC1	Y483	Q63HR2	0.935817
SRC	P12931	PIK3R1	Y607	P27986	0.858838
SRC	P12931	ABL2	Y231	P42684	0.791048
SRC	P12931	ZAP70	Y69	P43403	0.969035
SRC	P12931	FGR	Y180	P09769	0.969423
SRC	P12931	FYN	Y185	P06241	0.969423
SRC	P12931	YES1	Y194	P07947	0.969423
SRC	P12931	SRC	Y521	P12931	0.648028
SRC	P12931	VAV1	Y826	P15498	0.947995
SRC	P12931	VAV3	Y173	Q9UKW4	0.896622
SRC	P12931	TNS1	Y609	Q9HBL0	0.908339
SRC	P12931	TNS1	Y796	Q9HBL0	0.444779
SRC	P12931	CBLB	Y889	Q13191	0.704231
SRC	P12931	APBB3	Y291	O95704	0.717352
SRC	P12931	ANKS1A	Y454	Q92625	0.680003
SRC	P12931	CSK	Y263	P41240	0.871967
SRC	P12931	PTK2	Y397	Q05397	0.957421
SRC	P12931	PTK2	Y1007	Q05397	0.867812
SRC	P12931	CTNNB1	Y142	P35222	0.647832
ZAP70-C	P43403	EPHA4	Y602	P54764	0.956248
ZAP70-C	P43403	NTRK3	Y516	Q16288	0.962351
ZAP70-C	P43403	RET	Y1062	P07949	0.955927
ZAP70-C	P43403	PLCG2	Y1217	P16885	0.435345
ZAP70-C	P43403	NCK1	Y268	P16333	0.317429
ZAP70-C	P43403	DOK1	Y398	Q99704	0.943764
ZAP70-C	P43403	IRS1	Y732	P35568	0.730215

Table 6.2: Sub micromolar interactions identified in these studies (Continued)

ZAP70-C	P43403	IRS2	Y675	Q9Y4H2	0.375981
SYK-C	P43405	MST1R	Y1360	Q04912	0.82143
SYK-C	P43405	NTRK1	Y496	P04629	0.849088
SYK-C	P43405	PDGFRA	Y574	P16234	0.598208
SYK-C	P43405	PDGFRB	Y1009	P09619	0.371276
SYK-C	P43405	PDGFRB	Y1021	P09619	0.702923
SYK-C	P43405	EPHA7	Y791	Q15375	0.428996
SYK-C	P43405	PLCG2	Y1245	P16885	0.871387
SYK-C	P43405	NCK1	Y268	P16333	0.535432
SYK-C	P43405	EPHB3	Y754	P54753	0.761628
SYK-C	P43405	IRS1	Y46	P35568	0.826141
SYK-C	P43405	IRS1	Y989	P35568	0.802592
SYK-C	P43405	IRS2	Y675	Q9Y4H2	0.895185
SYK-C	P43405	PIK3R2	Y365	O00459	0.80629
SYK-C	P43405	SHC3	Y424	Q92529	0.80629
SYK-C	P43405	ABL1	Y191	P00519	0.542141
SYK-C	P43405	TNS1	Y366	Q9HBL0	0.408698
TEC	P42680	EPHA4	Y596	P54764	0.465051
TEC	P42680	EPHB1	Y600	P54762	0.637167
TEC	P42680	EPHB2	Y602	P29323	0.637167
TEC	P42680	FGFR1	Y653	P11362	0.4387
TEC	P42680	FLT3	Y597	P36888	0.448936
TEC	P42680	INSR	Y999	P06213	0.912736
TEC	P42680	INSR	Y1011	P06213	0.830824
TEC	P42680	KIT	Y900	P10721	0.937649
TEC	P42680	MET	Y1313	P08581	0.991099
TEC	P42680	MST1R	Y1317	Q04912	0.990729
TEC	P42680	NTRK1	Y496	P04629	0.655992
TEC	P42680	ERBB2	Y1139	P04626	0.995131
TEC	P42680	ERBB2	Y1221	P04626	0.602349
TEC	P42680	FES	Y811	P07332	0.851665
TEC	P42680	NCK1	Y268	P16333	0.285169
TEC	P42680	SH2D3A	Y231	Q9BRG2	0.870873
TEC	P42680	VAV1	Y160	P15498	0.748368
TEC	P42680	DOK1	Y315	Q99704	0.900355
TEC	P42680	IRS2	Y823	Q9Y4H2	0.876621
TEC	P42680	ABL1	Y191	P00519	0.688003
TEC	P42680	CSK	Y263	P41240	0.970701
TEC	P42680	CTNNB1	Y142	P35222	0.162082
LYN	P07948	FGFR3	Y724	P22607	0.568999

Table 6.2: Sub micromolar interactions identified in these studies (Continued)

LYN	P07948	FLT1	Y1327	P17948	0.493988
LYN	P07948	FLT3	Y591	P36888	0.786342
LYN	P07948	INSR	Y1011	P06213	0.616429
LYN	P07948	KIT	Y721	P10721	0.462819
LYN	P07948	MET	Y1313	P08581	0.562721
LYN	P07948	MET	Y1356	P08581	0.61833
LYN	P07948	MST1R	Y1317	Q04912	0.725729
LYN	P07948	PDGFRA	Y572	P16234	0.874822
LYN	P07948	PDGFRB	Y581	P09619	0.921378
LYN	P07948	PDGFRB	Y1009	P09619	0.73063
LYN	P07948	PDGFRB	Y1021	P09619	0.945782
LYN	P07948	RET	Y981	P07949	0.544262
LYN	P07948	ERBB2	Y1221	P04626	0.466276
LYN	P07948	ABL1	Y276	P00519	0.751777
LYN	P07948	FGR	Y412	P09769	0.669368
LYN	P07948	PLCG1	Y472	P19174	0.78483
LYN	P07948	PLCG1	Y771	P19174	0.818827
LYN	P07948	PLCG1	Y783	P19174	0.846372
LYN	P07948	PLCG2	Y743	P16885	0.766496
LYN	P07948	PLCG2	Y1217	P16885	0.866726
LYN	P07948	RASA1	Y615	P20936	0.177009
LYN	P07948	SH2D2A	Y39	Q9NP31	0.915167
LYN	P07948	VAV1	Y160	P15498	0.91412
LYN	P07948	CBL	Y368	P22681	0.968486
LYN	P07948	EPHA3	Y937	P29320	0.784812
LYN	P07948	IRS1	Y612	P35568	0.449398
LYN	P07948	IRS1	Y732	P35568	0.559194
LYN	P07948	IRS1	Y896	P35568	0.66083
LYN	P07948	IRS2	Y823	Q9Y4H2	0.960953
LYN	P07948	PIK3R1	Y607	P27986	0.905318
LYN	P07948	PIK3R1	Y463	P27986	0.719716
LYN	P07948	SYK	Y203	P43405	0.655063
LYN	P07948	VAV3	Y173	Q9UKW4	0.913258
LYN	P07948	SHB	Y336	Q15464	0.45712
LYN	P07948	ANKS1A	Y454	Q92625	0.820219
LYN	P07948	PTK2	Y925	Q05397	0.881321
VAV1	P15498	MET	Y1313	P08581	0.378954
VAV1	P15498	MET	Y1356	P08581	0.515973
VAV1	P15498	ERBB2	Y1139	P04626	0.860416
VAV1	P15498	ABL1	Y276	P00519	0.968244

Table 6.2: Sub micromolar interactions identified in these studies (Continued)

VAV1	P15498	PLCG2	Y1245	P16885	0.772974
VAV1	P15498	CBL	Y368	P22681	0.691798
VAV1	P15498	CBL	Y371	P22681	0.695921
VAV1	P15498	CBLB	Y363	Q13191	0.695921
VAV1	P15498	CBL	Y700	P22681	0.89631
VAV1	P15498	DOK1	Y398	Q99704	0.745427
VAV1	P15498	IRS1	Y465	P35568	0.832949
VAV1	P15498	IRS2	Y675	Q9Y4H2	0.590692
TNS3	Q68CZ2	EPHB1	Y600	P54762	0.915587
TNS3	Q68CZ2	EPHB2	Y602	P29323	0.915587
TNS3	Q68CZ2	FGFR3	Y724	P22607	0.521275
TNS3	Q68CZ2	FLT1	Y1333	P17948	0.165855
TNS3	Q68CZ2	FLT3	Y591	P36888	0.708676
TNS3	Q68CZ2	INSR	Y1011	P06213	0.918871
TNS3	Q68CZ2	KDR	Y996	P35968	0.847783
TNS3	Q68CZ2	KDR	Y1214	P35968	0.547381
TNS3	Q68CZ2	MET	Y1230	P08581	0.928767
TNS3	Q68CZ2	MET	Y1313	P08581	0.855099
TNS3	Q68CZ2	MST1R	Y1317	Q04912	0.582801
TNS3	Q68CZ2	PDGFRB	Y740	P09619	0.532523
TNS3	Q68CZ2	PDGFRB	Y778	P09619	0.356537
TNS3	Q68CZ2	RET	Y1029	P07949	0.906173
TNS3	Q68CZ2	RET	Y1062	P07949	0.974042
TNS3	Q68CZ2	AXL	Y759	P30530	0.88015
TNS3	Q68CZ2	VAV1	Y160	P15498	0.904452
TNS3	Q68CZ2	VAV2	Y159	P52735	0.997128
TNS3	Q68CZ2	CBL	Y368	P22681	0.778722
TNS3	Q68CZ2	DOK1	Y315	Q99704	0.816009
TNS3	Q68CZ2	ABL1	Y191	P00519	0.686554
TNS3	Q68CZ2	VAV3	Y173	Q9UKW4	0.621131
TNS3	Q68CZ2	TNS1	Y339	Q9HBL0	0.621933
BLK	P51451	ALK	Y1092	Q9UM73	0.311961
BLK	P51451	ALK	Y1096	Q9UM73	0.754373
BLK	P51451	ALK	Y1507	Q9UM73	0.689454
BLK	P51451	AXL	Y866	P30530	0.979741
BLK	P51451	CSF1R	Y561	P07333	0.242463
BLK	P51451	EPHB1	Y600	P54762	0.80471
BLK	P51451	EPHB2	Y602	P29323	0.80471
BLK	P51451	EPHB2	Y596	P29323	0.588141
BLK	P51451	FGFR1	Y463	P11362	0.449709

Table 6.2: Sub micromolar interactions identified in these studies (Continued)

BLK	P51451	FGFR1	Y730	P11362	0.6997
BLK	P51451	FGFR3	Y724	P22607	0.51551
BLK	P51451	FGFR3	Y760	P22607	0.709331
BLK	P51451	FLT1	Y1327	P17948	0.578464
BLK	P51451	FLT3	Y591	P36888	0.617824
BLK	P51451	IGF1R	Y1280	P08069	0.642896
BLK	P51451	INSR	Y999	P06213	0.794899
BLK	P51451	INSR	Y1011	P06213	0.281975
BLK	P51451	KDR	Y996	P35968	0.892938
BLK	P51451	FLT4	Y1063	P35916	0.938482
BLK	P51451	KDR	Y1054	P35968	0.938482
BLK	P51451	KDR	Y1214	P35968	0.937494
BLK	P51451	KIT	Y721	P10721	0.931329
BLK	P51451	KIT	Y900	P10721	0.166929
BLK	P51451	KIT	Y936	P10721	0.572169
BLK	P51451	MET	Y1313	P08581	0.279024
BLK	P51451	MET	Y1356	P08581	0.979099
BLK	P51451	MET	Y1365	P08581	0.548638
BLK	P51451	MST1R	Y1317	Q04912	0.452987
BLK	P51451	NTRK1	Y496	P04629	0.656727
BLK	P51451	NTRK3	Y516	Q16288	0.352913
BLK	P51451	PDGFRA	Y572	P16234	0.845157
BLK	P51451	PDGFRA	Y574	P16234	0.982432
BLK	P51451	PDGFRA	Y731	P16234	0.852887
BLK	P51451	PDGFRB	Y562	P09619	0.958547
BLK	P51451	PDGFRB	Y751	P09619	0.672591
BLK	P51451	PDGFRB	Y1021	P09619	0.933105
BLK	P51451	RET	Y791	P07949	0.221836
BLK	P51451	RET	Y900	P07949	0.896467
BLK	P51451	RET	Y1062	P07949	0.914228
BLK	P51451	RET	Y1096	P07949	0.768643
BLK	P51451	ROS1	Y2274	P08922	0.412125
BLK	P51451	ROS1	Y2334	P08922	0.687176
BLK	P51451	TEK	Y1048	Q02763	0.266521
BLK	P51451	TEK	Y1102	Q02763	0.662038
BLK	P51451	ERBB4	Y1066	Q15303	0.451814
BLK	P51451	ERBB4	Y1284	Q15303	0.945438
BLK	P51451	EGFR	Y1016	P00533	0.97281
BLK	P51451	EGFR	Y1172	P00533	0.827142
BLK	P51451	ERBB2	Y877	P04626	0.80374

Table 6.2: Sub micromolar interactions identified in these studies (Continued)

BLK	P51451	ERBB2	Y1023	P04626	0.578631
BLK	P51451	ERBB2	Y1221	P04626	0.275989
BLK	P51451	ERBB2	Y1222	P04626	0.238877
BLK	P51451	ERBB3	Y1197	P21860	0.696158
BLK	P51451	ERBB3	Y1276	P21860	0.844846
BLK	P51451	EPHA2	Y772	P29317	0.697581
BLK	P51451	EPHA7	Y597	Q15375	0.972784
BLK	P51451	ABL2	Y515	P42684	0.776505
BLK	P51451	ABL1	Y276	P00519	0.334744
BLK	P51451	EPHA1	Y599	P21709	0.579535
BLK	P51451	PLCG1	Y472	P19174	0.542661
BLK	P51451	PLCG1	Y771	P19174	0.93885
BLK	P51451	PLCG1	Y783	P19174	0.947249
BLK	P51451	PLCG2	Y1217	P16885	0.952709
BLK	P51451	RASA1	Y460	P20936	0.878273
BLK	P51451	RASA1	Y615	P20936	0.306404
BLK	P51451	SH2D2A	Y39	Q9NP31	0.762461
BLK	P51451	SH2D2A	Y305	Q9NP31	0.990522
BLK	P51451	VAV2	Y159	P52735	0.646544
BLK	P51451	CBL	Y371	P22681	0.772872
BLK	P51451	CBLB	Y363	Q13191	0.772872
BLK	P51451	DOK1	Y315	Q99704	0.960368
BLK	P51451	DOK1	Y398	Q99704	0.21348
BLK	P51451	DOK2	Y345	O60496	0.588753
BLK	P51451	EPHB3	Y754	P54753	0.954192
BLK	P51451	ERBB2	Y1005	P04626	0.846865
BLK	P51451	IRS1	Y46	P35568	0.899254
BLK	P51451	IRS1	Y896	P35568	0.516524
BLK	P51451	IRS2	Y675	Q9Y4H2	0.603569
BLK	P51451	IRS2	Y823	Q9Y4H2	0.746569
BLK	P51451	PIK3R1	Y607	P27986	0.972204
BLK	P51451	ABL1	Y191	P00519	0.87592
BLK	P51451	SYK	Y203	P43405	0.654192
BLK	P51451	LYN	Y501	P07948	0.923185
BLK	P51451	VAV1	Y826	P15498	0.335587
BLK	P51451	TNS1	Y903	Q9HBL0	0.940374
BLK	P51451	CTNNB1	Y670	P35222	0.236333
TNS1	Q9HBL0	MET	Y1356	P08581	0.875463
TNS1	Q9HBL0	NTRK3	Y516	Q16288	0.611884
TNS1	Q9HBL0	ROS1	Y2334	P08922	0.987129

Table 6.2: Sub micromolar interactions identified in these studies (Continued)

TNS1	Q9HBL0	FRS2	Y436	Q8WU20	0.391508
TNS1	Q9HBL0	PTK6	Y342	Q13882	0.89789
TNS1	Q9HBL0	PLCG1	Y775	P19174	0.993887
TNS1	Q9HBL0	DAB1	Y198	O75553	0.480213
TNS1	Q9HBL0	DOK1	Y315	Q99704	0.818917
TNS1	Q9HBL0	IRS1	Y732	P35568	0.622766
NCK2	O43639	EPHA3	Y596	P29320	0.951239
NCK2	O43639	EPHA3	Y602	P29320	0.776285
NCK2	O43639	EPHA4	Y602	P54764	0.698356
NCK2	O43639	EPHB1	Y600	P54762	0.565206
NCK2	O43639	EPHB2	Y602	P29323	0.565206
NCK2	O43639	FGFR1	Y653	P11362	0.805978
NCK2	O43639	FGFR1	Y730	P11362	0.948439
NCK2	O43639	FLT1	Y1213	P17948	0.663572
NCK2	O43639	FLT1	Y1327	P17948	0.668134
NCK2	O43639	FLT3	Y591	P36888	0.398276
NCK2	O43639	FLT4	Y1063	P35916	0.409639
NCK2	O43639	KDR	Y1054	P35968	0.409639
NCK2	O43639	KDR	Y1214	P35968	0.587666
NCK2	O43639	KIT	Y900	P10721	0.273641
NCK2	O43639	KIT	Y936	P10721	0.439134
NCK2	O43639	MET	Y1356	P08581	0.765058
NCK2	O43639	MST1R	Y1317	Q04912	0.310058
NCK2	O43639	NTRK1	Y496	P04629	0.84544
NCK2	O43639	NTRK1	Y791	P04629	0.374247
NCK2	O43639	NTRK2	Y706	Q16620	0.593753
NCK2	O43639	NTRK3	Y709	Q16288	0.593753
NCK2	O43639	NTRK3	Y516	Q16288	0.40704
NCK2	O43639	PDGFRB	Y771	P09619	0.883413
NCK2	O43639	TEK	Y1048	Q02763	0.981106
NCK2	O43639	FRS2	Y306	Q8WU20	0.569164
NCK2	O43639	EGFR	Y1138	P00533	0.464281
NCK2	O43639	ERBB2	Y1023	P04626	0.521967
NCK2	O43639	ERBB2	Y1196	P04626	0.69839
NCK2	O43639	EPHA2	Y575	P29317	0.963606
NCK2	O43639	EPHA2	Y588	P29317	0.812319
NCK2	O43639	EPHA2	Y735	P29317	0.890666
NCK2	O43639	EPHA2	Y921	P29317	0.914271
NCK2	O43639	FYN	Y420	P06241	0.693538
NCK2	O43639	SRC	Y419	P12931	0.693538

Table 6.2: Sub micromolar interactions identified in these studies (Continued)

NCK2	O43639	YES1	Y426	P07947	0.693538
NCK2	O43639	EPHA1	Y605	P21709	0.936811
NCK2	O43639	SYK	Y348	P43405	0.582365
NCK2	O43639	TEC	Y206	P42680	0.970587
NCK2	O43639	LYN	Y508	P07948	0.386666
NCK2	O43639	TXK	Y91	P42681	0.394609
NCK2	O43639	TXK	Y420	P42681	0.839778
NCK2	O43639	FER	Y402	P16591	0.949682
NCK2	O43639	LCK	Y192	P06239	0.830437
NCK2	O43639	FES	Y811	P07332	0.979915
NCK2	O43639	PLCG1	Y775	P19174	0.894273
NCK2	O43639	PLCG1	Y783	P19174	0.633912
NCK2	O43639	PLCG2	Y753	P16885	0.721693
NCK2	O43639	PLCG2	Y1217	P16885	0.952832
NCK2	O43639	PLCG2	Y1245	P16885	0.718534
NCK2	O43639	CRKL	Y207	P46109	0.658348
NCK2	O43639	JAK3	Y785	P52333	0.865833
NCK2	O43639	LCP2	Y128	Q13094	0.575424
NCK2	O43639	BLNK	Y178	Q8WV28	0.707321
NCK2	O43639	SH2D2A	Y39	Q9NP31	0.435623
NCK2	O43639	SH2D2A	Y280	Q9NP31	0.650341
NCK2	O43639	VAV1	Y160	P15498	0.242317
NCK2	O43639	VAV1	Y174	P15498	0.875792
NCK2	O43639	VAV2	Y159	P52735	0.554906
NCK2	O43639	VAV2	Y172	P52735	0.657495
NCK2	O43639	INPPL1	Y886	O15357	0.845583
NCK2	O43639	SHB	Y246	Q15464	0.568756
NCK2	O43639	CBL	Y337	P22681	0.760231
NCK2	O43639	CBL	Y368	P22681	0.347346
NCK2	O43639	CBL	Y700	P22681	0.529221
NCK2	O43639	DAB1	Y198	O75553	0.721225
NCK2	O43639	DAB1	Y220	O75553	0.747136
NCK2	O43639	DAB1	Y232	O75553	0.795318
NCK2	O43639	DOK1	Y146	Q99704	0.45217
NCK2	O43639	DOK1	Y315	Q99704	0.334554
NCK2	O43639	EPHA3	Y937	P29320	0.82661
NCK2	O43639	EPHB3	Y754	P54753	0.94914
NCK2	O43639	EPHB3	Y924	P54753	0.872637
NCK2	O43639	EPHB4	Y596	P54760	0.766664
NCK2	O43639	FLT1	Y1053	P17948	0.5096

Table 6.2: Sub micromolar interactions identified in these studies (Continued)

NCK2	O43639	IRS1	Y465	P35568	0.660747
NCK2	O43639	IRS1	Y662	P35568	0.73198
NCK2	O43639	IRS1	Y732	P35568	0.881102
NCK2	O43639	IRS1	Y989	P35568	0.684974
NCK2	O43639	IRS2	Y823	Q9Y4H2	0.557295
NCK2	O43639	GAB1	Y406	Q13480	0.660844
NCK2	O43639	ABL1	Y272	P00519	0.387665
NCK2	O43639	PIK3CB	Y772	P42338	0.969031
NCK2	O43639	PIK3CD	Y440	O00329	0.857561
NCK2	O43639	SRC	Y521	P12931	0.964647
NCK2	O43639	SYK	Y203	P43405	0.553831
NCK2	O43639	SHC3	Y406	Q92529	0.467301
NCK2	O43639	RIN1	Y632	Q13671	0.505348
NCK2	O43639	VAV3	Y173	Q9UKW4	0.979011
NCK2	O43639	HSH2D	Y265	Q96JZ2	0.875152
NCK2	O43639	SHB	Y297	Q15464	0.958097
NCK2	O43639	SHB	Y336	Q15464	0.592232
NCK2	O43639	TNS1	Y1440	Q9HBL0	0.732241
NCK2	O43639	PTK2	Y861	Q05397	0.84555
VAV3	Q9UKW4	FGFR3	Y724	P22607	0.631686
VAV3	Q9UKW4	IGF1R	Y1280	P08069	0.634733
VAV3	Q9UKW4	INSR	Y1011	P06213	0.718289
VAV3	Q9UKW4	MET	Y1313	P08581	0.716443
VAV3	Q9UKW4	MET	Y1356	P08581	0.509291
VAV3	Q9UKW4	MST1R	Y1317	Q04912	0.374723
VAV3	Q9UKW4	NTRK1	Y496	P04629	0.655709
VAV3	Q9UKW4	NTRK1	Y676	P04629	0.629983
VAV3	Q9UKW4	NTRK2	Y706	Q16620	0.973482
VAV3	Q9UKW4	NTRK3	Y709	Q16288	0.973482
VAV3	Q9UKW4	NTRK2	Y707	Q16620	0.943959
VAV3	Q9UKW4	NTRK3	Y710	Q16288	0.943959
VAV3	Q9UKW4	NTRK3	Y516	Q16288	0.863065
VAV3	Q9UKW4	PDGFRB	Y581	P09619	0.944868
VAV3	Q9UKW4	RET	Y1096	P07949	0.934777
VAV3	Q9UKW4	ERBB2	Y1023	P04626	0.79232
VAV3	Q9UKW4	ERBB2	Y1221	P04626	0.570909
VAV3	Q9UKW4	ERBB2	Y1222	P04626	0.324798
VAV3	Q9UKW4	RET	Y952	P07949	0.626448
VAV3	Q9UKW4	EPHA2	Y960	P29317	0.470523
VAV3	Q9UKW4	ABL2	Y515	P42684	0.905284

Table 6.2: Sub micromolar interactions identified in these studies (Continued)

VAV3	Q9UKW4	ABL1	Y276	P00519	0.619277
VAV3	Q9UKW4	ZAP70	Y474	P43403	0.676668
VAV3	Q9UKW4	SYK	Y525	P43405	0.955027
VAV3	Q9UKW4	TXK	Y91	P42681	0.736731
VAV3	Q9UKW4	PLCG1	Y771	P19174	0.778522
VAV3	Q9UKW4	PLCG2	Y743	P16885	0.955008
VAV3	Q9UKW4	PLCG2	Y753	P16885	0.979992
VAV3	Q9UKW4	GRAP2	Y45	O75791	0.656461
VAV3	Q9UKW4	SH3BP2	Y183	P78314	0.511169
VAV3	Q9UKW4	JAK3	Y785	P52333	0.953899
VAV3	Q9UKW4	BLNK	Y72	Q8WV28	0.761605
VAV3	Q9UKW4	BLNK	Y84	Q8WV28	0.855743
VAV3	Q9UKW4	BLNK	Y178	Q8WV28	0.872183
VAV3	Q9UKW4	RASA1	Y460	P20936	0.841192
VAV3	Q9UKW4	RASA1	Y615	P20936	0.25379
VAV3	Q9UKW4	DAB1	Y198	O75553	0.912819
VAV3	Q9UKW4	DAB1	Y220	O75553	0.707196
VAV3	Q9UKW4	DOK1	Y203	Q99704	0.985796
VAV3	Q9UKW4	DOK1	Y362	Q99704	0.881641
VAV3	Q9UKW4	DOK1	Y398	Q99704	0.75636
VAV3	Q9UKW4	DOK2	Y345	O60496	0.746521
VAV3	Q9UKW4	EPHB3	Y600	P54753	0.787584
VAV3	Q9UKW4	IRS1	Y896	P35568	0.735172
VAV3	Q9UKW4	IRS2	Y675	Q9Y4H2	0.984852
VAV3	Q9UKW4	ANKS1A	Y454	Q92625	0.769611
VAV2	P52735	EPHA3	Y602	P29320	0.666383
VAV2	P52735	EPHA4	Y596	P54764	0.924083
VAV2	P52735	EPHB1	Y600	P54762	0.338282
VAV2	P52735	EPHB2	Y602	P29323	0.338282
VAV2	P52735	FGFR3	Y724	P22607	0.397303
VAV2	P52735	FLT3	Y597	P36888	0.517517
VAV2	P52735	IGF1R	Y1161	P08069	0.628211
VAV2	P52735	INSR	Y1185	P06213	0.628211
VAV2	P52735	PDGFRB	Y775	P09619	0.300923
VAV2	P52735	RET	Y1096	P07949	0.518714
VAV2	P52735	ERBB4	Y1162	Q15303	0.388247
VAV2	P52735	EGFR	Y1016	P00533	0.19408
VAV2	P52735	EGFR	Y1092	P00533	0.493044
VAV2	P52735	EGFR	Y1138	P00533	0.527405
VAV2	P52735	ERBB2	Y1023	P04626	0.201917

Table 6.2: Sub micromolar interactions identified in these studies (Continued)

VAV2	P52735	ERBB2	Y1196	P04626	0.203923
VAV2	P52735	EPHA2	Y772	P29317	0.520572
VAV2	P52735	ZAP70	Y315	P43403	0.635398
VAV2	P52735	PLCG2	Y1245	P16885	0.787083
VAV2	P52735	NCK1	Y268	P16333	0.619488
VAV2	P52735	BLNK	Y178	Q8WV28	0.231245
VAV2	P52735	VAV2	Y172	P52735	0.992273
VAV2	P52735	CBL	Y700	P22681	0.48309
VAV2	P52735	DAB1	Y220	O75553	0.358264
VAV2	P52735	DOK1	Y315	Q99704	0.536042
VAV2	P52735	EPHB4	Y596	P54760	0.608327
VAV2	P52735	IRS1	Y896	P35568	0.693549
VAV2	P52735	CSK	Y263	P41240	0.957677
ITK	Q08881	ALK	Y1092	Q9UM73	0.372164
ITK	Q08881	AXL	Y821	P30530	0.893144
ITK	Q08881	FGFR3	Y724	P22607	0.467283
ITK	Q08881	FGFR3	Y760	P22607	0.286035
ITK	Q08881	FLT1	Y1327	P17948	0.414692
ITK	Q08881	FLT3	Y591	P36888	0.483081
ITK	Q08881	IGF1R	Y1281	P08069	0.855365
ITK	Q08881	INSR	Y1011	P06213	0.449406
ITK	Q08881	KIT	Y721	P10721	0.771895
ITK	Q08881	KIT	Y900	P10721	0.221157
ITK	Q08881	MET	Y1356	P08581	0.721717
ITK	Q08881	MST1R	Y1317	Q04912	0.263779
ITK	Q08881	NTRK1	Y496	P04629	0.927361
ITK	Q08881	NTRK2	Y706	Q16620	0.95243
ITK	Q08881	NTRK3	Y709	Q16288	0.95243
ITK	Q08881	NTRK2	Y817	Q16620	0.390874
ITK	Q08881	NTRK3	Y516	Q16288	0.402405
ITK	Q08881	PDGFRB	Y581	P09619	0.582678
ITK	Q08881	PDGFRB	Y778	P09619	0.585723
ITK	Q08881	RET	Y791	P07949	0.226029
ITK	Q08881	RET	Y981	P07949	0.251441
ITK	Q08881	RET	Y1096	P07949	0.657518
ITK	Q08881	ROS1	Y2274	P08922	0.674864
ITK	Q08881	ROS1	Y2334	P08922	0.741821
ITK	Q08881	ERBB2	Y1023	P04626	0.642546
ITK	Q08881	ERBB2	Y1222	P04626	0.215427
ITK	Q08881	EPHA2	Y772	P29317	0.903655

Table 6.2: Sub micromolar interactions identified in these studies (Continued)

ITK	Q08881	EPHA7	Y614	Q15375	0.695234
ITK	Q08881	ABL1	Y276	P00519	0.536265
ITK	Q08881	SYK	Y323	P43405	0.993644
ITK	Q08881	LCK	Y192	P06239	0.861133
ITK	Q08881	FES	Y811	P07332	0.924129
ITK	Q08881	PLCG1	Y472	P19174	0.903925
ITK	Q08881	PLCG1	Y775	P19174	0.961216
ITK	Q08881	PLCG2	Y743	P16885	0.92498
ITK	Q08881	PLCG2	Y1217	P16885	0.90778
ITK	Q08881	GRAP2	Y45	O75791	0.7629
ITK	Q08881	NCK1	Y268	P16333	0.954886
ITK	Q08881	JAK3	Y785	P52333	0.961036
ITK	Q08881	BLNK	Y72	Q8WV28	0.947949
ITK	Q08881	RASA1	Y460	P20936	0.499338
ITK	Q08881	RASA1	Y615	P20936	0.432281
ITK	Q08881	SH2D2A	Y290	Q9NP31	0.862876
ITK	Q08881	SH2D3C	Y495	Q8N5H7	0.870204
ITK	Q08881	VAV1	Y174	P15498	0.816334
ITK	Q08881	VAV2	Y172	P52735	0.871924
ITK	Q08881	CBL	Y368	P22681	0.580656
ITK	Q08881	CBL	Y371	P22681	0.917349
ITK	Q08881	CBLB	Y363	Q13191	0.917349
ITK	Q08881	CBL	Y700	P22681	0.862738
ITK	Q08881	DAB1	Y198	O75553	0.952965
ITK	Q08881	DOK1	Y146	Q99704	0.970119
ITK	Q08881	DOK1	Y315	Q99704	0.579054
ITK	Q08881	DOK1	Y398	Q99704	0.612668
ITK	Q08881	EPHA3	Y937	P29320	0.794982
ITK	Q08881	EPHB3	Y754	P54753	0.77223
ITK	Q08881	IRS1	Y465	P35568	0.829644
ITK	Q08881	IRS1	Y732	P35568	0.695192
ITK	Q08881	IRS1	Y1179	P35568	0.604916
ITK	Q08881	IRS2	Y675	Q9Y4H2	0.98248
ITK	Q08881	GAB1	Y406	Q13480	0.606705
ITK	Q08881	ZAP70	Y319	P43403	0.954391
ITK	Q08881	PIK3R1	Y607	P27986	0.653629
ITK	Q08881	ABL1	Y191	P00519	0.673676
ITK	Q08881	SYK	Y203	P43405	0.704784
ITK	Q08881	VAV1	Y826	P15498	0.674055
ITK	Q08881	PTPN6	Y377	P29350	0.940099

Table 6.2: Sub micromolar interactions identified in these studies (Continued)

ITK	Q08881	SHB	Y336	Q15464	0.435671
ITK	Q08881	TNS1	Y366	Q9HBL0	0.995223
ITK	Q08881	TNS1	Y609	Q9HBL0	0.76557
ITK	Q08881	DOK3	Y208	Q7L591	0.726065
ITK	Q08881	PTK2	Y5	Q05397	0.697399
YES1	P07947	ALK	Y1092	Q9UM73	0.543299
YES1	P07947	ALK	Y1096	Q9UM73	0.685897
YES1	P07947	AXL	Y821	P30530	0.780827
YES1	P07947	AXL	Y866	P30530	0.871889
YES1	P07947	EPHB1	Y600	P54762	0.877021
YES1	P07947	EPHB2	Y602	P29323	0.877021
YES1	P07947	FGFR1	Y463	P11362	0.678075
YES1	P07947	FGFR1	Y605	P11362	0.798665
YES1	P07947	FGFR1	Y730	P11362	0.890589
YES1	P07947	FGFR3	Y724	P22607	0.632292
YES1	P07947	FLT1	Y1327	P17948	0.787302
YES1	P07947	FLT1	Y1333	P17948	0.486804
YES1	P07947	FLT3	Y591	P36888	0.920378
YES1	P07947	FLT3	Y597	P36888	0.22779
YES1	P07947	FLT3	Y599	P36888	0.169964
YES1	P07947	FLT4	Y1337	P35916	0.896426
YES1	P07947	IGF1R	Y1161	P08069	0.967256
YES1	P07947	INSR	Y1185	P06213	0.967256
YES1	P07947	IGF1R	Y1165	P08069	0.866891
YES1	P07947	INSR	Y1189	P06213	0.866891
YES1	P07947	INSR	Y1011	P06213	0.539684
YES1	P07947	KDR	Y801	P35968	0.925086
YES1	P07947	FLT4	Y1063	P35916	0.793059
YES1	P07947	KDR	Y1054	P35968	0.793059
YES1	P07947	KIT	Y721	P10721	0.740977
YES1	P07947	KIT	Y936	P10721	0.575454
YES1	P07947	MET	Y1313	P08581	0.570601
YES1	P07947	MET	Y1356	P08581	0.585255
YES1	P07947	MET	Y1365	P08581	0.811167
YES1	P07947	MST1R	Y1317	Q04912	0.462757
YES1	P07947	MST1R	Y1353	Q04912	0.62886
YES1	P07947	NTRK1	Y496	P04629	0.907454
YES1	P07947	NTRK3	Y516	Q16288	0.287207
YES1	P07947	PDGFRA	Y574	P16234	0.654427
YES1	P07947	PDGFRA	Y988	P16234	0.866575

Table 6.2: Sub micromolar interactions identified in these studies (Continued)

YES1	P07947	PDGFRB	Y751	P09619	0.992637
YES1	P07947	PDGFRB	Y763	P09619	0.693615
YES1	P07947	RET	Y791	P07949	0.359942
YES1	P07947	RET	Y900	P07949	0.79969
YES1	P07947	RET	Y981	P07949	0.317781
YES1	P07947	RET	Y1096	P07949	0.601162
YES1	P07947	ROS1	Y2274	P08922	0.756808
YES1	P07947	ROS1	Y2334	P08922	0.919651
YES1	P07947	TEK	Y1048	Q02763	0.457668
YES1	P07947	TEK	Y1102	Q02763	0.920997
YES1	P07947	FRS2	Y196	Q8WU20	0.838552
YES1	P07947	EGFR	Y1092	P00533	0.934067
YES1	P07947	EGFR	Y1172	P00533	0.809628
YES1	P07947	ERBB2	Y1023	P04626	0.926775
YES1	P07947	ERBB2	Y1222	P04626	0.254196
YES1	P07947	ERBB3	Y1197	P21860	0.546518
YES1	P07947	ERBB3	Y1289	P21860	0.361518
YES1	P07947	RET	Y952	P07949	0.238772
YES1	P07947	EPHA2	Y960	P29317	0.630127
YES1	P07947	EPHA7	Y614	Q15375	0.395618
YES1	P07947	EPHA7	Y791	Q15375	0.982929
YES1	P07947	ABL2	Y515	P42684	0.790254
YES1	P07947	ABL1	Y276	P00519	0.451235
YES1	P07947	FYN	Y420	P06241	0.920565
YES1	P07947	SRC	Y419	P12931	0.920565
YES1	P07947	YES1	Y426	P07947	0.920565
YES1	P07947	EPHA1	Y599	P21709	0.779634
YES1	P07947	EPHA1	Y605	P21709	0.610979
YES1	P07947	EPHA1	Y781	P21709	0.767157
YES1	P07947	SYK	Y323	P43405	0.731821
YES1	P07947	TXK	Y91	P42681	0.728357
YES1	P07947	GRB2	Y209	P62993	0.730525
YES1	P07947	GRAP2	Y45	O75791	0.262348
YES1	P07947	SH2D2A	Y290	Q9NP31	0.562926
YES1	P07947	CBL	Y368	P22681	0.837451
YES1	P07947	CBL	Y774	P22681	0.574869
YES1	P07947	DAB1	Y198	O75553	0.677169
YES1	P07947	DOK1	Y203	Q99704	0.88107
YES1	P07947	DOK1	Y296	Q99704	0.569766
YES1	P07947	DOK1	Y315	Q99704	0.751018

Table 6.2: Sub micromolar interactions identified in these studies (Continued)

YES1	P07947	DOK1	Y377	Q99704	0.811104
YES1	P07947	DOK2	Y299	O60496	0.647832
YES1	P07947	EPHA3	Y937	P29320	0.660281
YES1	P07947	EPHA5	Y656	P54756	0.610199
YES1	P07947	EPHB1	Y634	P54762	0.748088
YES1	P07947	ERBB2	Y1127	P04626	0.544232
YES1	P07947	IRS1	Y465	P35568	0.984137
YES1	P07947	IRS1	Y732	P35568	0.698915
YES1	P07947	IRS1	Y896	P35568	0.74887
YES1	P07947	IRS2	Y823	Q9Y4H2	0.867405
YES1	P07947	PIK3R1	Y368	P27986	0.158593
YES1	P07947	PIK3R1	Y467	P27986	0.324605
YES1	P07947	PIK3R1	Y556	P27986	0.899202
YES1	P07947	PIK3CB	Y772	P42338	0.762953
YES1	P07947	PIK3CD	Y440	O00329	0.931903
YES1	P07947	ABL2	Y683	P42684	0.816455
YES1	P07947	ABL1	Y191	P00519	0.97613
YES1	P07947	SRC	Y521	P12931	0.748584
YES1	P07947	SYK	Y203	P43405	0.514539
YES1	P07947	TEC	Y519	P42680	0.931513
YES1	P07947	PTPN11	Y304	Q06124	0.770958
YES1	P07947	PTPN11	Y584	Q06124	0.773108
YES1	P07947	SHB	Y336	Q15464	0.664768
YES1	P07947	ANKS1A	Y454	Q92625	0.305026
YES1	P07947	ANKS1A	Y833	Q92625	0.618299
YES1	P07947	CTNNB1	Y333	P35222	0.774805
SH2D1A	O60880	EPHB1	Y778	P54762	0.603919
SH2D1A	O60880	FLT1	Y1327	P17948	0.998294
SH2D1A	O60880	FLT3	Y597	P36888	0.680484
SH2D1A	O60880	MST1R	Y1317	Q04912	0.741659
SH2D1A	O60880	NTRK1	Y496	P04629	0.786467
SH2D1A	O60880	RET	Y981	P07949	0.553292
SH2D1A	O60880	DAB1	Y198	O75553	0.535907
SH2D1A	O60880	ERBB2	Y735	P04626	0.831209
SH2D1A	O60880	IRS1	Y465	P35568	0.782444
SH2D1A	O60880	TNS1	Y366	Q9HBL0	0.921502
SH2D1A	O60880	TNS1	Y796	Q9HBL0	0.340946
SH2D1A	O60880	TNS1	Y1144	Q9HBL0	0.556188
SH2D1A	O60880	MAPRE1	Y124	Q15691	0.88945
STAP1	Q9ULZ2	ALK	Y1507	Q9UM73	0.337285

Table 6.2: Sub micromolar interactions identified in these studies (Continued)

STAP1	Q9ULZ2	NTRK1	Y496	P04629	0.244684
STAP1	Q9ULZ2	NTRK2	Y706	Q16620	0.296647
STAP1	Q9ULZ2	NTRK3	Y709	Q16288	0.296647
STAP1	Q9ULZ2	PDGFRB	Y775	P09619	0.87605
STAP1	Q9ULZ2	ERBB3	Y1276	P21860	0.777912
STAP1	Q9ULZ2	SRC	Y216	P12931	0.956353
STAP1	Q9ULZ2	CSF1R	Y923	P07333	0.743592
STAP1	Q9ULZ2	ZAP70	Y493	P43403	0.496419
STAP1	Q9ULZ2	EPHA3	Y937	P29320	0.778831
STAP1	Q9ULZ2	EPHB1	Y575	P54762	0.765845
STAP1	Q9ULZ2	ROS1	Y2110	P08922	0.402391
STAP1	Q9ULZ2	FGR	Y34	P09769	0.354288
STAP1	Q9ULZ2	FGR	Y180	P09769	0.385959
STAP1	Q9ULZ2	FYN	Y185	P06241	0.385959
STAP1	Q9ULZ2	YES1	Y194	P07947	0.385959
STAP1	Q9ULZ2	FER	Y229	P16591	0.561097
STAP1	Q9ULZ2	CRK	Y251	P46108	0.694957
STAP1	Q9ULZ2	NCK1	Y105	P16333	0.900628
STAP1	Q9ULZ2	CHN2	Y21	P52757	0.304796
STAP1	Q9ULZ2	TNS1	Y1254	Q9HBL0	0.543282
STAP1	Q9ULZ2	CBL	Y455	P22681	0.156049
STAP1	Q9ULZ2	ANKS1A	Y454	Q92625	0.542409
STAP1	Q9ULZ2	CTNNB1	Y333	P35222	0.885761
MATK	P42679	NTRK3	Y516	Q16288	0.754724
MATK	P42679	FGR	Y523	P09769	0.513811
MATK	P42679	SH2D3A	Y231	Q9BRG2	0.658169
MATK	P42679	CBL	Y368	P22681	0.54414
MATK	P42679	SYK	Y203	P43405	0.724206
MATK	P42679	VAV3	Y173	Q9UKW4	0.522787
MATK	P42679	ANKS1A	Y454	Q92625	0.939014
MATK	P42679	ITK	Y180	Q08881	0.591884
CRKL	P46109	ALK	Y1092	Q9UM73	0.219929
CRKL	P46109	FGFR1	Y605	P11362	0.695285
CRKL	P46109	FGFR1	Y653	P11362	0.448418
CRKL	P46109	FGFR1	Y654	P11362	0.95011
CRKL	P46109	FGFR3	Y577	P22607	0.53939
CRKL	P46109	FGFR3	Y648	P22607	0.483277
CRKL	P46109	FGFR3	Y724	P22607	0.45485
CRKL	P46109	FLT1	Y1327	P17948	0.888565
CRKL	P46109	FLT4	Y1063	P35916	0.926868

Table 6.2: Sub micromolar interactions identified in these studies (Continued)

CRKL	P46109	KDR	Y1054	P35968	0.926868
CRKL	P46109	KDR	Y1214	P35968	0.594696
CRKL	P46109	KIT	Y721	P10721	0.461127
CRKL	P46109	KIT	Y900	P10721	0.409294
CRKL	P46109	NTRK1	Y496	P04629	0.413195
CRKL	P46109	NTRK2	Y706	Q16620	0.769762
CRKL	P46109	NTRK3	Y709	Q16288	0.769762
CRKL	P46109	NTRK2	Y707	Q16620	0.887397
CRKL	P46109	NTRK3	Y710	Q16288	0.887397
CRKL	P46109	RET	Y981	P07949	0.140384
CRKL	P46109	RET	Y1062	P07949	0.695025
CRKL	P46109	ERBB4	Y1150	Q15303	0.297338
CRKL	P46109	EGFR	Y1016	P00533	0.611695
CRKL	P46109	ERBB2	Y1139	P04626	0.763613
CRKL	P46109	ABL1	Y276	P00519	0.400045
CRKL	P46109	ZAP70	Y248	P43403	0.792141
CRKL	P46109	AXL	Y759	P30530	0.460065
CRKL	P46109	CSF1R	Y923	P07333	0.520611
CRKL	P46109	HCK	Y209	P08631	0.412363
CRKL	P46109	FES	Y811	P07332	0.593265
CRKL	P46109	PLCG1	Y472	P19174	0.655119
CRKL	P46109	PLCG2	Y1245	P16885	0.493439
CRKL	P46109	GRB2	Y209	P62993	0.424817
CRKL	P46109	GRAP2	Y45	O75791	0.808536
CRKL	P46109	NCK1	Y268	P16333	0.310166
CRKL	P46109	RIN1	Y36	Q13671	0.778559
CRKL	P46109	SH2D3A	Y231	Q9BRG2	0.858953
CRKL	P46109	RASA1	Y460	P20936	0.818124
CRKL	P46109	VAV2	Y159	P52735	0.824773
CRKL	P46109	VAV2	Y172	P52735	0.614711
CRKL	P46109	CBL	Y337	P22681	0.792233
CRKL	P46109	CBL	Y368	P22681	0.632281
CRKL	P46109	CBL	Y371	P22681	0.948081
CRKL	P46109	CBLB	Y363	Q13191	0.948081
CRKL	P46109	CBL	Y700	P22681	0.416924
CRKL	P46109	CBL	Y774	P22681	0.431384
CRKL	P46109	STAT1	Y701	P42224	0.861119
CRKL	P46109	DAB1	Y220	O75553	0.430091
CRKL	P46109	DAB1	Y232	O75553	0.443463
CRKL	P46109	DOK1	Y146	Q99704	0.857527

Table 6.2: Sub micromolar interactions identified in these studies (Continued)

CRKL	P46109	DOK1	Y377	Q99704	0.912864
CRKL	P46109	DOK1	Y409	Q99704	0.716559
CRKL	P46109	DOK2	Y139	O60496	0.712137
CRKL	P46109	ERBB2	Y1127	P04626	0.71267
CRKL	P46109	FLT1	Y1048	P17948	0.396923
CRKL	P46109	IRS1	Y46	P35568	0.709646
CRKL	P46109	IRS1	Y465	P35568	0.75858
CRKL	P46109	IRS1	Y732	P35568	0.678611
CRKL	P46109	IRS1	Y989	P35568	0.589271
CRKL	P46109	IRS2	Y675	Q9Y4H2	0.540616
CRKL	P46109	IRS2	Y823	Q9Y4H2	0.835534
CRKL	P46109	GAB1	Y259	Q13480	0.436496
CRKL	P46109	GAB1	Y307	Q13480	0.256631
CRKL	P46109	PIK3R1	Y528	P27986	0.452313
CRKL	P46109	SRC	Y338	P12931	0.351545
CRKL	P46109	LYN	Y265	P07948	0.474606
CRKL	P46109	LYN	Y460	P07948	0.674566
CRKL	P46109	SHC3	Y342	Q92529	0.750788
CRKL	P46109	SHB	Y297	Q15464	0.860242
CRKL	P46109	TNS1	Y1345	Q9HBL0	0.70022
CRKL	P46109	CBLB	Y709	Q13191	0.569345
CRKL	P46109	CBLB	Y889	Q13191	0.377268
CRKL	P46109	DOK4	Y255	Q8TEW6	0.225536
ABL1	P00519	FGFR1	Y653	P11362	0.355881
ABL1	P00519	FGFR3	Y724	P22607	0.503969
ABL1	P00519	FLT1	Y1327	P17948	0.849695
ABL1	P00519	KIT	Y721	P10721	0.830683
ABL1	P00519	KIT	Y936	P10721	0.425751
ABL1	P00519	MET	Y1313	P08581	0.84276
ABL1	P00519	MET	Y1356	P08581	0.398738
ABL1	P00519	MST1R	Y1317	Q04912	0.422593
ABL1	P00519	RET	Y1096	P07949	0.590385
ABL1	P00519	FRS2	Y349	Q8WU20	0.779255
ABL1	P00519	ERBB2	Y1139	P04626	0.858463
ABL1	P00519	ERBB2	Y1221	P04626	0.702392
ABL1	P00519	EPHA7	Y614	Q15375	0.410672
ABL1	P00519	EPHA1	Y605	P21709	0.169489
ABL1	P00519	LCK	Y192	P06239	0.672862
ABL1	P00519	FES	Y811	P07332	0.270901
ABL1	P00519	PLCG1	Y783	P19174	0.940071

Table 6.2: Sub micromolar interactions identified in these studies (Continued)

ABL1	P00519	GRB2	Y209	P62993	0.612147
ABL1	P00519	CRK	Y221	P46108	0.769494
ABL1	P00519	CRKL	Y207	P46109	0.416854
ABL1	P00519	NCK1	Y268	P16333	0.477597
ABL1	P00519	SHC1	Y349	P29353	0.655595
ABL1	P00519	SH2D3A	Y231	Q9BRG2	0.683377
ABL1	P00519	SH2D2A	Y39	Q9NP31	0.543909
ABL1	P00519	PTPN6	Y564	P29350	0.973907
ABL1	P00519	INPPL1	Y986	O15357	0.418427
ABL1	P00519	DAB1	Y220	O75553	0.854103
ABL1	P00519	DOK1	Y315	Q99704	0.778252
ABL1	P00519	DOK1	Y362	Q99704	0.704623
ABL1	P00519	DOK1	Y377	Q99704	0.765606
ABL1	P00519	DOK1	Y398	Q99704	0.930068
ABL1	P00519	DOK1	Y409	Q99704	0.924244
ABL1	P00519	DOK2	Y139	O60496	0.822369
ABL1	P00519	DOK2	Y345	O60496	0.475108
ABL1	P00519	EPHB3	Y600	P54753	0.660109
ABL1	P00519	EPHB3	Y608	P54753	0.801441
ABL1	P00519	ERBB2	Y1127	P04626	0.491165
ABL1	P00519	IRS1	Y989	P35568	0.992784
ABL1	P00519	IRS2	Y675	Q9Y4H2	0.724796
ABL1	P00519	IRS2	Y823	Q9Y4H2	0.805011
ABL1	P00519	EPHA2	Y930	P29317	0.59984
ABL1	P00519	FGR	Y180	P09769	0.609982
ABL1	P00519	FYN	Y185	P06241	0.609982
ABL1	P00519	YES1	Y194	P07947	0.609982
ABL1	P00519	SRC	Y187	P12931	0.958418
ABL1	P00519	RIN1	Y632	Q13671	0.457947
ABL1	P00519	SH2D2A	Y260	Q9NP31	0.997651
ABL1	P00519	HSH2D	Y265	Q96JZ2	0.993784
ABL1	P00519	TNS1	Y366	Q9HBL0	0.821566
ABL1	P00519	TNS1	Y903	Q9HBL0	0.945005
ABL1	P00519	ANKS1A	Y454	Q92625	0.889422
ABL1	P00519	PTK2	Y861	Q05397	0.672341
ABL1	P00519	CTNNB1	Y333	P35222	0.683762
BTK	Q06187	NTRK3	Y516	Q16288	0.9837
BTK	Q06187	ABL1	Y412	P00519	0.518411
BTK	Q06187	FES	Y811	P07332	0.432744
BTK	Q06187	VAV2	Y172	P52735	0.82651

Table 6.2: Sub micromolar interactions identified in these studies (Continued)

BTK	Q06187	CBL	Y368	P22681	0.769571
BTK	Q06187	DOK1	Y398	Q99704	0.232044
BTK	Q06187	CSK	Y263	P41240	0.99661
RASA1-C	P20936	FGFR1	Y605	P11362	0.599984
RASA1-C	P20936	DOK1	Y315	Q99704	0.485755
RASA1-C	P20936	DOK1	Y398	Q99704	0.715569
RASA1-C	P20936	DOK2	Y299	O60496	0.175922
RASA1-C	P20936	FLT3	Y768	P36888	0.933255
RASA1-C	P20936	INSR	Y1149	P06213	0.176842
RASA1-C	P20936	IRS1	Y989	P35568	0.708626
RASA1-C	P20936	IRS2	Y675	Q9Y4H2	0.88627
RASA1-C	P20936	IRS2	Y823	Q9Y4H2	0.495175
RASA1-C	P20936	ABL1	Y272	P00519	0.505701
RASA1-C	P20936	TYRO3	Y681	Q06418	0.82646
RASA1-C	P20936	SHB	Y268	Q15464	0.758566
RIN1	Q13671	EPHB1	Y600	P54762	0.883072
RIN1	Q13671	EPHB2	Y602	P29323	0.883072
RIN1	Q13671	FGFR1	Y463	P11362	0.869991
RIN1	Q13671	FGFR3	Y724	P22607	0.513299
RIN1	Q13671	FLT3	Y591	P36888	0.605648
RIN1	Q13671	INSR	Y1011	P06213	0.985535
RIN1	Q13671	MET	Y1313	P08581	0.678785
RIN1	Q13671	NTRK2	Y707	Q16620	0.903324
RIN1	Q13671	NTRK3	Y710	Q16288	0.903324
RIN1	Q13671	PDGFRA	Y572	P16234	0.853178
RIN1	Q13671	PDGFRB	Y579	P09619	0.86938
RIN1	Q13671	PDGFRB	Y581	P09619	0.678939
RIN1	Q13671	EPHA2	Y588	P29317	0.32045
RIN1	Q13671	EPHA7	Y614	Q15375	0.654796
RIN1	Q13671	PTPN6	Y536	P29350	0.380923
RIN1	Q13671	CBL	Y368	P22681	0.877574
RIN1	Q13671	CBL	Y371	P22681	0.841153
RIN1	Q13671	CBLB	Y363	Q13191	0.841153
RIN1	Q13671	CBL	Y774	P22681	0.411072
RIN1	Q13671	DAB1	Y198	O75553	0.866356
RIN1	Q13671	EPHB3	Y614	P54753	0.654991
RIN1	Q13671	EPHB3	Y754	P54753	0.783583
RIN1	Q13671	IRS1	Y896	P35568	0.662331
RIN1	Q13671	FGR	Y180	P09769	0.763023
RIN1	Q13671	FYN	Y185	P06241	0.763023

Table 6.2: Sub micromolar interactions identified in these studies (Continued)

RIN1	Q13671	YES1	Y194	P07947	0.763023
RIN1	Q13671	FYN	Y213	P06241	0.605996
RIN1	Q13671	YES1	Y222	P07947	0.605996
SH2D3A	Q9BRG2	EPHB1	Y600	P54762	0.966169
SH2D3A	Q9BRG2	EPHB2	Y602	P29323	0.966169
SH2D3A	Q9BRG2	FGFR1	Y730	P11362	0.788883
SH2D3A	Q9BRG2	FGFR3	Y760	P22607	0.42686
SH2D3A	Q9BRG2	FLT3	Y597	P36888	0.800497
SH2D3A	Q9BRG2	FLT3	Y599	P36888	0.44494
SH2D3A	Q9BRG2	INSR	Y1011	P06213	0.453908
SH2D3A	Q9BRG2	MET	Y1313	P08581	0.827226
SH2D3A	Q9BRG2	MET	Y1356	P08581	0.549067
SH2D3A	Q9BRG2	MST1R	Y1317	Q04912	0.500147
SH2D3A	Q9BRG2	NTRK1	Y496	P04629	0.702813
SH2D3A	Q9BRG2	PDGFRA	Y572	P16234	0.899985
SH2D3A	Q9BRG2	PDGFRB	Y579	P09619	0.916942
SH2D3A	Q9BRG2	PDGFRB	Y581	P09619	0.342383
SH2D3A	Q9BRG2	RET	Y1062	P07949	0.458924
SH2D3A	Q9BRG2	EGFR	Y944	P00533	0.859063
SH2D3A	Q9BRG2	ERBB2	Y1023	P04626	0.948664
SH2D3A	Q9BRG2	EPHA2	Y791	P29317	0.66773
SH2D3A	Q9BRG2	EPHA7	Y597	Q15375	0.741536
SH2D3A	Q9BRG2	EPHA7	Y791	Q15375	0.466488
SH2D3A	Q9BRG2	ABL2	Y515	P42684	0.562387
SH2D3A	Q9BRG2	TEC	Y206	P42680	0.998668
SH2D3A	Q9BRG2	LCK	Y192	P06239	0.957713
SH2D3A	Q9BRG2	LCP2	Y128	Q13094	0.138652
SH2D3A	Q9BRG2	BLNK	Y72	Q8WV28	0.810974
SH2D3A	Q9BRG2	CBL	Y371	P22681	0.630585
SH2D3A	Q9BRG2	CBLB	Y363	Q13191	0.630585
SH2D3A	Q9BRG2	DAB1	Y198	O75553	0.401498
SH2D3A	Q9BRG2	DOK1	Y377	Q99704	0.866017
SH2D3A	Q9BRG2	EPHB3	Y754	P54753	0.888254
SH2D3A	Q9BRG2	EPHB4	Y581	P54760	0.957693
SH2D3A	Q9BRG2	FLT4	Y853	P35916	0.706449
SH2D3A	Q9BRG2	IRS1	Y465	P35568	0.977151
SH2D3A	Q9BRG2	IRS1	Y732	P35568	0.582665
SH2D3A	Q9BRG2	ABL1	Y204	P00519	0.926085
SH2D3A	Q9BRG2	MST1R	Y1017	Q04912	0.908901
SH2D3A	Q9BRG2	ABL1	Y191	P00519	0.714675

Table 6.2: Sub micromolar interactions identified in these studies (Continued)

SH2D3A	Q9BRG2	FGR	Y180	P09769	0.967097
SH2D3A	Q9BRG2	FYN	Y185	P06241	0.967097
SH2D3A	Q9BRG2	YES1	Y194	P07947	0.967097
SH2D3A	Q9BRG2	SRC	Y187	P12931	0.907968
SH2D3A	Q9BRG2	SYK	Y203	P43405	0.627685
SH2D3A	Q9BRG2	VAV1	Y826	P15498	0.699675
SH2D3A	Q9BRG2	DOK3	Y208	Q7L591	0.572099
SH2D3A	Q9BRG2	CSK	Y263	P41240	0.717583
SHC1	P29353	FLT1	Y1327	P17948	0.914727
SHC1	P29353	KIT	Y936	P10721	0.98892
SHC1	P29353	MET	Y1365	P08581	0.79406
SHC1	P29353	MST1R	Y1317	Q04912	0.640478
SHC1	P29353	RET	Y1062	P07949	0.670424
SHC1	P29353	EPHA7	Y597	Q15375	0.968278
SHC1	P29353	SRC	Y216	P12931	0.896582
SHC1	P29353	FES	Y811	P07332	0.722493
SHC1	P29353	VAV2	Y159	P52735	0.459699
SHC1	P29353	VAV2	Y172	P52735	0.89636
SHC1	P29353	DOK1	Y146	Q99704	0.509697
SHC1	P29353	KIT	Y553	P10721	0.811566
SHC1	P29353	ROS1	Y2323	P08922	0.658073
SHC1	P29353	PIK3R3	Y195	Q92569	0.374549
SHC1	P29353	SYK	Y203	P43405	0.638904
SHC1	P29353	FYN	Y214	P06241	0.814939
SHC1	P29353	YES1	Y223	P07947	0.814939
SHC1	P29353	VAV3	Y173	Q9UKW4	0.993958
SHC1	P29353	APBB3	Y291	O95704	0.375934
SHC1	P29353	ANKS1A	Y454	Q92625	0.467479
SHF	Q7M4L6	AXL	Y821	P30530	0.853941
SHF	Q7M4L6	EPHA4	Y596	P54764	0.933605
SHF	Q7M4L6	FGFR1	Y463	P11362	0.524018
SHF	Q7M4L6	FGFR3	Y724	P22607	0.86276
SHF	Q7M4L6	FLT3	Y591	P36888	0.962523
SHF	Q7M4L6	INSR	Y1011	P06213	0.718041
SHF	Q7M4L6	MET	Y1356	P08581	0.720497
SHF	Q7M4L6	MST1R	Y1317	Q04912	0.778691
SHF	Q7M4L6	NTRK1	Y496	P04629	0.884303
SHF	Q7M4L6	NTRK3	Y516	Q16288	0.521326
SHF	Q7M4L6	PDGFRA	Y572	P16234	0.94582
SHF	Q7M4L6	PDGFRB	Y1021	P09619	0.883908

Table 6.2: Sub micromolar interactions identified in these studies (Continued)

SHF	Q7M4L6	RET	Y981	P07949	0.461952
SHF	Q7M4L6	RET	Y1096	P07949	0.959153
SHF	Q7M4L6	ROS1	Y2274	P08922	0.674233
SHF	Q7M4L6	ROS1	Y2334	P08922	0.573481
SHF	Q7M4L6	ERBB2	Y1023	P04626	0.480214
SHF	Q7M4L6	ERBB2	Y1222	P04626	0.327447
SHF	Q7M4L6	PLCG2	Y753	P16885	0.696075
SHF	Q7M4L6	DAB1	Y198	O75553	0.66202
SHF	Q7M4L6	DOK1	Y203	Q99704	0.912882
SHF	Q7M4L6	IRS1	Y989	P35568	0.488923
SHF	Q7M4L6	SRC	Y521	P12931	0.865283
SHF	Q7M4L6	SYK	Y203	P43405	0.545188
SHF	Q7M4L6	RASA1	Y239	P20936	0.512163
HSH2D	Q96JZ2	CBL	Y371	P22681	0.812317
HSH2D	Q96JZ2	CBLB	Y363	Q13191	0.812317
HSH2D	Q96JZ2	IRS2	Y675	Q9Y4H2	0.494771
HSH2D	Q96JZ2	GAB1	Y242	Q13480	0.29667
HSH2D	Q96JZ2	GAB1	Y259	Q13480	0.345522
HSH2D	Q96JZ2	GAB1	Y373	Q13480	0.545967
HSH2D	Q96JZ2	SRC	Y521	P12931	0.981861
HSH2D	Q96JZ2	TNS1	Y339	Q9HBL0	0.886332
SH2B3	Q9UQQ2	EPHA3	Y779	P29320	0.82436
SH2B3	Q9UQQ2	EPHA4	Y779	P54764	0.82436
SH2B3	Q9UQQ2	EPHA5	Y833	P54756	0.82436
SH2B3	Q9UQQ2	EPHB1	Y600	P54762	0.900365
SH2B3	Q9UQQ2	EPHB2	Y602	P29323	0.900365
SH2B3	Q9UQQ2	FLT1	Y1327	P17948	0.390351
SH2B3	Q9UQQ2	FLT3	Y591	P36888	0.950048
SH2B3	Q9UQQ2	FLT3	Y599	P36888	0.851233
SH2B3	Q9UQQ2	KIT	Y900	P10721	0.47522
SH2B3	Q9UQQ2	PDGFRB	Y1009	P09619	0.718058
SH2B3	Q9UQQ2	PDGFRB	Y1021	P09619	0.717367
SH2B3	Q9UQQ2	RET	Y981	P07949	0.503835
SH2B3	Q9UQQ2	ERBB3	Y1197	P21860	0.680832
SH2B3	Q9UQQ2	SYK	Y203	P43405	0.924567
GRB14	Q14449	NTRK1	Y496	P04629	0.914836
GRB14	Q14449	ERBB2	Y1221	P04626	0.736905
GRB14	Q14449	ABL1	Y412	P00519	0.33996
GRB14	Q14449	GRB2	Y209	P62993	0.952851
GRB14	Q14449	CBL	Y368	P22681	0.922923

Table 6.2: Sub micromolar interactions identified in these studies (Continued)

GRB14	Q14449	EPHA3	Y937	P29320	0.593884
GRB14	Q14449	IRS1	Y989	P35568	0.72146
GRB14	Q14449	CSK	Y263	P41240	0.868519
GRB7	Q14451	ALK	Y1092	Q9UM73	0.45134
GRB7	Q14451	ALK	Y1096	Q9UM73	0.518757
GRB7	Q14451	FGFR1	Y730	P11362	0.511729
GRB7	Q14451	FGFR3	Y724	P22607	0.428939
GRB7	Q14451	FLT1	Y1327	P17948	0.33368
GRB7	Q14451	FLT3	Y599	P36888	0.513266
GRB7	Q14451	FLT4	Y1337	P35916	0.69102
GRB7	Q14451	IGF1R	Y1281	P08069	0.828358
GRB7	Q14451	INSR	Y1011	P06213	0.716986
GRB7	Q14451	FLT4	Y1063	P35916	0.929303
GRB7	Q14451	KDR	Y1054	P35968	0.929303
GRB7	Q14451	KDR	Y1214	P35968	0.745536
GRB7	Q14451	KIT	Y900	P10721	0.340715
GRB7	Q14451	KIT	Y936	P10721	0.785127
GRB7	Q14451	MET	Y1313	P08581	0.247611
GRB7	Q14451	MET	Y1356	P08581	0.258721
GRB7	Q14451	MET	Y1365	P08581	0.663834
GRB7	Q14451	MST1R	Y1317	Q04912	0.244613
GRB7	Q14451	NTRK1	Y496	P04629	0.583892
GRB7	Q14451	NTRK2	Y707	Q16620	0.890769
GRB7	Q14451	NTRK3	Y710	Q16288	0.890769
GRB7	Q14451	NTRK3	Y516	Q16288	0.413316
GRB7	Q14451	PDGFRB	Y740	P09619	0.792496
GRB7	Q14451	PDGFRB	Y1009	P09619	0.681753
GRB7	Q14451	RET	Y791	P07949	0.239469
GRB7	Q14451	RET	Y1096	P07949	0.73196
GRB7	Q14451	ROS1	Y2274	P08922	0.436249
GRB7	Q14451	TEK	Y1102	Q02763	0.413963
GRB7	Q14451	ERBB2	Y1023	P04626	0.866054
GRB7	Q14451	ERBB2	Y1222	P04626	0.267605
GRB7	Q14451	ERBB3	Y1197	P21860	0.632773
GRB7	Q14451	ERBB3	Y1276	P21860	0.888851
GRB7	Q14451	RET	Y952	P07949	0.654856
GRB7	Q14451	EPHA2	Y588	P29317	0.752548
GRB7	Q14451	ABL2	Y515	P42684	0.753065
GRB7	Q14451	ABL1	Y134	P00519	0.905994
GRB7	Q14451	ABL2	Y161	P42684	0.905994

Table 6.2: Sub micromolar interactions identified in these studies (Continued)

GRB7	Q14451	ABL1	Y276	P00519	0.952167
GRB7	Q14451	ABL1	Y412	P00519	0.253791
GRB7	Q14451	FGR	Y412	P09769	0.861392
GRB7	Q14451	ZAP70	Y474	P43403	0.670074
GRB7	Q14451	PLCG1	Y771	P19174	0.755982
GRB7	Q14451	PLCG2	Y1217	P16885	0.790899
GRB7	Q14451	GRAP2	Y45	O75791	0.772831
GRB7	Q14451	SH3BP2	Y174	P78314	0.738357
GRB7	Q14451	BLNK	Y189	Q8WV28	0.945351
GRB7	Q14451	RASA1	Y615	P20936	0.205507
GRB7	Q14451	VAV1	Y160	P15498	0.677236
GRB7	Q14451	PTPN6	Y564	P29350	0.76629
GRB7	Q14451	EPHB4	Y774	P54760	0.942949
GRB7	Q14451	IRS1	Y46	P35568	0.658507
GRB7	Q14451	IRS1	Y465	P35568	0.960939
GRB7	Q14451	IRS1	Y732	P35568	0.630271
GRB7	Q14451	IRS1	Y896	P35568	0.733502
GRB7	Q14451	IRS1	Y989	P35568	0.918165
GRB7	Q14451	IRS1	Y1179	P35568	0.565889
GRB7	Q14451	IRS2	Y823	Q9Y4H2	0.896322
GRB7	Q14451	SYK	Y203	P43405	0.759572
SHC3	Q92529	MET	Y1313	P08581	0.862081
SHC3	Q92529	MST1R	Y1317	Q04912	0.719822
SHC3	Q92529	NTRK1	Y496	P04629	0.93445
SHC3	Q92529	FGR	Y412	P09769	0.572803
SHC3	Q92529	DOK1	Y146	Q99704	0.32464
SHC3	Q92529	DOK2	Y139	O60496	0.589732
SHC3	Q92529	EPHA3	Y937	P29320	0.795754
SHC3	Q92529	SRC	Y187	P12931	0.502884
SHC3	Q92529	APBB3	Y291	O95704	0.583725
SHC3	Q92529	ANKS1A	Y454	Q92625	0.804342
TENC1	Q63HR2	FGFR3	Y724	P22607	0.716622
TENC1	Q63HR2	FLT1	Y1213	P17948	0.737434
TENC1	Q63HR2	KDR	Y1214	P35968	0.411641
TENC1	Q63HR2	KIT	Y721	P10721	0.883698
TENC1	Q63HR2	KIT	Y900	P10721	0.385778
TENC1	Q63HR2	KIT	Y936	P10721	0.713415
TENC1	Q63HR2	MET	Y1313	P08581	0.730233
TENC1	Q63HR2	MET	Y1356	P08581	0.453973
TENC1	Q63HR2	MST1R	Y1317	Q04912	0.477267

Table 6.2: Sub micromolar interactions identified in these studies (Continued)

TENC1	Q63HR2	NTRK3	Y516	Q16288	0.848777
TENC1	Q63HR2	PDGFRB	Y581	P09619	0.519886
TENC1	Q63HR2	PDGFRB	Y740	P09619	0.526871
TENC1	Q63HR2	PDGFRB	Y771	P09619	0.573199
TENC1	Q63HR2	ERBB4	Y1150	Q15303	0.319027
TENC1	Q63HR2	ERBB2	Y1139	P04626	0.930297
TENC1	Q63HR2	ERBB3	Y1276	P21860	0.455476
TENC1	Q63HR2	ERBB3	Y1328	P21860	0.484319
TENC1	Q63HR2	RET	Y952	P07949	0.586642
TENC1	Q63HR2	EPHA2	Y772	P29317	0.769131
TENC1	Q63HR2	EPHA7	Y597	Q15375	0.857655
TENC1	Q63HR2	PLCG2	Y1245	P16885	0.976023
TENC1	Q63HR2	VAV1	Y160	P15498	0.828568
TENC1	Q63HR2	VAV1	Y174	P15498	0.770818
TENC1	Q63HR2	CBL	Y368	P22681	0.740432
TENC1	Q63HR2	CBL	Y371	P22681	0.395747
TENC1	Q63HR2	CBLB	Y363	Q13191	0.395747
TENC1	Q63HR2	CBL	Y700	P22681	0.880105
TENC1	Q63HR2	EPHA3	Y937	P29320	0.914168
TENC1	Q63HR2	IRS1	Y46	P35568	0.684961
TENC1	Q63HR2	IRS1	Y465	P35568	0.92929
TENC1	Q63HR2	IRS1	Y896	P35568	0.675015
TENC1	Q63HR2	IRS2	Y675	Q9Y4H2	0.888165
TENC1	Q63HR2	KIT	Y553	P10721	0.841111
TENC1	Q63HR2	PDGFRB	Y934	P09619	0.856345
TENC1	Q63HR2	PIK3CD	Y936	O00329	0.569839
TENC1	Q63HR2	ABL2	Y303	P42684	0.437476
TENC1	Q63HR2	LYN	Y473	P07948	0.517021
TENC1	Q63HR2	PTPN11	Y584	Q06124	0.957671
TENC1	Q63HR2	PTPN6	Y377	P29350	0.831243
TENC1	Q63HR2	CBL	Y731	P22681	0.707449
TENC1	Q63HR2	ANKS1A	Y454	Q92625	0.957821
TENC1	Q63HR2	CSK	Y263	P41240	0.988652
TENC1	Q63HR2	PTK2	Y861	Q05397	0.750946
TENC1	Q63HR2	CTNNB1	Y64	P35222	0.782971
PTPN6-C	P29350	PLCG2	Y1245	P16885	0.819332
FER	P16591	EPHA3	Y779	P29320	0.998793
FER	P16591	EPHA4	Y779	P54764	0.998793
FER	P16591	EPHA5	Y833	P54756	0.998793
FER	P16591	CBL	Y368	P22681	0.586912

Table 6.2: Sub micromolar interactions identified in these studies (Continued)

FER	P16591	DOK1	Y398	Q99704	0.261434
FER	P16591	CSK	Y263	P41240	0.73436
PLCG2-N	P16885	EPHA3	Y779	P29320	0.757021
PLCG2-N	P16885	EPHA4	Y779	P54764	0.757021
PLCG2-N	P16885	EPHA5	Y833	P54756	0.757021
PLCG2-N	P16885	FGFR1	Y730	P11362	0.854809
PLCG2-N	P16885	FLT3	Y597	P36888	0.607513
PLCG2-N	P16885	INSR	Y1011	P06213	0.98185
PLCG2-N	P16885	KIT	Y570	P10721	0.64871
PLCG2-N	P16885	MET	Y1313	P08581	0.566648
PLCG2-N	P16885	MST1R	Y1317	Q04912	0.822868
PLCG2-N	P16885	NTRK1	Y676	P04629	0.937962
PLCG2-N	P16885	NTRK3	Y516	Q16288	0.776769
PLCG2-N	P16885	ERBB2	Y1221	P04626	0.554374
PLCG2-N	P16885	ERBB2	Y1222	P04626	0.335818
PLCG2-N	P16885	RET	Y952	P07949	0.742948
PLCG2-N	P16885	ABL1	Y412	P00519	0.248846
PLCG2-N	P16885	FGR	Y523	P09769	0.393876
PLCG2-N	P16885	ZAP70	Y474	P43403	0.63844
PLCG2-N	P16885	PLCG1	Y783	P19174	0.821303
PLCG2-N	P16885	CBL	Y368	P22681	0.783213
PLCG2-N	P16885	IRS1	Y989	P35568	0.878899
PLCG2-N	P16885	PDGFRA	Y958	P16234	0.732083
PLCG2-N	P16885	PIK3CB	Y772	P42338	0.979196
PLCG2-N	P16885	SYK	Y203	P43405	0.651119
SH2B2	O14492	EPHA7	Y791	Q15375	0.559303
SH2B2	O14492	ITK	Y512	Q08881	0.893845
SH2B2	O14492	EPHA3	Y937	P29320	0.9614
SH2B2	O14492	ZAP70	Y164	P43403	0.493915
SH2B2	O14492	VAV3	Y173	Q9UKW4	0.692229
SH2B2	O14492	TNS1	Y339	Q9HBL0	0.378155
BCAR3	O75815	ALK	Y1096	Q9UM73	0.494037
BCAR3	O75815	FGFR3	Y724	P22607	0.356396
BCAR3	O75815	FLT1	Y1327	P17948	0.292102
BCAR3	O75815	FLT3	Y599	P36888	0.363848
BCAR3	O75815	INSR	Y1011	P06213	0.868934
BCAR3	O75815	FLT4	Y1063	P35916	0.637009
BCAR3	O75815	KDR	Y1054	P35968	0.637009
BCAR3	O75815	KDR	Y1214	P35968	0.773519
BCAR3	O75815	KIT	Y936	P10721	0.622139

Table 6.2: Sub micromolar interactions identified in these studies (Continued)

BCAR3	O75815	MET	Y1313	P08581	0.67768
BCAR3	O75815	MET	Y1356	P08581	0.557414
BCAR3	O75815	MST1R	Y1317	Q04912	0.502697
BCAR3	O75815	NTRK1	Y496	P04629	0.691486
BCAR3	O75815	NTRK1	Y676	P04629	0.427529
BCAR3	O75815	NTRK3	Y516	Q16288	0.411087
BCAR3	O75815	PDGFRB	Y581	P09619	0.654723
BCAR3	O75815	PDGFRB	Y1021	P09619	0.891068
BCAR3	O75815	RET	Y1096	P07949	0.773999
BCAR3	O75815	EGFR	Y1172	P00533	0.765942
BCAR3	O75815	ERBB2	Y1023	P04626	0.41601
BCAR3	O75815	ERBB2	Y1222	P04626	0.246846
BCAR3	O75815	ERBB3	Y1276	P21860	0.564928
BCAR3	O75815	EPHA7	Y597	Q15375	0.917322
BCAR3	O75815	ABL2	Y515	P42684	0.686584
BCAR3	O75815	FGR	Y523	P09769	0.687912
BCAR3	O75815	PLCG1	Y771	P19174	0.758139
BCAR3	O75815	PLCG1	Y775	P19174	0.898303
BCAR3	O75815	PLCG2	Y1245	P16885	0.756659
BCAR3	O75815	SH2D3C	Y495	Q8N5H7	0.956048
BCAR3	O75815	VAV1	Y160	P15498	0.940536
BCAR3	O75815	VAV2	Y159	P52735	0.925868
BCAR3	O75815	CBL	Y371	P22681	0.791885
BCAR3	O75815	CBLB	Y363	Q13191	0.791885
BCAR3	O75815	DAB1	Y198	O75553	0.649585
BCAR3	O75815	DOK1	Y315	Q99704	0.855614
BCAR3	O75815	EPHB3	Y754	P54753	0.301087
BCAR3	O75815	IRS1	Y989	P35568	0.896659
BCAR3	O75815	IRS2	Y675	Q9Y4H2	0.914456
BCAR3	O75815	IRS2	Y823	Q9Y4H2	0.760997
BCAR3	O75815	ABL2	Y231	P42684	0.970578
BCAR3	O75815	ABL1	Y191	P00519	0.658787
BCAR3	O75815	FGR	Y180	P09769	0.839369
BCAR3	O75815	FYN	Y185	P06241	0.839369
BCAR3	O75815	YES1	Y194	P07947	0.839369
BCAR3	O75815	VAV1	Y826	P15498	0.660316
BCAR3	O75815	TNS1	Y796	Q9HBL0	0.571856
BCAR3	O75815	STAT1	Y203	P42224	0.926146
BCAR3	O75815	CSK	Y263	P41240	0.824616
SH2D1B	O14796	FLT1	Y1327	P17948	0.959526

Table 6.2: Sub micromolar interactions identified in these studies (Continued)

SH2D1B	O14796	INSR	Y1011	P06213	0.570802
SH2D1B	O14796	MET	Y1356	P08581	0.534264
SH2D1B	O14796	MST1R	Y1317	Q04912	0.884884
SH2D1B	O14796	NTRK1	Y757	P04629	0.848683
SH2D1B	O14796	PDGFRB	Y579	P09619	0.842866
SH2D1B	O14796	CBL	Y371	P22681	0.44226
SH2D1B	O14796	CBLB	Y363	Q13191	0.44226
SH2D1B	O14796	DOK1	Y315	Q99704	0.917328
SH2D1B	O14796	EPHB1	Y634	P54762	0.520868
SH2D1B	O14796	EPHB3	Y754	P54753	0.720247
SH2D1B	O14796	FLT4	Y830	P35916	0.753181
SH2D1B	O14796	IRS1	Y465	P35568	0.668617
SH2D1B	O14796	IRS2	Y823	Q9Y4H2	0.935713
SH2D1B	O14796	GAB1	Y373	Q13480	0.377863
SH2D1B	O14796	KIT	Y553	P10721	0.935996
SH2D1B	O14796	PIK3R1	Y556	P27986	0.360513
SH2D1B	O14796	PIK3C2B	Y685	O00750	0.730411
SH2D1B	O14796	PIK3R1	Y699	P27986	0.730411
SH2D1B	O14796	PIK3CB	Y772	P42338	0.79986
SH2D1B	O14796	PIK3CB	Y962	P42338	0.861442
SH2D1B	O14796	ABL1	Y191	P00519	0.729082
SH2D1B	O14796	SRC	Y521	P12931	0.938069
SH2D1B	O14796	TNS1	Y366	Q9HBL0	0.898278
SH2D1B	O14796	CSK	Y263	P41240	0.896904
SH2D1B	O14796	PTK2	Y861	Q05397	0.377777
SH2D1B	O14796	PTK2B	Y906	Q14289	0.77001
SHE	Q5VZ18	TEK	Y1048	Q02763	0.860664
SHE	Q5VZ18	IRS1	Y465	P35568	0.868732
SHE	Q5VZ18	IRS2	Y675	Q9Y4H2	0.66999
SHE	Q5VZ18	GAB1	Y406	Q13480	0.779488
SLA2	Q9H6Q3	EPHB1	Y600	P54762	0.92209
SLA2	Q9H6Q3	EPHB2	Y602	P29323	0.92209
SLA2	Q9H6Q3	FLT3	Y591	P36888	0.782272
SLA2	Q9H6Q3	FLT3	Y599	P36888	0.546351
SLA2	Q9H6Q3	INSR	Y1011	P06213	0.918463
SLA2	Q9H6Q3	FLT4	Y1063	P35916	0.996178
SLA2	Q9H6Q3	KDR	Y1054	P35968	0.996178
SLA2	Q9H6Q3	KIT	Y570	P10721	0.8511
SLA2	Q9H6Q3	KIT	Y900	P10721	0.71062
SLA2	Q9H6Q3	MET	Y1313	P08581	0.669879

Table 6.2: Sub micromolar interactions identified in these studies (Continued)

SLA2	Q9H6Q3	NTRK3	Y516	Q16288	0.642477
SLA2	Q9H6Q3	PDGFRB	Y1021	P09619	0.925795
SLA2	Q9H6Q3	ABL1	Y276	P00519	0.922494
SLA2	Q9H6Q3	ABL1	Y412	P00519	0.228597
SLA2	Q9H6Q3	PLCG1	Y775	P19174	0.96763
SLA2	Q9H6Q3	PLCG1	Y783	P19174	0.933353
SLA2	Q9H6Q3	DAB1	Y198	O75553	0.805459
SLA2	Q9H6Q3	DOK1	Y146	Q99704	0.987742
SHD	Q96IW2	ERBB4	Y1150	Q15303	0.627641
SH3BP2	P78314	MST1R	Y1360	Q04912	0.479254
SH3BP2	P78314	ERBB2	Y1139	P04626	0.638327
SH3BP2	P78314	ABL1	Y412	P00519	0.445064
SH3BP2	P78314	BLNK	Y72	Q8WV28	0.301613
SH3BP2	P78314	VAV2	Y172	P52735	0.96058
SH3BP2	P78314	PTPN6	Y564	P29350	0.296235
SH3BP2	P78314	CBL	Y368	P22681	0.618432
SH3BP2	P78314	IRS1	Y732	P35568	0.760589
SH3BP2	P78314	KIT	Y553	P10721	0.795158
SH3BP2	P78314	CSK	Y263	P41240	0.846633
SH3BP2	P78314	PTK2	Y1007	Q05397	0.971083
SH3BP2	P78314	CTNNB1	Y64	P35222	0.973008
TXK	P42681	FGFR3	Y724	P22607	0.636714
TXK	P42681	FLT3	Y599	P36888	0.652799
TXK	P42681	MET	Y1313	P08581	0.565677
TXK	P42681	MST1R	Y1317	Q04912	0.41949
TXK	P42681	PDGFRB	Y740	P09619	0.907376
TXK	P42681	RET	Y981	P07949	0.910854
BLNK	Q8WV28	DOK1	Y315	Q99704	0.953814
JAK2	O60674	PDGFRB	Y740	P09619	0.98565
HCK	P08631	FLT1	Y1327	P17948	0.918355
HCK	P08631	INSR	Y1011	P06213	0.854272
HCK	P08631	KIT	Y936	P10721	0.771467
HCK	P08631	MET	Y1313	P08581	0.697985
HCK	P08631	NTRK3	Y516	Q16288	0.764975
HCK	P08631	ROS1	Y2274	P08922	0.901643
HCK	P08631	EPHA2	Y735	P29317	0.857514
HCK	P08631	EPHA2	Y772	P29317	0.777762
HCK	P08631	ABL1	Y276	P00519	0.839866
HCK	P08631	ABL1	Y412	P00519	0.184251
HCK	P08631	SYK	Y323	P43405	0.955935

Table 6.2: Sub micromolar interactions identified in these studies (Continued)

HCK	P08631	FES	Y811	P07332	0.525171
HCK	P08631	PLCG1	Y472	P19174	0.759282
HCK	P08631	PLCG1	Y775	P19174	0.943007
HCK	P08631	PLCG2	Y1217	P16885	0.617216
HCK	P08631	GRAP2	Y45	O75791	0.629852
HCK	P08631	SH3BP2	Y183	P78314	0.889483
HCK	P08631	SH2D2A	Y290	Q9NP31	0.750748
HCK	P08631	VAV1	Y174	P15498	0.97876
HCK	P08631	CBL	Y368	P22681	0.834459
HCK	P08631	DAB1	Y198	O75553	0.982772
HCK	P08631	DOK1	Y146	Q99704	0.752051
HCK	P08631	DOK1	Y315	Q99704	0.704688
HCK	P08631	DOK1	Y398	Q99704	0.21887
HCK	P08631	EPHA3	Y937	P29320	0.969613
HCK	P08631	EPHA5	Y656	P54756	0.909587
HCK	P08631	ERBB2	Y1005	P04626	0.841927
HCK	P08631	ERBB2	Y1127	P04626	0.518496
HCK	P08631	FLT1	Y1048	P17948	0.933053
HCK	P08631	FLT3	Y969	P36888	0.895423
HCK	P08631	IRS1	Y662	P35568	0.995321
HCK	P08631	PDGFRB	Y934	P09619	0.803922
HCK	P08631	PIK3R1	Y607	P27986	0.97921
HCK	P08631	VAV3	Y173	Q9UKW4	0.812208
HCK	P08631	TNS1	Y1144	Q9HBL0	0.597145
HCK	P08631	DOK4	Y255	Q8TEW6	0.518617
HCK	P08631	ANKS1A	Y454	Q92625	0.453355
PTK6	Q13882	FGFR3	Y724	P22607	0.481767
PTK6	Q13882	FLT3	Y599	P36888	0.615964
PTK6	Q13882	MET	Y1313	P08581	0.581419
PTK6	Q13882	MST1R	Y1317	Q04912	0.656706
PTK6	Q13882	ERBB2	Y1139	P04626	0.596626
PTK6	Q13882	AXL	Y702	P30530	0.340438
PTK6	Q13882	FES	Y811	P07332	0.695225
PTK6	Q13882	PLCG2	Y1217	P16885	0.82153
PTK6	Q13882	JAK3	Y785	P52333	0.770936
PTK6	Q13882	VAV2	Y159	P52735	0.558588
PTK6	Q13882	CBL	Y368	P22681	0.856633
PTK6	Q13882	IRS2	Y823	Q9Y4H2	0.748847
PTK6	Q13882	PIK3R1	Y607	P27986	0.918981
PTK6	Q13882	SYK	Y203	P43405	0.643201

Table 6.2: Sub micromolar interactions identified in these studies (Continued)

PTK6	Q13882	VAV3	Y173	Q9UKW4	0.672018
PTK6	Q13882	SHB	Y336	Q15464	0.208212
PTK6	Q13882	TNS1	Y339	Q9HBL0	0.961328
PTK6	Q13882	CBL	Y731	P22681	0.688723
PTK6	Q13882	CBLB	Y889	Q13191	0.489144
PTK6	Q13882	CTNNB1	Y64	P35222	0.934059
BMX	P51813	MET	Y1313	P08581	0.720563
BMX	P51813	NTRK3	Y516	Q16288	0.605955
BMX	P51813	RET	Y1096	P07949	0.858643
BMX	P51813	EGFR	Y1172	P00533	0.722513
BMX	P51813	EPHA7	Y614	Q15375	0.542996
BMX	P51813	IRS2	Y675	Q9Y4H2	0.859645
BMX	P51813	PDGFRA	Y613	P16234	0.339029
BMX	P51813	PIK3CB	Y772	P42338	0.857509
BMX	P51813	PIK3CB	Y962	P42338	0.999141
BMX	P51813	PIK3CD	Y440	O00329	0.74516
BMX	P51813	ABL2	Y683	P42684	0.715014
BMX	P51813	SYK	Y203	P43405	0.634323
BMX	P51813	VAV3	Y173	Q9UKW4	0.636309
BMX	P51813	PTPN6	Y377	P29350	0.508892
BMX	P51813	PTPN6	Y390	P29350	0.824666
JAK3	P52333	FGFR1	Y463	P11362	0.525197
JAK3	P52333	FLT1	Y1333	P17948	0.36201
JAK3	P52333	PDGFRB	Y1021	P09619	0.916916
JAK3	P52333	VAV3	Y173	Q9UKW4	0.225368
SUPT6H	Q7KZ85	FGFR1	Y585	P11362	0.864715
SUPT6H	Q7KZ85	MET	Y1356	P08581	0.559482
SUPT6H	Q7KZ85	RET	Y1062	P07949	0.760979
SUPT6H	Q7KZ85	PLCG2	Y1245	P16885	0.686971
SUPT6H	Q7KZ85	IRS1	Y465	P35568	0.754652
SUPT6H	Q7KZ85	IRS2	Y823	Q9Y4H2	0.87079
GRB10	Q13322	EPHA3	Y596	P29320	0.778055
GRB10	Q13322	FGFR1	Y463	P11362	0.559947
GRB10	Q13322	FGFR3	Y724	P22607	0.757221
GRB10	Q13322	FGFR3	Y760	P22607	0.379215
GRB10	Q13322	FLT1	Y1213	P17948	0.649781
GRB10	Q13322	FLT1	Y1327	P17948	0.810267
GRB10	Q13322	FLT3	Y591	P36888	0.590679
GRB10	Q13322	FLT3	Y599	P36888	0.597995
GRB10	Q13322	KDR	Y996	P35968	0.996883

Table 6.2: Sub micromolar interactions identified in these studies (Continued)

GRB10	Q13322	KDR	Y1214	P35968	0.963463
GRB10	Q13322	MET	Y1313	P08581	0.677635
GRB10	Q13322	MET	Y1356	P08581	0.310468
GRB10	Q13322	NTRK1	Y676	P04629	0.931614
GRB10	Q13322	NTRK2	Y706	Q16620	0.899509
GRB10	Q13322	NTRK3	Y709	Q16288	0.899509
GRB10	Q13322	PDGFRB	Y581	P09619	0.814658
GRB10	Q13322	PDGFRB	Y1009	P09619	0.729117
GRB10	Q13322	PDGFRB	Y1021	P09619	0.907036
GRB10	Q13322	RET	Y1062	P07949	0.928312
GRB10	Q13322	RET	Y1096	P07949	0.636598
GRB10	Q13322	ROS1	Y2274	P08922	0.635648
GRB10	Q13322	TEK	Y1102	Q02763	0.439297
GRB10	Q13322	FRS2	Y306	Q8WU20	0.71758
GRB10	Q13322	ERBB2	Y1023	P04626	0.669002
GRB10	Q13322	ERBB2	Y1222	P04626	0.238161
GRB10	Q13322	ERBB3	Y1197	P21860	0.715254
GRB10	Q13322	RET	Y952	P07949	0.868027
GRB10	Q13322	EPHA2	Y628	P29317	0.69929
GRB10	Q13322	EPHA7	Y614	Q15375	0.8508
GRB10	Q13322	ABL2	Y515	P42684	0.909842
GRB10	Q13322	ABL1	Y412	P00519	0.429343
GRB10	Q13322	FGR	Y412	P09769	0.886526
GRB10	Q13322	FYN	Y420	P06241	0.860677
GRB10	Q13322	SRC	Y419	P12931	0.860677
GRB10	Q13322	YES1	Y426	P07947	0.860677
GRB10	Q13322	ZAP70	Y248	P43403	0.612234
GRB10	Q13322	ZAP70	Y474	P43403	0.716557
GRB10	Q13322	PLCG1	Y472	P19174	0.920346
GRB10	Q13322	PLCG1	Y771	P19174	0.84914
GRB10	Q13322	PLCG2	Y743	P16885	0.882296
GRB10	Q13322	PLCG2	Y1217	P16885	0.891161
GRB10	Q13322	JAK3	Y785	P52333	0.868351
GRB10	Q13322	RASA1	Y460	P20936	0.627014
GRB10	Q13322	RASA1	Y615	P20936	0.20624
GRB10	Q13322	SH2D2A	Y39	Q9NP31	0.631467
GRB10	Q13322	VAV1	Y160	P15498	0.801708
GRB10	Q13322	CBL	Y368	P22681	0.807108
GRB10	Q13322	DAB1	Y198	O75553	0.92431
GRB10	Q13322	DOK1	Y362	Q99704	0.591827

Table 6.2: Sub micromolar interactions identified in these studies (Continued)

GRB10	Q13322	DOK2	Y299	O60496	0.384779
GRB10	Q13322	EPHA5	Y656	P54756	0.683118
GRB10	Q13322	IRS1	Y46	P35568	0.968586
GRB10	Q13322	IRS1	Y465	P35568	0.998518
GRB10	Q13322	IRS1	Y732	P35568	0.823034
GRB10	Q13322	IRS1	Y896	P35568	0.895896
GRB10	Q13322	IRS2	Y823	Q9Y4H2	0.699428
GRB10	Q13322	GAB1	Y373	Q13480	0.863045
GRB10	Q13322	GAB1	Y406	Q13480	0.584951
GRB10	Q13322	PIK3CB	Y962	P42338	0.963318
GRB10	Q13322	SYK	Y203	P43405	0.772257
GRB10	Q13322	TNS1	Y339	Q9HBL0	0.490715
FES	P07332	FGFR1	Y585	P11362	0.732101
FES	P07332	FYN	Y420	P06241	0.733602
FES	P07332	SRC	Y419	P12931	0.733602
FES	P07332	YES1	Y426	P07947	0.733602
FES	P07332	SYK	Y203	P43405	0.524532
TNS4	Q8IZW8	EPHB1	Y600	P54762	0.590108
TNS4	Q8IZW8	EPHB2	Y602	P29323	0.590108
TNS4	Q8IZW8	FGFR3	Y724	P22607	0.5199
TNS4	Q8IZW8	FLT1	Y1213	P17948	0.414545
TNS4	Q8IZW8	KDR	Y1214	P35968	0.185156
TNS4	Q8IZW8	KIT	Y936	P10721	0.452862
TNS4	Q8IZW8	MET	Y1356	P08581	0.444885
TNS4	Q8IZW8	PDGFRB	Y771	P09619	0.238891
TNS4	Q8IZW8	PDGFRB	Y775	P09619	0.637354
TNS4	Q8IZW8	ERBB4	Y1208	Q15303	0.414408
TNS4	Q8IZW8	ERBB2	Y1139	P04626	0.736658
TNS4	Q8IZW8	ERBB3	Y1328	P21860	0.853656
TNS4	Q8IZW8	EPHA2	Y772	P29317	0.652663
TNS4	Q8IZW8	EPHA7	Y791	Q15375	0.407779
TNS4	Q8IZW8	PTPN6	Y564	P29350	0.497664
TNS4	Q8IZW8	CBL	Y774	P22681	0.856737
TNS4	Q8IZW8	DAB1	Y232	O75553	0.639806
TNS4	Q8IZW8	DOK1	Y315	Q99704	0.843359
TNS4	Q8IZW8	DOK1	Y398	Q99704	0.930117
TNS4	Q8IZW8	EPHA5	Y656	P54756	0.685047
TNS4	Q8IZW8	EPHB3	Y754	P54753	0.458759
TNS4	Q8IZW8	IRS1	Y46	P35568	0.828215
TNS4	Q8IZW8	IRS1	Y896	P35568	0.591391

Table 6.2: Sub micromolar interactions identified in these studies (Continued)

TNS4	Q8IZW8	IRS2	Y823	Q9Y4H2	0.993151
TNS4	Q8IZW8	SHB	Y297	Q15464	0.380368
TNS4	Q8IZW8	TNS1	Y339	Q9HBL0	0.712314
TNS4	Q8IZW8	ANKS1A	Y454	Q92625	0.551364
PIK3R3-N	Q92569	FGFR1	Y730	P11362	0.500412
PIK3R3-N	Q92569	FGFR3	Y724	P22607	0.224147
PIK3R3-N	Q92569	IGF1R	Y1346	P08069	0.72992
PIK3R3-N	Q92569	INSR	Y1011	P06213	0.624803
PIK3R3-N	Q92569	INSR	Y1361	P06213	0.417651
PIK3R3-N	Q92569	KDR	Y1059	P35968	0.587181
PIK3R3-N	Q92569	KIT	Y721	P10721	0.148005
PIK3R3-N	Q92569	KIT	Y900	P10721	0.16118
PIK3R3-N	Q92569	MET	Y1365	P08581	0.644616
PIK3R3-N	Q92569	MST1R	Y1317	Q04912	0.306182
PIK3R3-N	Q92569	NTRK1	Y496	P04629	0.877985
PIK3R3-N	Q92569	NTRK3	Y516	Q16288	0.716839
PIK3R3-N	Q92569	PDGFRA	Y742	P16234	0.211803
PIK3R3-N	Q92569	PDGFRB	Y771	P09619	0.16925
PIK3R3-N	Q92569	ROS1	Y2334	P08922	0.835472
PIK3R3-N	Q92569	ERBB4	Y1056	Q15303	0.912233
PIK3R3-N	Q92569	EGFR	Y1016	P00533	0.951999
PIK3R3-N	Q92569	EGFR	Y1092	P00533	0.555743
PIK3R3-N	Q92569	EGFR	Y1138	P00533	0.78676
PIK3R3-N	Q92569	ERBB3	Y1054	P21860	0.945303
PIK3R3-N	Q92569	ERBB3	Y1197	P21860	0.320616
PIK3R3-N	Q92569	ERBB3	Y1276	P21860	0.607545
PIK3R3-N	Q92569	RET	Y952	P07949	0.351387
PIK3R3-N	Q92569	EPHA7	Y597	Q15375	0.749327
PIK3R3-N	Q92569	ABL2	Y515	P42684	0.525211
PIK3R3-N	Q92569	FGR	Y412	P09769	0.394922
PIK3R3-N	Q92569	EPHA1	Y605	P21709	0.857363
PIK3R3-N	Q92569	GRB2	Y209	P62993	0.818709
PIK3R3-N	Q92569	NCK1	Y268	P16333	0.461985
PIK3R3-N	Q92569	BLNK	Y84	Q8WV28	0.309163
PIK3R3-N	Q92569	VAV2	Y172	P52735	0.957145
PIK3R3-N	Q92569	CBL	Y368	P22681	0.541972
PIK3R3-N	Q92569	CBL	Y371	P22681	0.348621
PIK3R3-N	Q92569	CBLB	Y363	Q13191	0.348621
PIK3R3-N	Q92569	CBL	Y700	P22681	0.874884
PIK3R3-N	Q92569	DOK1	Y398	Q99704	0.803042

Table 6.2: Sub micromolar interactions identified in these studies (Continued)

PIK3R3-N	Q92569	ERBB2	Y1127	P04626	0.552762
PIK3R3-N	Q92569	IRS1	Y465	P35568	0.254603
PIK3R3-N	Q92569	IRS1	Y612	P35568	0.3301
PIK3R3-N	Q92569	IRS1	Y732	P35568	0.346878
PIK3R3-N	Q92569	IRS1	Y896	P35568	0.745123
PIK3R3-N	Q92569	IRS1	Y941	P35568	0.354162
PIK3R3-N	Q92569	IRS1	Y989	P35568	0.449961
PIK3R3-N	Q92569	IRS2	Y653	Q9Y4H2	0.579357
PIK3R3-N	Q92569	IRS2	Y675	Q9Y4H2	0.442295
PIK3R3-N	Q92569	PDGFRB	Y934	P09619	0.187995
PIK3R3-N	Q92569	PIK3CB	Y246	P42338	0.467183
PIK3R3-N	Q92569	FGR	Y209	P09769	0.600016
PIK3R3-N	Q92569	LYN	Y473	P07948	0.834271
PIK3R3-N	Q92569	BTK	Y225	Q06187	0.886019
PIK3R3-N	Q92569	SH2D3C	Y183	Q8N5H7	0.248673
PIK3R3-N	Q92569	STAT5A	Y694	P42229	0.802729
PIK3R3-N	Q92569	CBL	Y731	P22681	0.450964
PIK3R3-N	Q92569	ANKS1A	Y454	Q92625	0.80046
PIK3R3-N	Q92569	CTNNB1	Y64	P35222	0.7427
PIK3R3-N	Q92569	CTNNB1	Y86	P35222	0.564123
PIK3R3-C	Q92569	FGFR1	Y605	P11362	0.756545
PIK3R3-C	Q92569	FGFR3	Y724	P22607	0.235694
PIK3R3-C	Q92569	FGFR3	Y770	P22607	0.461049
PIK3R3-C	Q92569	FLT3	Y589	P36888	0.461049
PIK3R3-C	Q92569	FLT1	Y1333	P17948	0.785137
PIK3R3-C	Q92569	KIT	Y721	P10721	0.997247
PIK3R3-C	Q92569	NTRK3	Y516	Q16288	0.94605
PIK3R3-C	Q92569	PDGFRB	Y740	P09619	0.179778
PIK3R3-C	Q92569	CSF1R	Y923	P07333	0.898656
PIK3R3-C	Q92569	PLCG2	Y1245	P16885	0.87787
PIK3R3-C	Q92569	NCK1	Y268	P16333	0.471766
PIK3R3-C	Q92569	SH2D3A	Y231	Q9BRG2	0.607423
PIK3R3-C	Q92569	CBL	Y368	P22681	0.953896
PIK3R3-C	Q92569	CBL	Y371	P22681	0.668943
PIK3R3-C	Q92569	CBLB	Y363	Q13191	0.668943
PIK3R3-C	Q92569	IRS1	Y465	P35568	0.559534
PIK3R3-C	Q92569	IRS1	Y989	P35568	0.728693
PIK3R3-C	Q92569	IRS2	Y675	Q9Y4H2	0.846564
PIK3R3-C	Q92569	IRS2	Y823	Q9Y4H2	0.790033
PIK3R3-C	Q92569	CBL	Y731	P22681	0.228392

Table 6.2: Sub micromolar interactions identified in these studies (Continued)

PIK3R3-C	Q92569	IRS4	Y921	O14654	0.737564
PIK3R2-N	O00459	AXL	Y821	P30530	0.255535
PIK3R2-N	O00459	CSF1R	Y723	P07333	0.623378
PIK3R2-N	O00459	FGFR1	Y605	P11362	0.83266
PIK3R2-N	O00459	FGFR1	Y730	P11362	0.550045
PIK3R2-N	O00459	FGFR3	Y724	P22607	0.187271
PIK3R2-N	O00459	IGF1R	Y1346	P08069	0.599752
PIK3R2-N	O00459	INSR	Y1011	P06213	0.451329
PIK3R2-N	O00459	INSR	Y1361	P06213	0.21691
PIK3R2-N	O00459	KDR	Y1059	P35968	0.460323
PIK3R2-N	O00459	KIT	Y900	P10721	0.158886
PIK3R2-N	O00459	MET	Y1313	P08581	0.27235
PIK3R2-N	O00459	MET	Y1356	P08581	0.48317
PIK3R2-N	O00459	MST1R	Y1317	Q04912	0.311527
PIK3R2-N	O00459	MST1R	Y1360	Q04912	0.538928
PIK3R2-N	O00459	NTRK3	Y516	Q16288	0.926999
PIK3R2-N	O00459	PDGFRA	Y742	P16234	0.144509
PIK3R2-N	O00459	PDGFRB	Y740	P09619	0.255318
PIK3R2-N	O00459	PDGFRB	Y775	P09619	0.585683
PIK3R2-N	O00459	ROS1	Y2274	P08922	0.706561
PIK3R2-N	O00459	TEK	Y1048	Q02763	0.962066
PIK3R2-N	O00459	ERBB4	Y1056	Q15303	0.885027
PIK3R2-N	O00459	EGFR	Y1092	P00533	0.445087
PIK3R2-N	O00459	EGFR	Y1138	P00533	0.610805
PIK3R2-N	O00459	ERBB2	Y1023	P04626	0.32545
PIK3R2-N	O00459	ERBB2	Y1139	P04626	0.819383
PIK3R2-N	O00459	ERBB3	Y1054	P21860	0.464131
PIK3R2-N	O00459	ERBB3	Y1197	P21860	0.279326
PIK3R2-N	O00459	ERBB3	Y1199	P21860	0.547884
PIK3R2-N	O00459	ABL2	Y515	P42684	0.211589
PIK3R2-N	O00459	FGR	Y523	P09769	0.504471
PIK3R2-N	O00459	TXK	Y420	P42681	0.368572
PIK3R2-N	O00459	PLCG1	Y783	P19174	0.486987
PIK3R2-N	O00459	GRB2	Y209	P62993	0.804746
PIK3R2-N	O00459	NCK1	Y268	P16333	0.43131
PIK3R2-N	O00459	SH3BP2	Y183	P78314	0.715898
PIK3R2-N	O00459	JAK3	Y785	P52333	0.63162
PIK3R2-N	O00459	BLNK	Y72	Q8WV28	0.382587
PIK3R2-N	O00459	BLNK	Y84	Q8WV28	0.427679
PIK3R2-N	O00459	SH2D3A	Y231	Q9BRG2	0.741316

Table 6.2: Sub micromolar interactions identified in these studies (Continued)

PIK3R2-N	O00459	VAV2	Y172	P52735	0.518707
PIK3R2-N	O00459	CBL	Y337	P22681	0.96038
PIK3R2-N	O00459	CBL	Y368	P22681	0.555761
PIK3R2-N	O00459	CBL	Y371	P22681	0.527177
PIK3R2-N	O00459	CBLB	Y363	Q13191	0.527177
PIK3R2-N	O00459	CBL	Y700	P22681	0.487285
PIK3R2-N	O00459	DOK1	Y146	Q99704	0.715066
PIK3R2-N	O00459	ERBB2	Y1127	P04626	0.579233
PIK3R2-N	O00459	IRS1	Y465	P35568	0.1754
PIK3R2-N	O00459	IRS1	Y612	P35568	0.286453
PIK3R2-N	O00459	IRS1	Y632	P35568	0.623725
PIK3R2-N	O00459	IRS1	Y896	P35568	0.593692
PIK3R2-N	O00459	IRS1	Y989	P35568	0.360433
PIK3R2-N	O00459	IRS2	Y653	Q9Y4H2	0.509648
PIK3R2-N	O00459	IRS2	Y675	Q9Y4H2	0.32933
PIK3R2-N	O00459	PDGFRB	Y934	P09619	0.252797
PIK3R2-N	O00459	PIK3R2	Y365	O00459	0.781059
PIK3R2-N	O00459	SHC3	Y424	Q92529	0.781059
PIK3R2-N	O00459	PIK3R2	Y605	O00459	0.874755
PIK3R2-N	O00459	PIK3CB	Y246	P42338	0.742448
PIK3R2-N	O00459	SYK	Y203	P43405	0.707288
PIK3R2-N	O00459	PTK6	Y114	Q13882	0.99134
PIK3R2-N	O00459	JAK3	Y981	P52333	0.566404
PIK3R2-N	O00459	STAT5A	Y694	P42229	0.711786
PIK3R2-N	O00459	CBL	Y731	P22681	0.235796
PIK3R2-N	O00459	IRS4	Y921	O14654	0.259791
PIK3R2-N	O00459	ANKS1A	Y454	Q92625	0.805612
PIK3R2-N	O00459	PTK2B	Y849	Q14289	0.938913
DAB1	O75553	MST1R	Y1317	Q04912	0.54767
DAB1	O75553	IRS1	Y465	P35568	0.996483
DAB1	O75553	IRS2	Y675	Q9Y4H2	0.923732
DAB2	P98082	DOK1	Y315	Q99704	0.953693
NUMBL	Q9Y6R0	FGFR1	Y585	P11362	0.870022
NUMBL	Q9Y6R0	MET	Y1356	P08581	0.446074
NUMBL	Q9Y6R0	NTRK1	Y496	P04629	0.871145
NUMBL	Q9Y6R0	RET	Y1062	P07949	0.549413
NUMBL	Q9Y6R0	ROS1	Y2334	P08922	0.831127
NUMBL	Q9Y6R0	NCK1	Y268	P16333	0.935082
NUMBL	Q9Y6R0	IRS1	Y465	P35568	0.769519
NUMBL	Q9Y6R0	IRS1	Y989	P35568	0.96537

Table 6.2: Sub micromolar interactions identified in these studies (Continued)

NUMB	P49757	ERBB3	Y1289	P21860	0.688588
SHC2	P98077	FGFR3	Y724	P22607	0.536382
SHC2	P98077	FLT3	Y591	P36888	0.714134
SHC2	P98077	INSR	Y1011	P06213	0.573644
SHC2	P98077	KDR	Y996	P35968	0.635291
SHC2	P98077	MET	Y1230	P08581	0.698177
SHC2	P98077	MET	Y1313	P08581	0.90214
SHC2	P98077	MET	Y1356	P08581	0.561741
SHC2	P98077	MST1R	Y1317	Q04912	0.646097
SHC2	P98077	NTRK3	Y516	Q16288	0.622085
SHC2	P98077	PDGFRB	Y562	P09619	0.902254
SHC2	P98077	PDGFRB	Y579	P09619	0.796316
SHC2	P98077	PDGFRB	Y740	P09619	0.508218
SHC2	P98077	PDGFRB	Y1021	P09619	0.697985
SHC2	P98077	RET	Y1029	P07949	0.695054
SHC2	P98077	RET	Y1096	P07949	0.771903
SHC2	P98077	EGFR	Y1172	P00533	0.824948
SHC2	P98077	ABL1	Y412	P00519	0.448718
SHC2	P98077	PLCG2	Y1245	P16885	0.799926
SHC2	P98077	DOK1	Y402	Q99704	0.801563
SHC2	P98077	ABL2	Y231	P42684	0.955135
SHC1-PTB	P29353	ALK	Y1092	Q9UM73	0.701593
SHC1-PTB	P29353	ALK	Y1096	Q9UM73	0.612222
SHC1-PTB	P29353	ALK	Y1507	Q9UM73	0.322462
SHC1-PTB	P29353	FGFR1	Y653	P11362	0.702376
SHC1-PTB	P29353	FGFR1	Y730	P11362	0.323243
SHC1-PTB	P29353	FLT4	Y1337	P35916	0.335467
SHC1-PTB	P29353	IGF1R	Y980	P08069	0.956031
SHC1-PTB	P29353	INSR	Y999	P06213	0.854868
SHC1-PTB	P29353	INSR	Y1011	P06213	0.947498
SHC1-PTB	P29353	KIT	Y900	P10721	0.3917
SHC1-PTB	P29353	MET	Y1313	P08581	0.696655
SHC1-PTB	P29353	MET	Y1356	P08581	0.570236
SHC1-PTB	P29353	NTRK1	Y496	P04629	0.576407
SHC1-PTB	P29353	NTRK1	Y676	P04629	0.723206
SHC1-PTB	P29353	NTRK2	Y516	Q16620	0.41416
SHC1-PTB	P29353	PDGFRA	Y574	P16234	0.300106
SHC1-PTB	P29353	ERBB4	Y1242	Q15303	0.713939
SHC1-PTB	P29353	ERBB4	Y1284	Q15303	0.53015
SHC1-PTB	P29353	EGFR	Y1138	P00533	0.388092

Table 6.2: Sub micromolar interactions identified in these studies (Continued)

SHC1-PTB	P29353	ERBB2	Y1023	P04626	0.877826
SHC1-PTB	P29353	ERBB2	Y1196	P04626	0.571858
SHC1-PTB	P29353	ERBB2	Y1221	P04626	0.583772
SHC1-PTB	P29353	EPHA2	Y735	P29317	0.689082
SHC1-PTB	P29353	ABL1	Y276	P00519	0.953334
SHC1-PTB	P29353	FGR	Y412	P09769	0.629607
SHC1-PTB	P29353	FGR	Y523	P09769	0.945145
SHC1-PTB	P29353	SRC	Y216	P12931	0.508687
SHC1-PTB	P29353	PLCG1	Y775	P19174	0.963615
SHC1-PTB	P29353	JAK3	Y785	P52333	0.805383
SHC1-PTB	P29353	INPPL1	Y986	O15357	0.312206
SHC1-PTB	P29353	DOK1	Y146	Q99704	0.546272
SHC1-PTB	P29353	IRS1	Y732	P35568	0.802505
SHC1-PTB	P29353	IRS1	Y989	P35568	0.773927
SHC1-PTB	P29353	SYK	Y203	P43405	0.778369
SHC1-PTB	P29353	ANKS1A	Y833	Q92625	0.637643
DOK1	Q99704	ALK	Y1096	Q9UM73	0.728568
DOK1	Q99704	AXL	Y821	P30530	0.568248
DOK1	Q99704	AXL	Y866	P30530	0.916121
DOK1	Q99704	EPHB2	Y912	P29323	0.872626
DOK1	Q99704	FGFR1	Y463	P11362	0.558966
DOK1	Q99704	FLT3	Y591	P36888	0.724501
DOK1	Q99704	FLT3	Y597	P36888	0.357462
DOK1	Q99704	FLT3	Y599	P36888	0.26234
DOK1	Q99704	INSR	Y1011	P06213	0.569571
DOK1	Q99704	KIT	Y900	P10721	0.182644
DOK1	Q99704	MET	Y1003	P08581	0.863337
DOK1	Q99704	MET	Y1230	P08581	0.761542
DOK1	Q99704	MET	Y1313	P08581	0.173679
DOK1	Q99704	MET	Y1356	P08581	0.491896
DOK1	Q99704	PDGFRA	Y572	P16234	0.73293
DOK1	Q99704	PDGFRB	Y740	P09619	0.92818
DOK1	Q99704	PDGFRB	Y751	P09619	0.590363
DOK1	Q99704	PDGFRB	Y1009	P09619	0.728491
DOK1	Q99704	PDGFRB	Y1021	P09619	0.952081
DOK1	Q99704	RET	Y1096	P07949	0.545897
DOK1	Q99704	ROS1	Y2274	P08922	0.365737
DOK1	Q99704	ROS1	Y2334	P08922	0.730627
DOK1	Q99704	ERBB2	Y1023	P04626	0.582152
DOK1	Q99704	PLCG2	Y1245	P16885	0.729787

Table 6.2: Sub micromolar interactions identified in these studies (Continued)

DOK1	Q99704	INSR	Y1149	P06213	0.934878
DOK1	Q99704	CSK	Y263	P41240	0.925293
DOK2	O60496	FGFR3	Y724	P22607	0.737005
DOK2	O60496	NTRK1	Y496	P04629	0.942248
DOK2	O60496	RET	Y1062	P07949	0.862249
DOK2	O60496	ABL2	Y515	P42684	0.831347
DOK2	O60496	ABL1	Y276	P00519	0.650633
DOK2	O60496	VAV2	Y159	P52735	0.897972
DOK2	O60496	CBL	Y368	P22681	0.94491
DOK2	O60496	CSK	Y263	P41240	0.992938
DOK4	Q8TEW6	FGFR1	Y463	P11362	0.948323
DOK4	Q8TEW6	MET	Y1356	P08581	0.742546
DOK4	Q8TEW6	IRS1	Y465	P35568	0.620847
DOK4	Q8TEW6	IRS2	Y823	Q9Y4H2	0.762194
DOK4	Q8TEW6	GAB1	Y242	Q13480	0.358118
DOK4	Q8TEW6	GAB1	Y259	Q13480	0.365096
DOK5	Q9P104	PDGFRB	Y1021	P09619	0.808282
DOK5	Q9P104	PLCG2	Y1245	P16885	0.761905
IRS1	P35568	PDGFRB	Y1021	P09619	0.841574
IRS4	O14654	PLCG2	Y1245	P16885	0.630501
FRS3	O43559	NTRK1	Y496	P04629	0.688318
FRS3	O43559	RET	Y1062	P07949	0.696125
FRS3	O43559	ABL1	Y488	P00519	0.84047
FRS3	O43559	IRS2	Y675	Q9Y4H2	0.761283
ANKS1A	Q92625	FGFR1	Y463	P11362	0.452842
ANKS1A	Q92625	FGFR3	Y770	P22607	0.853093
ANKS1A	Q92625	FLT3	Y589	P36888	0.853093
ANKS1A	Q92625	PDGFRB	Y1021	P09619	0.832722
ANKS1A	Q92625	RET	Y1062	P07949	0.988126
ANKS1A	Q92625	FRS2	Y436	Q8WU20	0.32211
ANKS1A	Q92625	EGFR	Y1172	P00533	0.817516
ANKS1A	Q92625	ERBB2	Y1139	P04626	0.903046
APPL1	Q9UKG1	MET	Y1313	P08581	0.648983
APPL1	Q9UKG1	ZAP70	Y126	P43403	0.32182
GULP1	Q9UBP9	AXL	Y821	P30530	0.501512
GULP1	Q9UBP9	EPHB1	Y600	P54762	0.57623
GULP1	Q9UBP9	EPHB2	Y602	P29323	0.57623
GULP1	Q9UBP9	FLT3	Y591	P36888	0.845127
GULP1	Q9UBP9	FLT3	Y597	P36888	0.592763
GULP1	Q9UBP9	FLT3	Y599	P36888	0.436238

Table 6.2: Sub micromolar interactions identified in these studies (Continued)

GULP1	Q9UBP9	INSR	Y1011	P06213	0.593207
GULP1	Q9UBP9	KIT	Y936	P10721	0.921791
GULP1	Q9UBP9	MET	Y1003	P08581	0.454465
GULP1	Q9UBP9	MET	Y1230	P08581	0.906948
GULP1	Q9UBP9	MET	Y1234	P08581	0.63235
GULP1	Q9UBP9	MET	Y1313	P08581	0.607378
GULP1	Q9UBP9	MET	Y1356	P08581	0.532448
GULP1	Q9UBP9	MST1R	Y1360	Q04912	0.995928
GULP1	Q9UBP9	PDGFRA	Y572	P16234	0.597337
GULP1	Q9UBP9	PDGFRB	Y579	P09619	0.863653
GULP1	Q9UBP9	PDGFRB	Y740	P09619	0.66385
GULP1	Q9UBP9	PDGFRB	Y751	P09619	0.453731
GULP1	Q9UBP9	PDGFRB	Y775	P09619	0.95902
GULP1	Q9UBP9	PDGFRB	Y1021	P09619	0.703334
GULP1	Q9UBP9	RET	Y981	P07949	0.424132
GULP1	Q9UBP9	RET	Y1029	P07949	0.982662
GULP1	Q9UBP9	RET	Y1062	P07949	0.64938
GULP1	Q9UBP9	RET	Y1096	P07949	0.822959
GULP1	Q9UBP9	EGFR	Y1125	P00533	0.702493
GULP1	Q9UBP9	IRS1	Y732	P35568	0.849669
GULP1	Q9UBP9	IRS1	Y896	P35568	0.699241
GULP1	Q9UBP9	ROS1	Y2110	P08922	0.634215
TNS1-PTB	Q9HBL0	EPHA7	Y791	Q15375	0.680334
TENC1-PTB	Q63HR2	ERBB3	Y1054	P21860	0.34174
TENC1-PTB	Q63HR2	EPHA7	Y791	Q15375	0.832303
TENC1-PTB	Q63HR2	FGR	Y523	P09769	0.145152
TENC1-PTB	Q63HR2	EPHA1	Y599	P21709	0.99187
TENC1-PTB	Q63HR2	LCK	Y192	P06239	0.295724
TENC1-PTB	Q63HR2	DOK1	Y315	Q99704	0.938282
TENC1-PTB	Q63HR2	ROS1	Y2110	P08922	0.393144
TENC1-PTB	Q63HR2	ABL1	Y191	P00519	0.92347
TENC1-PTB	Q63HR2	SYK	Y203	P43405	0.395918
TENC1-PTB	Q63HR2	FYN	Y531	P06241	0.773591
TENC1-PTB	Q63HR2	YES1	Y537	P07947	0.773591
CCM2	Q9BSQ5	PLCG2	Y1245	P16885	0.881716
ANKS1B	Q7Z6G8	MET	Y1313	P08581	0.644095
ANKS1B	Q7Z6G8	PDGFRB	Y1021	P09619	0.884444
ANKS1B	Q7Z6G8	ABL1	Y412	P00519	0.894799
ANKS1B	Q7Z6G8	ZAP70	Y292	P43403	0.76104
ANKS1B	Q7Z6G8	ZAP70	Y315	P43403	0.834369

Table 6.2: Sub micromolar interactions identified in these studies (Continued)

ANKS1B	Q7Z6G8	ZAP70	Y474	P43403	0.747184
ANKS1B	Q7Z6G8	CBL	Y368	P22681	0.994338
ANKS1B	Q7Z6G8	IRS2	Y823	Q9Y4H2	0.918242
DOK6	Q6PKX4	FLT1	Y1333	P17948	0.365173
DOK6	Q6PKX4	PDGFRB	Y1021	P09619	0.811197
DOK6	Q6PKX4	ZAP70	Y492	P43403	0.253591
DOK6	Q6PKX4	LCK	Y505	P06239	0.673593
DOK6	Q6PKX4	DOK1	Y398	Q99704	0.578489
DOK6	Q6PKX4	GAB1	Y307	Q13480	0.382919
DOK6	Q6PKX4	GAB1	Y472	Q13480	0.535772
APBB1-NC	O00213	FGFR1	Y463	P11362	0.893491
APBB1-NC	O00213	FGFR3	Y724	P22607	0.781596
APBB1-NC	O00213	FGFR3	Y760	P22607	0.284467
APBB1-NC	O00213	KIT	Y900	P10721	0.921657
APBB1-NC	O00213	MET	Y1313	P08581	0.609947
APBB1-NC	O00213	MET	Y1356	P08581	0.567844
APBB1-NC	O00213	MST1R	Y1317	Q04912	0.48237
APBB1-NC	O00213	NTRK1	Y496	P04629	0.897435
APBB1-NC	O00213	NTRK3	Y516	Q16288	0.96863
APBB1-NC	O00213	RET	Y1062	P07949	0.54266
APBB1-NC	O00213	ABL1	Y412	P00519	0.750048
APBB1-NC	O00213	IRS1	Y896	P35568	0.553994
APBB1-NC	O00213	IRS1	Y1179	P35568	0.970284
APBB1-NC	O00213	IRS2	Y823	Q9Y4H2	0.807003
APBB2-NC	Q92870	NTRK3	Y516	Q16288	0.749227
APBB2-NC	Q92870	DOK1	Y315	Q99704	0.87709
APBB2-NC	Q92870	ABL1	Y191	P00519	0.933695
APBB3-NC	O95704	PLCG2	Y1245	P16885	0.946783
APBB3-NC	O95704	CBL	Y368	P22681	0.912086
APBB3-NC	O95704	EPHB3	Y924	P54753	0.385251
APBB3-NC	O95704	IRS1	Y989	P35568	0.813134
CBL	P22681	AXL	Y821	P30530	0.877172
CBL	P22681	AXL	Y866	P30530	0.936307
CBL	P22681	EPHB1	Y778	P54762	0.914351
CBL	P22681	FGFR1	Y605	P11362	0.800067
CBL	P22681	FGFR3	Y724	P22607	0.921497
CBL	P22681	FLT1	Y1327	P17948	0.390255
CBL	P22681	FLT3	Y599	P36888	0.263014
CBL	P22681	FLT4	Y1337	P35916	0.806653
CBL	P22681	IGF1R	Y1281	P08069	0.484803

Table 6.2: Sub micromolar interactions identified in these studies (Continued)

CBL	P22681	INSR	Y1011	P06213	0.838048
CBL	P22681	KIT	Y900	P10721	0.439409
CBL	P22681	KIT	Y936	P10721	0.852357
CBL	P22681	MET	Y1234	P08581	0.884883
CBL	P22681	MET	Y1313	P08581	0.43049
CBL	P22681	MET	Y1365	P08581	0.91234
CBL	P22681	MST1R	Y1317	Q04912	0.391109
CBL	P22681	MST1R	Y1360	Q04912	0.943777
CBL	P22681	NTRK3	Y516	Q16288	0.586438
CBL	P22681	PDGFRB	Y1021	P09619	0.728491
CBL	P22681	ROS1	Y2274	P08922	0.827528
CBL	P22681	TEK	Y1102	Q02763	0.656324
CBL	P22681	ERBB4	Y1150	Q15303	0.539476
CBL	P22681	ERBB2	Y877	P04626	0.917709
CBL	P22681	ERBB2	Y1023	P04626	0.932632
CBL	P22681	ERBB2	Y1112	P04626	0.988212
CBL	P22681	ERBB2	Y1221	P04626	0.55019
CBL	P22681	ERBB2	Y1222	P04626	0.308569
CBL	P22681	PLCG2	Y753	P16885	0.756607
CBL	P22681	CBL	Y368	P22681	0.864434
CBL	P22681	INSR	Y1149	P06213	0.860252
CBL	P22681	GAB1	Y285	Q13480	0.934788
CBL	P22681	TNS1	Y339	Q9HBL0	0.528601
PIK3R2-C	O00459	RET	Y1096	P07949	0.719235
PIK3R2-C	O00459	DOK1	Y146	Q99704	0.623798
PIK3R2-C	O00459	DOK2	Y139	O60496	0.888514
PIK3R2-C	O00459	FLT1	Y1053	P17948	0.140497
PIK3R2-C	O00459	IRS1	Y662	P35568	0.828726
PIK3R2-C	O00459	PTPN6	Y301	P29350	0.627026
PIK3R3-NC	Q92569	AXL	Y821	P30530	0.657743
PIK3R3-NC	Q92569	FGFR1	Y730	P11362	0.474357
PIK3R3-NC	Q92569	FGFR3	Y724	P22607	0.267028
PIK3R3-NC	Q92569	IGF1R	Y1161	P08069	0.625473
PIK3R3-NC	Q92569	INSR	Y1185	P06213	0.625473
PIK3R3-NC	Q92569	IGF1R	Y1280	P08069	0.929501
PIK3R3-NC	Q92569	IGF1R	Y1346	P08069	0.586984
PIK3R3-NC	Q92569	INSR	Y1011	P06213	0.313409
PIK3R3-NC	Q92569	INSR	Y1361	P06213	0.243616
PIK3R3-NC	Q92569	KDR	Y1059	P35968	0.762151
PIK3R3-NC	Q92569	KIT	Y900	P10721	0.183787

Table 6.2: Sub micromolar interactions identified in these studies (Continued)

PIK3R3-NC	Q92569	MET	Y1313	P08581	0.300051
PIK3R3-NC	Q92569	MST1R	Y1317	Q04912	0.265298
PIK3R3-NC	Q92569	PDGFRA	Y742	P16234	0.162098
PIK3R3-NC	Q92569	PDGFRB	Y740	P09619	0.397489
PIK3R3-NC	Q92569	PDGFRB	Y775	P09619	0.721229
PIK3R3-NC	Q92569	PDGFRB	Y1021	P09619	0.609036
PIK3R3-NC	Q92569	RET	Y981	P07949	0.368778
PIK3R3-NC	Q92569	ERBB4	Y1056	Q15303	0.845634
PIK3R3-NC	Q92569	FRS2	Y196	Q8WU20	0.963482
PIK3R3-NC	Q92569	FRS2	Y306	Q8WU20	0.621464
PIK3R3-NC	Q92569	FRS2	Y349	Q8WU20	0.87593
PIK3R3-NC	Q92569	EGFR	Y1092	P00533	0.761228
PIK3R3-NC	Q92569	EGFR	Y1138	P00533	0.943412
PIK3R3-NC	Q92569	EGFR	Y1172	P00533	0.723479
PIK3R3-NC	Q92569	ERBB2	Y1196	P04626	0.875449
PIK3R3-NC	Q92569	ERBB2	Y1221	P04626	0.556073
PIK3R3-NC	Q92569	ERBB3	Y1199	P21860	0.646337
PIK3R3-NC	Q92569	FYN	Y420	P06241	0.254837
PIK3R3-NC	Q92569	SRC	Y419	P12931	0.254837
PIK3R3-NC	Q92569	YES1	Y426	P07947	0.254837
PIK3R3-NC	Q92569	ZAP70	Y315	P43403	0.911487
PIK3R3-NC	Q92569	LCP2	Y128	Q13094	0.95075
PIK3R3-NC	Q92569	SH2D2A	Y39	Q9NP31	0.564425
PIK3R3-NC	Q92569	VAV1	Y174	P15498	0.430338
PIK3R3-NC	Q92569	CBL	Y371	P22681	0.346544
PIK3R3-NC	Q92569	CBLB	Y363	Q13191	0.346544
PIK3R3-NC	Q92569	DOK1	Y315	Q99704	0.772111
PIK3R3-NC	Q92569	IRS1	Y989	P35568	0.204048
PIK3R3-NC	Q92569	IRS2	Y653	Q9Y4H2	0.583628
PIK3R3-NC	Q92569	GAB1	Y259	Q13480	0.78733
PIK3R3-NC	Q92569	PDGFRA	Y613	P16234	0.169158
PIK3R3-NC	Q92569	NCK2	Y50	O43639	0.616749
PIK3R3-NC	Q92569	VAV3	Y173	Q9UKW4	0.66962
PIK3R3-NC	Q92569	PTPN6	Y301	P29350	0.928051
PIK3R3-NC	Q92569	CBL	Y731	P22681	0.251014
PIK3R3-NC	Q92569	CBLB	Y709	Q13191	0.305185
PIK3R2-NC	O00459	FGFR1	Y730	P11362	0.558408
PIK3R2-NC	O00459	FGFR3	Y724	P22607	0.229568
PIK3R2-NC	O00459	FLT1	Y1213	P17948	0.628015
PIK3R2-NC	O00459	IGF1R	Y1346	P08069	0.941536

Table 6.2: Sub micromolar interactions identified in these studies (Continued)

PIK3R2-NC	O00459	KIT	Y721	P10721	0.158754
PIK3R2-NC	O00459	MST1R	Y1317	Q04912	0.292133
PIK3R2-NC	O00459	NTRK3	Y516	Q16288	0.613315
PIK3R2-NC	O00459	ERBB4	Y1056	Q15303	0.772274
PIK3R2-NC	O00459	EGFR	Y1138	P00533	0.717774
PIK3R2-NC	O00459	ERBB3	Y1276	P21860	0.341317
PIK3R2-NC	O00459	ERBB3	Y1289	P21860	0.516252
PIK3R2-NC	O00459	NCK1	Y268	P16333	0.771296
PIK3R2-NC	O00459	VAV2	Y172	P52735	0.862663
PIK3R2-NC	O00459	CBL	Y371	P22681	0.617489
PIK3R2-NC	O00459	CBLB	Y363	Q13191	0.617489
PIK3R2-NC	O00459	IRS1	Y896	P35568	0.408697
PIK3R2-NC	O00459	IRS1	Y989	P35568	0.228816
PIK3R2-NC	O00459	IRS2	Y653	Q9Y4H2	0.505608
LCK	P06239	EPHA3	Y779	P29320	0.893664
LCK	P06239	EPHA4	Y779	P54764	0.893664
LCK	P06239	EPHA5	Y833	P54756	0.893664
LCK	P06239	FGFR3	Y724	P22607	0.71417
LCK	P06239	FLT1	Y1327	P17948	0.795837
LCK	P06239	INSR	Y1011	P06213	0.731166
LCK	P06239	KIT	Y721	P10721	0.519325
LCK	P06239	KIT	Y900	P10721	0.599839
LCK	P06239	KIT	Y936	P10721	0.870901
LCK	P06239	MET	Y1313	P08581	0.33765
LCK	P06239	MET	Y1356	P08581	0.95673
LCK	P06239	ERBB3	Y1289	P21860	0.416355
LCK	P06239	EPHA7	Y614	Q15375	0.856101
LCK	P06239	EPHA1	Y599	P21709	0.562484
LCK	P06239	EPHA1	Y605	P21709	0.723717
LCK	P06239	PLCG2	Y1217	P16885	0.795307
LCK	P06239	VAV1	Y174	P15498	0.78843
LCK	P06239	CBL	Y368	P22681	0.996805
LCK	P06239	DOK1	Y315	Q99704	0.561315
LCK	P06239	EPHA3	Y937	P29320	0.646067
LCK	P06239	EPHA5	Y656	P54756	0.521736
LCK	P06239	ERBB2	Y1127	P04626	0.723004
LCK	P06239	FLT1	Y1048	P17948	0.717697
LCK	P06239	FLT3	Y969	P36888	0.920208
LCK	P06239	KIT	Y553	P10721	0.674019
LCK	P06239	FGFR2	Y466	P21802	0.940568

Table 6.2: Sub micromolar interactions identified in these studies (Continued)

LCK	P06239	PIK3R1	Y528	P27986	0.970238
LCK	P06239	PIK3C2B	Y685	O00750	0.964672
LCK	P06239	PIK3R1	Y699	P27986	0.964672
LCK	P06239	ABL1	Y191	P00519	0.793807
LCK	P06239	FGR	Y180	P09769	0.567284
LCK	P06239	FYN	Y185	P06241	0.567284
LCK	P06239	YES1	Y194	P07947	0.567284
LCK	P06239	SYK	Y203	P43405	0.862977
LCK	P06239	PLCG1	Y1253	P19174	0.792398
LCK	P06239	CHN2	Y21	P52757	0.797007
LCK	P06239	PTPN6	Y301	P29350	0.527871
LCK	P06239	TNS4	Y150	Q8IZW8	0.562618
LCK	P06239	SHB	Y297	Q15464	0.735368
LCK	P06239	TNS1	Y366	Q9HBL0	0.76999
LCK	P06239	CBL	Y731	P22681	0.901779
LCK	P06239	CBLB	Y889	Q13191	0.835729
LCK	P06239	APBB3	Y291	O95704	0.49301
LCK	P06239	IRS4	Y921	O14654	0.791007
LCK	P06239	ANKS1A	Y833	Q92625	0.791877
LCK	P06239	CSK	Y263	P41240	0.969775
LCK	P06239	PTK2	Y397	Q05397	0.783774
LCK	P06239	PTK2	Y407	Q05397	0.953714
LCK	P06239	PTK2	Y861	Q05397	0.663407
LCK	P06239	PTK2	Y925	Q05397	0.499888
SH2D2A	Q9NP31	PDGFRB	Y771	P09619	0.607596
SH2D2A	Q9NP31	ERBB2	Y1139	P04626	0.654339
SH2D2A	Q9NP31	PLCG2	Y1245	P16885	0.922343
SH2D2A	Q9NP31	CBL	Y700	P22681	0.972193
SH2D2A	Q9NP31	DAB1	Y198	O75553	0.495338
SH2D2A	Q9NP31	IRS1	Y465	P35568	0.900128
SH2D2A	Q9NP31	IRS1	Y732	P35568	0.949546
SH2D2A	Q9NP31	IRS1	Y989	P35568	0.802336
SH2D2A	Q9NP31	CSK	Y263	P41240	0.898666
SH2D3C	Q8N5H7	ALK	Y1092	Q9UM73	0.381734
SH2D3C	Q8N5H7	ALK	Y1096	Q9UM73	0.549853
SH2D3C	Q8N5H7	EPHB1	Y600	P54762	0.962653
SH2D3C	Q8N5H7	EPHB2	Y602	P29323	0.962653
SH2D3C	Q8N5H7	EPHB2	Y596	P29323	0.739096
SH2D3C	Q8N5H7	FGFR1	Y463	P11362	0.864898
SH2D3C	Q8N5H7	FGFR1	Y730	P11362	0.621391

Table 6.2: Sub micromolar interactions identified in these studies (Continued)

SH2D3C	Q8N5H7	FGFR3	Y724	P22607	0.298312
SH2D3C	Q8N5H7	FLT1	Y1327	P17948	0.316663
SH2D3C	Q8N5H7	FLT3	Y591	P36888	0.836358
SH2D3C	Q8N5H7	FLT3	Y597	P36888	0.378353
SH2D3C	Q8N5H7	FLT3	Y599	P36888	0.286201
SH2D3C	Q8N5H7	FLT4	Y1337	P35916	0.7077
SH2D3C	Q8N5H7	IGF1R	Y1280	P08069	0.524607
SH2D3C	Q8N5H7	IGF1R	Y1281	P08069	0.316681
SH2D3C	Q8N5H7	INSR	Y1011	P06213	0.628714
SH2D3C	Q8N5H7	KIT	Y900	P10721	0.405702
SH2D3C	Q8N5H7	KIT	Y936	P10721	0.681898
SH2D3C	Q8N5H7	MET	Y1313	P08581	0.341611
SH2D3C	Q8N5H7	MST1R	Y1317	Q04912	0.235489
SH2D3C	Q8N5H7	MST1R	Y1360	Q04912	0.885484
SH2D3C	Q8N5H7	NTRK1	Y496	P04629	0.495529
SH2D3C	Q8N5H7	NTRK1	Y676	P04629	0.979604
SH2D3C	Q8N5H7	NTRK3	Y516	Q16288	0.537946
SH2D3C	Q8N5H7	PDGFRB	Y1021	P09619	0.908834
SH2D3C	Q8N5H7	RET	Y791	P07949	0.496501
SH2D3C	Q8N5H7	RET	Y1062	P07949	0.976337
SH2D3C	Q8N5H7	RET	Y1096	P07949	0.53939
SH2D3C	Q8N5H7	ROS1	Y2274	P08922	0.796667
SH2D3C	Q8N5H7	TEK	Y1048	Q02763	0.31579
SH2D3C	Q8N5H7	TEK	Y1102	Q02763	0.649007
SH2D3C	Q8N5H7	ERBB2	Y1023	P04626	0.948881
SH2D3C	Q8N5H7	ERBB2	Y1222	P04626	0.315431
SH2D3C	Q8N5H7	ABL2	Y515	P42684	0.475032
SH2D3C	Q8N5H7	DAB1	Y198	O75553	0.699674
SH2D3C	Q8N5H7	DOK1	Y203	Q99704	0.979938
SH2D3C	Q8N5H7	IRS1	Y465	P35568	0.904383
SH2D3C	Q8N5H7	IRS1	Y896	P35568	0.535081
SH2D3C	Q8N5H7	IRS1	Y1179	P35568	0.80332
SH2D3C	Q8N5H7	IRS2	Y675	Q9Y4H2	0.71887
SH2D3C	Q8N5H7	IRS2	Y823	Q9Y4H2	0.979542
SH2D3C	Q8N5H7	GAB1	Y373	Q13480	0.63155
SH2D3C	Q8N5H7	SRC	Y521	P12931	0.90118
SH2D3C	Q8N5H7	SYK	Y203	P43405	0.629236
SH2B1	Q9NRF2	PDGFRB	Y1021	P09619	0.879998
SH2B1	Q9NRF2	GRB2	Y209	P62993	0.788918
SH2B1	Q9NRF2	VAV3	Y173	Q9UKW4	0.533039

Table 6.2: Sub micromolar interactions identified in these studies (Continued)

RASA1-NC	P20936	ALK	Y1092	Q9UM73	0.626474
RASA1-NC	P20936	ALK	Y1096	Q9UM73	0.68284
RASA1-NC	P20936	AXL	Y866	P30530	0.909161
RASA1-NC	P20936	FGFR1	Y766	P11362	0.92155
RASA1-NC	P20936	FGFR3	Y724	P22607	0.34659
RASA1-NC	P20936	FLT1	Y1327	P17948	0.463713
RASA1-NC	P20936	FLT4	Y1337	P35916	0.545616
RASA1-NC	P20936	IGF1R	Y1280	P08069	0.91097
RASA1-NC	P20936	IGF1R	Y1346	P08069	0.490879
RASA1-NC	P20936	INSR	Y1011	P06213	0.780154
RASA1-NC	P20936	FLT4	Y1063	P35916	0.699334
RASA1-NC	P20936	KDR	Y1054	P35968	0.699334
RASA1-NC	P20936	KIT	Y570	P10721	0.51353
RASA1-NC	P20936	KIT	Y900	P10721	0.498773
RASA1-NC	P20936	MET	Y1313	P08581	0.419338
RASA1-NC	P20936	MET	Y1356	P08581	0.342958
RASA1-NC	P20936	MST1R	Y1317	Q04912	0.519472
RASA1-NC	P20936	NTRK1	Y496	P04629	0.697821
RASA1-NC	P20936	NTRK2	Y706	Q16620	0.91031
RASA1-NC	P20936	NTRK3	Y709	Q16288	0.91031
RASA1-NC	P20936	NTRK3	Y516	Q16288	0.50186
RASA1-NC	P20936	PDGFRB	Y1009	P09619	0.761799
RASA1-NC	P20936	RET	Y791	P07949	0.515646
RASA1-NC	P20936	RET	Y806	P07949	0.520195
RASA1-NC	P20936	RET	Y1096	P07949	0.785543
RASA1-NC	P20936	TEK	Y1102	Q02763	0.514791
RASA1-NC	P20936	ERBB4	Y1221	Q15303	0.781575
RASA1-NC	P20936	ERBB2	Y1023	P04626	0.899355
RASA1-NC	P20936	ERBB2	Y1222	P04626	0.300823
RASA1-NC	P20936	ERBB3	Y1276	P21860	0.942986
RASA1-NC	P20936	ABL1	Y276	P00519	0.689004
RASA1-NC	P20936	ABL1	Y412	P00519	0.139186
RASA1-NC	P20936	RASA1	Y615	P20936	0.307835
RASA1-NC	P20936	VAV1	Y174	P15498	0.684902
RASA1-NC	P20936	VAV2	Y159	P52735	0.956125
RASA1-NC	P20936	CBL	Y371	P22681	0.704434
RASA1-NC	P20936	CBLB	Y363	Q13191	0.704434
RASA1-NC	P20936	DOK2	Y139	O60496	0.8378
RASA1-NC	P20936	IRS1	Y941	P35568	0.695478
RASA1-NC	P20936	IRS2	Y823	Q9Y4H2	0.797816

Table 6.2: Sub micromolar interactions identified in these studies (Continued)

RASA1-NC	P20936	PIK3R2	Y365	O00459	0.878477
RASA1-NC	P20936	SHC3	Y424	Q92529	0.878477
RASA1-NC	P20936	SRC	Y521	P12931	0.672195
RASA1-NC	P20936	SYK	Y203	P43405	0.986425
RASA1-NC	P20936	IRS4	Y921	O14654	0.622386
RASA1-NC	P20936	CSK	Y263	P41240	0.904032
PLCG2-C	P16885	FLT3	Y597	P36888	0.825676
PLCG2-C	P16885	RET	Y981	P07949	0.562782
PLCG2-C	P16885	ABL1	Y204	P00519	0.987962
PLCG2-NC	P16885	ALK	Y1092	Q9UM73	0.543996
PLCG2-NC	P16885	ALK	Y1096	Q9UM73	0.938776
PLCG2-NC	P16885	ALK	Y1131	Q9UM73	0.60643
PLCG2-NC	P16885	FGFR1	Y463	P11362	0.81399
PLCG2-NC	P16885	FGFR1	Y730	P11362	0.683063
PLCG2-NC	P16885	FGFR3	Y724	P22607	0.252343
PLCG2-NC	P16885	FLT1	Y1327	P17948	0.514331
PLCG2-NC	P16885	IGF1R	Y1280	P08069	0.56637
PLCG2-NC	P16885	IGF1R	Y1281	P08069	0.824529
PLCG2-NC	P16885	IGF1R	Y1346	P08069	0.662383
PLCG2-NC	P16885	INSR	Y1011	P06213	0.511922
PLCG2-NC	P16885	FLT4	Y1063	P35916	0.873841
PLCG2-NC	P16885	KDR	Y1054	P35968	0.873841
PLCG2-NC	P16885	KIT	Y721	P10721	0.83522
PLCG2-NC	P16885	KIT	Y900	P10721	0.325984
PLCG2-NC	P16885	MET	Y1356	P08581	0.404987
PLCG2-NC	P16885	MST1R	Y1317	Q04912	0.479559
PLCG2-NC	P16885	NTRK1	Y496	P04629	0.672929
PLCG2-NC	P16885	NTRK1	Y676	P04629	0.974187
PLCG2-NC	P16885	NTRK3	Y516	Q16288	0.488847
PLCG2-NC	P16885	PDGFRA	Y574	P16234	0.888509
PLCG2-NC	P16885	PDGFRB	Y771	P09619	0.923141
PLCG2-NC	P16885	PDGFRB	Y1021	P09619	0.829302
PLCG2-NC	P16885	RET	Y1029	P07949	0.46012
PLCG2-NC	P16885	EGFR	Y1092	P00533	0.939561
PLCG2-NC	P16885	ERBB2	Y877	P04626	0.852092
PLCG2-NC	P16885	ERBB2	Y1023	P04626	0.592124
PLCG2-NC	P16885	ERBB2	Y1196	P04626	0.968809
PLCG2-NC	P16885	ERBB2	Y1221	P04626	0.44514
PLCG2-NC	P16885	ERBB3	Y1276	P21860	0.826813
PLCG2-NC	P16885	ABL1	Y276	P00519	0.543012

Table 6.2: Sub micromolar interactions identified in these studies (Continued)

PLCG2-NC	P16885	FGR	Y523	P09769	0.957014
PLCG2-NC	P16885	EPHA1	Y599	P21709	0.866723
PLCG2-NC	P16885	EPHB4	Y581	P54760	0.456748
PLCG2-NC	P16885	IRS1	Y732	P35568	0.984798
PLCG2-NC	P16885	VAV3	Y173	Q9UKW4	0.585296
PLCG2-NC	P16885	SHB	Y336	Q15464	0.810495
PTPN6-N	P29350	PDGFRB	Y740	P09619	0.9752
PTPN6-N	P29350	RET	Y1029	P07949	0.980756
PTPN6-N	P29350	VAV2	Y159	P52735	0.438642
PTPN6-N	P29350	FLT1	Y1053	P17948	0.322372
PTPN6-N	P29350	IRS1	Y896	P35568	0.446783
PTPN6-NC	P29350	TEK	Y1048	Q02763	0.552983
SYK-N	P43405	ALK	Y1092	Q9UM73	0.811594
SYK-N	P43405	EPHB1	Y600	P54762	0.959097
SYK-N	P43405	EPHB2	Y602	P29323	0.959097
SYK-N	P43405	FGFR1	Y730	P11362	0.79148
SYK-N	P43405	FLT1	Y1327	P17948	0.730361
SYK-N	P43405	FLT3	Y597	P36888	0.580203
SYK-N	P43405	FLT4	Y1337	P35916	0.601583
SYK-N	P43405	MET	Y1313	P08581	0.579525
SYK-N	P43405	MET	Y1365	P08581	0.775436
SYK-N	P43405	MST1R	Y1317	Q04912	0.822837
SYK-N	P43405	NTRK3	Y516	Q16288	0.684779
SYK-N	P43405	PDGFRA	Y731	P16234	0.562725
SYK-N	P43405	PDGFRB	Y775	P09619	0.938515
SYK-N	P43405	RET	Y791	P07949	0.756238
SYK-N	P43405	RET	Y900	P07949	0.308295
SYK-N	P43405	RET	Y981	P07949	0.365889
SYK-N	P43405	TEK	Y1048	Q02763	0.728166
SYK-N	P43405	TEK	Y1102	Q02763	0.996068
SYK-N	P43405	ERBB2	Y1221	P04626	0.621918
SYK-N	P43405	ERBB2	Y1222	P04626	0.38546
SYK-N	P43405	ERBB3	Y1276	P21860	0.835128
SYK-N	P43405	RET	Y952	P07949	0.989995
SYK-N	P43405	ABL1	Y412	P00519	0.384715
SYK-N	P43405	FYN	Y420	P06241	0.726417
SYK-N	P43405	SRC	Y419	P12931	0.726417
SYK-N	P43405	YES1	Y426	P07947	0.726417
SYK-N	P43405	RASA1	Y460	P20936	0.85097
SYK-N	P43405	RASA1	Y615	P20936	0.432996

Table 6.2: Sub micromolar interactions identified in these studies (Continued)

SYK-N	P43405	SH2D2A	Y39	Q9NP31	0.792051
SYK-N	P43405	DOK2	Y345	O60496	0.363701
SYK-N	P43405	EPHA5	Y967	P54756	0.981014
SYK-N	P43405	IRS1	Y896	P35568	0.762976
SYK-N	P43405	TYRO3	Y681	Q06418	0.872891
SYK-N	P43405	PIK3R1	Y467	P27986	0.723379
SYK-N	P43405	PIK3CB	Y772	P42338	0.779417
SYK-N	P43405	ZAP70	Y69	P43403	0.588645
SYK-N	P43405	SRC	Y338	P12931	0.659999
SYK-N	P43405	JAK2	Y119	O60674	0.209591
SYK-N	P43405	SHB	Y272	Q15464	0.412757
SYK-N	P43405	TNS1	Y339	Q9HBL0	0.674441
SYK-N	P43405	IRS4	Y921	O14654	0.577975
SYK-N	P43405	INPPL1	Y1135	O15357	0.92321
SYK-NC	P43405	ALK	Y1092	Q9UM73	0.447309
SYK-NC	P43405	ALK	Y1096	Q9UM73	0.819903
SYK-NC	P43405	EPHA4	Y602	P54764	0.965445
SYK-NC	P43405	EPHB1	Y600	P54762	0.810192
SYK-NC	P43405	EPHB2	Y602	P29323	0.810192
SYK-NC	P43405	EPHB1	Y778	P54762	0.670969
SYK-NC	P43405	FGFR1	Y463	P11362	0.364204
SYK-NC	P43405	FGFR1	Y653	P11362	0.462512
SYK-NC	P43405	FGFR3	Y724	P22607	0.735469
SYK-NC	P43405	FGFR3	Y760	P22607	0.444274
SYK-NC	P43405	FLT1	Y1213	P17948	0.775183
SYK-NC	P43405	FLT1	Y1327	P17948	0.904181
SYK-NC	P43405	FLT3	Y591	P36888	0.523166
SYK-NC	P43405	FLT3	Y599	P36888	0.363407
SYK-NC	P43405	INSR	Y1011	P06213	0.937644
SYK-NC	P43405	KDR	Y1214	P35968	0.514659
SYK-NC	P43405	KIT	Y721	P10721	0.59525
SYK-NC	P43405	KIT	Y900	P10721	0.298658
SYK-NC	P43405	KIT	Y936	P10721	0.385503
SYK-NC	P43405	MET	Y1313	P08581	0.817337
SYK-NC	P43405	MET	Y1356	P08581	0.785316
SYK-NC	P43405	MST1R	Y1317	Q04912	0.257265
SYK-NC	P43405	NTRK1	Y676	P04629	0.327239
SYK-NC	P43405	NTRK2	Y702	Q16620	0.924976
SYK-NC	P43405	NTRK3	Y705	Q16288	0.924976
SYK-NC	P43405	NTRK2	Y706	Q16620	0.930604

Table 6.2: Sub micromolar interactions identified in these studies (Continued)

SYK-NC	P43405	NTRK3	Y709	Q16288	0.930604
SYK-NC	P43405	PDGFRA	Y574	P16234	0.378253
SYK-NC	P43405	PDGFRB	Y562	P09619	0.655582
SYK-NC	P43405	PDGFRB	Y579	P09619	0.931748
SYK-NC	P43405	PDGFRB	Y771	P09619	0.976826
SYK-NC	P43405	PDGFRB	Y775	P09619	0.440792
SYK-NC	P43405	RET	Y900	P07949	0.607624
SYK-NC	P43405	RET	Y981	P07949	0.339786
SYK-NC	P43405	RET	Y1096	P07949	0.748231
SYK-NC	P43405	ROS1	Y2274	P08922	0.978553
SYK-NC	P43405	TEK	Y1102	Q02763	0.705143
SYK-NC	P43405	ERBB4	Y1150	Q15303	0.595647
SYK-NC	P43405	EGFR	Y1172	P00533	0.571332
SYK-NC	P43405	ERBB2	Y1023	P04626	0.670592
SYK-NC	P43405	ERBB2	Y1221	P04626	0.365035
SYK-NC	P43405	ERBB3	Y1197	P21860	0.613176
SYK-NC	P43405	ERBB3	Y1276	P21860	0.573242
SYK-NC	P43405	RET	Y952	P07949	0.807682
SYK-NC	P43405	EPHA2	Y628	P29317	0.659309
SYK-NC	P43405	EPHA2	Y960	P29317	0.307696
SYK-NC	P43405	ABL2	Y515	P42684	0.822875
SYK-NC	P43405	ABL1	Y276	P00519	0.864362
SYK-NC	P43405	ABL1	Y412	P00519	0.430713
SYK-NC	P43405	FGR	Y412	P09769	0.852834
SYK-NC	P43405	ZAP70	Y248	P43403	0.955232
SYK-NC	P43405	ZAP70	Y474	P43403	0.72578
SYK-NC	P43405	TXK	Y91	P42681	0.811066
SYK-NC	P43405	BLNK	Y189	Q8WV28	0.667216
SYK-NC	P43405	RASA1	Y615	P20936	0.309195
SYK-NC	P43405	PTPN6	Y564	P29350	0.931509
SYK-NC	P43405	CBL	Y368	P22681	0.933607
SYK-NC	P43405	CBL	Y371	P22681	0.748832
SYK-NC	P43405	CBLB	Y363	Q13191	0.748832
SYK-NC	P43405	CBL	Y774	P22681	0.861974
SYK-NC	P43405	DAB1	Y198	O75553	0.953851
SYK-NC	P43405	DAB1	Y220	O75553	0.443868
SYK-NC	P43405	DOK1	Y146	Q99704	0.826895
SYK-NC	P43405	DOK2	Y345	O60496	0.700307
SYK-NC	P43405	IRS1	Y896	P35568	0.616144
SYK-NC	P43405	IRS1	Y1179	P35568	0.551704

Table 6.2: Sub micromolar interactions identified in these studies (Continued)

SYK-NC	P43405	IRS2	Y675	Q9Y4H2	0.91288
SYK-NC	P43405	SRC	Y521	P12931	0.784728
SYK-NC	P43405	SYK	Y203	P43405	0.715826
SYK-NC	P43405	VAV1	Y826	P15498	0.901898
SYK-NC	P43405	SHB	Y272	Q15464	0.734447
SYK-NC	P43405	TNS1	Y903	Q9HBL0	0.903128
SYK-NC	P43405	IRS4	Y921	O14654	0.677963
INPPL1	O15357	KIT	Y900	P10721	0.344976
INPPL1	O15357	MST1R	Y1317	Q04912	0.676942
INPPL1	O15357	TNS1	Y366	Q9HBL0	0.746222
INPPL1	O15357	TNS1	Y796	Q9HBL0	0.387599
INPPL1	O15357	CBLB	Y889	Q13191	0.713757
ZAP70-N	P43403	NTRK3	Y516	Q16288	0.867725
ZAP70-N	P43403	FRS2	Y196	Q8WU20	0.652037
ZAP70-N	P43403	FYN	Y420	P06241	0.438844
ZAP70-N	P43403	SRC	Y419	P12931	0.438844
ZAP70-N	P43403	YES1	Y426	P07947	0.438844
ZAP70-N	P43403	PLCG2	Y1217	P16885	0.297265
ZAP70-N	P43403	DOK1	Y315	Q99704	0.992807
ZAP70-N	P43403	FLT1	Y1053	P17948	0.590569
ZAP70-N	P43403	IRS1	Y896	P35568	0.498934
ZAP70-N	P43403	GAB1	Y406	Q13480	0.803257
ZAP70-N	P43403	PIK3R3	Y341	Q92569	0.94236
ZAP70-N	P43403	ABL2	Y683	P42684	0.513786
ZAP70-N	P43403	FGR	Y180	P09769	0.681028
ZAP70-N	P43403	FYN	Y185	P06241	0.681028
ZAP70-N	P43403	YES1	Y194	P07947	0.681028
ZAP70-N	P43403	SYK	Y203	P43405	0.572743
ZAP70-N	P43403	TNS1	Y366	Q9HBL0	0.852759
ZAP70-NC	P43403	ALK	Y1092	Q9UM73	0.462672
ZAP70-NC	P43403	ALK	Y1096	Q9UM73	0.4824
ZAP70-NC	P43403	AXL	Y866	P30530	0.960221
ZAP70-NC	P43403	FGFR1	Y653	P11362	0.887557
ZAP70-NC	P43403	FGFR1	Y730	P11362	0.45763
ZAP70-NC	P43403	FGFR3	Y724	P22607	0.995236
ZAP70-NC	P43403	FLT1	Y1327	P17948	0.893576
ZAP70-NC	P43403	FLT3	Y597	P36888	0.537925
ZAP70-NC	P43403	FLT3	Y599	P36888	0.498379
ZAP70-NC	P43403	MET	Y1313	P08581	0.837078
ZAP70-NC	P43403	MST1R	Y1317	Q04912	0.565985

Table 6.2: Sub micromolar interactions identified in these studies (Continued)

ZAP70-NC	P43403	NTRK3	Y516	Q16288	0.476746
ZAP70-NC	P43403	PDGFRA	Y731	P16234	0.587634
ZAP70-NC	P43403	RET	Y900	P07949	0.367413
ZAP70-NC	P43403	RET	Y981	P07949	0.87992
ZAP70-NC	P43403	TEK	Y1048	Q02763	0.762477
ZAP70-NC	P43403	NCK1	Y268	P16333	0.822284
ZAP70-NC	P43403	RASA1	Y615	P20936	0.374943
ZAP70-NC	P43403	CBL	Y700	P22681	0.613807
ZAP70-NC	P43403	DOK1	Y315	Q99704	0.976211
ZAP70-NC	P43403	IRS1	Y465	P35568	0.94864
ZAP70-NC	P43403	GAB1	Y373	Q13480	0.740566
ZAP70-NC	P43403	SYK	Y203	P43405	0.820327
ZAP70-NC	P43403	TNS1	Y339	Q9HBL0	0.408614
SHB	Q15464	EPHB1	Y600	P54762	0.488475
SHB	Q15464	EPHB2	Y602	P29323	0.488475
SHB	Q15464	FGFR1	Y463	P11362	0.515537
SHB	Q15464	FLT3	Y591	P36888	0.582967
SHB	Q15464	INSR	Y992	P06213	0.799455
SHB	Q15464	INSR	Y1011	P06213	0.646292
SHB	Q15464	KDR	Y996	P35968	0.697336
SHB	Q15464	FLT4	Y1063	P35916	0.840804
SHB	Q15464	KDR	Y1054	P35968	0.840804
SHB	Q15464	KDR	Y1214	P35968	0.885113
SHB	Q15464	MET	Y1003	P08581	0.704016
SHB	Q15464	MET	Y1230	P08581	0.689469
SHB	Q15464	MET	Y1234	P08581	0.862347
SHB	Q15464	MET	Y1313	P08581	0.343401
SHB	Q15464	MST1R	Y1317	Q04912	0.864931
SHB	Q15464	PDGFRB	Y562	P09619	0.733825
SHB	Q15464	PDGFRB	Y581	P09619	0.799038
SHB	Q15464	PDGFRB	Y740	P09619	0.453919
SHB	Q15464	PDGFRB	Y751	P09619	0.356384
SHB	Q15464	PDGFRB	Y1009	P09619	0.568205
SHB	Q15464	PDGFRB	Y1021	P09619	0.811647
SHB	Q15464	RET	Y1062	P07949	0.465949
SHB	Q15464	RET	Y1096	P07949	0.823944
SHB	Q15464	EGFR	Y1069	P00533	0.875899
SHB	Q15464	EGFR	Y1125	P00533	0.920206
SHB	Q15464	ERBB2	Y1023	P04626	0.535646
SHB	Q15464	ERBB2	Y1221	P04626	0.295504

Table 6.2: Sub micromolar interactions identified in these studies (Continued)

SHB	Q15464	CSF1R	Y923	P07333	0.847531
SHB	Q15464	TEC	Y206	P42680	0.708688
SHB	Q15464	PLCG2	Y753	P16885	0.827631
SHB	Q15464	PLCG2	Y1245	P16885	0.75859
SHB	Q15464	CRKL	Y207	P46109	0.258296
SHB	Q15464	INPPL1	Y986	O15357	0.933448
SHB	Q15464	CBL	Y368	P22681	0.908981
SHB	Q15464	IRS1	Y896	P35568	0.628243
SHB	Q15464	SYK	Y203	P43405	0.487639
SHB	Q15464	SYK	Y244	P43405	0.660686
SHB	Q15464	VAV3	Y173	Q9UKW4	0.40617
SHB	Q15464	ANKS1A	Y454	Q92625	0.440588